FINAL REPORT

Determining Blue-eye Trevalla stock structure and improving methods for stock assessment

Alan Williams, Paul Hamer, Malcolm Haddon, Simon Robertson, Franziska Althaus,

Mark Green, Johnathan Kool

January 2017

FRDC Project No 2013/015

ISBN 978-1-4863-0756-2

FRDC report: Determining Blue-eye Trevalla stock structure and improving methods for stock assessment, Hobart, May, 2017. FRDC Project No 2013/015. 123p. Williams, A. Hamer, P, Haddon, M, Robertson, S, Althaus, F, Green, M. and Kool, J. (2016). - Online

Determining Blue-eye Trevalla stock structure and improving methods for stock assessment

FRDC Project No 2013/015

2017

The Fisheries Research and Development Corporation plans, invests in and manages fisheries research and development throughout Australia. It is a statutory authority within the portfolio of the federal Minister for Agriculture, Fisheries and Forestry, jointly funded by the Australian Government and the fishing industry.

Researcher Contact Details

Name:	Alan Williams
Address:	Castray Esplanade Hobart TAS 7001
Phone:	03 6232 5222
Fax:	
Email:	Alan.Williams@csiro.au

FRDC Contact Details

Address:	25 Geils Court Deakin ACT 2600
Phone:	02 6285 0400
Fax:	02 6285 0499
Email:	frdc@frdc.com.au
Web:	www.frdc.com.au

In submitting this report, the researcher has agreed to FRDC publishing this material in its edited form.

Contents

Tables

Figures

Acknowledgments

Undertaking this multidisciplinary project, and capturing the necessary data on Blue-eye Trevalla, was possible only with the input and help of a wide range of people outside the project team.

We would like to acknowledge other staff at our institutions – CSIRO, Fisheries Victoria, Fish Ageing Services (FAS), and Geoscience Australia – for their contribution of time and expertise to various aspects of the project, including (at CSIRO) project administration (Deb Vince and Marilen Silverio) and communication (Kirsten Lea). Jodie Kemp (Fisheries Victoria) played a key role assisting with otolith preparations and data processing.

We are indebted to several colleagues for help in sourcing, sharing and discussing relevant data, and especially helping to source physical collections of otoliths: notably, Corey Wakefield from the Department of Fisheries, Western Australia and Kyne Krusic-Golub from FAS. Ken Graham was instrumental in making the collection of otoliths from Blue-eye catches on the Tasmantid Seamounts during a previous AFMA-funded project (see Williams *et al.* 2013), when considerable assistance was provided by Fortuna Seafoods Pty Ltd (Mike and Joe Rowley) and Whan & Boxsell Pty Ltd. (Adam Whan and Jason Boxsell). The AFMA Observer Program and Fishery Independent surveys are acknowledged for their contributions to the available data and samples for Blue-eye Trevalla, whilst additional assistance was given in accessing material from areas poorly covered in Commonwealth data: by Veronika Silberschneider and David Makin (NSW Fisheries) and Eva Lai (Department of Fisheries, Western Australia). Kevin Rowling also generously contributed information and knowledge of the species' life history and fishery background from an Australian perspective, and Peter Horn, Malcolm Francis and Crispin Middleton (NIWA) a valuable perspective of the state of knowledge of Blue-eye ecology and stock assessment in New Zealand waters.

In particular, we would like to draw attention to the role of the fishing industry in the project: several fishers generously and openly shared their knowledge of Blue-eye Trevalla ecology (e.g. spawning times and areas). Will Mure, Russell Potter and crew from the FV *Diana*, as well as staff at Mures Restaurant in Hobart, all had key roles in producing the project's main outreach product – a web-linked video (https://www.youtube.com/watch?v=fLjKeicR9C4&feature=youtu.be) and media release.

We would like to acknowledge the role of the National Environmental Research Program (NERP) Biodiversity Hub and Scott Nichol from Geoscience Australia for facilitated the involvement of Johnathan Kool and the opportunity to use the Conn4D ecological dispersal model to simulate movements of Blue-eye during their early life stages. Dr Jeff Leis kindly reviewed the dispersal modelling component of the work.

Valuable comments were provided by many attendees at SlopeRAG during project presentations in 2014 and 2015.

Finally, we acknowledge the Fisheries Research and Development Corporation (FRDC) and CSIRO Wealth from Ocean Business Unit (Marine Resources and Industry Theme) (CSIRO WfO) for providing the funding that enabled the project to go ahead.

Executive Summary

What the project achieved

The first spatial mapping of Blue-eye Trevalla stocks in Australian waters was completed between 2013 and 2016 using a variety of techniques, novel approaches, leading edge technology, a synthesis of historical data, and input from knowledgeable commercial fishers.

Each of our three primary analyses provided evidence for stock structure within the broad southern Australian distribution of Blue-eye Trevalla: spatial differences in age and growth (phenotypic variation) and otolith chemistry of the adult life stage implied there was local and regional residency by adults. Dispersal potential indicated a broader scale connectivity amongst regional populations was likely during early life. By overlaying these spatial patterns, we identified four broad Blue-eye 'stock areas': West, South, East and Seamounts-Lord Howe. Each of these stock areas represents an interconnected 'meta-population', i.e. a group of discrete adult sub-populations resident on the continental slope and seamounts without extensive migration between them. Stock areas do not reflect truly separated biological stocks because there is some exchange between them during pelagic early life history, and some of the adult sub-populations act as larger 'sinks' than others, i.e. benefiting more from recruitment derived from 'upstream' spawning areas.

These findings will help identify spatial management options for fishery managers (other than additional spatial closures). New options have the potential to enhance the effectiveness of the present stock assessment and management arrangements through an appropriately-set Total Allowable Catch (TAC). Options would need to account for the area of Blue-eye habitat already protected in each of the stock areas, and a preliminary analysis is provided. This study can be used as the basis to develop and evaluate options for other species with similar characteristics of broad distribution, unknown spatial sub-structure, and management plans that presently lack spatial and temporal dimensions.

A multidisciplinary approach increased certainty in the results by enabling a comparison and validation of conclusions from different methods. The work was only possible though a collaboration that combined the knowledge and specialist skills of a group of researchers from CSIRO, Fisheries Victoria, Geoscience Australia and the Fish Ageing Services (FAS), and with the generous contribution of time and knowledge from commercial fishers.

Project background

Blue-eye Trevalla (*Hyperoglyphe antarctica*) is a deep water fish that commands a premium price as an iconic seafood species in Australia's domestic fish markets. Despite this prominence, a number of important knowledge gaps have hampered its fishery management in Australian waters. Thus, although the species ranges widely across southern temperate Australia and extends to sub-tropical latitudes on both east and west coasts, it is currently managed as a single stock. The primary developmental need for the Blue-eye stock assessment is a better understanding of 'stock structure'.

Project aim

Defining Blue-eye Trevalla stock structure was the primary aim of the project. In this context, stock structure means spatial patterns that delineate natural sub-populations, which represent meaningful sub-units for managers of the Blue-eye fishery.

Methodology

1. Data collation and biology The starting point of the study was to locate and compile pre-existing data for Blue-eye Trevalla in Australian waters. This was done by reviewing the relevant literature and examining commercial catch data used in stock assessments (to 2013), compiling observer-collected length frequency and biological data, accessing additional collections (e.g. otoliths), and speaking with knowledgeable commercial fishers and researchers. The primary aim of this component of the project was to provide the best background information and data to all other project components, and to provide a centralised and documented archive for future work on Blue-eye Trevalla.

2. Otolith ageing A large collection of otoliths (n= 1573) were aged as part of this study. The collection was spatially selected across the Blue-eye Trevalla's Australian range to provide representative data from key areas. Length frequency and daily increment analyses were also completed. The primary aims were to (1) estimate the age composition of Blue-eye Trevalla catch from key areas; (2) enable the modelling of growth parameters in the key areas (Results Chapter 3); and (3) establish the position of the first annual zone on the sectioned otolith to support the determination of habitat usage from otolith microchemistry (Results Chapter 4).

3. Spatial analysis of age and growth Growth curves (using age data from Results Chapter 2) were fitted for 15 different regions between the GAB and the NSW/Queensland border, and from the Tasmantid Seamount chain and Lord Howe Rise. The primary aims were to (1) determine what would be required, in terms of selecting age groups and associated length groups, to make valid comparisons of the growth characteristics of Blue-eye between regions; (2) determine the growth characteristics of multiple Blue-eye from key areas using the von Bertalanffy growth model; (3) determine whether there are any trends in growth patterns through the species' geographical distribution by formally comparing the growth characteristics of the various populations studied; and (4) discuss the implications for the current assumptions concerning stock structure of the growth characteristics discovered.

4. Otolith chemistry The chemistry of Blue-eye Trevalla was examined using two complementary methods to make inferences on population structure and processes that might be influencing population structure across their Australian range. Otolith (trace) elemental chemistry analysis examined life history profiles and stable isotope ratio (carbon and oxygen) analysis examined specific life history stages (early life history, recent life history). This involved comparisons of otolith chemistry across 10 seamount locations extending from off southern QLD to Tasmania, including Lord Howe, and five slope locations extending from southern WA around Tasmania and along the NSW coast. The primary aims were to: (1) compare otolith elemental chemistry life history profiles among different slope and seamount fishery locations, and (2) compare stable isotope ratios ($\delta^{13}C$ and $\delta^{18}O$) for the early life history (juvenile/pelagic) and demersal adult life stages among different slope and seamount locations

5. Ecological dispersal modelling A sophisticated biophysical dispersal model (Conn4D) was used to evaluate the expected trajectory of Blue-eye Trevalla early life history stages transported via advection and diffusion in 3D space over time. The model used oceanographic data in conjunction with individual-based behaviour, and incorporated relevant elements of Blue-eye ecology identified by reviewing the literature and through discussions with knowledgeable commercial fishers (Results Chapter 1). The primary aims were to (1) quantify the potential connectivity of Blue-eye Trevalla between spawning areas and fishing grounds to infer species sub-structure (stock structure) across its Australian range, and (2) interpret the results in the context of fishery management.

Results/key findings

1. Data collation and biology All historical data have been compiled and quality checked, with summaries provided as archives and for use by the other project components. Additional data and otolith collections (from NSW, WA and offshore seamounts) were accessed and incorporated. Summaries of historical spatial distribution of catch, length frequency distribution, observer-collected data, early life history, and general ecology (e.g. spawning times and areas) are provided in the report, and have been used extensively in analyses by the other project components.

2. Otolith ageing Spatially explicit length frequency distributions of Blue–eye Trevalla catches from continental slope and seamount fishery areas was found to vary with location. The length frequencies of the subsets of fish that were aged are representative of both the total catch (most areas), and the size range of fish taken by the commercial fishery. Modal fish size from the Tasmantid Seamounts was consistently greater than those of the non-Tasmantid Seamounts and slope fishery areas, age composition was similar across all areas of capture, but there were higher frequencies of older fish on most of the Tasmantid seamounts (except Barcoo Seamount). Age interpretation of Blue-eye otoliths is documented for the first

time; this includes the first analysis of daily increments. Daily age results suggest the established interpretation of the zone structure for annual ageing is correct.

3. Spatial analysis of age and growth The growth of Blue-eye Trevalla differs across the range of areas sampled. The length-at-age, on average, was largest on (1) the Tasmantid Seamounts, and declined progressively on (2) the Lord Howe Rise, (3) the NSW slope and Gascoyne and unknown Queensland Seamounts, and (4) areas from eastern Bass Strait to Kangaroo Island. Blue-eye Trevalla is a relatively long-lived species (Horn *et al.* 2010 estimated a maximum age of 76 years) and for their growth patterns to become spatially distinct implies that sub-populations must remain relatively isolated from one another.

4. Otolith chemistry The otolith chemistry life history profiles and stable isotope analyses show strong differences among seamount and continental slope samples depending on the life history stage compared. Seamount samples were characterised by highly enriched barium zones in the early life history that appeared related to exposure to warmer water and consistent with the separation of slope and seamount fish early in the life history, and prior to movement to the demersal habitat. However, analysis of the inner core region of the otoliths, representing the first few months of pelagic life, showed much more homogeneity across slope and seamount areas. This is possibly a signal that broad larval dispersal and mixing of individuals from different slope and seamount spawning areas occurs early in the pelagic larval phase. Patterns in the outer edge of the otoliths, representing the period of life just prior to capture, showed finer geographic variation than for the pelagic juvenile stages, indicating local residency in the areas of capture. Overall the results are consistent with recruitment of Blue-eye to seamount and continental shelf areas from a broadly dispersed/mixed larval pool, but adult populations constituting separate resident sub-populations (meta-population with local adult residency).

5. Ecological dispersal modelling Dispersal model results implied there are four sub-regional areas having different patterns of potential recruitment: ‘West’ – comprising continental slope fishing grounds off Western Australia, South Australia and western Victoria to western Tasmania; ‘South’ – continental slope grounds around Tasmania and north-eastwards to eastern Bass Strait; ‘East’ – fishing grounds on the NSW continental slope and Tasmantid seamounts; and ‘Offshore’ – fishing grounds on the Lord Howe Rise. The South stock appears relatively resilient in having the broadest potential range of strong sources of Blue-eye recruits, and is likely to lead to a relatively high genetic diversity. However, it is also the area of greatest economic importance for Blue-eye Trevalla being the area from which the highest historical catches have been taken.

Implications for relevant stakeholders

The project found independent lines of evidence for stock structure (‘stock areas’) within the broad southern Australian distribution of Blue-eye Trevalla. This indicates the need for some form of spatial management of the resource, and provides the basis for developing options for managers of the Blue-eye fishery. The value of the results for all stakeholders, especially the fishing industry, is to provide a greater confidence in the stock assessment leading, potentially, to a less risk-averse setting of the Blue-eye Trevalla TAC.

Recommendations

That the project results be considered in relation to potential spatial management options (other than additional spatial closures) for the Blue-eye Trevalla resource in Australian waters. These options include separate TACs for different stock areas, a voluntary agreement about the spread of catch across stock areas, or some other management initiative that helps prevent serial depletion (sequential over-catch in certain areas), and considers ‘upstream’ management of ‘source areas’ to help ensure that downstream ‘sink’ areas are replenished.

Keywords

Blue-eye Trevalla; *Hyperoglyphe antarctica*; stock structure; age and growth; otolith chemistry; dispersal modelling; stock assessment; fishery spatial management

Introduction

This proposal was developed because there is a need, and an opportunity, to improve the management of Blue-eye Trevalla (*Hyperoglyphe antarctica*) – one of Australia's premium commercial scalefish, and an iconic species of south eastern regions including Tasmania.

Blue-eye Trevalla is currently managed as a single stock, and its assessment is characterised by several key uncertainties (Haddon, 2015a). These uncertainties negatively influence the Blue-eye Trevalla Total Allowable Catch (TAC), which reduced dramatically from 785 tonnes in 2007 to 335 tonnes in 2016 – a decline of over 50% in 9 years.

Uncertainties in the stock assessment primarily stem from complex spatial structure in the fishery (e.g. Fay *et al.* 2011), and uncertainty about stock structure. Blue-eye Trevalla range from WA to southern Qld, and tend to associate with seamounts and steep features on the upper continental slope (Figure 1) where they exhibit different biological properties in different areas, e.g. size and age structure, possibly linked to productivity. Historically, Blue-eye Trevalla have been caught mostly by relatively discrete target fisheries (especially auto-longline and dropline), but now a substantial catch is being taken by a new fishing method (hydraulic handline fishing variously referred to as 'power-handline' or 'minor-line'). In certain areas there is also a substantial but unquantified predation by Orcas (*Orcinus orca*), particularly on auto-longline caught fish. All of these factors have the potential to create uncertainties in the stock assessment analyses, particularly the CPUE time-series (Haddon, 2015a).

Blue-eye Trevalla is both a target species, and an incidental catch from fishing on the upper continental slope for other species such as Pink Ling (*Genypterus blacodes*). Although the Blue-eye Trevalla TAC was not fully caught in previous years, quota shortage in 2011/12 led to idle vessels and difficulties in balancing quota accounts when fish are taken incidentally. Catchwatch (AFMA, 2015) indicates that commercial Blue-eye Trevalla catch in recent years has been less than the TAC.

There is an opportunity now to improve our knowledge of Blue-eye Trevalla, and address several of the key uncertainties in its stock assessment. The opportunity exists because dialogue between research providers, industry and the Australian Fisheries Management Authority (AFMA) has identified the ways in which the stock assessment can be improved, and has identified the tools and information needed. The present project brought together the personnel and information necessary to re-develop and revise the stock assessment of Blue-eye Trevalla, and facilitate the uptake of results in management arrangements.

Knowledge of the Blue-eye Trevalla fishery will be improved principally through mapping and quantifying its complex spatial patterns – importantly including the species' stock structure – and building this information into the stock assessment. This is possible by applying leading-edge otolith-based techniques for stock discrimination, and applying spatially-based analytical techniques to historical catch and effort data. Two earlier studies of Blue-eye Trevalla stock structure suggested that genetic variation was not significant among Australian fishery regions (Bolch et al. 1993; Hindell et al. 2005). The comparison of otolith and genetic methods by Hindell et al. (2005, FRDC project 2003/045), while failing to detect genetic variation among Australian Blue-eye populations, did demonstrate some regional variation in whole otolith chemistry. This study recognised the limitations of whole otolith analyses for inferring population structure. For example, if larval and juvenile dispersal was broad, but adult fish were more locally resident this could not be resolved through a whole otolith approach, and it was suggested that a more refined life-history focussed otolith chemistry approach could be more informative of Blue-eye Trevalla population structure. Modern, cost-effective otolith-based stock discrimination techniques (e.g. otolith chemistry) are well suited to Blue-eye Trevalla because conventional tag/recapture approaches are not practical, and genetic discrimination can be blurred by low levels of gene flow across resident adult populations. Further, by applying high resolution sampling methods such as laser ablation and micro-milling to target particular life history stages (i.e. larval, juvenile, adult) within otoliths, it is possible to use otolith chemistry to investigate hypotheses of different models of population structure. New data and samples available to the project, included a comprehensive collection of Blue-eye Trevalla otoliths and fishery data from the Tasmantid seamount chain in the East Coast Deepwater Fishery (ECDF) collected during 2011-12 (Williams *et al.* 2013; 2016).

The prospective benefits to industry are enhancements to available TAC, and greater certainty for quota availability. The benefits to AFMA are reduced uncertainty of management arrangements, including stock assessment models that are risk-averse because they capture the spatial structure of Blue-eye Trevalla distribution and exploitation. A single-stock model for all Blue-eye Trevalla found within the Southern and Eastern Shark and Scalefish Fishery (SESSF) boundaries and the ECDF constitutes risk-prone management if these two areas hold separate stocks. By examining biological details that elucidate stock structure, this project will be able to provide an answer to whether these two areas hold separate stocks or not, and hence whether they should be assessed and managed separately or not. There is also a need and opportunity to incorporate new spatially-based arrangements into management of Blue-eye Trevalla in response to complex spatial patterns in the fishery that include a change of fishing methods through time, re-location of effort into underutilized locations (e.g. ECDF seamounts), and the series of recent and planned area closures that include Commonwealth Marine Reserves (CMR) in the Great Australian Bight (GAB), off the eastern seaboard and on the offshore Tasmantid Seamount Chain, and fishery closures being implemented by AFMA and NSW Fisheries to protect Harrisson's Dogfish (*Centrophorus harrissoni*) and Southern Dogfish (*Centrophorus zeehaani).*

Regionalisation of catches/ TACs is a risk-averse option when a species is spatially clustered into sub-populations (as Blue-eye Trevalla is). In such a situation, given a universal TAC without any spatial management of catch, there is a serious risk of regional serial depletion. The present work provides information necessary to avoid this as well as provide a detailed case study for the drivers and requirements for regionalisation of TACs more generally.

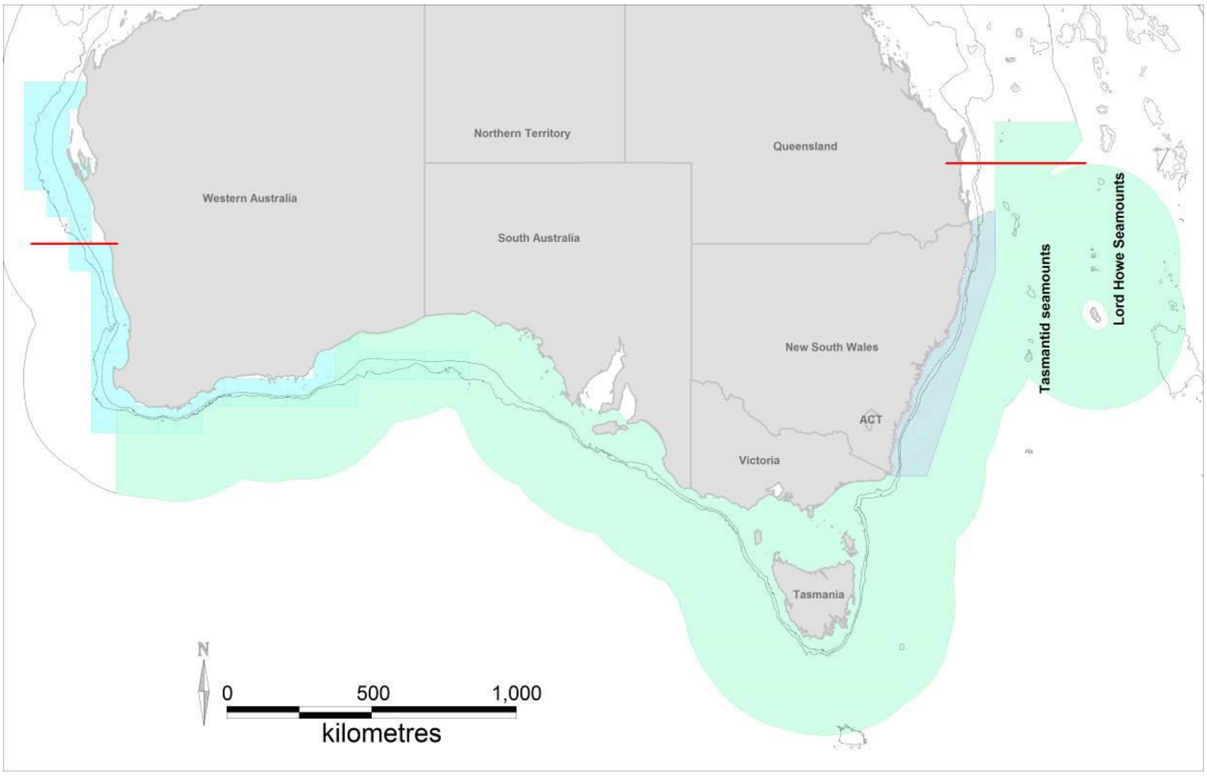

Figure 1 Overview map of study area showing the marine realm off southern Australia, identifying the upper slope (depth contours: 200 m and 1100 m) and seamount chains, as well as the fisheries jurisdiction areas of the Commonwealth Southern and Eastern Scalefish and Shark Fishery (SESSF) – green, NSW State Fisheries – purple hashed and WA State Fisheries CAES – cyan hashed. The red lines indicate the approximate extent of the modelled distribution of Blue-eye Trevalla (OBIS: http://www.obis.org.au/cgi-bin/cs_map.pl)

Objectives

The project had five primary objectives:

1. Define Blue-eye Trevalla sub-population structure, especially between the SESSF, ECDF and outside Australia's EZ, using otolith elemental and stable isotopic chemistry.
2. Evaluate the potential of other biological data (age, size frequency and maturation stage) to substantiate or refute potential sub-population spatial patterns.
3. Infer patterns of dispersal and recruitment using otolith chemistry in conjunction with ocean circulation models.
4. Develop methods to develop management options that capture the spatially and temporally complex Blue-eye Trevalla fishery and which account for extensive recent fishery and marine reserve closures.
5. Use Blue-eye Trevalla as a model to develop and evaluate options for other species.

These primary objectives were addressed by the integration of work completed in five main research areas that are presented here as separate chapters, each specifying its own sub-objectives:

- Data collation and biology
- Otolith ageing
- Spatial analysis of age and growth
- Otolith chemistry
- Ecological dispersal modelling

Method

Rationale

Blue-eye Trevalla is one of Australia's premium commercial scale-fish, and an iconic seafood species of south eastern regions including Tasmania. Despite this profile, Blue-eye Trevalla's biology, ecology and fishery status is relatively poorly documented relative to other SESSF quota species. Accordingly, an aim of this multidisciplinary project was to bring together all relevant historical biological information on Blue-eye Trevalla, as well as to generate new datasets.

Data sources

Commercial Blue-eye Trevalla catch data were sourced from official reporting data bases. All reported Blue-eye Trevalla catches (from 1985 onwards) in the spatial area of the Southern and Eastern Scalefish and Shark Fishery (SESSF) were extracted from the CSIRO mirror of the AFMA Logbook data base using spatial queries of reported shot locations (Figure 1, Table 1). Similar spatial catch data were requested for the jurisdictional areas of the NSW and WA state fisheries (Figure 1) from the NSW Department of Primary Industries and the Department of Fisheries Western Australia (Table 1). These data are described in Results Chapter 1.

Biological data including length frequency and sex distributions were extracted from the Integrated Scientific Monitoring Program (ISMP) data collated in the AFMA Observer data base (Table 1). These data are described in Results Chapter 1.

Otoliths are routinely collected by AFMA observers for determining age structure of commercial stocks, in conjunction with collecting biological data. Collected otoliths are lodged with Fish Ageing Services (FAS). An additional collection of otoliths and biological data was taken from Blue-eye Trevalla caught by hydraulic handline fishing on the Tasmantid seamount chain during an AFMA-funded study in 2011-12 (Williams *et al.* 2013). For ageing and otolith chemistry analysis we aimed to select otoliths from a limited age (size) class of fishes from a broad range of regions and the cohorts spawned within 2005–2007. Details of otolith selection, preparation and analysis for the current study are described in Results Chapters 2 and 3.

To understand the distribution of spawning adults and early life stages of Blue-eye Trevalla we reviewed the literature on Blue-eye Trevalla ontogeny and early life history and spoke with knowledgeable fishers regarding capture locations of spawning fish, in addition to examining the commercial catch and observer-collected biological data. The findings from these enquires are described in Results Chapter 1 and incorporated into the dispersal model described in Results Chapter 5.

Table 1 Blue-eye Trevalla data collated from commercial fisheries logbooks (AFMA) and observers, by broad gear groups (data extracts up to 2013). Total catch is shown for records in the AFMA logbooks, as well as for data received from NSW fisheries and WA Fisheries. The first year of data collection is indicated for each of the gear groups. AFMA observer data has separate tables for 'Length Frequency' and 'Biologicals', hence these are presented separately here.

A) AFMA Fisheries Data	**AutoLine (1997+)**	**Lines other (1988+)**	**Trawl (1985+)**	**Gillnet (1997+)**	**other gears (1986+)**	**Comment**
AFMA Logbook data – Catch table						
# operations	8049	8751	29556	1509	355	Data used for stock assessments in 2013
Total catch (t)	3419	3085	1826	302	175	
AFMA Observer data-base – Length Frequency						
# operations observed	821	672	227	55		% relative to all catch operations
% operations with LF data	10%	8%	1%	4%		
# individual measurements	24372	6890	6531	1583		
AFMA Observer data-base – Biologicals						
# operations observed	38	48	119	1		% relative to all catch operations
% operations with biologicals	0.5%	0.5%	0.4%	0.1%		
# individual measurements	3059	231	792	1		
B) State-based Fisheries Data						
WA state catch data		**(2010+)**		**(2010+)**		Data 2010-2013
Total Catch (t)		10		0.08		
NSW state catch data	**All gears collated (1984+)**					
Total Catch (t)	2181					

Results and Discussion

1. Data collation and biology

A foundation for the project was to locate and compile pre-existing data for Blue-eye Trevalla in Australian waters. This was done by a review of the relevant literature and examination of commercial catch data used in stock assessments (to 2013), compiling observer-collected length frequency and biological data, accessing additional collections (e.g. otoliths), and speaking with knowledgeable commercial fishers and researchers.

The sub-objective of this component of the project was to:

1. provide the best background information and data to all other project components, and to build a centralised and documented archive for future work on Blue-eye Trevalla.

Catch distribution

Commonwealth fisheries — AFMA data

Extracts for Blue-eye Trevalla catches from the AFMA logbook data base yielded a total of 48,220 fishing operations catching over 8,600 tonnes reported between 1985 and 2013 (Table 1). Blue-eye Trevalla are caught by a variety of gear types including lines, trawl, gillnets and few other fishing methods (Table 1). However the main commercial catch in Commonwealth waters (reported in the AFMA Logbook data-base) is from line fisheries, with auto-longline catches taking over in volume from other lines around 2003 (Table 1; Figure 2). Lower quantities but regular catches of Blue-eye Trevalla are also taken by trawls. The distribution of Blue-eye Trevalla catches is widespread on the continental slope around temperate and sub-tropical Australia, including offshore seamounts and oceanic ridges, but concentrated on the southeast (Figure 3).

The majority of the Blue-eye Trevalla catches are reported from upper continental slope depths between 200 and ~700 m with some reports from the shelf (<200 m) and lower slope to ~1100 m (Figure 3 inset).

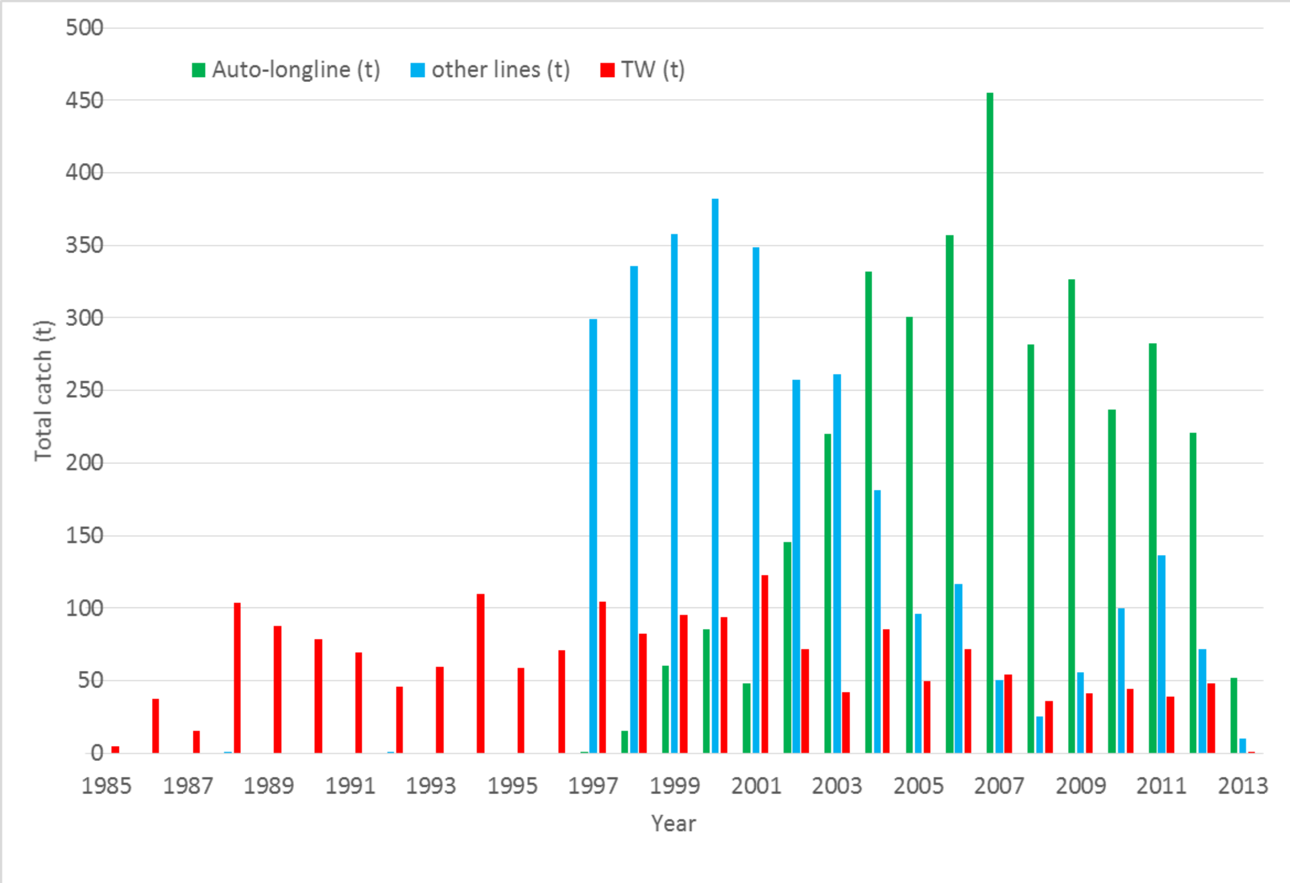

Figure 2 Total Blue-eye Trevalla catch (t) reported in AFMA logbooks by year for the three main gear types: auto-longline, other lines and trawl (TW)

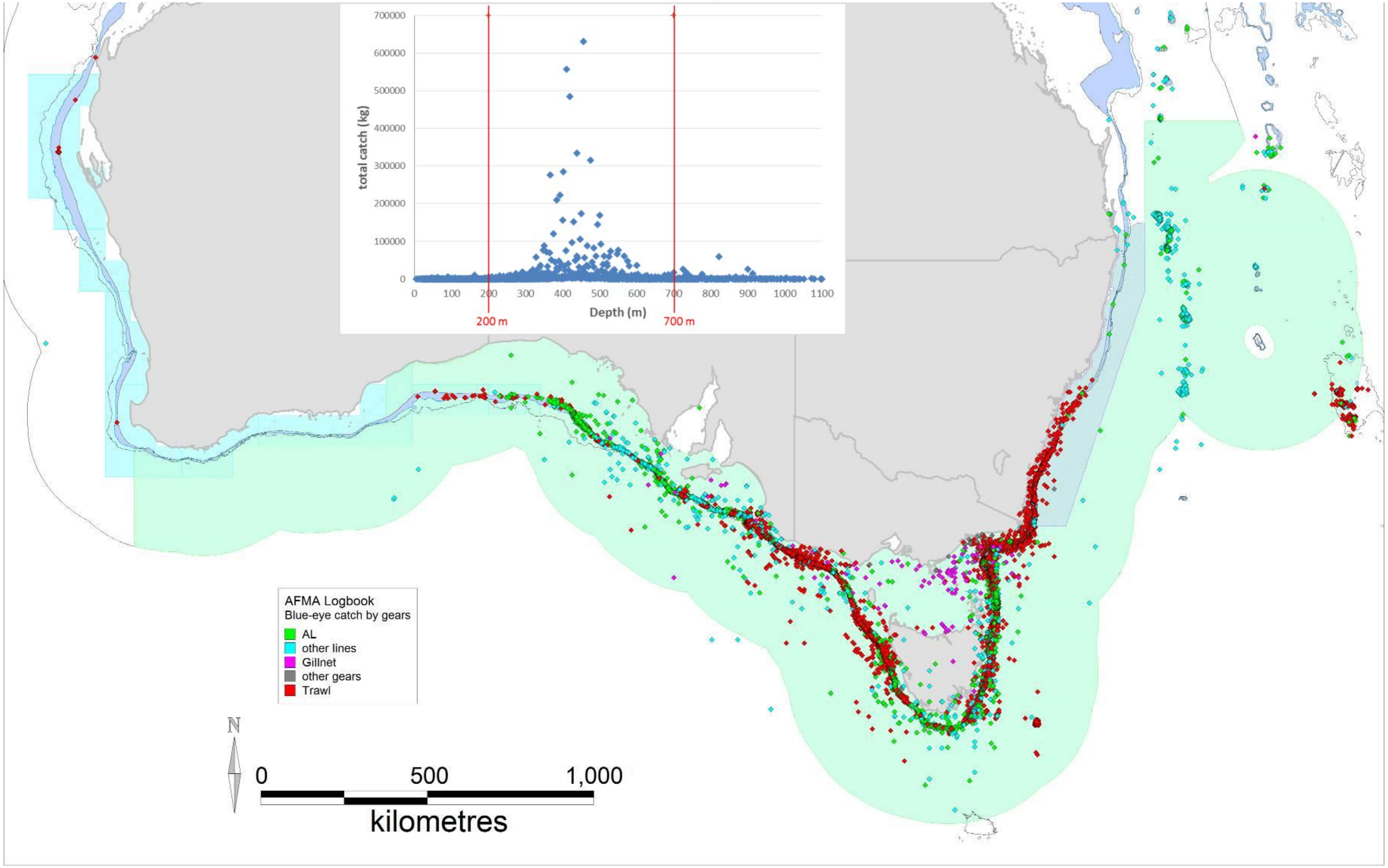

Figure 3 Spatial distribution of Blue-eye Trevalla catch records in AFMA logbook data between 1985 and 2013 (data used for stock assessment) by gear types (from Table 1). Also shown fisheries jurisdictions: SESSF – green, NSW Fisheries – purple hashed, WA Fisheries CAES – cyan hashed. Depth contours: 200 m and 1100 m. Upper slope depths (200-700 m) highlighted blue, grey line 1100 m contour. INSET: Scatter plot of total catch by depth identifying the upper slope (200-700 m). AL = Auto-longline.

New South Wales State Fisheries data

NSW Fisheries supplied Blue-eye Trevalla landings summary data by 12 latitudinal fishing zones (Figure 4a) from their catch and effort records. Data in this fishery is reported per fiscal year and was summarised for three time periods in accordance with major changes in reporting format: 1984/85-1996/97, 1997/98-2008/09 and 2009/10-2013/14. Caveats received with the NSW fisheries data summaries state that these data may include Commonwealth and other jurisdictions landings into NSW, particularly in the earliest reporting period (for 1984/85-1996/97). In addition, records of a second species – Deep Sea or Oceanic Blue Eye (*Schedophilus labyrinthicus*) – may be included in these data. The summary data received was not separated by gear type and no details of effort were supplied, due to commercial in confidence restrictions.

The NSW data report a total of 2,181 tonnes of Blue-eye Trevalla catches being landed between 1984 and 2013. The highest landings are observed for the first reporting period spanning 11 years (Figure 4a), however as mentioned in the caveat, these data are expected to include landings from Commonwealth waters outside the NSW jurisdictional boundary. Average catch per year (Figure 4b), shows that the spatial distribution of landings may be a reflection of port locations rather than fishing effort distribution. Landings in the earliest period were distributed over the entire NSW coast with peaks in zones 5 (off Tuncurry/ Newcastle), 3 (off Raleigh/ Port Macquarie) and 9 (off Tuross Heads/ Tathra). Similar peaks (except zone 5) are observed in the most recent data (2009-2013). Relatively high annual landings were reported in the southern part of NSW in 1996-2008 period.

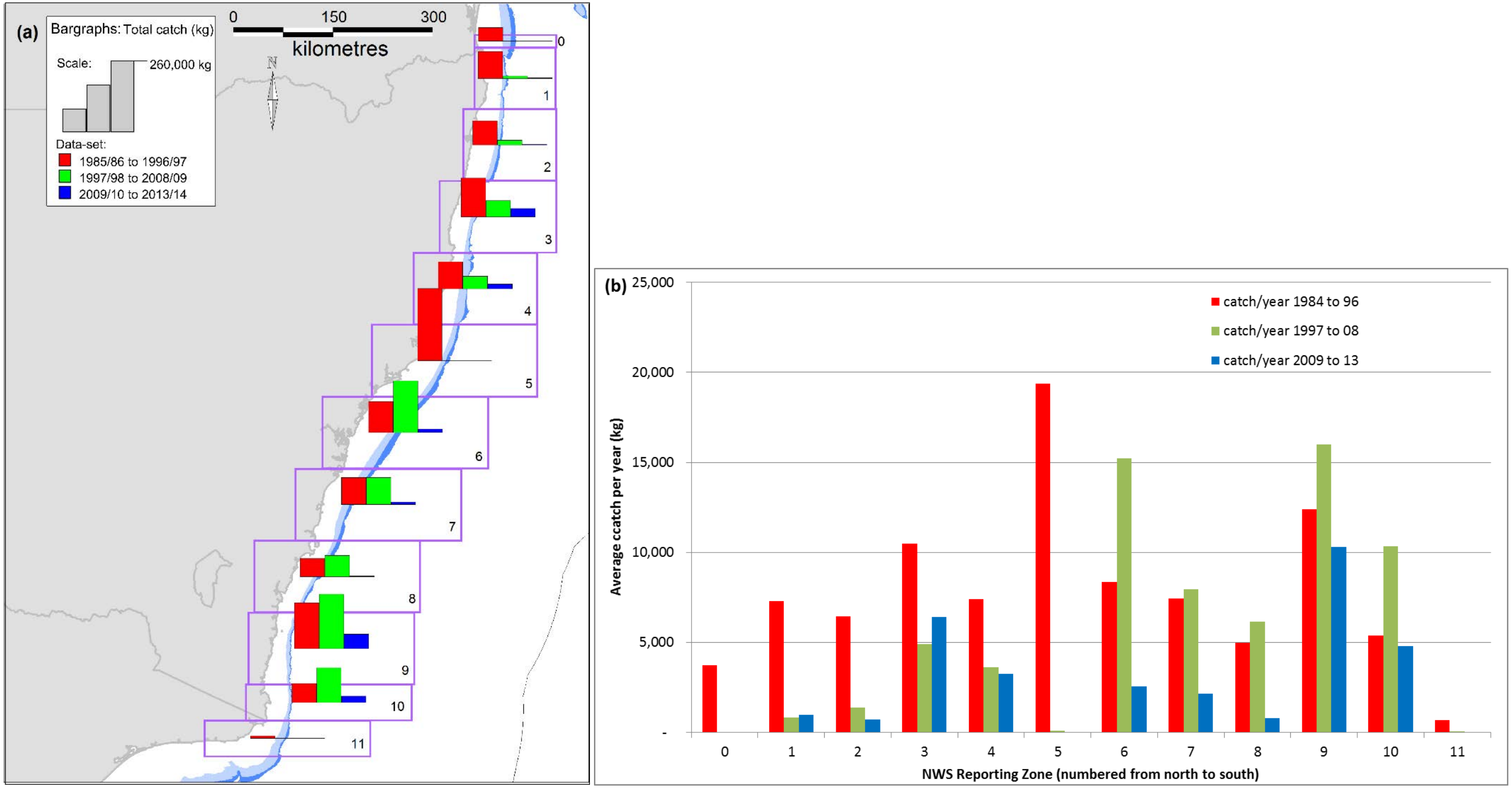

Figure 4 Blue-eye Trevalla catches (kg) reported: by NSW Fisheries for three reporting periods (NOTE: period 1984/85 to 1996/97 reports landings in NSW so this may include data from outside NSW zone - probably including seamounts; where data was reported over multiple zones we apportioned it evenly for this summary): (a) shows spatial distribution of the total catches by reporting period; for ease of comparison, (b) shows averaged annualised catches by reporting period and zone. Depth contours in (a): 200-700 m (light) and 700-1100 m (dark) coloured in two shades of blue.

Western Australia State Fisheries data

WA Fisheries supplied an extract from the Commercial Catch and Effort Statistics (CAES) database for the three fiscal years 2010/11 to 2012/13, by 'reporting block' and gear type (Figure 5). Blue-eye Trevalla was reported from 26 reporting blocks from as far north as Shark Bay to near Esperance in the south-eastern part of WA; however, the greatest volume of catch was from the southern WA coast (Figure 5). The bulk of Blue-eye Trevalla catches (10,012 kg) were from a variety of line methods (excluding auto-longline); a minor portion (79 kg) was caught in gillnets (Table 1). Annual Blue-eye Trevalla catches with line methods ranged between 2.9 and 3.9 tonnes.

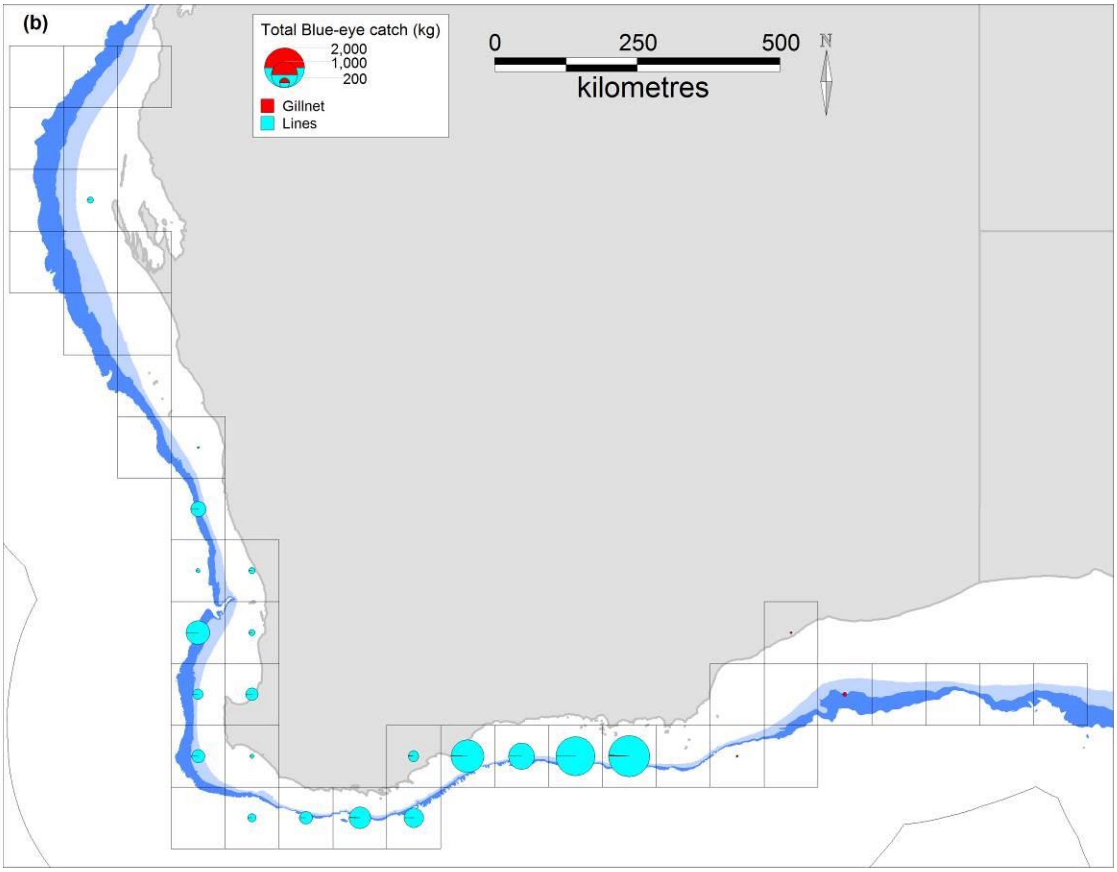

Figure 5 Blue-eye Trevalla catches (kg) reported by WA Fisheries CAES data reporting cells and gear type between FY 2010/11 and 2012/13. Depth contours 200-700 m (light) and 700-1100 m (dark) coloured in two shades of blue.

Spatial distribution of Blue-eye Trevalla catches

We summarised the reported Blue-eye Trevalla catches for 1997-2013 (2010-2013 for WA) on Australia's continental slope into broad regions, guided by the availability of otolith collections and broad geography (Figure 6). Figure 6 clearly shows that the bulk of Blue-eye Trevalla catches since 1997 were obtained from Eastern Bass Strait and Southern Tasmania, with sizeable catches off southern NSW and off Kangaroo Island/Portland. Catches off WA are minimal in comparison.

On the seamounts, the southern Lord Howe Rise yielded the highest catches (Figure 6), however if the Tasmantid seamounts are combined the total catch (~508,000 kg) is comparable to Southern NSW or West of Kangaroo Island.

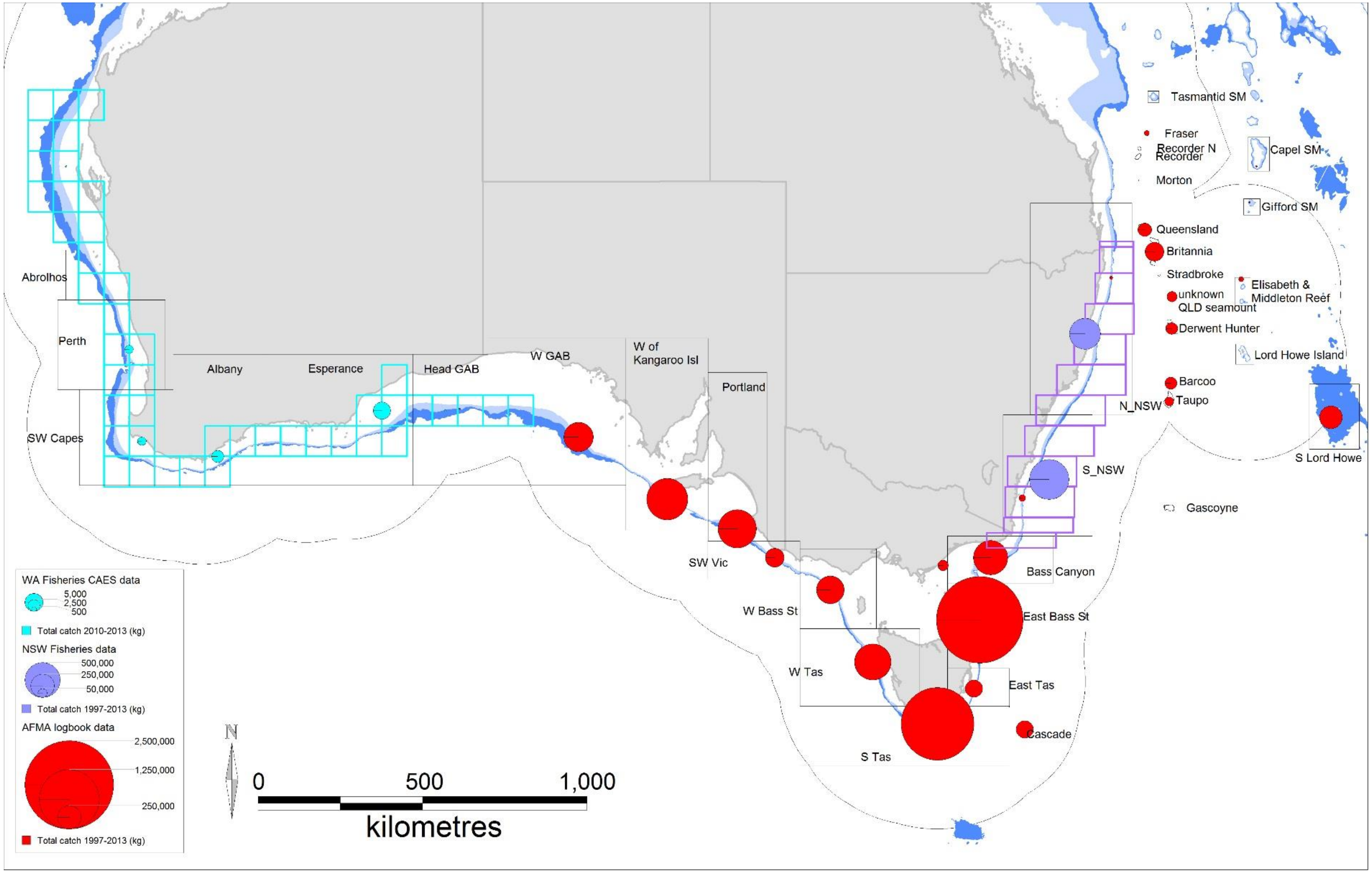

Figure 6 Distribution of total commercial catch of Blue-eye Trevalla for all gears combined by broad geographical regions for 1997 to 2013 (AFMA Logbook data and NSW Fisheries data) and for 2010-2013 for WA Fisheries CAES data (NOTE <u>different scales for the three data sets</u>). Also shown are the reporting grids for the NSW Fisheries (purple) and the WA Fisheries CAES (cyan) data. Depth contours 200-700 m (light) and 700-1100 m (dark) coloured in two shades of blue.

Length frequency distribution

Length frequency data were extracted from the AFMA Observer (ISMP) data-base by gear type and region (Table 2; Figure 7). Most observed Blue-eye Trevalla were caught by lines (62% auto-longline, 17% other line methods), with 17% trawl caught and 4% in gillnets. The observer data extracts for Blue-eye Trevalla length frequencies yielded measurements for a total of 39,376 fish, however, 320 records could not be geo-located and were thus excluded from our summaries (Table 2). The entire data set could not be presented by sex because 89% of the 39,056 geo-located fish were unsexed: the sexed fraction were 45% female and 55% male.

Individual length frequency graphs for selected regions are shown in Figure 8. For comparative graphical representation the regions were combined into four broad areas: the Tasmantid seamounts and Lord Howe Rise, and the continental slope areas of the eastern SESSF, and western SESSF (including eastern GAB). The southern Tas SESSF region was excluded from these graphs but is spatially indicated in Figure 7 and AFMA length frequency data presented in Figure 9. The majority of the data were from the continental slope: 36% west SESSF, 14% south of Tasmania, and 33% east SESSF. The seamounts regions represented a total of 17% of the data – 10% Tasmantid and 7% Lord Howe (Table 2).

Fish length (measured to caudal fork) ranged between 27 cm and 132 cm. Continental slope fishes were tightly clustered between ~42 and 75 cm lengths with few smaller/larger fish, particularly in the western SESSF (Figure 8 & Figure 9). Fish >75 cm were commonly recorded on the seamounts (Figure 8 & Figure 9). The Lord Howe seamounts have the widest spread of size classes of Blue-eye Trevalla; we note these data may also include some Oceanic Blue-eye (*Schedophilus labyrinthicus*) that is difficult to distinguish from Blue-eye Trevalla (*Hyperoglyphe antarctica*), but this is expected to have a very minor influence as they occur/attain comparable sizes.

Table 2 Summary of the geo-located length frequency data for Blue-eye Trevalla by region (Figure 7), reported in AFMA's Observer data-base (ISMP). Sizes (caudal length) are measured in cm.

Broad area	*Region*	*Number of fish*	*Size range*	*Size mode*	*Max number fish of one size*
West SESSF cont. slope	W GAB	2178	43-89	58	163
	W of Kangaroo Isl	5140	40-96	51	564
	Portland	1018	45-80	50	127
	SW Vic	1275	34-84	50	137
	W Bass St	1631	44-82	52	175
	W Tas	2966	36-85	50	353
Sth Tas SESSF cont. slope	S Tas	5338	27-92	50	758
East SESSF cont. slope	East Tas	484	46-81	50	64
	East Bass St	8612	37-104	50	759
	Bass Canyon	3501	43-93	50	251
	S_NSW	65	48-72	51	8
	N_NSW	151	47-86	68	11
Tasmantid seamounts	Gascoyne	1051	46-99	61	59
	Taupo	44	84-101	91	7
	Barcoo	658	50-97	77	47
	Derwent Hunter	350	53-101	84	20
	unknown QLD seamount	768	48-116	63	35
	Stradbroke	86	47-92	54	15
	Britannia	321	49-99	64	17
	Queensland	59	57-88	67	7
	Fraser	459	48-113	68	27
	Tasmantid SM	6	59-72	72	2
Lord Howe seamounts	S Lord Howe	2750	30-132	54	76
	Gifford SM	14	62-70	62	2
	Capel SM	23	47-80	52	3
	Outside identified regions	95	47-75	49	16

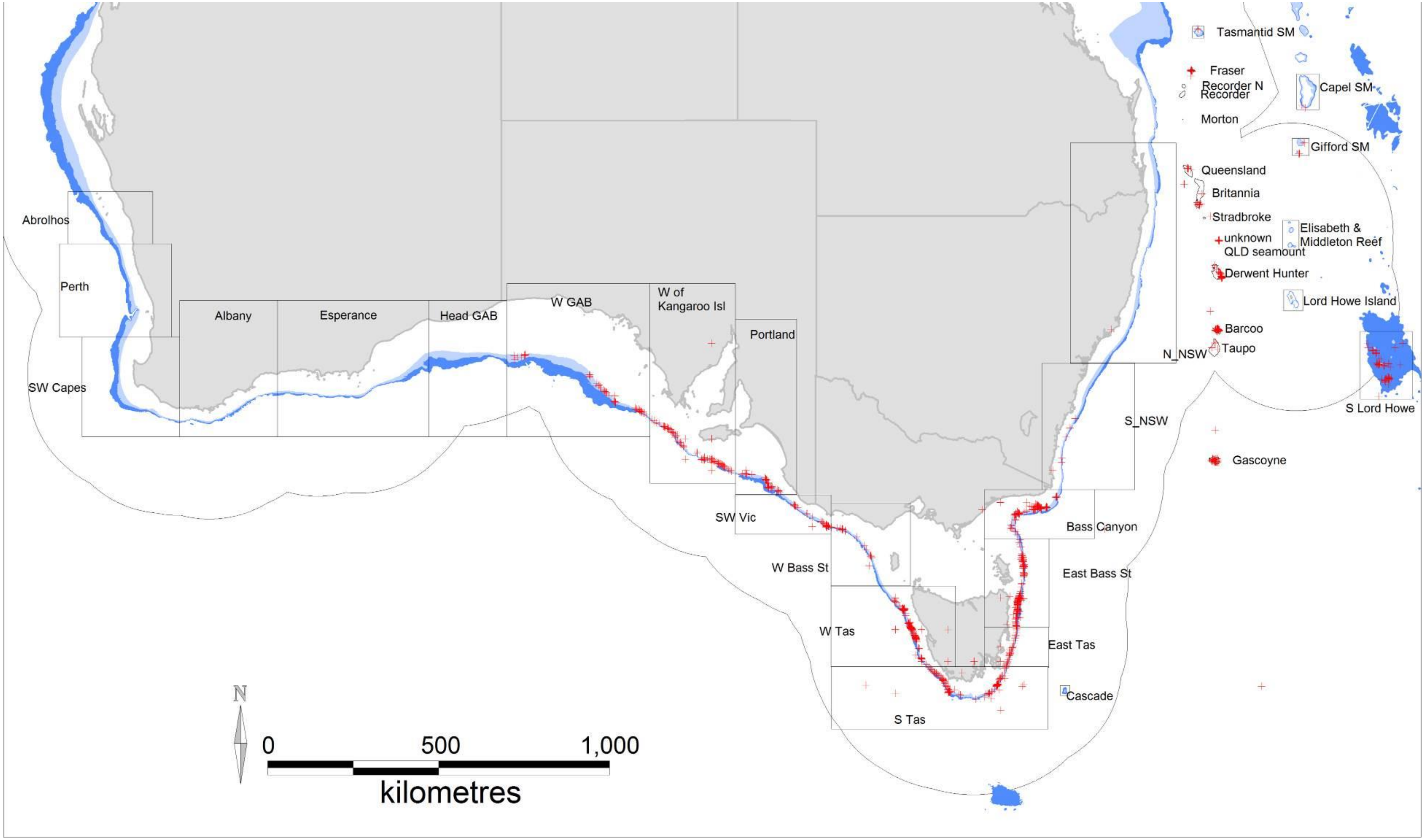

Figure 7 Spatial distribution of AFMA Observer collected length frequency data for Blue-eye Trevalla (re Table 2).

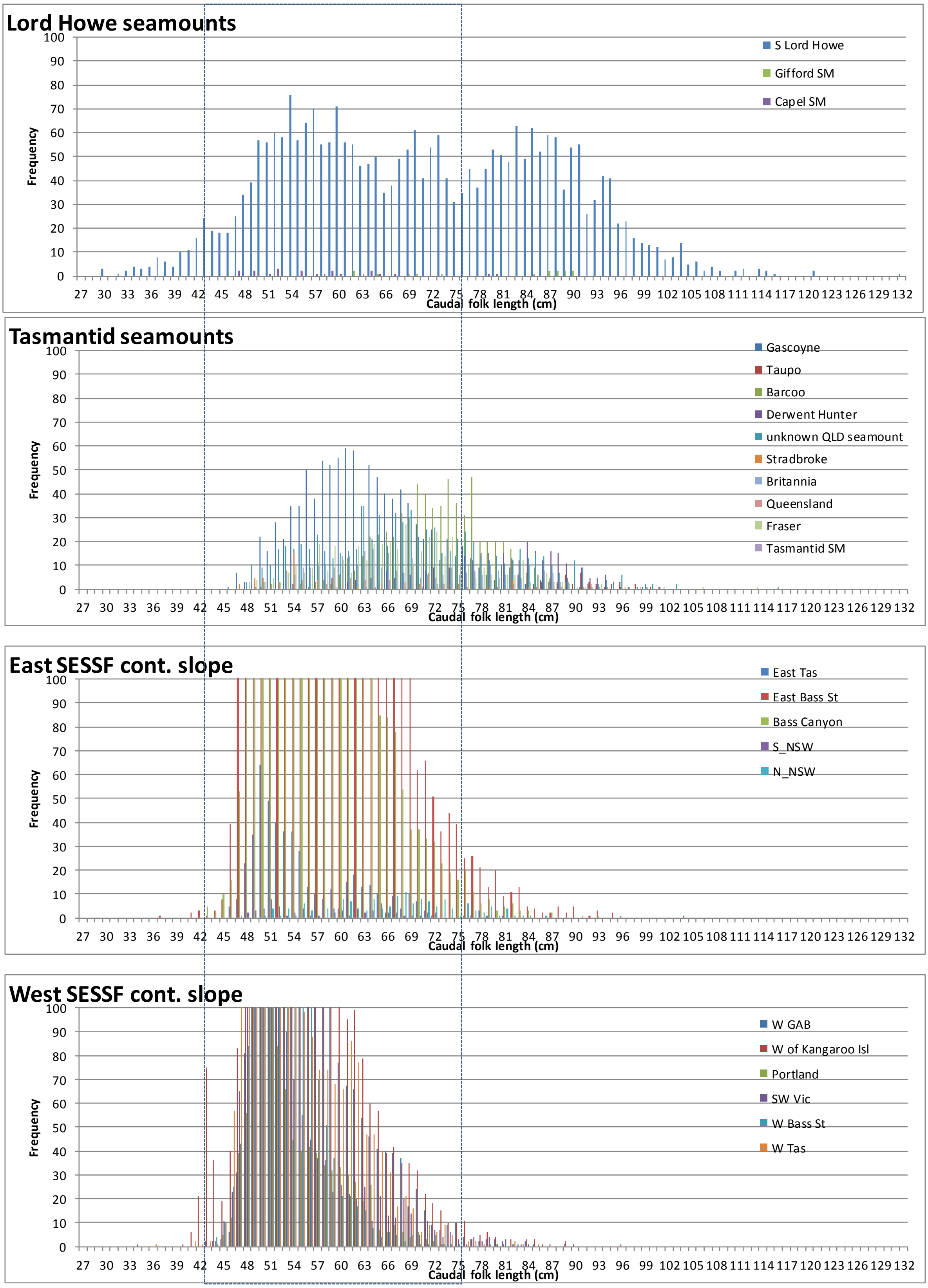

Figure 8 Length frequency plots per region (as per Table 2) summarised by larger areas. For comparative purposes the y-axes were truncated at 100 for the continental slope graphs. The 42-75 cm size range is highlighted

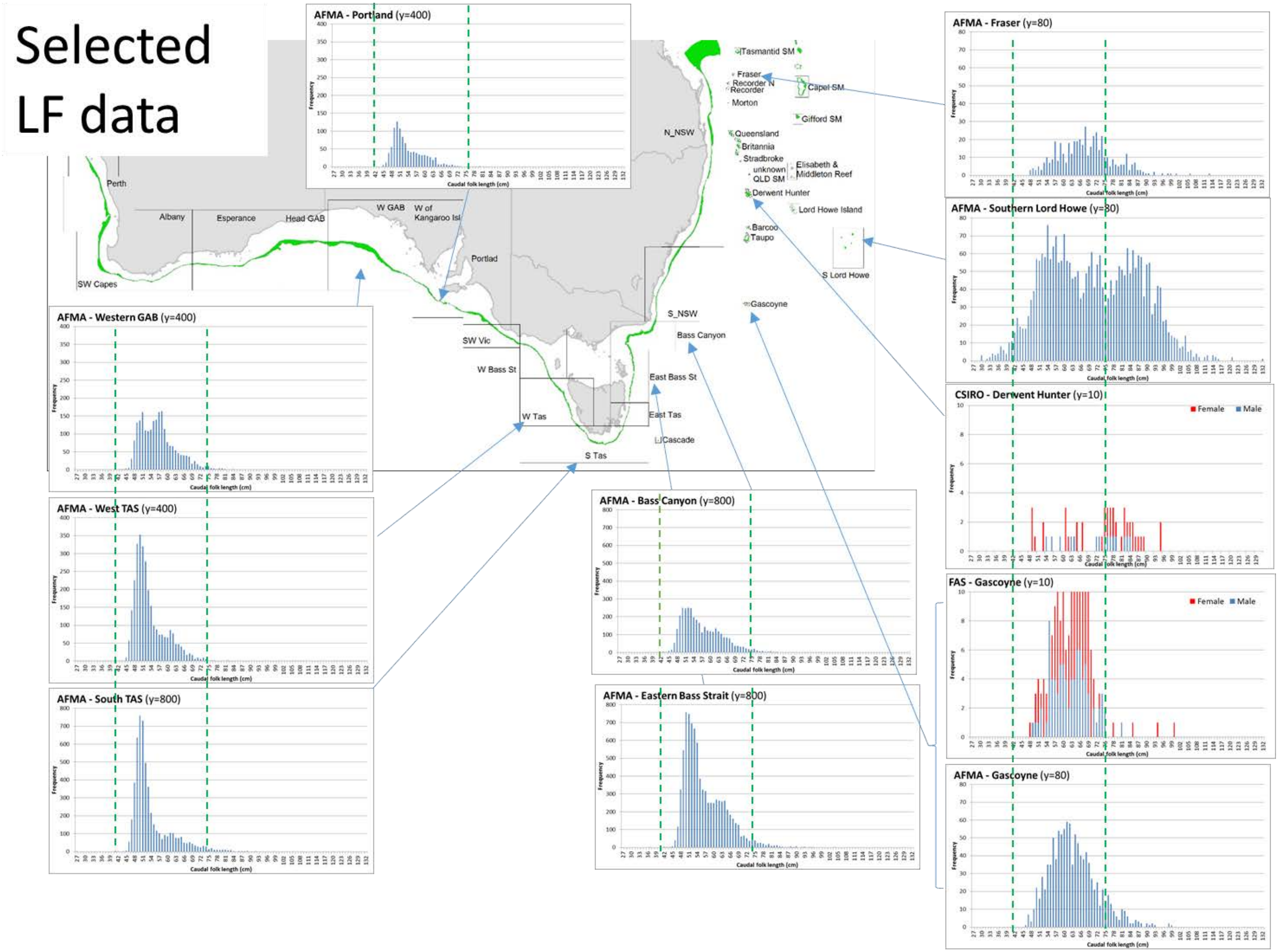

Figure 9 Length frequency distribution graphs for Blue-eye Trevalla caught in selected regions highlighting the 42-75 cm size-range over all graphs. Observation frequency varied between regions, thus note the difference in the Y-axes. The 42-75 cm size range is highlighted. Note the data at Derwent Hunter was collected during a CSIRO project investigating Blue-eye Trevalla catch on Tasmantid seamounts using power handlines and is not part of the AFMA observer data set.

Biology and ecology

Identifying aspects of biology and ecology – especially early life history – is necessary to infer connectivity among fishery sub-areas, including understanding how Blue-eye Trevalla recruits are dispersed by ocean currents. To improve our knowledge for Blue-eye Trevalla we reviewed the relevant literature, examined AFMA Observer commercial catch data (to 2013) used in stock assessments (Table 1) and length frequency data (Table 2).

The sparseness of the biological data collected by fishery observers is shown in the database summary (Table 1), with data taken from <0.6% of operations of any gear type. Data are also incomplete, for example, the great majority of biological records for sexed Blue-eye Trevalla did not include an indication of gonad stage (i.e. 'N/A' in data base); of the ones that were staged, most were reported at stage 1. Only 3 females and 10 males with gonads at stages 5 and 6, i.e. in late spawning stages, have been recorded (Table 4). On the other hand, interviews with fishers' revealed that ripe fish were regularly observed on most 'good Blue-eye Trevalla grounds', particularly in the late summer/early autumn.

Our literature review revealed many insightful individual studies but also showed that, compared to many other important commercial species, relatively little was known about Blue-eye Trevalla at a whole-of-fishery scale. This is in part because fishery-derived data are sparse, but also because the species has an unusual and elusive early life history. A summary of the information on the life history of Blue-eye Trevalla gathered from primary and grey literature, conversation with fisheries biologists and fishers as well as inference from closely related species is shown in Table 3, and represented graphically in Figure 10.

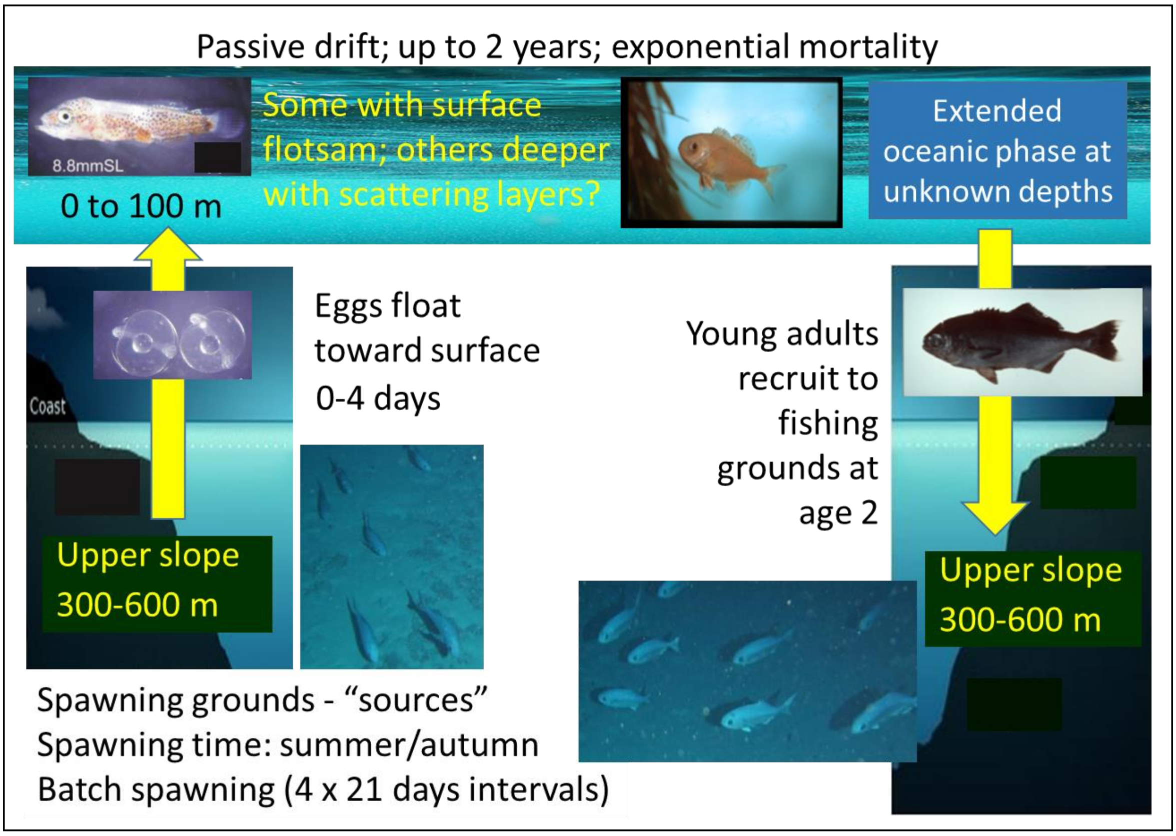

Figure 10 Diagram illustrating the life history of Blue-eye Trevalla as interpreted from literature and conversation with fishers; black text shows parameters incorporated into an ecological dispersal model (Results Chapter 5). [Images of eggs and larva from Connell, 2012]

It has long been known (e.g. Jones 1985) that Blue-eye Trevalla appear on Australian and New Zealand commercial fishing grounds at a length of about 35 to 45 cm, when they are estimated to be about 2 years old (Horn 1988), and therefore appear to be fast growing (Horn and Massey, 1989). During this period of recruitment to the fishery, they may school in mid- or near-surface waters (Duffy *et al.* 2000), but appear to reside primarily near the seabed (benthopelagic) on the upper continental slope, mainly in 200-650 m depth and often in association with abrupt seabed topography including hills and seamounts (Williams *et al.* 2016).

The species' distribution prior to the near-seabed adult phase is largely unknown because extensive net sampling programs over the Australian continental slope have collected only a few larvae (Bruce *et al.* 2001; 2002), and juveniles have been rarely observed (Last *et al.* 1993) The elusive nature of juveniles is such that only about 22 juveniles (7 to 9 cm SL) have been captured off New Zealand – two with general flotsam and at least 20 with a discarded and heavily encrusted trawl net (Duffy *et al.* 2000), and 4 individuals (3 to 6 cm; length measure not indicated) off eastern Tasmania in mid-June – dip netted beneath a floating raft of the brown kelp, *Phyllospora comosa* (Last *et al.* 1993) (Figure 11). This infers a near-surface, and probably lengthy, juvenile phase in association with floating objects, and is consistent with the behaviour of congeneric species such as the Atlantic Blue-eye, *H. perciforma*, or 'barrelfish', named for its common association with drifting logs and other floating objects.

There was some pre-existing information on spawning locations and times of Blue-eye Trevalla (Jones, 1985; Baelde, 1996), but for relatively small areas of the species' Australian distribution. These data were supplemented in this study by information provided by knowledgeable fishers. They reported that spawning Blue-eye Trevalla appear on consistently productive fishing grounds (e.g. location X & Y), indicating that spawning may occur at many locations, potentially along lengthy stretches of the continental slope. However, for the purposes of this study – and specifically in the ecological dispersal model (Results Chapter 5) – only confirmed spawning locations were included as sources. Additionally, we introduced single seed locations into each of the five Western Australian source areas where Blue-eye Trevalla occur, but where there is an absence of information of likely spawning areas. This resulted in a plausible distribution of source spawning locations across the range of the species (Results Chapter 5; Figure 57).

Table 3 Summary of key information on Blue-eye Trevalla, used to parametrize the ecological dispersal model in Results Chapter 5.

Topic	Information	Reference
Eggs	- 4-day incubation; buoyant	Connell (2012) SPRFMO 2007
Larvae	- Assumed pelagic and widely distributed by surface currents	Kailola *et al.* 1993
	- Inference from other Centrolophidae larvae (*Seriolla* spp, esp. the slope dwelling species *S. punctata*) within 25 km seaward of shelf break and in top 100 m, mostly top 50 m	Bruce *et al.* 2001
Juveniles	- 7–9 cm SL specimens collected offshore NZ west and east coast North Island in September (‘96 & ‘97), associated with drifting flotsam	Duffey *et al.* 2000
	- 3–6 cm (length measure not defined) specimens collected beyond shelf break off eastern Tasmania, associated with drifting macroalga	Last *et al.* 1993
Pre-adults	- Adopt demersal existence at size of 47-50 cm FL, about 2 years of age, off NZ	Horn 1988
	- 3–4 year olds in commercial catch	Baelde 1996
	- Rapid growth first two years, reaching 31 cm FL (0+) and 45 cm FL (1+)	Horn 1988
Maturity – age/size	- Average 71.3 cm FL (est. 11–12 yrs) female - Average 61.6 cm FL (est. 8–9 yrs) male	Baelde 1996
	- First spawn (females) at about 62 cm FL (est. 4–5 yrs)	Horn 1988
	- Immature fish 47–55 cm FL. Estimate maturity 4–5 years (aged using fish scales)	Jones 1985
	- Both sexes mature between 5 and 7 years	Horn and Massey 1989
Spawning - time	- Tasmanian BE gonads mature late Spring–Summer (Oct–Feb)	Baelde 1996
	- Tasmanian BE spawn Autumn (Mar–May)	Baelde 1996
	- South Australian BE had advanced gonads in April. Spent gonads in May.	Jones 1985
	- NZ BE from north island spawn in late summer	Horn and Massey 1989
	- Hydrated oocytes present in very large female (96 cm FL) taken of southern coast WA	Wakefield and Newman 2008
	- Spawn later than June of northern NSW	Kailola *et al.* 1993
Spawning - area	- Spawning aggregations off NSW	Rowlings 1994 pers.comm. in Baelde 1996
Spawning - method	- 3–4 batches per season	Baelde 1996
Maximum age	- At least 25 years and probably in excess of 40 years. Suggest earlier ageing studies inaccurate.	Paul *et al.* 2004 in SPRFMO 2007
	- Very large female from southern WA (96 cm FL) estimated to be 32 years	Wakefield and Newman 2008
	- Maximum age estimated at 42 years (zone counts)	Morison and Robertson 1995
	- Maximum age estimated at 76 years (radiocarbon dating)	Horn *et al.* 2010
Movement	- Can range 450 km north and south of tagging area in NZ – conclude single stock on eastern side	Horn 2012

Table 4 Blue-eye Trevalla gonad stage data from (A) females and (B) males by month of capture

A) FEMALE	**total number fish sampled: 1365**						
	Gonad stage NA	Gonad stage 1	Gonad stage 2	Gonad stage 3	Gonad stage 4	Gonad stage 5	Gonad stage 6
Total	**1128**	**134**	**59**	**26**	**14**	**3**	**1**
Jan	118						
Feb	161	15	1	1			
Mar	98						
Apr	163						
May	157						
Jun	19		1				
Jul	32	3	7	11	7	2	
Aug	128	102	32	10	1	1	
Sep	48	4	2				
Oct	38	10	14		1		
Nov	161		2	4	5		1
Dec	5						

B) MALE	**total number fish sampled: 1607**						
	Gonad stage NA	Gonad stage 1	Gonad stage 2	Gonad stage 3	Gonad stage 4	Gonad stage 5	Gonad stage 6
Total	**1205**	**287**	**55**	**38**	**12**	**9**	**1**
Jan	209						
Feb	152	28	1	4			
Mar	112			1			
Apr	136						
May	134						
Jun	41		1				
Jul	12	4	12	10	2		
Aug	149	125	21	17	4		
Sep	61	14					
Oct	36	68	13	4		3	1
Nov	144	48	7	2	6	6	
Dec	19						

Figure 11 Juvenile Blue-eye Trevalla (6-9 cm TL) – the only known specimens collected in Australian waters (Courtesy of the Australian National Fish Collection, CSIRO Hobart.)

2. Otolith ageing

Daily and annual ageing methods for otoliths of the Blue-eye Trevalla (*Hyperoglyphe antarctica*)

Introduction

Being able to confidently determine the chronological age of animals is one of the fundamental requirements for robust wild stock assessment and sustainable management, no less so for fish. The existing literature on Blue-eye Trevalla ageing is sparse, generally old and has focused on otolith increments in the New Zealand (Horn, 1988; Horn and Massey, 1989) and Australian fish stocks (Baelde, 1996) as well as fish scale increments from Australian fish (Jones 1985). More recently, radiocarbon ageing methods were used by Kalish and Johnston (2002) and Horn *et al.* (2010) to validate age estimates based on otolith increment counts.

This part of the project aimed to provide three key pieces of information to elucidate the stock structure and growth of Blue-eye Trevalla within its broad Australian range. These sub-objectives were to determine:

1. the age composition of Blue-eye Trevalla catch from spatially discrete areas of capture.
2. the position of the first annual zone on the sectioned otolith (Results in Chapter 4) [*this information will be used to investigate habitat usage by Blue-eye Trevalla from each area of capture*].
3. growth parameters for Blue-eye Trevalla in each area of capture (Results in Chapter 3).

Method

To examine these questions, otoliths were sourced, prepared and aged from ten seamounts and three continental slope areas from the South East Fishery.

Otolith samples and selection for ageing

Blue-eye Trevalla otolith samples were sourced from three collections: CSIRO (n=435), NSW Fisheries (n=57), and Fish Ageing Service (FAS) (n=1084) for a total of 1,576 otolith samples. See Table 5 for details and Figure 12 for geographic visualisation of the collection areas.

The CSIRO otoliths were collected during an Australian Fisheries Management Authority (AFMA) funded study investigating the capture of Harrisson's Dogfish (*Centrophorus harrissoni*) by fishing vessels targeting Blue-eye Trevalla on the Tasmantid Seamount chain (Williams *et al.* 2013). The otolith samples supplied by CSIRO were representative of the length frequency of the Blue-eye Trevalla catch in this study and were supplied as a pair of otoliths from each fish in envelopes. All but 3 of these samples were processed for ageing.

NSW Fisheries otoliths were collected from fish caught in the NSW slope fishery. These samples were supplied as prepared transverse sections mounted on glass slides. All of these samples were processed.

The FAS otolith samples were collected by the Integrated Scientific Monitoring Project (ISMP). ISMP samples generally contained a pair of dried otoliths from each fish in envelopes, but occasionally some sample envelopes only contained a single otolith.

Where insufficient otolith samples were obtained from specific areas of capture in the slope fishery, samples from adjacent capture areas were aggregated. To ensure the selected samples retained the length frequency distribution of the original dataset the original collection was randomly sub-sampled without replacement and a sum of squares was calculated between the new distribution and the original distribution by length class (see Results Figure 16). Sampling was halted when the distribution of the sub-sample qualitatively approximated the original distribution. After a satisfactory sub-sample was obtained, the selected fish were assigned a new batch. The length frequency was initially limited to 45–75 cm FL to provide comparable age-classes for the microchemistry component of the study. Initial sub-samples were either 50 or 100 per area; these were augmented later with additional samples from smaller and larger fish from corresponding areas after initial analysis to improve growth parameterisation; these results are presented separately.

Biological data associated with each sample.

The biological data (length, sex, capture location) for each sample had been recorded on the uniquely marked envelopes containing the otoliths and/or cross referenced to an accompanying data sheet. Biological data for each sample was entered into MS Excel and then transferred to an MS Access database.

Table 5 Details of otolith samples aged in this project including the mean start position for fishing operations from each area.

Source	*Habitat*	*Area*	*N*	*Mean Long. Start*	*Mean Lat. Start*
CSIRO	Seamount	Barcoo	197	156.275	-32.592
CSIRO	Seamount	Britannia	79	155.623	-28.325
CSIRO	Seamount	Derwent Hunter	52	156.254	-30.798
CSIRO	Seamount	Fraser	36	155.284	-24.439
CSIRO	Seamount	Queensland	2	155.182	-27.597
CSIRO	Seamount	Taupo	66	156.179	-33.184
FAS	Seamount	Gascoyne	238	156.203	-36.724
FAS	Seamount	LH3	50	162.451	-33.686
FAS	Seamount	LH4	50	162.691	-34.198
FAS	Seamount	unknown Qld SM	50	156.334	-29.791
FAS	Slope	Bass Canyon/East Flinders Is	254	148.761	-39.290
FAS	Slope	West BS/W Tas	291	144.346	-41.699
FAS	Slope	West KI/GAB	151	135.123	-35.704
NSWF	Slope	N_NSW	44	153.592	-29.375
NSWF	Slope	S_NSW	13	150.911	-35.418
Total			**1573**		

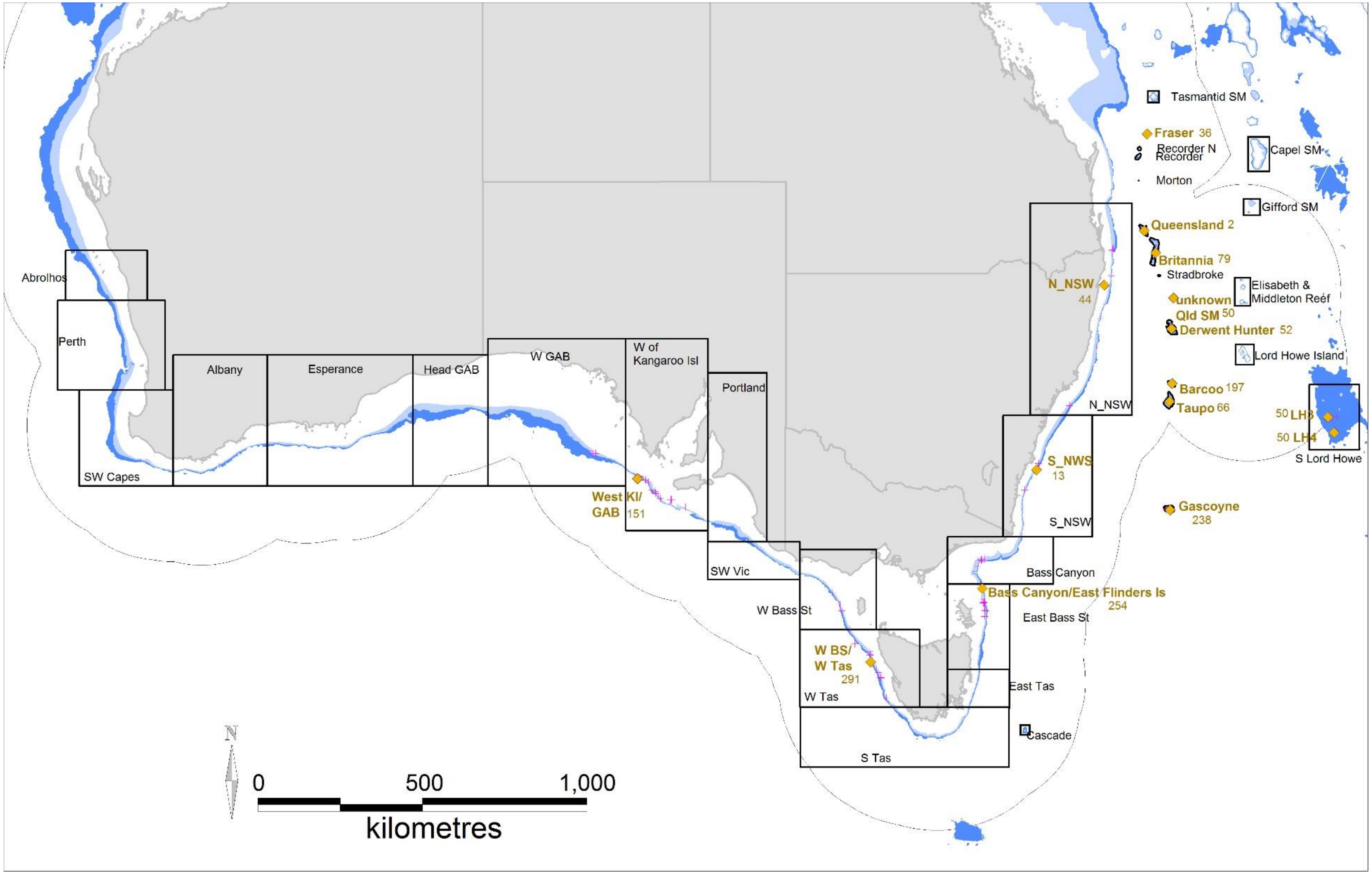

Figure 12 Sampling locations of Blue-eye Trevally aged in this project shown in orange with corresponding sample sizes.

Otolith preparation

All otoliths were prepared using the following protocol. One otolith from each pair was sectioned using a three stage process: embedding, sectioning, and mounting.

To embed the otoliths, a thin layer of clear polyester casting resin was poured on to the base of a silicon mould and left to partially cure. Otoliths were arranged in two rows of four (eight otoliths per block). Resin blocks were labelled and coated with another layer of resin. Blocks were then oven cured at 55°C for three hours.

Otolith sections were cut using a Gemmasta™ lapidary saw fitted with a diamond impregnated blade. From each column of otoliths, four sections were taken (approximately 300μm in thickness) to ensure the primordium of each otolith was included. Sections were cleaned and stored in vials until mounted on a slide. For identification, each vial contained a sample identification label.

A small amount of resin was poured on to a glass slide (50x75 mm). Otolith sections were pressed into the resin and the identification label placed at the top of the slide. Once the resin had semi-cured, further resin was applied to the preparations and two coverslips (22x60mm, No.1) were placed side by side on top of the resin. Slides were oven cured at 55°C for three hours.

Reading protocol

Sections were viewed with transmitted light at a magnification appropriate for Blue-eye Trevalla. Ages were estimated by counting the number of complete zones (translucent – opaque sequence) that have been validated as annual zones using radiocarbon ageing (Horn *et al.* 2010) and are further validated by our own otolith microstructure investigation presented in this report. Samples were aged along a transect from the primordium to the edge on the dorsal side of the sulcus (Figure 13).

Other information recorded in the database file was a readability score. This is a subjective measure of the sample's readability.

- A sample with a readability score of 1 is excellent.
- A readability score of 2 indicates a fairly unambiguous section.
- A readability score of 3 indicates that the sample age estimate may be ±2 years .
- A readability score of 4 indicates that the sample is subject to multiple interpretations.
- A readability score of 5 indicates that the sample could not be aged or the sample was missing from the envelopes.

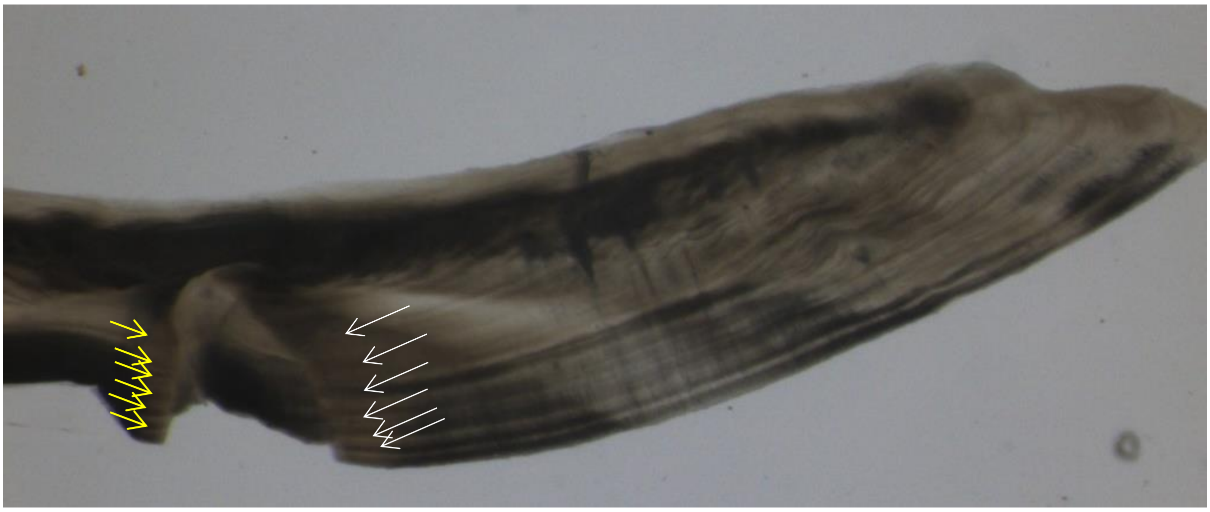

Figure 13 A representative Blue-eye Trevalla otolith transverse section showing zones counted as annual increments. Sample is from a 69 cm FL female collected from the Fraser Seamount. Estimated age=6. White arrows indicate positions of increments on the ventral side of the sulcus while the yellow lines show the counted zones on the dorsal side of the sulcus. Zone forming on the edge of the sample is not counted.

Comparison of age estimates

Following Central Ageing Facility (CAF) protocols (Morison *et al.* 1998), a minimum of 25% of samples were re-read. To avoid potential bias, all counts were made without knowledge of fish size, otolith weight, or previous count. Repeated readings of the same otoliths does not validate the assigned ages, but provides an indication of the size of the error to be expected within a set of age estimates due to intra-reader variation in otolith interpretation. Beamish and Fournier (1981) developed an index of average percent error (IAPE), which has become a common method for quantifying this variation. The IAPE is calculated as:

$$IAPE = \tfrac{100}{N}\sum_{j=1}^{N}\left[\tfrac{1}{R}\sum_{i=1}^{R}\frac{|X_{ij}-X_j|}{X_j}\right]$$

Where N is the number of fish aged, R is the number of times fish are aged, X_{ij} is the ith determination for the jth fish, and X_j is the average estimated age of the jth fish. The index has the property that differences in age estimates for younger fish will contribute more to the final value than will the same absolute error for older fish (Anderson *et al.* 1992).

To establish confidence intervals to these estimates of precision, a bootstrap technique was employed on the individual error estimates following methods described by Efron and Tibshirani (1993). Five thousand samples of error estimates (each the same size as the original) were randomly taken with replacement from the repeat readings, and a new IAPE calculated for each. The mean of these replicate IAPE's is the mean bootstrap IAPE and the standard deviation is the standard error of the mean. The bootstrap procedure exaggerates any bias present in the original estimate, so it is necessary to correct for this by adding the difference between the original statistic and the bootstrap mean, to the original estimate. The bias-corrected bootstrapped IAPE is thus calculated as:

Bias-corrected IAPE = Original IAPE + (Original IAPE – Mean Bootstrap IAPE)

The 95% confidence interval (CI) was calculated as:

95% CI = Bias-corrected IAPE ± (1.96 Standard deviation of Bootstrap IAPE)*

Examination of otolith microstructure

Five otoliths from small fish caught in the slope fishery were selected for 'daily' preparations from the FAS collection with the hope that the otolith microstructure (assumed daily growth zones) would provide information on the life history period targeted by the core microchemistry component and the inner isotope micro-milling. Additionally, if daily growth zones were clearly identifiable and continuous from the primordium to the first assumed opaque zone, the position and approximate age at first opaque zone formation could be verified.

To prepare the otolith in the transverse plane for daily age increment reading, otoliths were ground down in a 2-step process. During this process, the otolith preparation was continuously checked to ensure it reached the desired thickness of 50-80 µm.

Initially the otoliths were fixed on the edge (end) of a slide using thermoplastic mounting media (Crystal Bond 509) with the anterior side of the otolith hanging over the edge. Care was taken to ensure that the primordium was aligned with the edge of the slide (Figure 14). The otolith was ground down to the edge of the slide using 400, 800 and 1200 grit wet and dry paper.

Secondly the slide was reheated and the otolith removed and placed (ground side down) on another slide and fixed with Crystal Bond. The sample was then allowed to cool. Once cooled the otolith section was horizontally ground using increasingly finer grades (400, 800 and 1200 grit) of wet and dry sandpaper.

Daily otolith increment preparations were viewed at between 250 to 640 x magnification using a compound microscope illuminated with transmitted light. To conceal scratches and improve the clarity of the preparations, a small amount of immersion oil was used to cover the top surface of the preparation. Daily zones were counted from centre of the otolith section to the otolith edge on the dorsal side.

To estimate the daily resolution of subsequent otolith analyses, counts of daily zones were made for: (1) the area ablated to quantify the core microchemistry, (2) the area of inner/core otolith micro-milled for isotope analysis, (3) the area from the primordium to the first annual opaque zone, and (4) where possible the area from the first annual zone to the otolith edge (Figure 15). Several zones throughout areas 1 and 2 were also measured to provide an estimate of annual increment width.

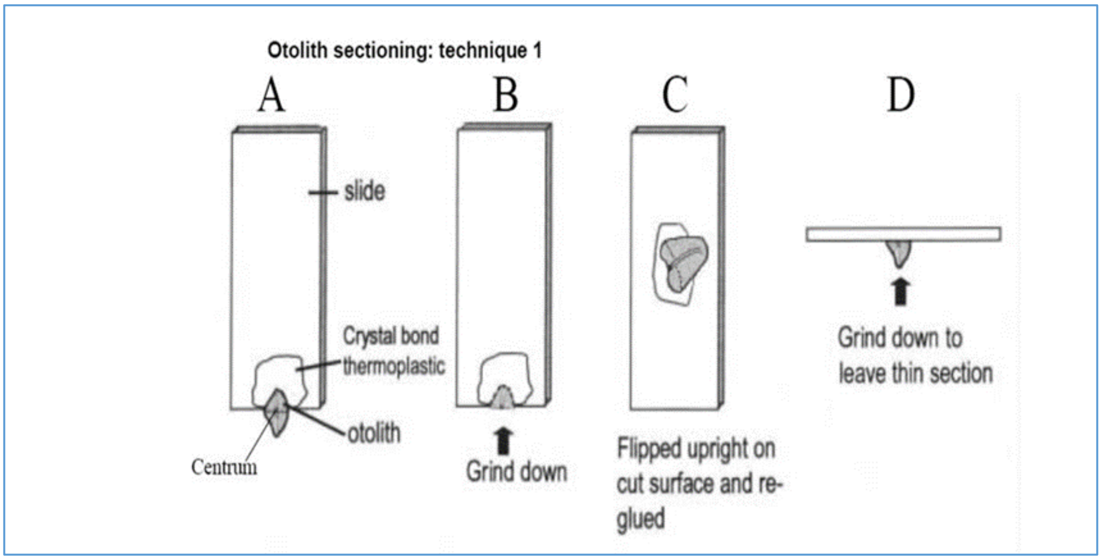

Figure 14 Illustration of the individual grinding process for preparation transverse otolith thin sections (Source: Robbins and Choat, 2002).

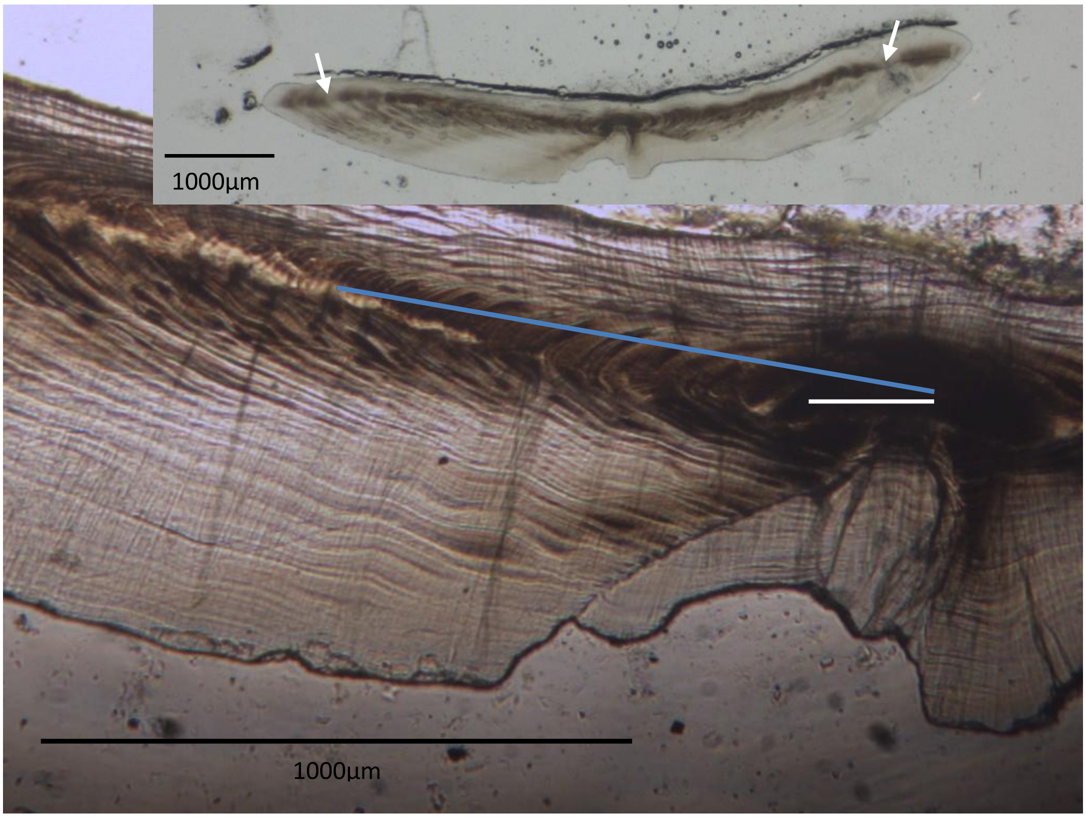

Figure 15 Image of a Blue-eye Trevalla section (sample 451_982_071) prepared for daily ageing. The blue line (1000µm) represents the area of the otolith micro-milled for the isotope analysis of the presumed juvenile period, and the white line (200µm) represents the approximate transect ablated to examine the core microchemistry. Arrows in the top image indicate the assumed first annual opaque zone used in the annual ageing protocol

Results

Length frequency of Blue-eye Trevalla catch from different areas

Length and age frequencies for the NSW slope samples were not plotted due to insufficient sample sizes (n = 57). The length frequency of the Blue–eye Trevalla catch from the slope fishery and the seamounts varies with catch location (Figure 16 & Figure 17). The length frequency of the subset aged was representative of the larger catch of fish that were between 45 and 75 cm FL long: these were taken from the following areas:

- Gascoyne Seamount
- Lord Howe 3 Seamount
- Lord Howe 4 Seamount
- Unknown Queensland Seamount
- West King Island / Great Australian Bight
- Western Bass Strait / West Tasmania
- Bass Canyon and East Finders Island (Figure 16).

The samples from the Tasmantid seamounts (Figure 17) were not restricted in length. The size of the fish ranged between 45 and 99 cm FL. These samples were representative of the catch from the Tasmantid seamount fishery.

The length modes of the catch from the CSIRO collected samples are consistently greater than that of the FAS and NSW Fisheries collected samples. Caution must be used interpreting the length frequency distributions of the collections as true representation of the site biomass as size classes may have been targeted for collection to ensure a wide distribution of the size/age data or the sample selection truncated with a specific size range.

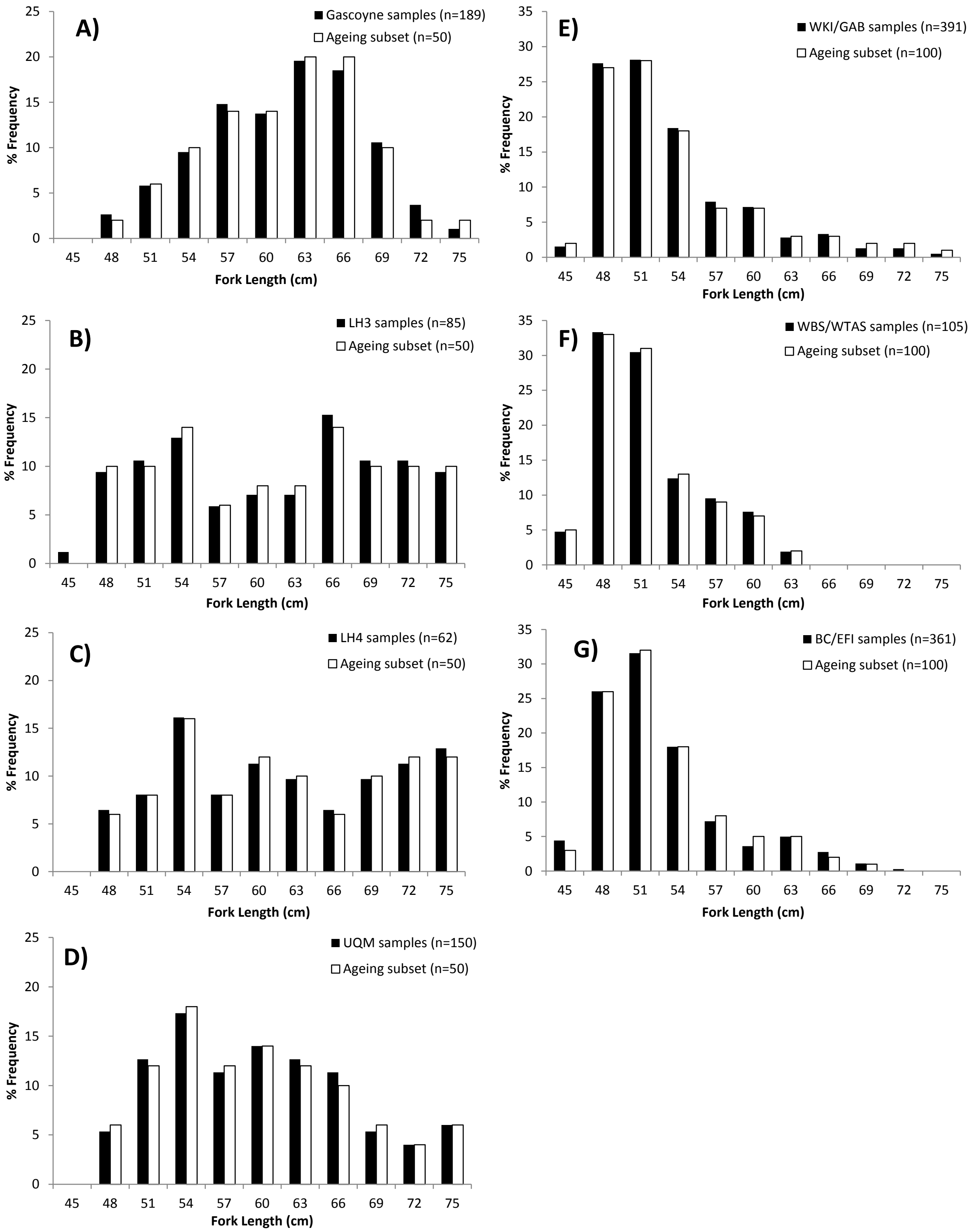

Figure 16 Length frequencies of the original Blue-eye Trevalla sample and the subset selected for ageing by area. Fork Length is truncated between 45 cm and 75 cm. A) Gascoyne Seamount, B) Lord Howe Seamount 3, C) Lord Howe Seamount 4, D) Unknown Queensland Seamount, E) West King Island / Great Australian Bight, F) West Bass Strait / West Tasmania and G) Bass Canyon and East Flinders Island. Solid bars indicate the parent length frequency and hollow bars indicate subset selected for ageing.

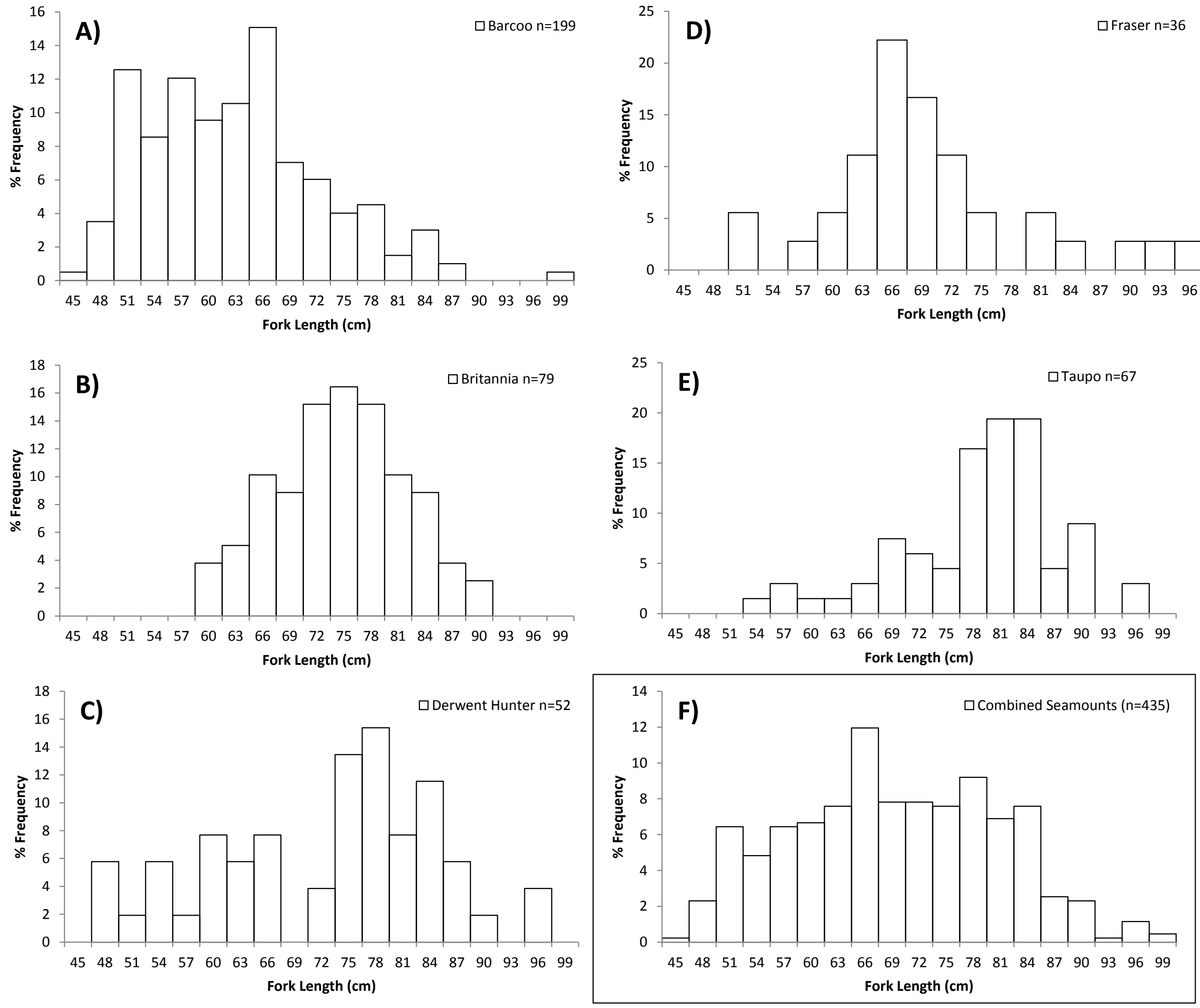

Figure 17 Length frequency of Blue-eye Trevalla from A) Barcoo, B) Britannia, C) Derwent Hunter, D) Fraser, E) Taupo and F) Combined samples (boxed). Note: no length frequency for Queensland Seamount is provided as only two samples were available from that location.

Age of Blue-eye Trevalla from different areas of capture

The age composition from the slope fishery was similar across all areas of capture. The age compositions from the non-Tasmantid seamounts were also similar to that of the slope fishery (Figure 18).

The age frequency from the Tasmantid seamounts shows higher frequencies of older fish compared with the non-Tasmantid seamounts and slope fishery. The age composition from the Barcoo Seamount appears to be similar to that of the slope fisheries (Figure 19).

An average percent error was calculated by re-ageing 25% of all of the samples. The bias-corrected IAPE with the frequency distribution of the boot strapped IAPE was only calculated for the combined Tasmantid data. IAPE calculated for other areas were within the confidence intervals of the combined Tasmantid dataset, which is shown in Figure 20.

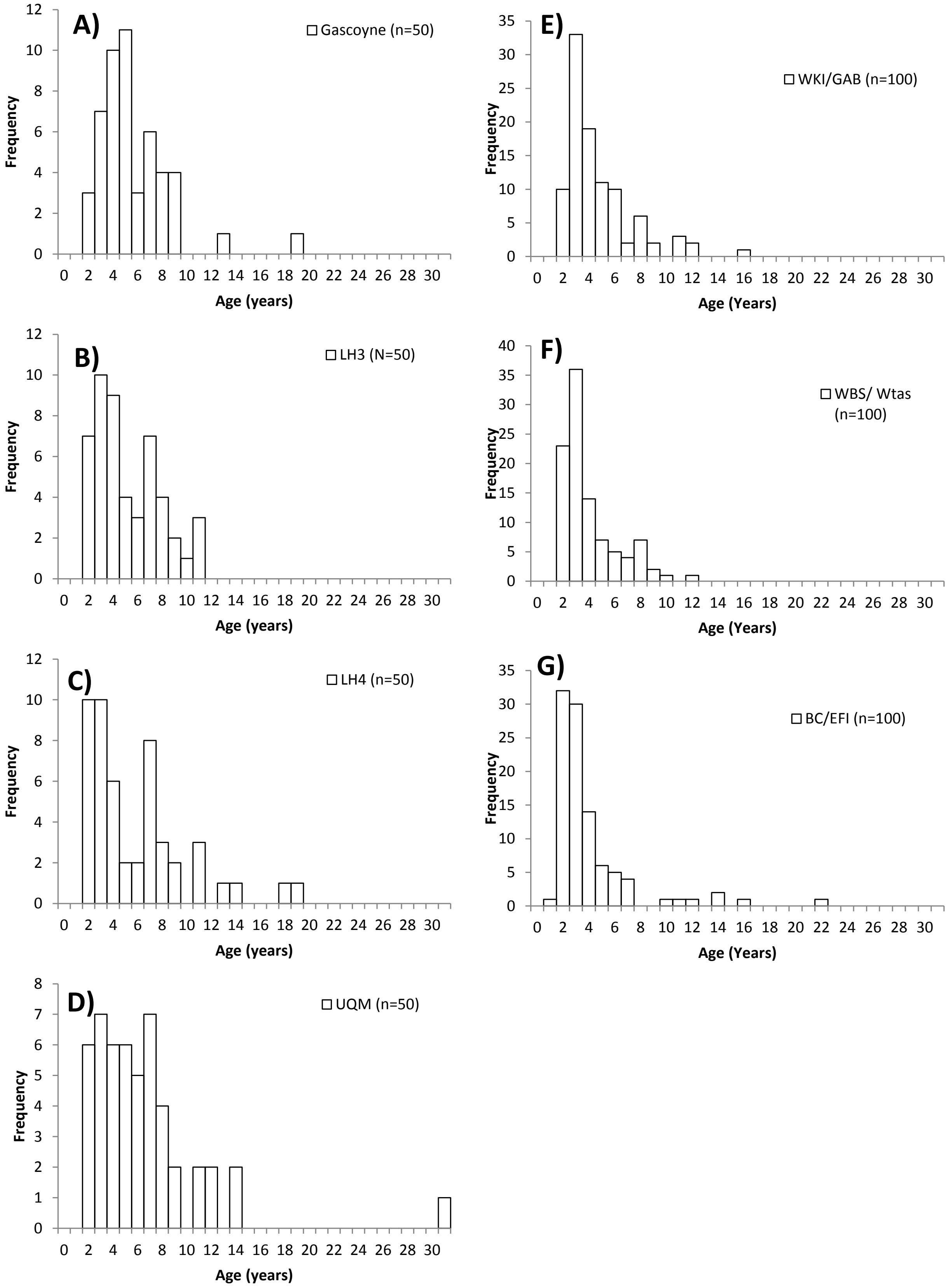

Figure 18 Age frequency for the subset of Blue-eye Trevalla chosen for ageing, where sample fork length is truncated between 45 cm and 75 cm. A) Gascoyne Seamount, B) Lord Howe Seamount 3, C) Lord Howe Seamount 4, D) Unknown Queensland Seamount, E) West King Island / Great Australian Bight, F) West Bass Strait / West Tasmania and G) Bass Canyon and East Flinders Island.

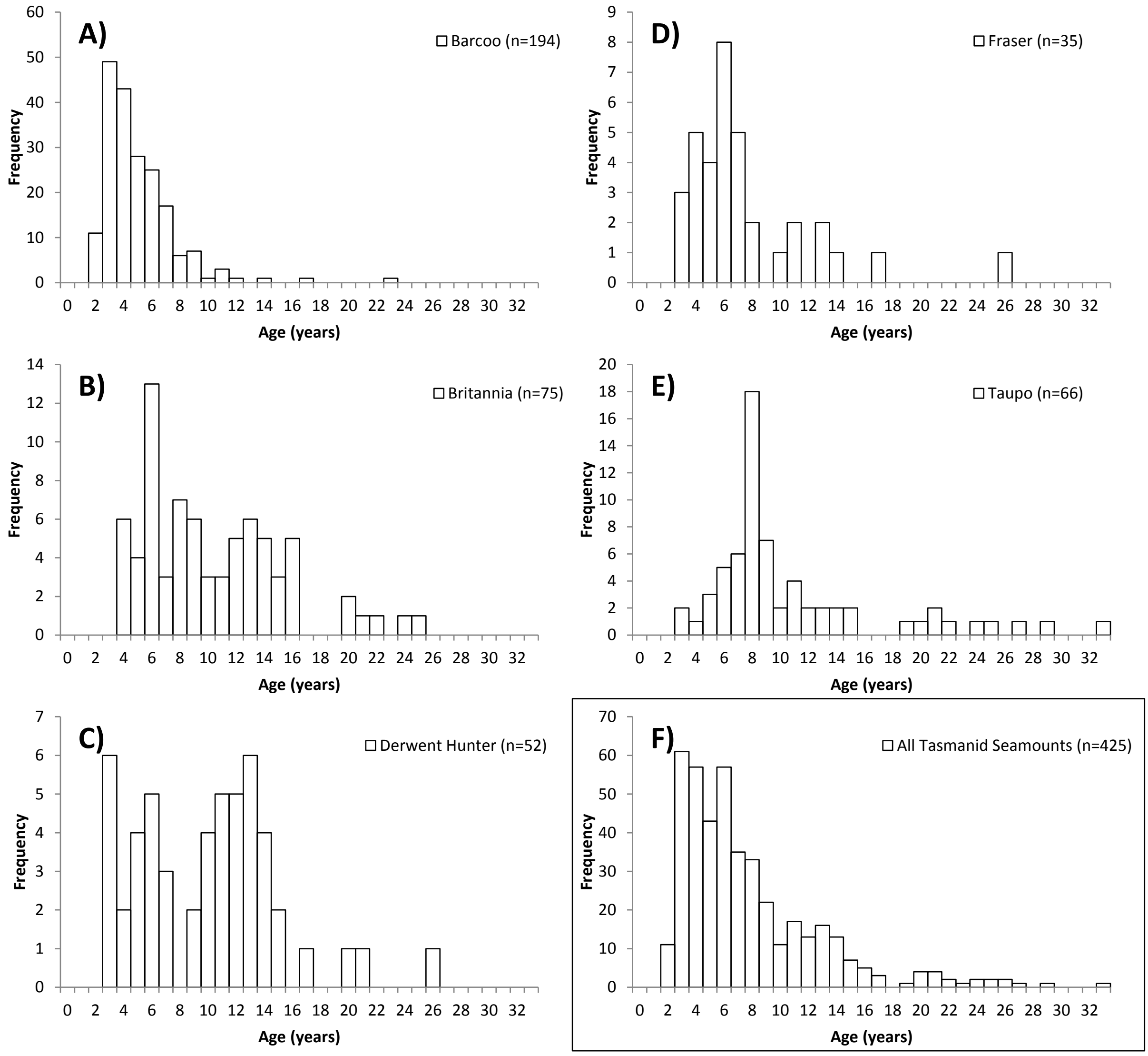

Figure 19 Age frequency for Blue-eye Trevalla from the Tasmantid Seamounts, A) Barcoo, B) Britannia, C) Derwent Hunter, D) Fraser, E) Taupo and F) is the combined age frequency for all Tasmantid Seamounts. Sample fork lengths ranged 45 to 99 cm.

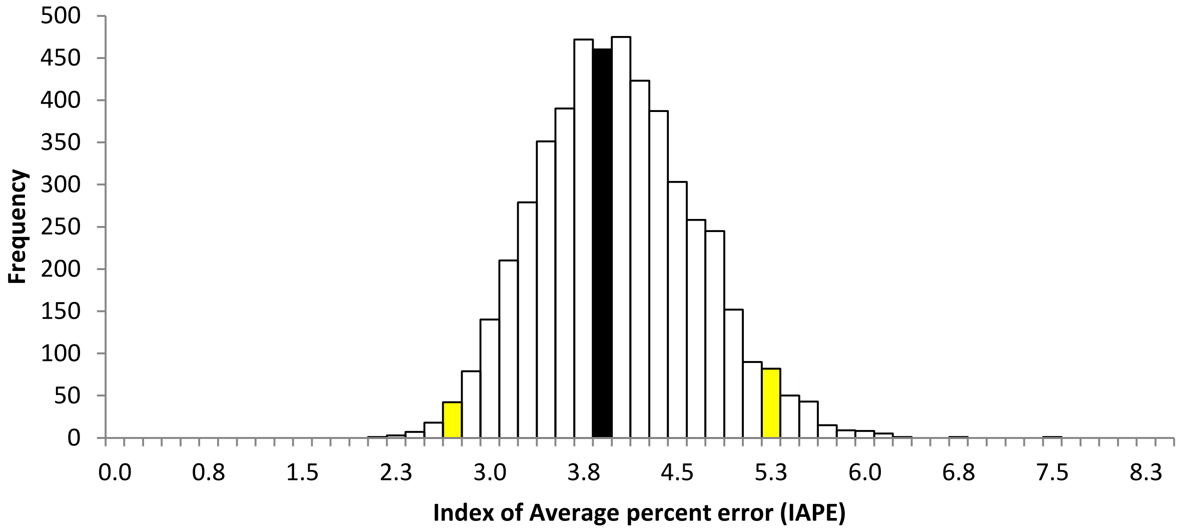

Figure 20 Bootstrapped index average percent error (IAPE) from Tasmantid Seamounts, where the original sample was 106 re-reads bootstrapped 5000 times. Black solid bar represents bias corrected IAPE while yellow solid bars indicate lower and upper 95% confidence intervals.

Otolith microstructure

Estimates of daily age were possible for two of the five samples prepared (sample 71 and 97). The readability of the thin sections and whether daily zones could be distinguished did change as they progressed towards the edge, and can be seen in three areas of the otolith section (Figure 21). The three areas are shown at higher magnification in Figure 22, Figure 23 and Figure 24. The zones within the core area (A) were the most difficult to interpret since the core was relatively diffuse and the opaque and translucent zone were closely spaced. This area consisted of between 30–40 increments (consisting of one opaque and subsequent translucent zone) which were approximately 5–6 µm apart. Post core area (B), the microstructure quickly transitioned to clear increments which were approximately 13–15 µm in width. The daily structure then transitioned to very fine increments (<2 µm) around the formation of the first annual opaque zone (C).

Generally, the microstructure of Blue-eye Trevalla otoliths was consistent with a pattern that suggested these structures were daily in nature. Using this interpretation, the inner areas of the otoliths examined were formed during a three to four month period, presumably in the juvenile phase (Figure 25). Specifically, the core area consisted of the first 30-40 daily increments and the area representing the isotope analysis was approximately 80-90 days. Total age was estimated at 457 and 404 days for the two samples. Unfortunately the zones on the marginal edge (area past the black arrow; Figure 25) of sample 97 were very difficult to interpret and the final count may be under-estimated. Estimated age at the first annual opaque zone was 340 days and 382 days for sample 71 and 97, respectively.

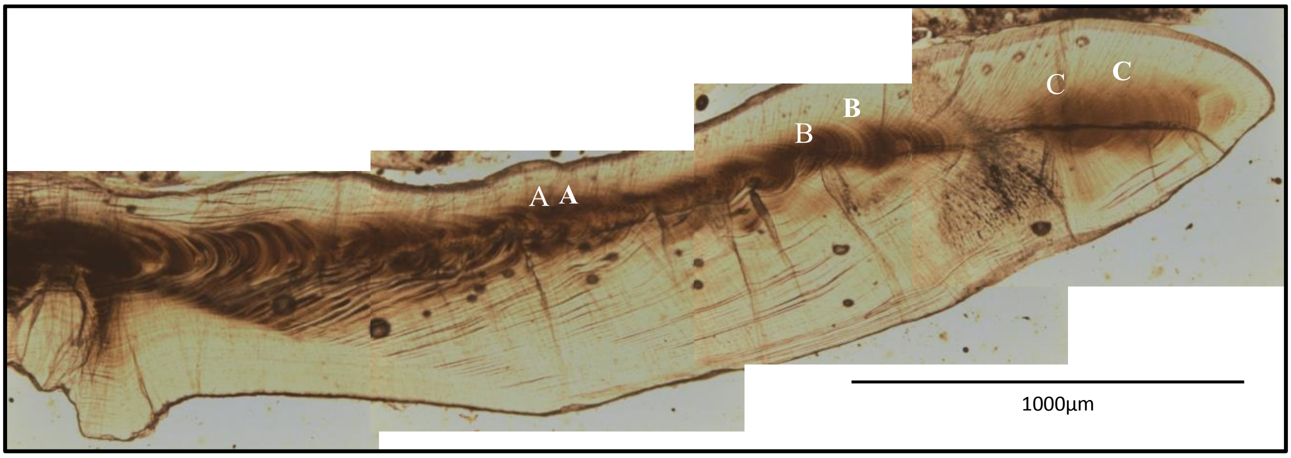

Figure 21 Dorsal side of the otolith shown in Figure 15 showing three areas of interest (A, B and C). These areas are photographed at higher magnifications in Figure 22, Figure 23 and Figure 24.

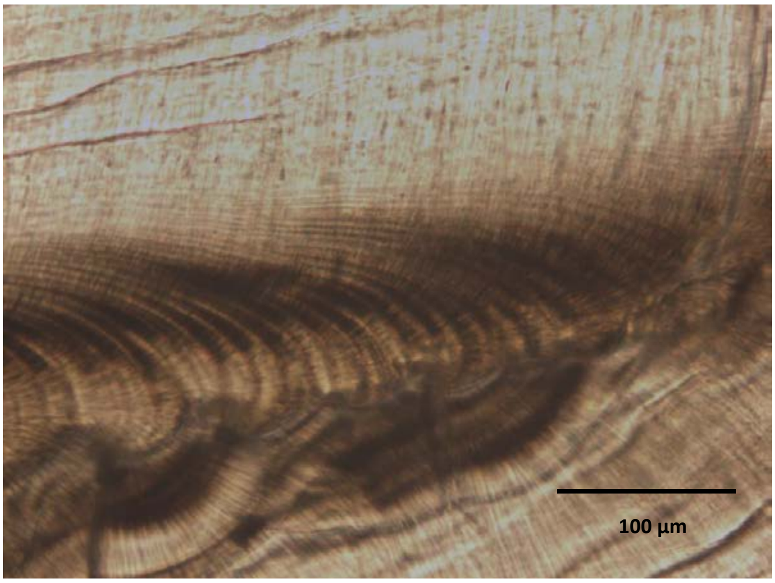

Figure 22 Higher magnification of section A showing clear daily zones.

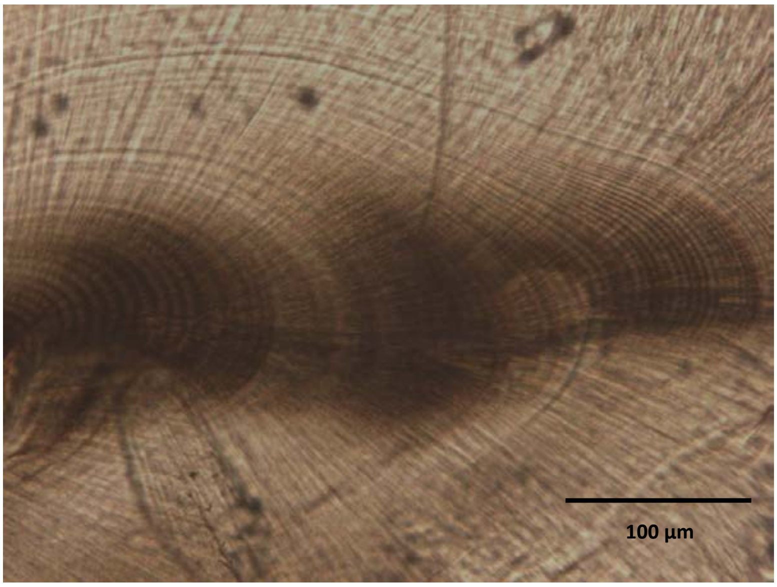

Figure 23 Higher magnification of section B showing clear daily zones.

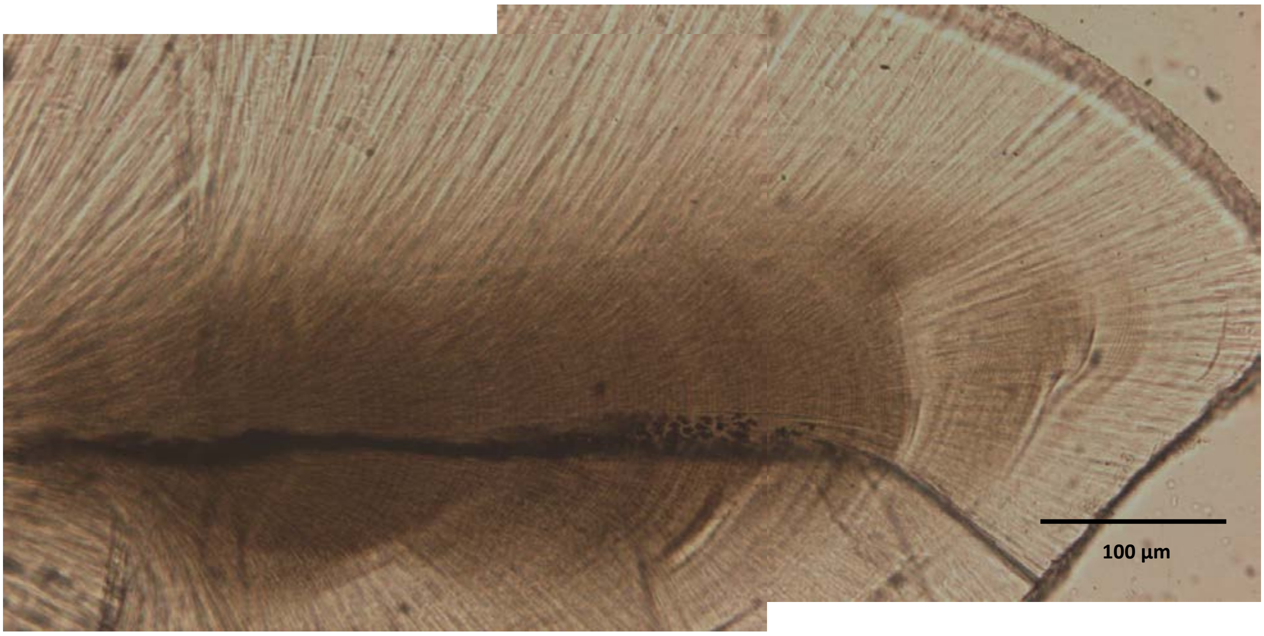

Figure 24 Higher magnification of section C showing clear daily zones. Daily zones in this region of the section tend to become less distinct, but are visible under the microscope.

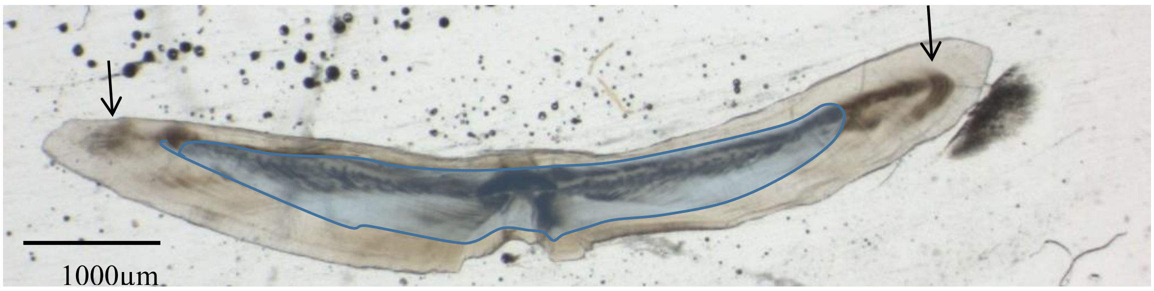

Figure 25 Age to the first annulus (indicated by the arrows) is approximately 320-340 days. The blue area encapsulates the first 4-5 months of age or approximately 120-140 days.

Augmented age and length frequencies from selected non-Tasmantid and slope fisheries (for growth parameters)

The length and age frequencies of the non-representative samples from selected non-Tasmantid and slope fisheries are shown Figure 26. These frequencies were generated to provide an indication of more realistic growth parameters. As they do not represent the catch from these areas (being augmented by smaller and large fish) they can provide no insight into the age or length composition of the catches of Blue-eye Trevalla from each of these areas.

Discussion

The position of the first and second zone was identified during the annual ageing. The distance from the primordium was measured for the microchemistry component of this study. The position of these marked zones was quantified using two samples. Although two samples were used to identify the first and second zones in the Blue eye Trevally otoliths, these data provided a preliminary point of reference for this study. Further daily ageing of otoliths from this species is indicated to understand the variance in the timing of zone formation. The number of samples used to construct age composition representative of the actual length-frequency in each of the areas of capture is relatively low. Given the low sample sizes, large variances in length and age composition were still evident with larger and older fish being present on the Tasmantid seamounts. To understand the underlying age composition of the fishery, it is necessary to age more samples and develop an age-length key which can be applied to length frequencies from the catch and adjust for gear selectivity. This component of understanding the age composition is beyond the scope of this study.

While the maximum age of this species is uncertain, the maximum validated age of Blue-eye has been validated (Horn *et al.* 2010) at 76 years and the periodicity of zone formation has been estimated (Robertson and Morison, 1998), neither method provides information on the interpretation of the otoliths. The ageing of Blue-eye from otolith thin sections is considered difficult due to the presence of multiple check marks, split zones and diffuse areas. This is particularly evident in the inner area of the otoliths that are assumed to represent the first two to three years of growth. Identification of the first, or innermost, growth increment is an important component of any age validation study. In studies which have validated increment periodicity rather than absolute age (as in chemical tagging studies), validation of the first increment is a mandatory adjunct to age determination; without a correctly defined starting point, age determinations will be consistently wrong by a constant amount (Campana, 2001).

These results present the first description of otolith microstructure for this species and indicate the potential for daily growth zones to provide valuable information on the early life history of this species. Even though only 2 samples were successfully prepared and aged, the microstructure of Blue-eye otoliths was consistent with a pattern that suggested that these structures were daily in nature (Pannella, 1971). Using this interpretation, the inner areas of the otoliths examined were formed during a three to four month period in the juvenile phase. Counts of daily zones to the first opaque zone were consistent across both samples examined, further suggesting that the first opaque zone forms at approximately one year of age. The preliminary examination of thin sections for daily increments undertaken during this study suggests the established interpretation of the first annulus (first annual opaque zone) is valid.

Structurally, the marked changes in daily zone optical clarity and width between areas of the otolith examined suggest transition points in their life history, this may be a change in growth, a shift in habitat or feeding, or possibly combinations of more than one factor. The two major transition points that we observed occurred at the end of the core area and at the end of the first annulus. The width of the daily zones in the post-core area out to the first annulus are reasonably wide compared to those reported in a range of species which have investigated otolith microstructure during the juvenile phase. This includes maximum increment widths of approximately 3.1 µm for Anchovy (*Engraulis japonicus*) (Namiki *et al.*, 2010), 4 µm for Chinook Salmon (*Oncorhynchus tshawytscha*) (Bradford, 1981), 3 µm for Walleye Pollock (*Theragra chalcogramma*) (Dougerty, 2008) and to the other extent up to 21 µm for bigeye tuna (*Thunnus obesus*) (Shaefer and Fuller, 2006) and 20 µm for Atlantic Bluefin Tuna (*Thunnus thynnus*) (La Mesa *et al.,* 2005). If the assumption that otolith growth and somatic growth is linked, this suggests that juvenile Blue-eye trevalla growth is rapid throughout this early life phase and that the relatively large length at age 1 (>40 cm) is not an unrealistic estimate.

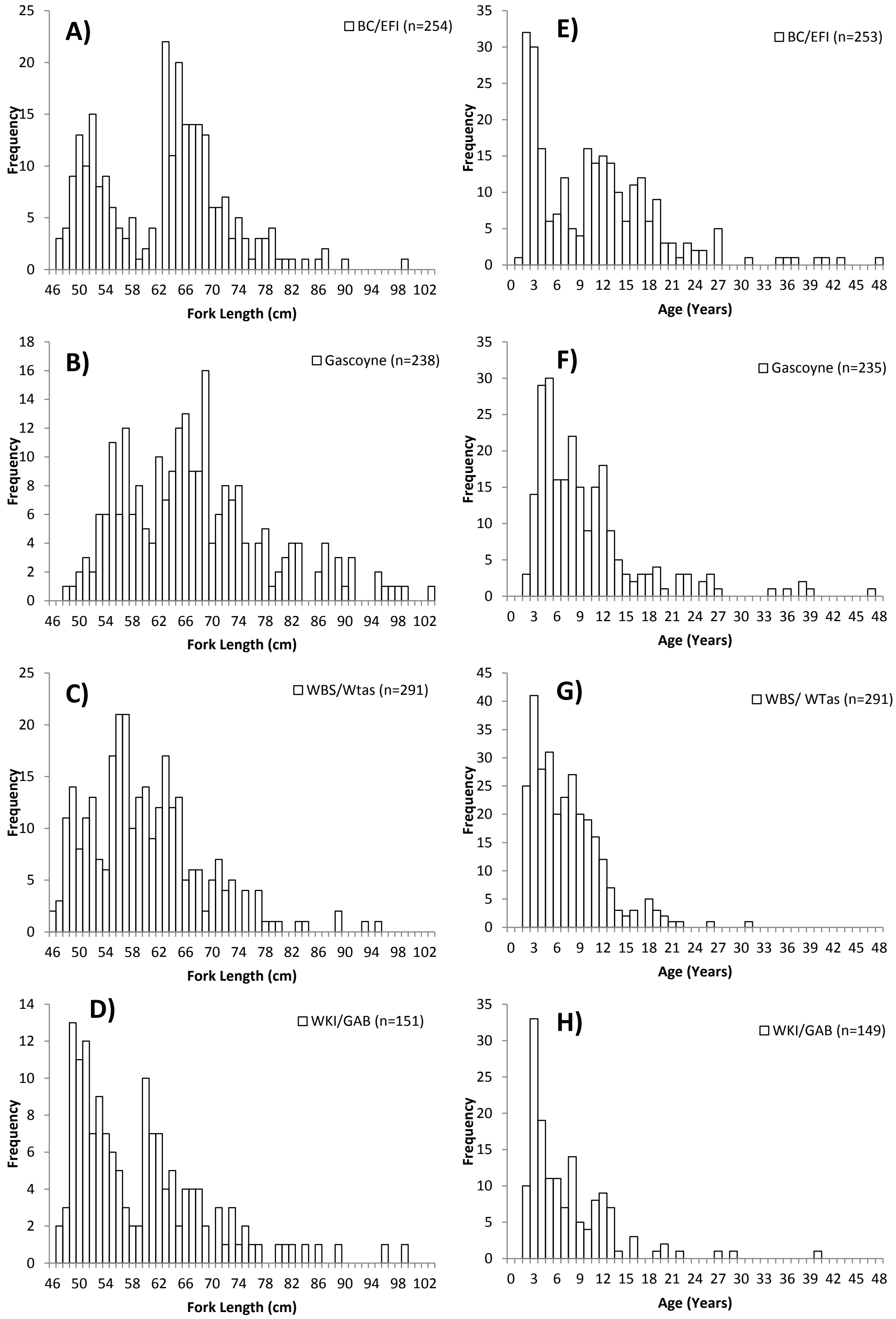

Figure 26. Length and age frequencies for areas where additional smaller and larger samples were added for growth parameterization. Length frequencies A) Bass Canyon / East Flinders Island, B) Gascoyne Seamount, C) West Bass Strait / West Tasmania and D) West King Island / Great Australian Bight. Age frequencies E) Bass Canyon / East Flinders Island, F) Gascoyne Seamount, G) West Bass Strait / West Tasmania and H) West King Island / Great Australian Bight. Lower numbers in age frequency compared to length frequency represent samples that could not be aged or were missing.

3. Spatial analysis of age and growth

Spatial variation in age and growth in Blue-eye Trevalla (*Hyperoglyphe antarctica*) supports the concept of separate populations on seamounts and the continental slope

Introduction

The Blue-eye Trevalla Fishery

Blue-eye Trevalla (*Hyperoglyphe antarctica*) is currently managed in Australia as a single stock ranging from WA to southern Queensland. Its stock assessment has several major uncertainties that arise primarily from the relatively complex spatial structure and are exhibited as spatial variation in CPUE, and in the sampled length and age composition of the commercial catch. This spatial heterogeneity, in turn, leads to uncertainty about stock structure (Fay *et al.* 2011). Recently, there have been changes introduced in the fishery brought about by the introduction of an array of marine closures as well as the development of depredation of Blue-eye catches by Orca on the auto-line fishery (such depredations had long been a feature of the drop-line fishery). Such events contribute to the variation observed in where fishing occurs, which then maintains or increases the variability in the monitoring data.

Blue-eye Trevalla is a relatively long-lived, late-maturing, high-value species in Australia's Southern and Eastern Scalefish and Shark fishery (SESSF) with an average annual total allowable catch of about 500t from 2003–2014, although with reductions and closures affecting catches in recent years. The fishery for this species has operated since the 1970s and occurs mainly on the continental slope with 96% of all records and associated catches taken between 200–650 m. Multiple gear types have been used through time with different methods focussing in different areas at different times. Most catches in early years were taken using drop-lining with a switch to auto-lining occurring across 2002–2004. Trawling has reported an average of about 55t per year from 1986–2014, and even gillnets were responsible for about 50 t of catch each year from 1997–2003 (Haddon, 2015).

Variation in Growth Characteristics

Some recent reductions in quota availability combined with closures around some of the more highly productive areas (e.g. off Flinders Island) have contributed to recent changes in the distribution of effort and the introduction of some novel fishing methods (e.g. hydraulic hand-line on sea-mounts off northern New South Wales). The Tasmantid seamounts had only been fished lightly from 2004 (Haddon, 2015) but from 2009 onwards there has been an increase in activity. The increased fishing on the Tasmantid seamounts led to renewed reports of larger fish with possibly a rather different body shape. This corroborated expectations that there was spatial heterogeneity in the biological characteristics of Blue-eye around the extent of the fishery. Such heterogeneity naturally leads to questions concerning the validity of assuming a single stock for Australian Blue-eye, principally: was the assumed biological/phenotypic variation due to multiple stocks, or to one stock with relatively sedentary adults with variation arising through spatially structured fishing (Haddon, 2015) through time.

This question was of interest to both managers and industry, as if there were more than one stock some stakeholders mooted the possibility of setting different/extra quota for any new stocks identified. Among a range of methods to test the question of stock structure, some of which are included in other chapters of this report, one way of exploring this question is to examine the growth characteristics of different populations spread about the range of the fishery. If the populations from different regions are sufficiently separated that they can exhibit different growth characteristics, which would constitute evidence of a degree of separation between those regions. This current work aims to estimate and compare the growth trajectories, in terms of average length-at-age, for populations of Blue-eye sampled from an array of geographically separate regions. Given the acknowledged spatial heterogeneity in samples taken from the fishery, making such estimates needs to be preceded by an effort to ensure that the data available are representative. If not, all ages and sizes can be sampled equally among regions, then at least the available data needs to be selected so as to compare like with like in terms of the range of ages compared.

This part of the project had four sub-objectives:

1. Determine what would be required, in terms of selecting age groups and associated length groups, to make valid comparisons of the growth characteristics of Blue-eye Trevalla between regions.
2. Given the outcome of objective 1, determine the growth characteristics of multiple Blue-eye Trevalla populations from around the coast using the von Bertalanffy (VB) growth model.
3. Determine whether there are any trends in growth patterns through the species' geographical distribution by formally comparing the growth characteristics of the various populations studied.
4. Discuss the implications for the current assumptions concerning stock structure of the growth characteristics discovered.

Methods

Ageing Data Characterization

Blue-eye Trevalla (*Hyperoglyphe antarctica*) is renowned for being spatially heterogeneous in its biological characteristics (mean size, body shape, age-structure of population, etc.) and its fishery characteristics (CPUE, length- and age-composition of catch, etc; Haddon, 2015). This heterogeneity has thwarted two previous attempts at producing a fully integrated stock assessment (Fay *et al.*, 2011). Whether this heterogeneity is reflected in how they grow in different places was investigated by comparing fish caught in widely different locations (Table 6, Table 7; Figure 27).

Otolith samples were obtained for both this and other purposes from Blue-eye taken at different locations around the coast, and these were classified into 15 regions or locations suitable for growth characterization. Some sites (namely Queensland and S_NSW) have only very small samples and so growth curves could not be fitted, although the consistency of the available length-at-age observations with other sites was considered. The complementary studies of otolith chemistry, documented elsewhere in this report, were intended to focus on particular cohorts so the complete range of sizes and ages were not always sampled at each site. The expectation therefore was that some censoring of ageing data would be necessary and growth comparisons made over only those regions of the growth trajectories in different areas that were well sampled and hence validly comparable.

Ageing of Blue-eye Trevalla otoliths used in this study followed methods developed by Fish Ageing Services which were modified from Morison *et al.* (1998). Descriptions of the method of ageing and the length and age frequencies for each region can be found elsewhere in this report (Chapter 1 and 2). Otolith samples were initially chosen to represent the catch length frequency. In an effort to obtain more biologically reasonable estimates of growth, otoliths from smaller and larger fish were added to regions where available. Extra samples were added to BassCanyon/EastFlinders, WBS/WTas, WestKI/GAB and Gascoyne. Although additional samples were available for other regions, smaller or larger fish were absent.

Table 6. Explanatory names for each site label (Figure 27).

Site	Description
Fraser	Fraser seamount
Queensland	Queensland seamount
Britannia	Britannia seamount
unknownQldSM	unknown Queensland seamount
DerwentHunter	Derwent and Hunter seamounts
Barcoo	Barcoo seamount
Taupo	Taupo seamount
N_NSW	Northern New South Wales coast
LH3	Lord Howe Rise 3
LH4	Lord Howe Rise 4
Gascoyne	Gascoyne sea mount
S_NWS	Southern New South Wales coast
BassCEastFI	Bass Canyon/East Flinders Island
WBS/WTas	Western Bass Strait and Western Tasmania
WestKI/GAB	Western King Island and Great Australian Bight
AllData	All data considered together

Table 7. The sample sizes and location ranges of the 15 different regions sampled. A total of 1516 records are available but 16 had no associated ages so 1500 records were usable. N and S relate to north and south, respectively. Useable denotes those records with ages and lengths. The ranges of the lengths and ages are also given.

			Length (cm FL)		Age		Longitude		Latitude	
Region	Records	Usable	First	Last	First	Last	West	East	LatS	LatN
Barcoo	197	192	47	99	2	23	156.275	156.275	-32.592	-32.592
BassCanyon/EastFlinders	254	253	47	99	1	48	148.367	148.900	-40.200	-38.333
Britannia	79	75	60	90	4	25	155.623	155.623	-28.325	-28.325
DerwentHunter	52	52	50	96	3	26	156.254	156.254	-30.798	-30.798
Fraser	36	35	53	99	3	26	155.284	155.284	-24.439	-24.439
Gascoyne	238	235	48	103	2	47	156.030	156.299	-36.741	-36.667
LH3	50	50	48	77	2	11	162.395	162.777	-33.703	-33.665
LH4	50	50	48	77	2	19	162.628	162.721	-34.237	-34.123
Queensland	2	2	69	71	6	7	155.182	155.182	-27.597	-27.597
N_NSW	45	45	47	94	2	29	152.219	153.942	-33.316	-28.171
S_NSW	12	12	47	84	2	37	150.315	151.241	-37.486	-34.658
Taupo	66	66	56	98	3	33	156.179	156.179	-33.184	-33.184
unknownQldSM	50	50	48	75	2	31	156.326	156.337	-29.792	-29.789
WBS/WTas	291	291	46	95	2	31	142.833	144.967	-42.867	-39.433
WestKI/GAB	151	149	47	99	2	40	132.900	137.017	-36.633	-34.483

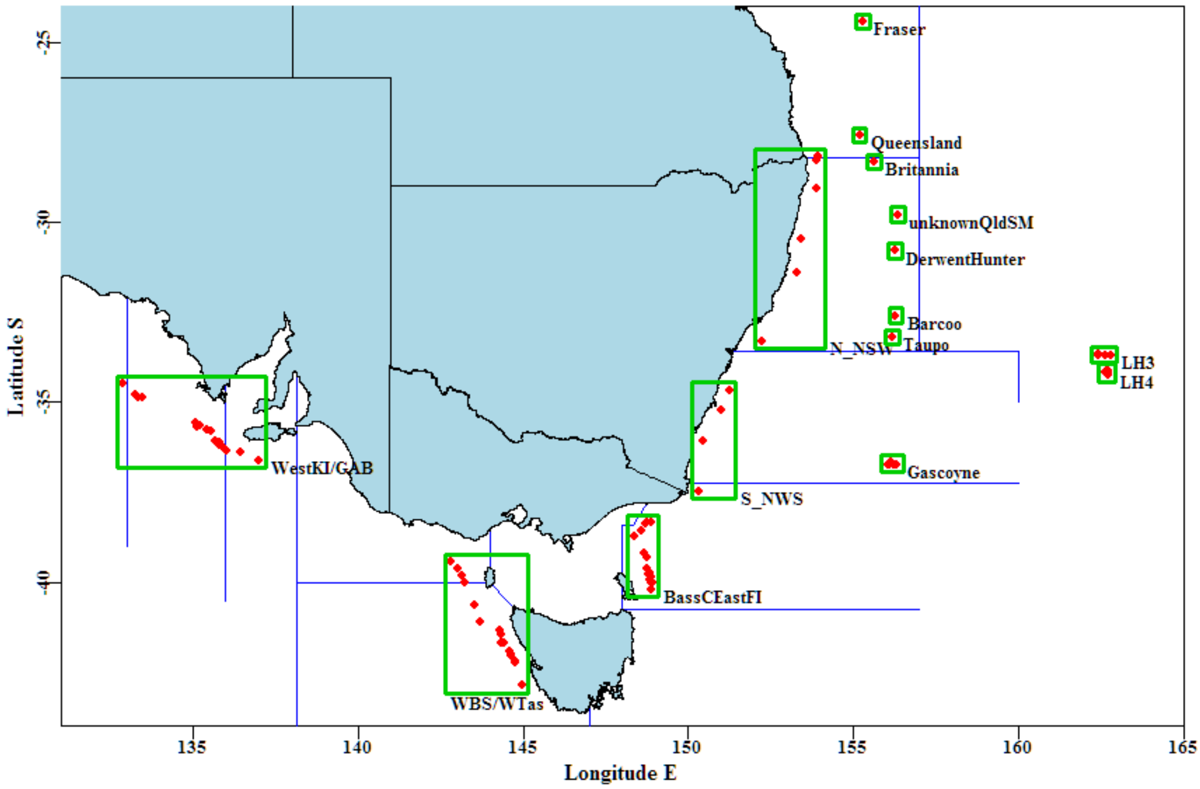

Figure 27. Schematic map of the locations of current samples, based on the latitudes and longitudes in the data set (Table 7). The red dots are the average locations of samples; green boxes are rectangles bracketing each set of data for a region; blue lines show statistical reporting areas. For site name descriptions see Table 8.

Modelling Length-at-Age

In all cases the von Bertalanffy growth (VB) curve (von Bertalanffy 1938) is used to describe the growth of the different Blue-eye Trevalla populations (equation 1).

$$\begin{aligned} L_{t,i} &= L_\infty\left(1 - e^{-K[t-t_0]}\right) + \varepsilon_i \\ \hat{L}_t &= L_\infty\left(1 - e^{-K[t-t_0]}\right) \end{aligned} \qquad (1)$$

where $\hat{L}_t$ is the predicted length at age t given the parameters L_∞, which is the asymptotic average maximum body size, K, which is a growth rate coefficient that determines how quickly the maximum is attained, and t_0, which is the hypothetical age at which the species has zero length. $L_{t,i}$ is the observed length of observation i for age t, and ε_i reflects the assumption that the residual errors about the growth curve would be normally distributed. Thus, ε_i is the residual value for the particular observation i from a normal distribution defined by N (mean=0, stddev=σ), where σ is the standard deviation of the residuals about the mean curve. The assumption of normality derives from the observed shape of the distribution of lengths from identifiable modes in length of young cohorts.

In all cases the growth models were fitted using maximum likelihood methods (Haddon, 2011), which both enabled an estimate to be made of the variance of the observations about the mean curve as well as, if required, enabling a relaxation of the assumption of that variance being constant (although this option is not presented here). The estimated negative log-likelihood (*–veLL*) is calculated:

$$SSQ = \sum_{i=1}^{n}\left(L_{t,i} - \hat{L}_t\right)^2 \qquad (2)$$

where SSQ is the sum of squared residuals from the n observed and predicted lengths for a given site. This can be used to estimate the expected variance (σ^2) or standard deviation (σ) of the spread of the residuals about the predicted growth curve:

$$\sigma = \sqrt{\frac{SSQ}{n}} \tag{3}$$

The negative log-likelihood for each growth curve could then be estimated as:

$$-veLL = -\frac{n}{2}\left(Ln\left(2\pi\right) + 2Ln\left(\sigma\right) + 1\right) \tag{4}$$

which is a simplification (Haddon, 2011) of the fully articulated calculation of the likelihood for each observation.

$$-veLL\left\{L_{t,i} \mid L_\infty, K, t_0, \sigma\right\} = nLn\left(\sigma\sqrt{2\pi}\right)^{-1} + \frac{1}{2\sigma^2}\sum_{i=1}^{n} -\left(L_{t,i} - \hat{L}_t\right)^2 \tag{5}$$

The total $-veLL$ is minimized to find the optimum model fit to the available data.

Growth Curve Comparisons

Various comparisons were made between the growth curves fitted to different subsets of the data using a likelihood ratio test. With growth curves the likelihood ratio test requires that the $-veLL$ obtained from fitting the two curves separately are combined and compared with the $-veLL$ obtained by pooling the data from the two sexes or sites and fitting a single growth curve. The basis of this test is that the two separate curves use six parameters while the single combined curve uses only three parameters. If the expected improvement obtained, in terms of increased likelihoods, through using six parameters is less than expected, as predicted using a χ^2 distribution, then the two curves are not significantly different (Haddon, 2011).

$$2 \times abs\left[LL\left(\theta\right)_{Max} - LL\left(\theta\right)\right] \le \chi^2_{3,1-\alpha} \tag{6}$$

where $\chi^2_{3,1-\alpha}$ is the $(1 - \alpha)^{th}$ quantile of the χ^2 distribution with 3 degree of freedom (e.g., for 95% confidence intervals $\alpha = 0.95$ and $1-\alpha = 0.05$, $\chi^2_{3,1-\alpha} = 7.81$ or $\alpha = 0.99$ and $1-\alpha = 0.01$, $\chi^2_{3,1-\alpha} = 11.34$). Thus, for two curves to be significantly different then fitting two curves instead of one has to increase the log-likelihood by at least 7.81 and ideally by more than 11.34.

Randomization Tests

Unfortunately, in many sites the representativeness of the larger and older animals is poor, which has the effect of potentially leading to misleading growth curve fits. In such cases it is plausible to censor the available data to focus on the ages for which each sample being compared contains sufficient numbers to permit a valid comparison. In addition, there are two sites with very low numbers of observations and eight sites that only have 35–75 observations (with an average of 53; Table 7). Most of these smaller samples are too sparse to permit a plausible comparison, although the option of combining samples from similar habitats remains. The option of combining data sets was used with the Tasmantid seamounts to allow for comparisons with sites on the continental slope. Such data manipulations can have the effect of breaking the assumption that the χ^2 distribution can be used to test whether any differences found between growth characteristics are unlikely (and hence significantly different). To avoid the problem that the χ^2 distribution might no longer represent a proper test of the significance of the likelihood ratio tests a randomization test was developed which generated the probability distribution of expected differences between two equivalent curves empirically.

Randomization forms the underlying basis of many parametric statistical tests (Fisher, 1936; Good, 1994; Manly, 1991, 1997). To generate the sampling distribution of the likelihood ratio test one might expect from two growth curves samples that are equivalent, the data pairs (lengths-at-age) from the two samples are randomly assorted between the two samples, and the likelihood ratio test run on the randomized data. This is repeated 1000 times to produce an empirical distribution of the likelihood ratios expected when the two samples really are random samples from the same pool of data. Thus, when the likelihood ratio from the original, non-randomly assorted, data is compared with that empirical distribution, if it sits in the central part of the distribution this constitutes evidence that the two samples are no different from random samples from the same underlying population of length-at-age samples. However, if the original likelihood ratio lies outside or at the extremes of the empirical distribution this is evidence that the two samples compared are unlikely to be samples from the same underlying population of possible samples.

The use of these methods can be illustrated by taking two of the larger samples (Bass Strait Canyon and Flinders Island compared with the sample from Western Tasmania and Western Bass Strait). With such relatively large sample sizes (Figure 28) the χ^2 distribution should provide a valid probability distribution for determining the significance of any differences between the regions. A standard likelihood ratio test of these two sites generated a likelihood ratio of 3.0701 which, using a χ^2 distribution with three degrees of freedom, is not significant (P = 0.1506). This lack of a significant difference is confirmed by the randomization test, which was conducted using a routine written in R (Figure 29).

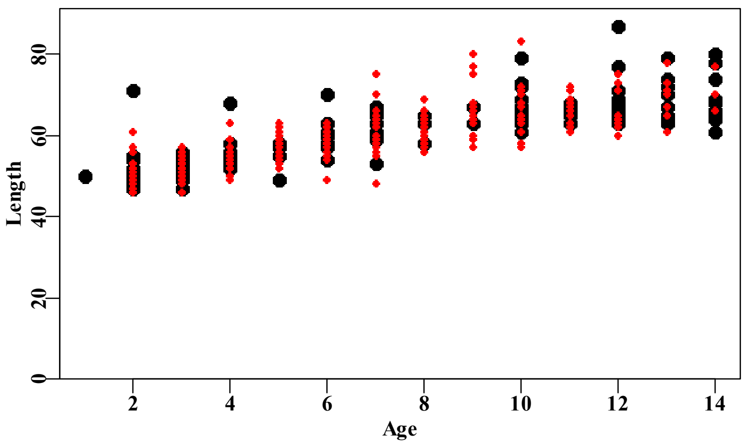

Figure 28. A combined plot illustrating the overlap of the data from ages 1–14 for Bass Strait Canyon and Flinders Island (182 large black dots) and Western Tasmania and Western Bass Strait (272 smaller red dots).

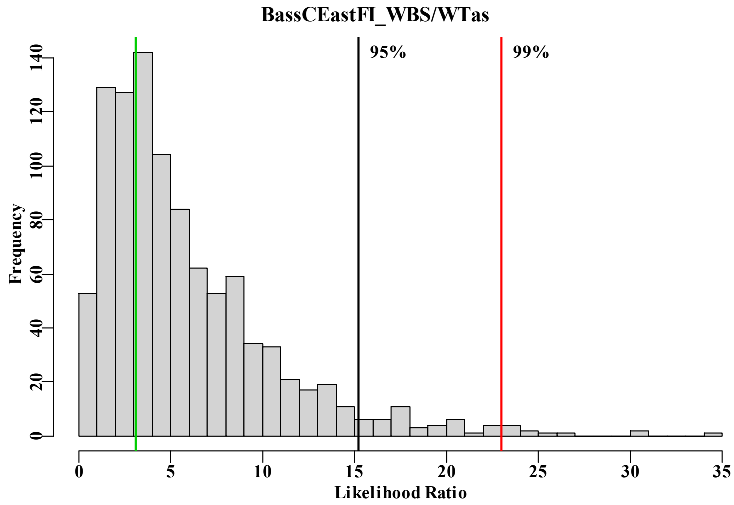

Figure 29. The empirical distribution of likelihood ratios obtained from randomizing the data from the two sites BassCEastFI vs WBS/WTas. The likelihood ratio values required for significant differences to be indicated are illustrated with the vertical black and red lines. The observed likelihood ratio is shown in green demonstrating that it is very typical of a random selection of the grouped data, meaning there is no significant difference in growth trajectory between the ages of 1–14 between the regions.

Before making comparisons between regions, however, differences were looked for between the sexes in those samples with sufficient numbers of males and females in the same region (Table 8). In these cases randomization tests were not used, but for some sites, the poorly represented ages greater than 14–15 needed to be censored so that the growth patterns over ages common to both sexes were compared.

Comparison of the Sexes

The samples from the fifteen locations had different numbers of each gender (Table 8). There were sufficient samples taken to compare the growth by sex at Barcoo, Western Bass Strait/Western Tasmania, Bass Canyon/Flinders Island, and Gascoyne; although older fish were poorly represented in the latter two and so data censorship was required with them.

Table 8. Counts of each gender in the available data. See Table 6 for expanded site names

Site	Male	Female	Juvenile	Unknown
Barcoo	87	105	0	0
BassCEastFI	109	138	1	5
Britannia	25	50	0	0
DerwentHunter	16	36	0	0
Fraser	10	25	0	0
Gascoyne	55	62	0	118
LH3	20	30	0	0
LH4	28	22	0	0
N_NSW	27	18	0	0
Queensland	1	1	0	0
S_NWS	6	5	0	1
Taupo	31	35	0	0
unknownQldSM	24	25	0	1
WBS/WTas	69	64	7	151
WestKI/GAB	23	15	69	42

Site Comparisons

Randomization tests using likelihood ratios were conducted to compare sites in series around the coasts (Table 9).

Table 9. The sites compared. Fraser, DerwentHunter, Taupo, and Britannia were combined. All three Tasmanian and GAB sites were compared (groups A), and then comparisons were performed sequentially around the coast, i.e. groups B with B, C with C, D with D.

Comparison Group	Region	Records	Usable	Length (cm FL) First	Length (cm FL) Last	Age First	Age Last
D	Fraser	36	35	53	99	3	26
D	DerwentHunter	52	52	50	96	3	26
D	Taupo	66	66	56	98	3	33
D	Britannia	79	75	60	90	4	25
D C	Barcoo	197	192	47	99	2	23
C B	Gascoyne	238	235	48	103	2	47
B A	BassCanyon/EastFlinders	254	253	47	99	1	48
A	WBS/WTas	291	291	46	95	2	31
A	WestKI/GAB	151	149	47	99	2	40

Results

Growth Differences by Sex

When the four sites with sufficient data are considered, no significant differences in growth between the sexes are seen within the data from Barcoo and Western Bass Strait/Western Tasmania (Figure 30; Table 10). However, highly significant differences in growth between sexes from all available samples taken from Bass Canyon/Eastern Flinders Island and from the Gascoyne (Figure 30; Table 10). The sampling of the older age classes in these areas, however, is not necessarily representative as it is relatively sparse and scattered. When only the length-at-age data for ages 2–13 or 2–14 are used then the significant differences disappear (Table 10). Visually this is very clear when comparing the predicted growth curves across the ages for which there is strong overlap across the two sexes (Figure 30).

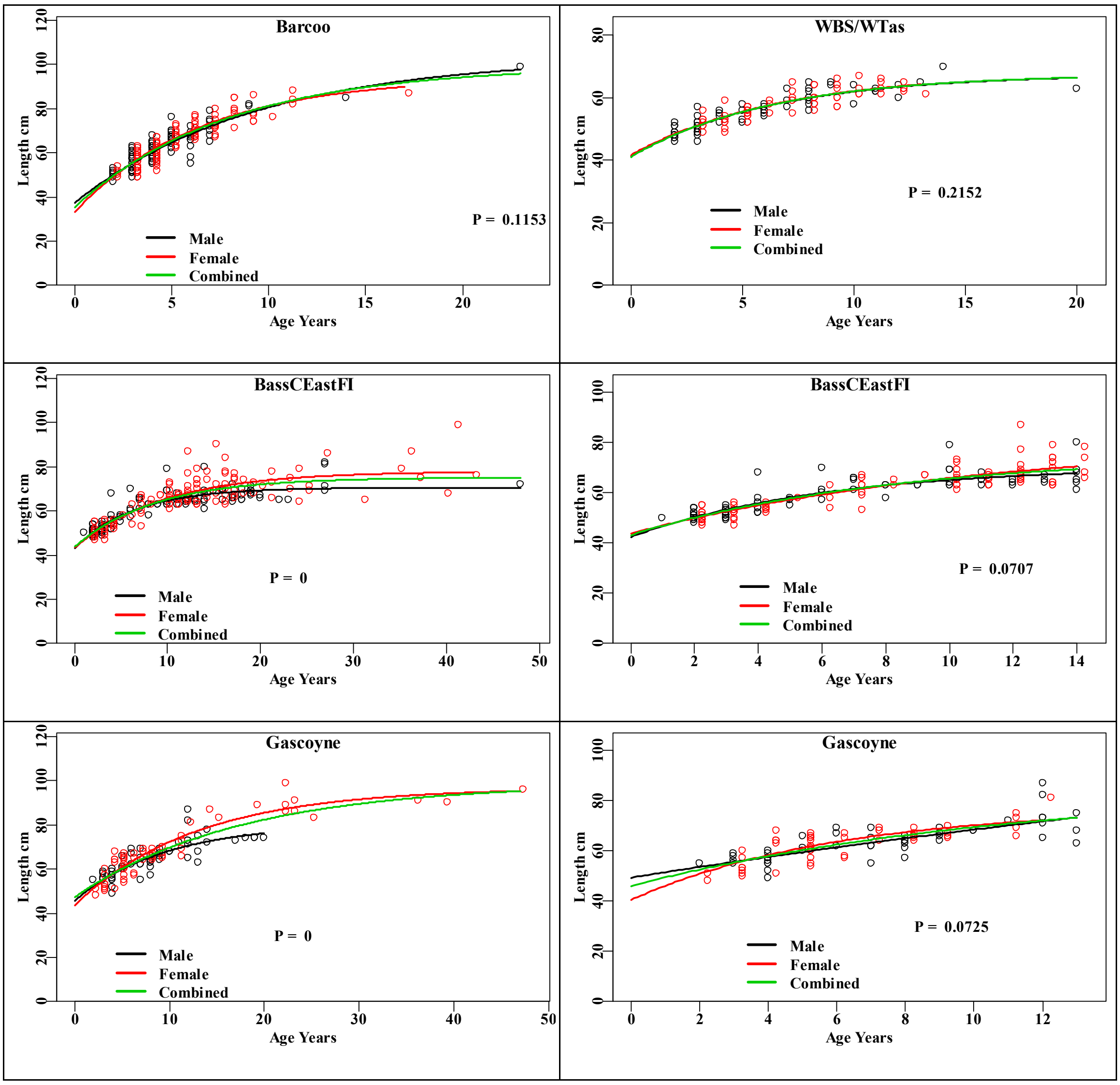

Figure 30. A comparison of the growth curves fitted to four sites with sufficient data to make a comparison between sexes. At Barcoo and WBS/WTas, no significant differences were found even when using all available age classes. At both the Gascoyne and Bass Strait Canyon/Eastern Flinders, sampling variation and sparsity in the older age classes led to statistically significant differences, which disappeared when the age classes were restricted to those less than 14–15 years. In each case the female data points have had 0.25 added to their ages in the plot to separate them from the males. A probability > 0.05 is not significant.

Table 10. A comparison of the growth curves for the two sexes at four sites: Barcoo, Western Bass Strait/Western Tasmania, Gascoyne, and Bass Canyon/Eastern Flinders. For the latter two the upper ages needed to be censored to enable comparisons where there were comparable data. Parameters are defined in the text at equation 1 and 2.

Site /Gender	L_∞	K	t_0	σ	-veLL	N_{obs}	L_{ratio}	$P(\chi^2)$
Barcoo								
Male	103.394	0.106	-4.218	4.131	246.857	87		
Female	94.333	0.154	-2.806	3.970	293.771	105		
Combined	99.278	0.126	-3.487	4.083	542.540	192	2.635	0.1734
WBS/WTas								
Male	67.606	0.155	-6.049	2.337	156.464	69		
Female	68.093	0.149	-6.359	2.512	149.745	64		
Combined	67.635	0.157	-5.989	2.423	306.440	133	0.462	0.2152
Gascoyne		Eventually limited to ages < 14						
Male	80.382	0.106	-7.934	4.477	160.488	55		
Female	96.727	0.078	-7.719	4.404	179.895	62		
Combined	98.767	0.057	-11.380	4.856	350.899	117	21.033	0.0000
Male	135.467	0.025	-18.097	4.623	141.553	48		
Female	77.015	0.167	-4.450	4.074	141.173	50		
Combined	85.719	0.089	-8.697	4.444	285.239	98	5.024	0.0725
BassCEastFI		Eventually limited to ages < 15						
Male	70.570	0.154	-6.126	3.715	297.704	109		
Female	78.394	0.098	-8.426	5.459	448.746	144		
Combined	75.475	0.110	-8.007	4.935	762.889	253	30.087	0.0000
Male	70.612	0.16	-5.672	3.65	217.12	80		
Female	81.327	0.09	-8.715	4	269.42	96		
Combined	75.272	0.12	-7.061	3.9	489.08	176	5.088	0.0707

These results, which did not even use randomization tests, indicate that there is at least evidence of no differences in the growth pattern between the sexes, at least up until the age of 15 years. In those cases where no difference was discovered, even when all ages were included in the analysis, the numbers of older fish are still so low that this result may have come about by chance; just as is being suggested for those sites where a significant difference was found between the sexes when the older age classes are included. In the following the sexes are not considered further; one advantage of this is that juveniles and unsexed fish can be included in the analyses, which can increase the number of observations significantly in some sites.

Growth Differences by Site

As with the comparison of sexes, care is needed when comparing growth curves between sites as not all sites have representative data across all ages. A growth curve was fitted to all available data combined for a visual comparison across all individual sites. A visual comparison of growth curve fits to the available data for each site indicates some major differences between sites especially when compared to the growth curve fitted to all data (Figure 31; Table 11). However, the common growth curve is not a simple average growth curve across sites as its parameter values will be biased towards those sites with the most data. Nevertheless, it provides a simple visual comparison showing some sites grow above the common trend and some below. At each site the different age classes and associated lengths have been sampled at different intensities (as is visible in the density of points on the plot of length-at-age for each site; Figure 31). In all cases fewer replicates are available in the older age classes at any site and the variation certainly increases with age and length.

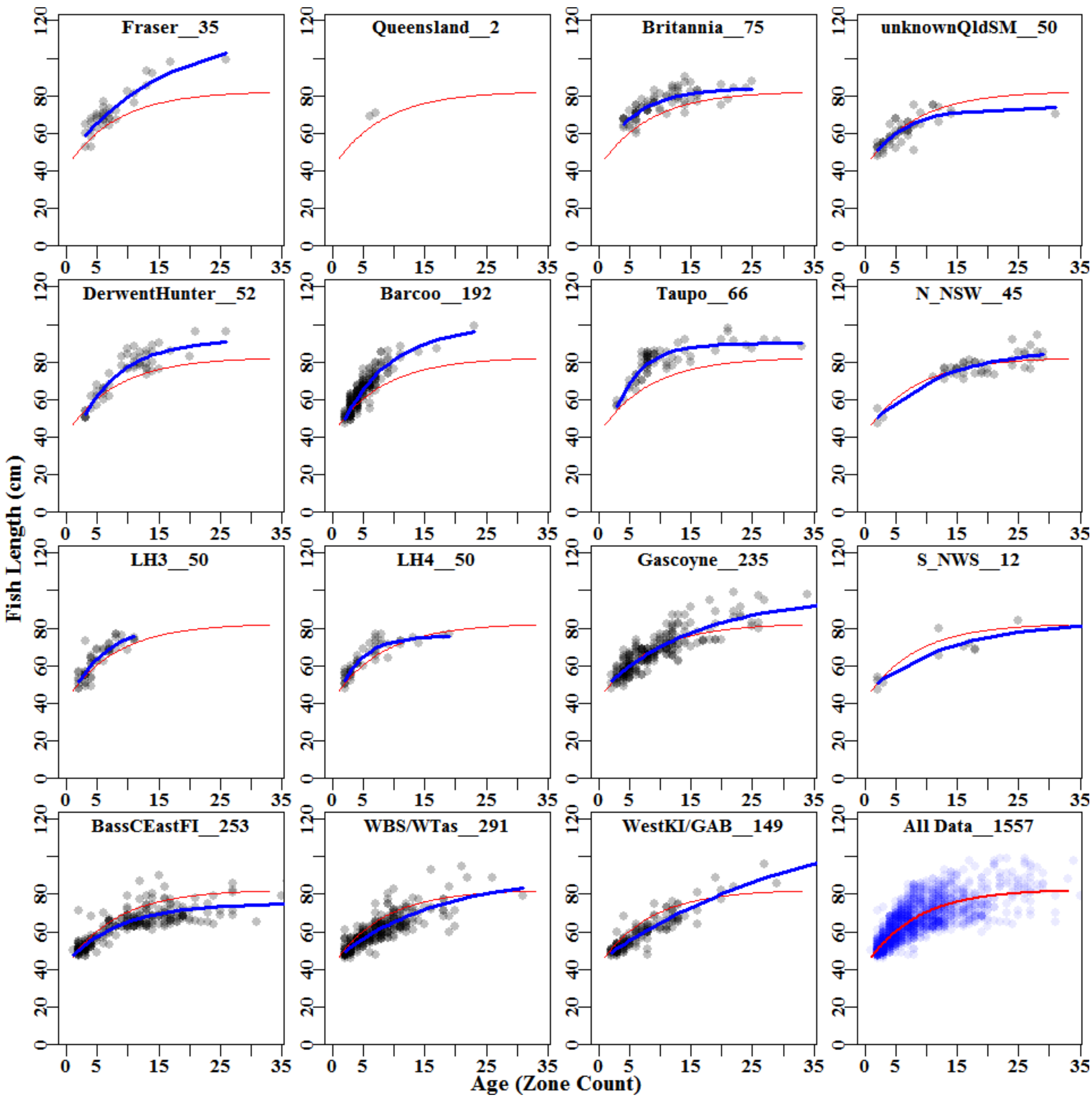

Figure 31. A plot of each region before any attempt at spatial grouping. The title in each case is the region name while the number is the usable sample size. The thicker blue line is the optimal fit to each data set while the red line is the optimal fit to all data combined (the graph at bottom right). The parameters for the general fit are L_∞ = 82.467, K = 0.1222, t_0 = -5.803, and sigma=6.721. The sites are arranged in sequence north to south and east to west around the coast (Figure 27). No curve was fitted to the two data points from the Queensland sea mount. The density of colour in each case represents the density of data points, with individual sites requiring only 1/3 the point density for the same density of colour shown in the all data combined graph.

All estimated cases have negative values for the t_0 parameter, which designates the hypothetical age at zero length, with some sites having extreme negative values less than -7.0 (Table 11). Some sites, such as N_NSW and S_NSW had poor t_0 parameter estimates due to small to very small sample sizes or poor representation of smaller, younger fish. Others sites such as Gascoyne, BassCEastFI, WBS/WTas, and WestKI/GAB had good sample sizes and seemingly good samples of smaller younger fish but still exhibited very negative values for t_0. Such large and unrealistic negative values suggest that the data for younger and smaller fish are unrepresentative, which is not surprising as such young animals are difficult to sample using commercial gear. Nevertheless, lacking the early years does not preclude the VB curve from providing a good description of the growth pattern over the specified restricted range of ages and sizes. However, when used over such restricted age ranges the parameters, especially the L_∞ and t_0, can no longer be considered as meaningful in any way.

Table 11. The parameter estimates from the naïve growth model fit to the data from each site. N_{obs} is the number of observations and *–veLL* is the negative log-likelihood. No estimates were made for the Queensland Seamount.

Site	N_{obs}	L_∞	K	t_0	σ	-veLL
Fraser	35	115.731	0.065	-7.837	4.478	102.140
Queensland	2					
Britannia	75	84.336	0.167	-4.775	4.008	210.538
unknownQldSM	50	73.960	0.165	-5.015	4.288	143.730
DerwentHunter	52	92.004	0.144	-2.771	4.602	153.169
Barcoo	192	99.322	0.126	-3.490	4.082	542.540
Taupo	66	89.989	0.226	-1.356	4.164	187.783
N_NSW	45	87.559	0.086	-7.960	3.933	125.472
LH3	50	81.594	0.178	-3.524	4.465	145.759
LH4	50	75.689	0.259	-2.528	3.288	130.453
Gascoyne	235	97.462	0.064	-9.912	5.138	718.087
S_NWS	12	84.112	0.073	-10.714	4.842	35.954
BassCEastFI	253	75.478	0.110	-8.012	4.936	762.889
WBS/WTas	291	90.624	0.060	-11.369	4.665	861.079
WestKI/GAB	149	129.223	0.027	-15.541	3.764	408.904
AllData	1557	82.467	0.122	-5.803	6.721	5175.785

Age Censoring

Older and larger fish are relatively poorly represented at all sites. When all data combined are considered (bottom right of Figure 31) relatively even densities of fish appear to be available across ages 2–15. A second analysis by site of ages 2–15 was conducted to determine whether some of the noisiness in the results can be damped by excluding potentially unrepresentative data.

The outcome of using this restricted data set was indeed less noisy with the modelled growth patterns compared with the combined data shown at Figure 32, Figure 33; and the VB variables tabulated at Table 13 and Table 14. The censored data clarifies the relative growth of each site relative to the overall approximate average (Figure 32), with the more north-easterly sites mostly being above the average growth curve, while the mid-eastern sites such as the Lord Howe Rise, the Northern and Southern NSW coast, plus the Gascoyne, were either just above the overall average or appeared to be sitting on top of it. Finally Eastern and Western Tasmania, Western Bass Strait, King Island and the GAB were clearly below the overall average and appeared to exhibit very similar growth trajectories even though their parameter values were rather different (Figure 32; Table 13).

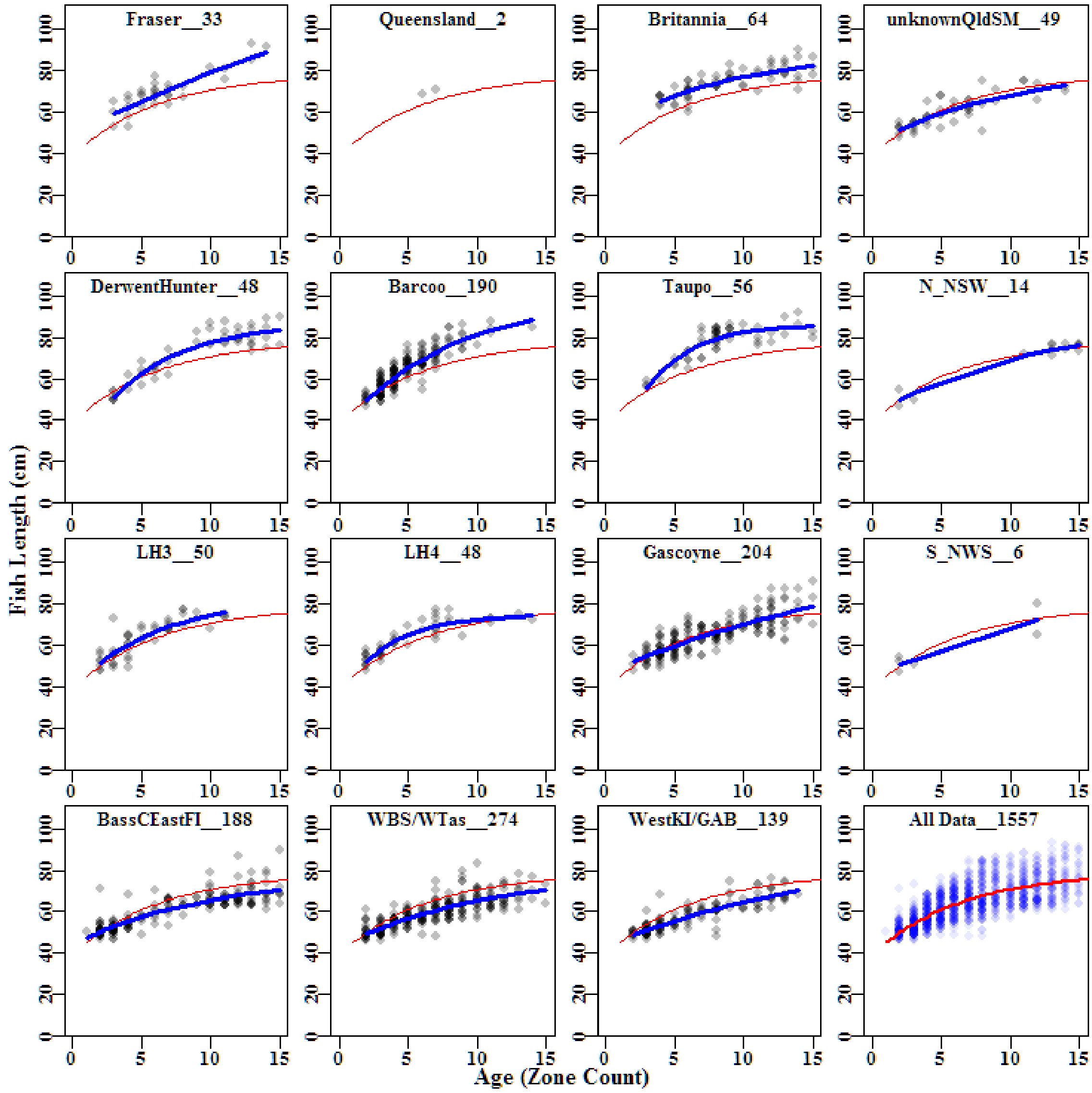

Figure 32. A plot of each region of fish aged 2–15 years, before any attempt at spatial grouping. The title includes the region name and sample size. The thick blue line is the optimal fit to each data set while the red line is the optimal fit to all data (ages 2–15) combined (the graph at bottom right). The parameters for the general fit are L_∞ = 78.753, K = 0.159, t_0 = -4.301, and σ = 6.290; all of which, except *K*, are smaller than when data with all ages are analysed. The sites are arranged in sequence down and around the coast (Figure 27). The density of colour in each case represents the density of data points, with individual sites requiring only 1/3 the point density for the same density of colour shown in the all data combined graph.

There was no consistent direction of change for the *Linf* and *K* parameters when the age data was censored down to between 2–15 years (Figure 33; Table 13), which also suggests that the older age classes were adding noise rather than information. However, one change, from an L_∞ of 115 cm FL to one of 178, cm FL would not be deemed an improvement and suggests that the older age classes at that site (Fraser; Table 12) were at least partially informative.

Table 12. The parameter estimates from the growth model fit to the data from each site when ages are censored to be between 2–15. N_{obs} is the number of observations and *–veLL* is the negative log-likelihood. No estimates were made for the Queensland sea mount.

Site	N_{obs}	L_∞	K	t_0	σ	-veLL
Fraser	35	178.575	0.026	-12.380	4.372	95.508
Queensland	2					
Britannia	75	88.352	0.122	-6.976	4.041	180.195
unknownQldSM	50	80.836	0.108	-7.347	4.254	140.506
DerwentHunter	52	86.753	0.195	-1.543	4.468	139.956
Barcoo	192	99.213	0.127	-3.457	4.083	536.881
Taupo	66	86.199	0.299	-0.443	4.088	158.314
LH3	50	81.606	0.178	-3.528	4.465	145.759
LH4	50	74.872	0.278	-2.283	3.341	126.003
N_NSW	45	85.562	0.103	-6.468	2.443	32.369
Gascoyne	235	114.695	0.042	-12.352	4.755	607.378
S_NWS	12	126.318	0.034	-12.884	4.874	18.036
BassCEastFI	253	79.155	0.094	-8.783	4.421	546.124
WBS/WTas	291	80.919	0.086	-8.933	4.149	778.666
WestKI/GAB	149	101.141	0.045	-12.758	3.538	372.881
AllData	1365	78.753	0.159	-4.301	6.290	4447.250

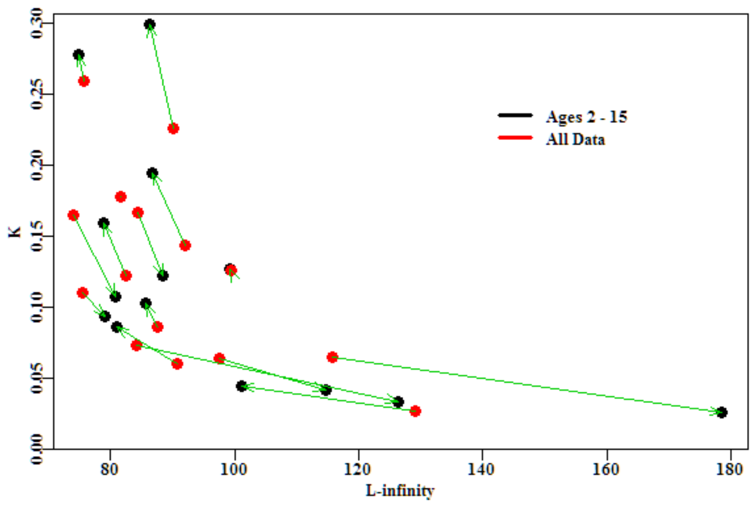

Figure 33. The direction of change in the L_∞ and K parameters when the ageing data are censored to be between 2–15. The direction of change is equally distributed between K increasing and L_∞ decreasing and vice versa.

Table 13. A generic characterization of each site 'Relative' to the overall growth curve fitted to all data together when ages are censored to be between 2–15. On Top (under 'Relative') means the curves are the same. 'Observations' is the number of observations. Consistent (under 'Comment') implies that the data by itself is consistent with the relative position but that the fitted curve, if there is one, is uncertain through minimal data being available.

Site	Relative	Comment	N_{obs}	L_∞	K
Fraser	Above	Fitted	33	178.575	0.026
Queensland	Above	Consistent	2	88.352	0.122
Britannia	Above	Fitted	64	80.836	0.108
unknownQldSM	On Top	Fitted	49	86.753	0.195
DerwentHunter	Above	Fitted	48	99.213	0.127
Barcoo	Above	Fitted	190	86.199	0.299
Taupo	Above	Fitted	56	81.606	0.178
LH3	Just Above	Fitted	50	74.872	0.278
LH4	Just Above	Fitted	48	85.562	0.103
N_NSW	On Top	Consistent	14	114.695	0.042
Gascoyne	On Top	Fitted	204	126.318	0.034
S_NWS	On Top	Consistent	6	79.155	0.094
BassCEastFI	Below	Fitted	188	80.919	0.086
WBS/WTas	Below	Fitted	274	101.141	0.045
WestKI/GAB	Below	Fitted	139	78.753	0.159

The von Bertalanffy parameters for the age-censored data (Table 12) exhibit no relation to whether the curve itself is above or below the overall average curve. This suggests that the von Bertalanffy curve itself is acting simply as an empirical description of the data and the parameter values should not be considered to reflect likely values. Rather they merely reflect the properties of the data available and some other curve may produce equally valid descriptions of that data. Nevertheless, the fact that some curves are above and others below the average curve and that property is related to the geographical position of the sites constitutes evidence that the growth of Blue-eye Trevalla around Tasmania and across into the GAB is expected, at least for ages 2–15, to lead to shorter fish for the same age than those found up in the north east and out on the seamounts of the east coast.

These growth differences are sufficient to remain apparent despite any mixing of adults that might occur across at least 15 year periods.

Spatial Grouping of Sites

The simple visual comparison of the individual curves against the curve fitted to all data illustrates there are differences between the sites but neither provides a valid test of those differences nor does it quantify those differences. The von Bertalanffy curve has two parameters (L_∞, and K) that relate to the extreme ends of the predicted curve where generally there is the least data. There have been re-parameterizations suggested that can improve the model fitting process but they do not improve the capacity for simple growth curve comparisons. For example, in the unknown Queensland Seamount there is a single observation aged 31 with the remaining 49 observations all less than 15 years old. A comparison of the growth with and without the 31 year old fish (Figure 34) leads to what appear to be very different von Bertalanffy parameters, however, the growth curves themselves overlap very closely over almost the full range of data from ages 2–14 (Figure 34). This illustrates why care is required when estimating a growth curve to represent a site; if un-representative data are included they can alter or bias a curve in unpredictable ways.

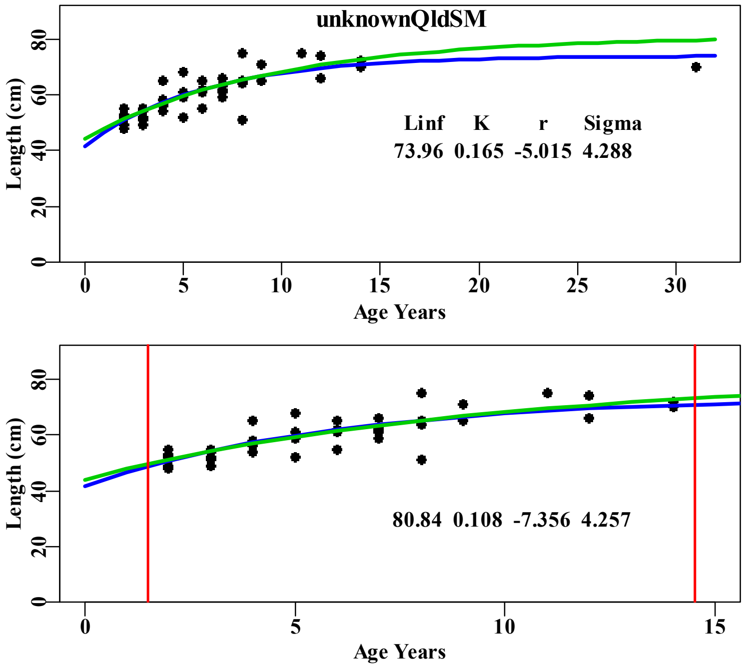

Figure 34. Comparing the von Bertalanffy curves between including and removing a single larger/older fish at the unknown Queensland seamount. Green line includes the single 31 year old fish, blue line is with this fish removed from the analysis. While the parameter values differ quite markedly the curves are very similar over the age range 2–14 years. The bottom graph is an expansion of the relevant section of the top graph.

Comparison of Regions using Restricted Age Classes

It is clear that few of the sampled locations have good coverage across the full size range and the related full age range. This is not surprising given that the sampling, at least outside of the seamounts, was for a restricted range of sizes (45–85 cm FL). The seamounts appear to have more regions that have more extensive size sampling (Table 7) with some of the seamounts (e.g. Taupo and Britannia) exhibiting a relatively wide coverage of ages, although with relatively sparse data along the full age range (Table 9). For comparisons to be valid some restriction on the number of age classes would be appropriate and some sites (some seamounts) would need to be combined. As a first trial, the growth of fish from different regions was only compared for fish aged between 2–15 years.

The comparisons made using the randomization tests (listed in Table 9Table 9) found some significant differences around the coast and some non-significant growth comparisons. The three sites BassCEastFI, WBS/WTas, and WestKI/GAB were each compared to the others and no significant differences were found when randomization tests were used (Figure 35).

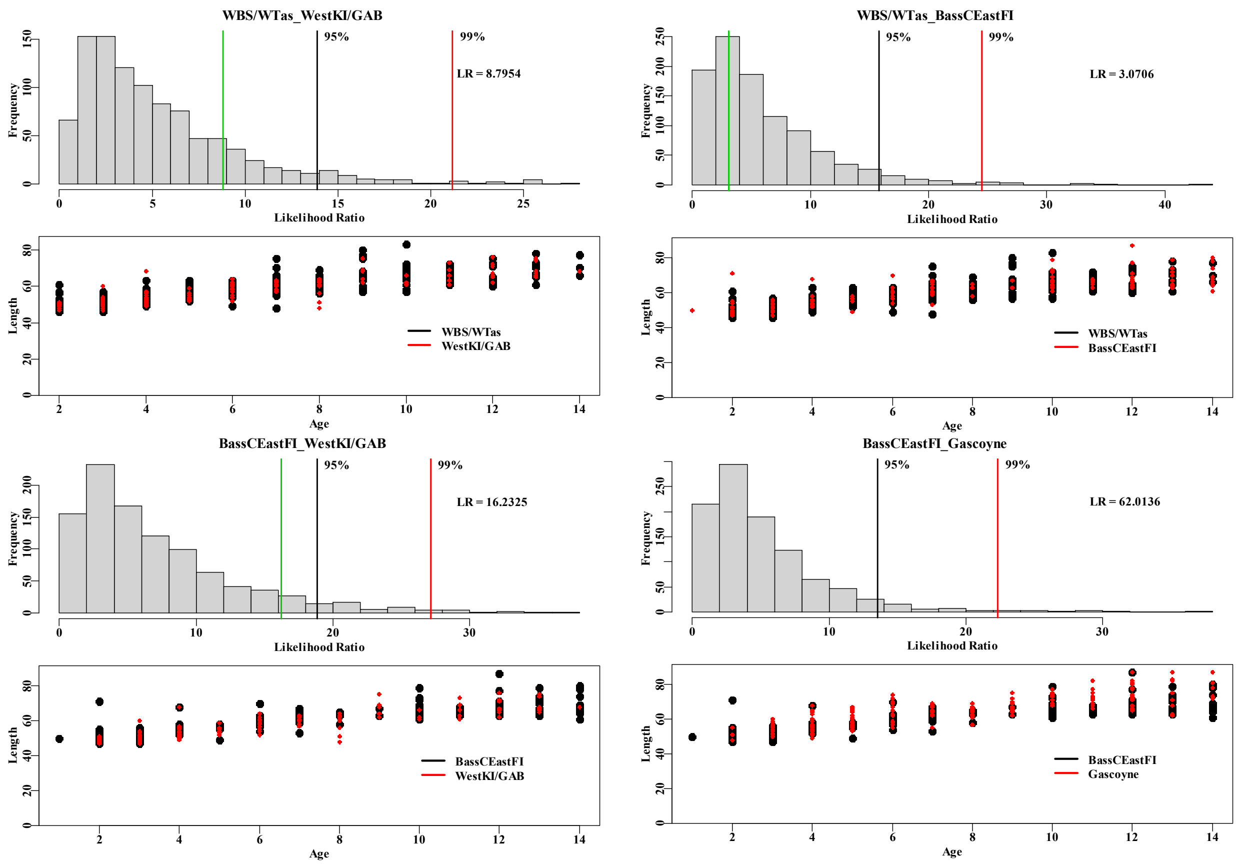

Figure 35. Comparisons between the Tasmanian sites and GAB, plus a comparison of the Bass Canyon/East Flinders Island with the Gascoyne site. None of the Tasmanian/GAB sites were significantly different whereas a highly significant difference was apparent between Bass Canyon/East Flinders Island and the Gascoyne site.

The Lord Howe Rise sites were not significantly different from one another, but Lord Howe combined differed significantly from both Barcoo and Gascoyne, with a greater difference from Gascoyne than from Barcoo (Figure 36).

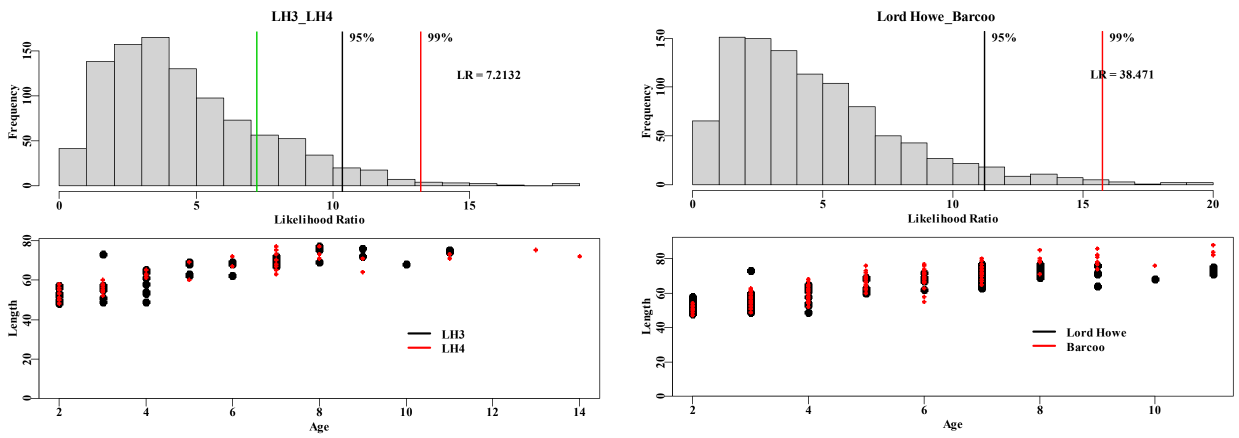

Figure 36. A comparison between the two Lord Howe Rise sites where even though the data from each site was sparse, no difference was found. In comparison with Barcoo the combined Lord Howe Rise data (from 2–11 years) remained significantly different suggesting that Barcoo fish grow to a larger size for the same age.

The various seamounts in the north all had relatively small sample sizes (Table 7) however, when plotted together their similarities can be observed (Figure 37) even though some of the sites have very noisy data that is unevenly distributed across the different ages. The Barcoo seamount has the most data although it has very few observations above the age of 11.

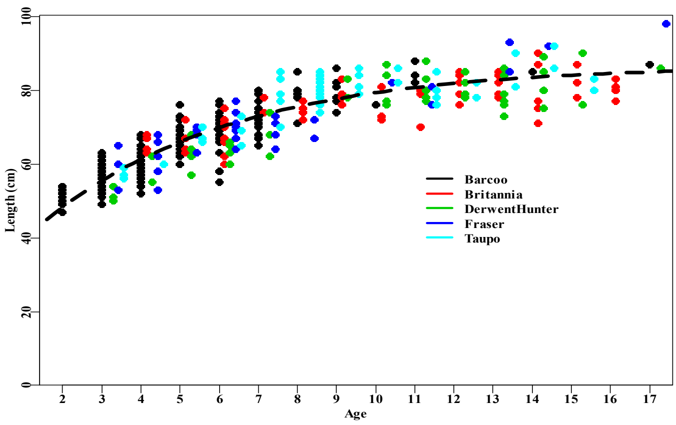

Figure 37. A plot of the data from five different seamounts from the north-east. The dashed line is the best fitting growth curve fitted to all these data combined.

A comparison was made between the combined seamounts and Barcoo between the ages 2–11 and this demonstrated no significant difference, whereas the seamounts against other sites exhibited highly significant differences (Figure 38).

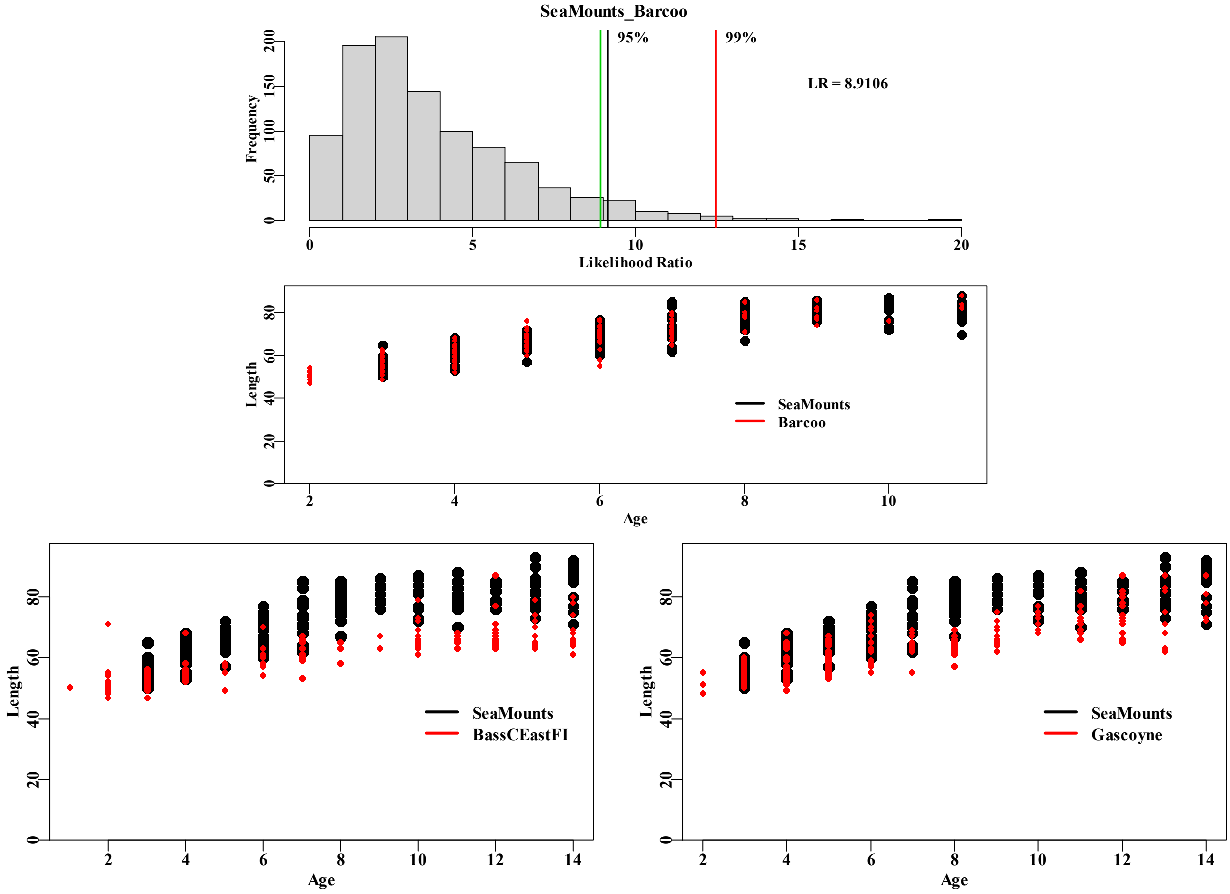

Figure 38. A plot of the data from five different seamounts from the north-east. The dashed line is the best fitting growth curve fitted to all these data combined.

It would appear that the Gascoyne sample is different from everywhere else, however, as indicated in Table 13 the data from the unknown QLDSM, the N_NSW, the S_NSW, and the Gascoyne all had curves or data that appeared to sit on top of the overall average growth curve. When the data from the unknown QldSM and the two NSW sites are combined and compared with the Gascoyne no significant differences are found, even though the data are relatively noisy and the age data is unevenly spread in the two groups (Figure 39).

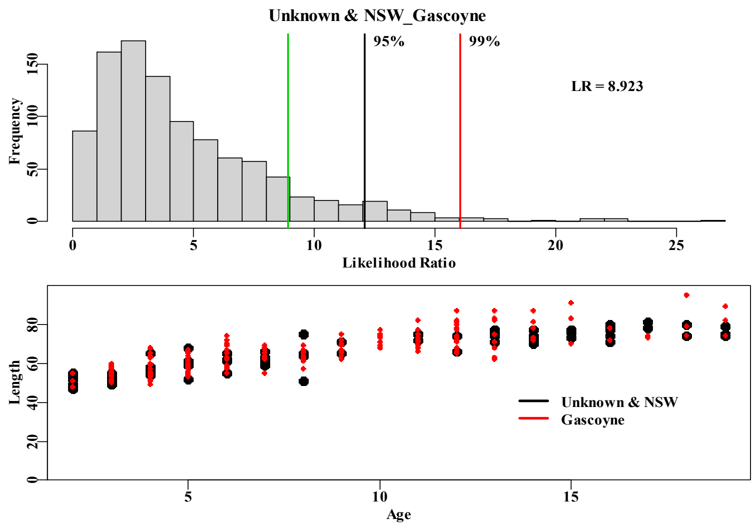

Figure 39. A randomization test comparison of the unknownQldSM plus the two NSW samples relative to the sample from the Gascoyne. When ages 2–15 are compared the two curves are very similar, less so, but still insignificant from 2–20, but finally, across ages 2–25 a significant difference at 5% (but not 1%) was found.

The various randomization tests conducted confirm the findings in Table 13Table 13, which indicates that differences exist in a series around the coast, with a few more complicated arrangements close to the NSW coast and the Gascoyne (with the unknown Queensland Seamount), and no significant differences around Tasmania and out past King Island and into the GAB (Figure 40 and Figure 41).

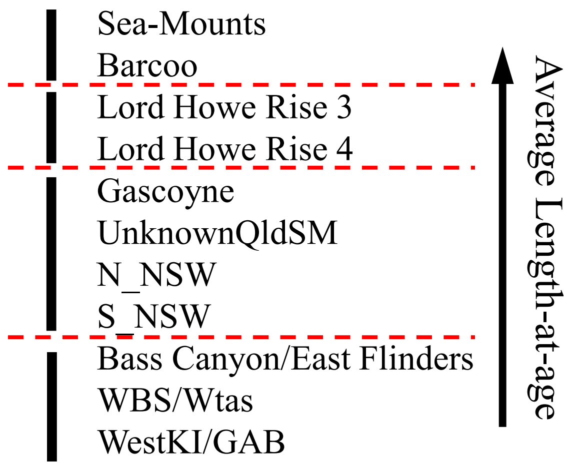

Figure 40. No significant differences between sites/regions are denoted by the thick vertical lines while significant differences are marked by the horizontal red dashed lines.

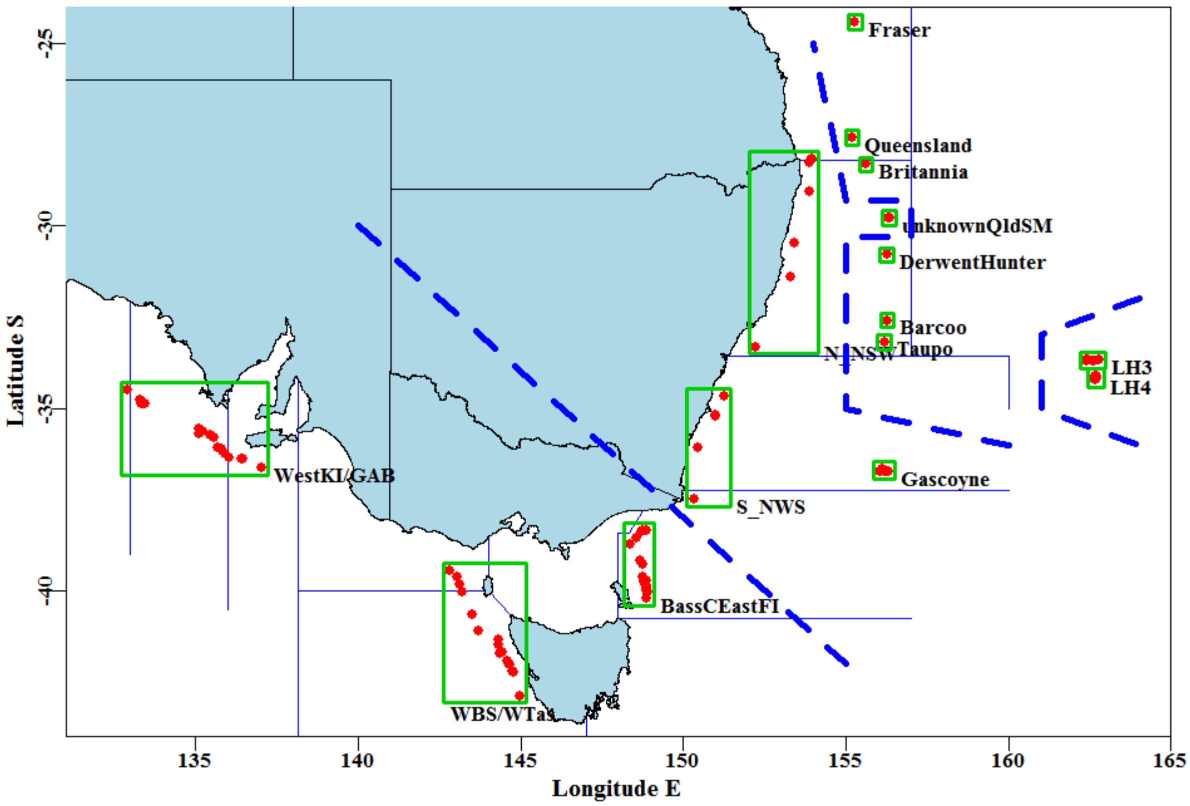

Figure 41. Schematic map of the sampled sites, based on the latitudes and longitudes in the data set (Table 7). The red dots are the average locations of samples while the green boxes are rectangles bracketing each set of data for a region. For site name descriptions see Table 6. The thick blue dashed lines separate regions that have significantly different growth characteristics, generally in the 2–15 age classes. Bass Canyon/East Flinders is in SESSF zone 20, WBS/Wtas is in zones 40–50, and WestKI/GAB is in GAB zones 84 and 85 (Haddon, 2015b).

Catches by Region

By taking the total reported catch data from Haddon (2015b, Table 5, p 13) these can be summarized into those catches taken in the SESSF zones 10–50 (with the minor catches in zone 60 being included), those in the northeast (zones 70, 91, and 92), and those in the GAB zone 83–85 (Table 14). Catches in the northeast were always a relatively small percentage except for two years in 2002–2003 and then between 2009 and 2013. Changes in TAC, changes in other fishing regulations (auto-line fishing no longer permitted on the Tasmantid seamounts), the advent of growing whale depredation on auto-line fishing, and finally the introduction of multiple marine closures, have led to relatively large changes in the distribution of fishing effort (Table 14Table 14).

Table 14. Summary reported catches taken by all methods in the three regions GAB, SESSF (zones 20–50), and in the north-east. Taken and summarized from Haddon, 2015b).

Year	Northeast	SESSF	GAB	Total	Northeast	SESSF	GAB
1997	10.975	435.502	16.843	463.320	2.37	94.00	3.64
1998	1.590	435.423	7.967	444.980	0.36	97.85	1.79
1999	21.640	517.456	7.044	546.140	3.96	94.75	1.29
2000	7.258	640.227	9.923	657.408	1.10	97.39	1.51
2001	42.856	488.208	48.991	580.055	7.39	84.17	8.45
2002	48.983	375.847	37.437	462.267	10.60	81.31	8.10
2003	74.978	416.524	70.485	561.987	13.34	74.12	12.54
2004	47.021	401.142	152.432	600.595	7.83	66.79	25.38
2005	14.758	326.040	100.616	441.414	3.34	73.86	22.79
2006	15.431	353.465	165.364	534.260	2.89	66.16	30.95
2007	16.174	386.751	152.539	555.464	2.91	69.63	27.46
2008	8.100	259.400	74.574	342.074	2.37	75.83	21.80
2009	43.004	348.180	32.416	423.600	10.15	82.20	7.65
2010	69.948	277.114	32.010	379.072	18.45	73.10	8.44
2011	147.192	207.540	75.426	430.158	34.22	48.25	17.53
2012	102.941	188.954	22.196	314.091	32.77	60.16	7.07
2013	43.887	190.029	29.874	263.790	16.64	72.04	11.32
2014	25.297	213.707	49.042	288.046	8.78	74.19	17.03

Discussion

Significant Growth Differences Detected

It should be emphasized that the seamounts in the north-east were combined solely on the basis of a visual comparison, and clearly there is some uncertainty associated with the NSW coast and the unknown Queensland seamount. Nevertheless, the differences in the growth characteristics between the south and west from the rest are clear, as was the difference between the Lord Howe Rise fish and the rest. We can thus conclude that the growth of Blue-eye Trevalla differs among fish taken in different areas around the coast, with, on average, a larger length-at-age from the Tasmantid seamounts, the Lord Howe Rise, the NSW Coast and the Gascoyne (and the unknown Queensland seamount), and finally the sites around Tasmania and in the GAB (Figure 40). Samples were not available from the Cascade Plateau and so these are not considered here further, although the expectation might be that they would be more similar in growth to the south and the west than to the Tasmantid or the Gascoyne seamounts. It would be interesting to discover to which group they were most similar as that might suggest whether the differences are habitat related (seamount versus slope), related to latitude (although West KI/GAB is on about the same latitude as the Gascoyne), or to properties of major water masses.

Implications for the Stock Assessment

The current stock assessment for Blue-eye Trevalla relies on the analysis of commercial catch rates from the auto-line and drop-line fisheries in SESSF zones 20–50 and GAB zones 83–85 from 1997–present in a Tier 4 assessment, with only token notice taken of trawl catch rates from 1986–present (Haddon, 2015b, 2015c). Commercial catch data from the north-east remains spread among too many different fishing methods to permit a consistent analysis of CPUE above the SESSF zone 20 (above the Bass Strait Canyon and Eastern Flinders Island). Nevertheless, in some recent years over 30% of all Commonwealth fishery catches came from the north-east (Tasmantid seamounts and Lord Howe Rise) (Table 14Table 14), so while the catches from that area are included in the assessment, the validity of assuming that the CPUE from the SESSF is representative of the stocks in the north-east is doubtful. This would appear to be especially the case now that it appears that the fish in SESSF zones 20–50 and the GAB growth rather differently to those in the north-east.

Blue-eye are relatively long-lived fish and for their growth patterns to become distinct implies that the populations in the large areas studied must remain relatively isolated from one another. Length-at-age differences, such as those found in the current investigation, could only arise if the fish populations were relatively discrete. While there may remain some movement of fish between areas, quite possibly enough to bring about relative genetic homogeneity, if it occurs it is clearly insufficient to prevent growth pattern differences arising and being maintained.

Often, biological stocks are defined in a purely genetic sense, but in long-lived species that do not exhibit large scale adult movements after settlement it is possible for phenotypic differences to arise from differences in their growth characteristics. Such spatial heterogeneity, if it arises, indicates that such populations do experience significant degrees of isolation irrespective of what any genetic analysis may indicate (Haddon and Willis, 1995). What this means is that there is a risk of serial depletion if the total allowable catch is estimated using the whole range of the species, but the fishery operates over a fraction of the area. This appears to have occurred to Blue-eye Trevalla, with the relative depletion (exploitation) of the population seemingly matching the relative depletion (exploitation) by area. The east coast of Tasmania, for example, was always the principle fishing ground for the drop-lining vessels early in the fishery. Thus, estimated catches from 1980 onwards reached nearly 1000 t, mainly from eastern Tasmania in 1986 and 1987 (Haddon, 2015b, Table 2). The west coast of Tasmania, on the other hand, has only been fished to any real extent since 1997, and the relative depletion of the two areas, as implied by their relative CPUE, reflects this.

If Blue-eye Trevalla continue to be treated as a single stock, despite the present evidence, then efforts should be made to ensure that catches (the TAC) are dispersed about the whole of the fishery approximately in proportion to the available abundance. The alternative is to recognize different stock areas and manage them differently in accordance with the relative separation and regional abundance, setting a separate TAC for each independent/identified region. The intent is to avoid depleting any single area at the expense of allowing other areas to develop relatively untouched populations. Catch levels that should be sustainable can be estimated for such spatially structured stocks. The problem of distributing those catches across such a wide ranging and spatially structured species is common to many other spatially heterogeneous species. Focussing effort and catch in the most convenient areas rather than spreading effort and resulting catch across a wide geographical area is understandable as it is more profitable and efficient to do so, at least until the easily accessible stocks become depleted. Nevertheless, some form of spatial management is needed, whether that be separate TACs for different areas, a voluntary agreement about the spread of catch, or some other form of spatial management. As long as the objective of spreading effort and catch approximately is in line with the relative availability this should help ensure that proposed catches remain sustainable.

4. Otolith chemistry

Application of otolith chemistry life history profiles and stable isotope analysis to resolve population structure of Blue-eye Trevalla (*Hyperoglyphe antarctica*)

Introduction

Blue-eye Trevalla (*Hyperoglyphe antarctica*) occur over hard bottom on the outer continental shelf and upper slope waters, and also offshore seamounts around the southern half of Australia and New Zealand. *H. antarctica* is an important high value commercial target species, and of growing availability to recreational fishers, throughout most of its distribution. In the Australian fishery, Blue-eye Trevalla is taken by the trawl and non-trawl sectors (primarily by auto-longline and drop-line). There is some evidence that spawning of *H. antarctica* is widespread around southern Australia, taking place in areas over the continental slope as well as on offshore seamounts. The time of spawning across the species range is not well known, with spawning in southern regions (i.e. around Tasmania to South Australia) thought to occur in autumn, but in more northern regions (i.e. northern New South Wales) in winter (Kailola *et al.* 1993, Jones 1995, Rowling 1994, Baelde 1996). The distribution of larvae and juveniles is not well known. Juvenile *H. antarctica* are believed to be pelagic up to the size of about 45 cm fork length (FL) (when about 2 to 3 years old), at which stage they are thought to move to a semi-demersal habitat, and appear to be fully recruited to benthic habitats at 300–600 m depth at a length of approximately 50 cm FL.

Little is known about the population structure of *H. antarctica*. This poor knowledge of population structure is an impediment to optimising assessment and management, and informing the need for spatial allocation of quota. Genetic studies (allozyme analyses) suggest that gene flow is sufficient to prevent genetic differentiation among fish collected from seamounts off New South Wales, Tasmania, and on-shelf waters around the Tasmanian coast (Bolch *et al.* 1993). This lack of spatial differentiation is not inconsistent with the hypothesis of a single population of *Hyperoglyphe antarctica* in Australian waters. Tagging trials off eastern Australia support the genetic studies, with some juvenile fish (around 50 cm length) remaining within a region for up to 3 months (Rowling pers. comm. in Blaede 1996) while others may move significant distances along the continental slope (K. Rowling, pers. com.). Movement between slope areas and offshore seamounts are however unknown. Studies from New Zealand suggest that *H. antarctica* may be relatively sedentary in the short term, but capable of movements over 100s of kms with time (Duffy *et al.* 2000; Horn 2003).

While the earlier studies of Blue-eye Trevalla stock structure have indicated that genetic variation was not significant among Australian fishery regions (Bolch *et al.* 1993; Hindell *et al.* 2005; Robertson *et al.* 2008), genetic homogeneity can be maintained over broad spatial scales even in situations where reproductive exchange and or movement is in fact limited over the same scales (Waples 1998). In these situations genetically homogeneous populations, may in fact be comprised of a number of `stocks' based on geographic variation of other phenotypic or vital rate parameters (e.g. growth rate, reproduction, size at maturity, fecundity, recruitment variation) that are critical for assessing fishery dynamics and managing impacts of fishing on population processes (Begg and Waldman 1999). Based on the results of Hindell *et al.* (2005) the genetic homogeneity observed by these previous studies cannot be taken as clear evidence for one Australia wide stock for management and assessment purposes, and further work is required to apply more sensitive approaches for resolving contemporary population structure.

The application of otolith chemistry is one such approach. The chemical and isotopic composition of fish otoliths can be influenced by variation in the physical and chemical properties of the ambient water, food composition and or physiology (Campana 1999; Campana and Thorrold 2001; Elsdon *et al.* 2008, Sturrock *et al.* 2012). Because the influences of these factors can vary geographically, differences in the chemical and isotopic composition of otoliths can be used to infer spatial separation of fish for parts of, or all of their lives. Furthermore, because otoliths grow continuously throughout a fish's life, and are metabolically inert, they provide a permanent record of variation in trace elemental and isotopic composition (Campana 1999). These properties have allowed otolith chemistry to provide information on migration behaviour, environmental history, and population structure of fish (Campana and Thorrold 2001; Elsdon *et al.* 2008).

Analyses of otolith chemistry can be conducted in various ways to infer population structure of fish. In many instances stock structure studies have applied a 'top down' type approach (Thresher 1999) whereby older life-stages are sampled in a structured way (such as by fishery areas/zones) and their otolith chemistry is compared to detect differences among sample groups that can support inferences of spatial separation and stock structure. An alternative to this is the 'bottom-up approach' whereby small juveniles or larvae are sampled in nursery/spawning areas to detect specific 'nursery area' chemical signatures or tags. The same cohorts of fish are then sampled as adults, and the proportions of particular source area tags in the adult samples from specific areas (or fishery regions) is used to inform meta-population structure and source sink relationships (i.e. Hamer *et al.* 2011). This approach assumes that all source areas can be sampled, which is problematic for oceanic species such as for Blue-eye Trevalla that have wide distributions and no clearly defined nursery areas.

In a preliminary study of Blue-eye Trevalla stock structure around Australia and New Zealand, Hindell *et al.* (2005) applied a 'top-down' approach to provide evidence of regional variation in 'whole' otolith chemistry of young adults in spite of genetic homogeneity across the sampling areas. While this study supported the further application of otolith chemistry over genetics for more detailed investigations of Blue-eye Trevalla stock structure, the analysis of 'whole' otoliths (i.e. dissolution of the entire otolith in acid and analysis of the resultant solution) homogenises the chemical variation that occurs within the otolith. This approach loses valuable information on the variation in otolith chemistry that occurs across different life history stages, and in some situations can lead to misinformed interpretation of stock structure. For example, if larval and juvenile dispersal was broad with major mixing among different spawning sources, but adult fish were more locally resident, this could not be resolved through a whole otolith approach, and in fact differences in whole otolith chemistry could occur and be misinterpreted as indicative of reproductively separate populations. Hindell *et al.* (2005) recognised the limitations of the whole otolith approach for inferring population structure of Blue-eye Trevalla and recommended that a more refined life history based otolith chemistry approach could be more informative of stock structure.

This study was developed to build on the earlier (Hindell *et al.* 2005) study by applying a combination of otolith life history profiles of elemental chemistry and sampling of stable isotopes in specific otolith growth zones (life stages) to investigate alternative hypothesise of Blue-eye Trevalla population structure between seamounts and areas of the Australian continental shelf, including Tasmania. Life history profiles involve continuous analysis of the otolith chemistry from the otolith core (larval/early juvenile period) to the otolith margin (point of capture). The otoliths are sectioned through the core region and the thin sections are sampled, typically using laser ablation, with the ablated material analysed by an ICP-MS (inductively coupled plasma mass spectrometer). The resultant data is a continuous profile of elemental chemistry from the core to the margin that can then be related to microstructural features such as annual growth increments to provide a life history chronology of otolith chemical variation. Aspects of these profiles, such as different phases or years of the life history, can then be compared among samples from different areas to detect variation that indicates separation at various points in the life history.

Profile analyses, conducted with laser ablation ICP-MS, measure a range of individual elements, with those typically most informative and detectable in otolith studies being: Barium (Ba), Strontium (Sr), Magnesium (Mg), and Manganese (Mn), measured as their respective ratios to Calcium (Ca), but numerous others have been reported (Campana 1999). Elements are not simply deposited into otolith material in proportion to their ambient concentrations but at rates that are mediated through complex physiological processes, which are not yet fully understood (Campana 1999; Sturrock *et al.* 2012; 2014; Izzo *et al.* 2015). At least for Ba and Sr, there is a weight of evidence that chemical composition of the ambient water can be a major influence on their incorporation rates into otoliths, but for other commonly used elements such as Mg and Mn the role of physiology, growth rate and or metabolic affects may overwhelm ambient concentration effects where variation is low (Kalish 1989; Bath *et al.* 2000; Elsdon and Gillanders 2003; 2004; De Vries *et al.* 2005; Martin and Thorrold 2005; Walther and Thorrold 2006; Hamer and Jenkins 2007, DiMaria *et al.* 2010; Woodcock *et al.* 2012; Sturrock *et al.* 2015). Irrespective of the causal processes that drive variation in otolith elemental compositions, consistent differences among individuals from different areas can be used to infer patterns of separation over time or life-stages.

Stable isotope ratios of carbon ($^{13}C/^{12}C$, i.e. $\delta^{13}C$) and oxygen ($^{18}O/^{16}O$, i.e. $\delta^{18}O$) have also been utilized in studies of fish population structure (Campana 1999, Campana and Thorrold 2001). Measurements of these ratios are conducted with different instrumentation than the elemental profiles above. The analysis requires small amounts of ground powder to be extracted from the otolith section, typically > 50 µg, that are then dissolved in acid with the resultant CO_2 gas analysed by an isotope ratio mass spectrometer. The sample material is extracted from otoliths using computer controlled milling drills (micro-mills). While it does not achieve the same micro-scale resolution as laser sampling, it can still target specific periods in the life history. $\delta^{18}O$ has been shown to be a useful indicator of temperatures experienced by fish due to the fact that the fractionation of $^{18}O/^{16}O$ in otoliths is in close equilibrium to that of the surrounding seawater, and is strongly influenced by temperature (Iacumin *et al.* 1992; Thorrold *et al.* 1997b; Dufour *et al.* 1998; Gao and Beamish 1999; Weidman and Millner 2000; Begg and Weidman 200). Unlike $^{18}O/^{16}O$, the $^{13}C/^{12}C$ ratios in otoliths are not in equilibrium with the surrounding water, and it is thought that much of this disequilibria is related to metabolic effects (Thorrold *et al.* 1997a). Variation in the $^{13}C/^{12}C$ isotopic composition of otolith carbonate is likely to be related to variation in both environmental conditions and physiology/metabolism (Kalish 1991a; 1991b; Iacumin *et al.* 1992; Thorrold *et al.* 1997b; Schwarcz *et al.* 1998; Weidman and Millner 2000). In the case of $\delta^{18}O$, where the influence of temperature is clearly established, it is possible to make some a-priori predictions as to the nature of regional differences in $\delta^{1}8O$ under different stock structure hypotheses based on knowledge of water temperature variation. In the current study samples are being compared among fishing regions separated over a latitudinal range of approximately 24°- 44° S and a longitudinal range from 115°-159° E. If sustained stock structure exists we would therefore expect that $\delta^{18}O$ at least will show clear variation among sampling regions.

Focussing on life history stages using laser ablation (elemental chemistry) and micro-mill sampling (stable isotopes) provides a more inferentially powerful approach than whole otolith analysis. It allows more detailed inferences on population structure, but also processes that might be driving population structure. The sub-objectives for this part of our study were to:

1. Compare otolith elemental chemistry life history profiles among different slope and seamount fishery locations

2. Compare stable isotope ratios ($\delta^{13}C$ and $\delta^{18}O$) for the early life history (juvenile/pelagic) and demersal adult life stages among different slope and seamount locations

We interpret the data from these two approaches in relation to two hypothesise of Blue-eye Trevalla population structure:

Hypothesis 1: seamount and continental shelf Blue-eye Trevalla fisheries are based on separate stocks that are replenished from different larval sources (i.e. true stock separation)

Hypothesis 2: recruitment of Blue-eye Trevalla to seamount and continental shelf areas is derived from a broadly dispersed/mixed larval pool, but adult populations constitute separate resident sub-populations (meta-population with local adult residency).

Methodology

Sample collection

This study compared otolith chemistry life history profiles across the chronological structure of transverse sections of adult Blue-eye Trevalla otoliths from 10 seamount and 5 continental slope regions around Australia and the Tasman Sea (Table 15). Otoliths were sourced from archived collections held by CSIRO, New South Wales Fisheries, Western Australian Fisheries, and Fish Ageing Services (FAS). Otoliths in these archives were generally removed from freshly caught or chilled fish within 24 hours of capture, and stored in paper envelopes. For most of the regions we were able to constrain the comparisons to three cohorts born between 2005 and 2007 with samples collected between 2010 and 2013 (Table 15). NSW samples were only available from 2009 and were comprised of larger older fish from cohorts between 1973 and 1997, and for Cascade Plateau, samples were only available from collections in 2004, and were again mostly older fish from cohorts between 1975 and 1984 (Table 15). While it is not ideal to conduct spatial comparison among samples collected or born in different years (Gillanders 2002), this was unavoidable. However, by only comparing the same increment zones across areas, and statistically assessing the influences of cohort variation on spatial variation using linear mixed models it possible to limit the influence of temporal differences in sampling or birth years on spatial comparisons (see below).

Table 15 Summary of samples used for life history otolith chemistry profiles and stable isotope analyses

Region	*n*	*Size FL cm (mean, range)*	*Sex M, F, U*	*Age years (mean, range)*	*Cohort (sample number)*
WA-Esp. (slope)	13	61, 55-69	9,4,0	8, 7-12	2002 (1), 2006 (6), 2007 (6)
WKI/GAB (slope)	16	55, 50-68	2,1,13	5, 4-7	2005 (1), 2006 (6), 2007 (9)
WBT (slope)	10	57, 54-63	4,3,3	6, 4-7	2005 (2), 2006 (5), 2007 (2) 2008 (1)
BSC (slope)	13	59, 54-67	6,7,0	6, 4-8	2004 (1), 2005(1), 2006 (4), 2007 (6), 2008 (1)
Sth-NSW (slope)*	22	77, 65-94	16,6,0	20, 12-36	1973 (1), 1979 (1), 1982 (1), 1983 (1), 1985 (3), 1986 (1), 1989 (2), 1991 (2), 1992 (1), 1993 (4), 1994 (1), 1996 (2) , 1997 (2)
CASC (seamount)	9	82, 77-88	0,0,9	24, 20-29	1975 (1), 1976 (1), 1978 (3), 1981 (1), 1983 (1), 1984 (2)
GASC (seamount)	10	67, 64-69	4,6,0	7, 6-8	2005 (1), 2006 (5), 2007 (4)
LH3 (seamount)	12	67, 62-72	6,6,0	6, 5-7	2006 (6), 2006 (4), 2007 (2)
LH4 (seamount)	10	70, 63-77	4,6,0	7, 5-7	2005 (5), 2006 (3), 2007 (1), 2008 (1)
TPO (seamount)	11	72, 65-85	6,5,0	6, 5-7	2004 (1), 2005 (4), 2006 (4), 2007 (2)
BCO (seamount)	12	68, 63-76	6,6,0	6, 5-7	2004 (1), 2005 (5), 2006 (6)
DH(seamount)	12	66, 57-83	4,8,0	6, 5-10	2002 (1), 2003 (1), 2005 (1), 2006 (6), 2007 (3)
'Unknown'. Qld (seamount)	12	61, 52-68	6,6,0	6, 4-8	2004 (1), 2006 (5), 2007 (5), 2008 (1)
BRIT (seamount)	12	67, 60-72	6,6,0	6, 5-7	2003 (2), 2004 (1), 2005(4), 2006 (4)
FRS (seamount)	10	69, 63-77	5,5,0	6, 5-7	2004 (2), 2005 (4), 2006 (4)
Overall	**184**	**67, 50-94**	**84, 75, 25**	**8, 4-36 (all) 6, 4-12 (excl. Sth-NSW, CASC)**	

Otolith preparation

One whole sagitta was selected for each fish. It was embedded separately in epoxy resin (Struers Epofix), sectioned to approximately 400 µm in thickness in the transverse plane to incorporate the core region, and polished with aluminium oxide lapping film lubricated with Milli-Q water. Each polished section was fixed to a microscope with epoxy resin, cured and the slide then sonicated in Milli-Q water for 5 minutes, liberally rinsed prior to drying in a laminar flow cabinet and stored in a plastic container. The birth year (i.e. cohort) was determined from the count of annual increments and the known capture date (ageing as per Results Chapter 2).

Elemental analysis

Laser ablation inductively coupled plasma mass spectrometry (LA-ICP-MS, Laser - New Wave UP213, ICP-MS – Thermo Scientific Element 2, Fisheries Victoria, Queenscliff, Victoria, Australia) was used to obtain age-related element:Ca profiles. The laser was programmed to traverse the otolith section from the core to the margin along the ventral side of the sulcus. The laser path initially traversed a short path (280–300 µm) towards the ventral tip to capture the early life history zone (i.e. core-c, first 1–2 months of pelagic life, refer Chapter 2) before deviating on a straight path towards the proximal margin cross-cutting the annual increment zones, before deviating again to run for a short period (~250 µm) along the otolith margin to capture the marginal chemistry (i.e. region of capture, termed edge - e) (Figure 42a). This axis was chosen for analysis because it is one of the clearest for differentiating the opaque zones for fish ageing. Laser settings were: beam diameter 40 µm, fluence 10 J cm^{-2}, and repetition rate 6 Hz, with 8 µm s^{-1} stage movement along the transect path. Ablation occurred in helium that was mixed with argon for injection to the plasma. Each transect path was pre-ablated as a final surface cleaning step (fluence 6 J cm^{-2}, repetition rate 5 Hz, and 60 µm s^{-1} stage movement along the transect path). The ICP-MS measured the isotopes of ^{25}Mg, ^{55}Mn, ^{88}Sr, ^{138}Ba, and ^{43}Ca. The latter was used as the internal standard to adjust for variation in ablation yield. The Ca concentration of otolith matrix was 38.8% by weight (Yoshinaga, *et al.* 2000). Blanks were obtained by analysing sample gases for approximately 50 x ICP-MS scans of the selected isotopes (elements) prior to sample ablation, and the averages of the blank counts were subtracted from the sample counts prior to calibration. Calibration was achieved with the National Institute of Standards (NIST) 612 certified reference pellet (Lahaye *et al.* 1997) analysed by 100 scan transects (first 30 scans as blanks) between every four otolith transects. Samples were prepared, mounted and analysed in random order with respect to collection areas. Data are presented as molar ratios to Ca.

The profiles for each element:Ca ratio was matched to fish age (i.e. yearly growth zones) using the opaque zones in the otolith macrostructure (see Results Chapter 2). After analysis by laser ablation ICP-MS, a digital image of the otolith was recorded from which the increment widths were measured from the core to the otolith margin adjacent to the trench left by the ablation path on the surface of the otolith section (Figure 42a). Using these distances, the known rate of movement of the laser beam across the otolith and the time taken for individual ICP-MS scans of the isotopes the consecutive element:Ca measurements were divided into consecutive age (years) zones using a MACRO program in Excel, with the core and edge regions being demarcated by the deviations in the laser transect path (i.e. Figure 42a). The element:Ca measurements for each annual age, core and edge zone were then integrated to provide average element:Ca ratio data for each zone that were used for further statistical analysis.

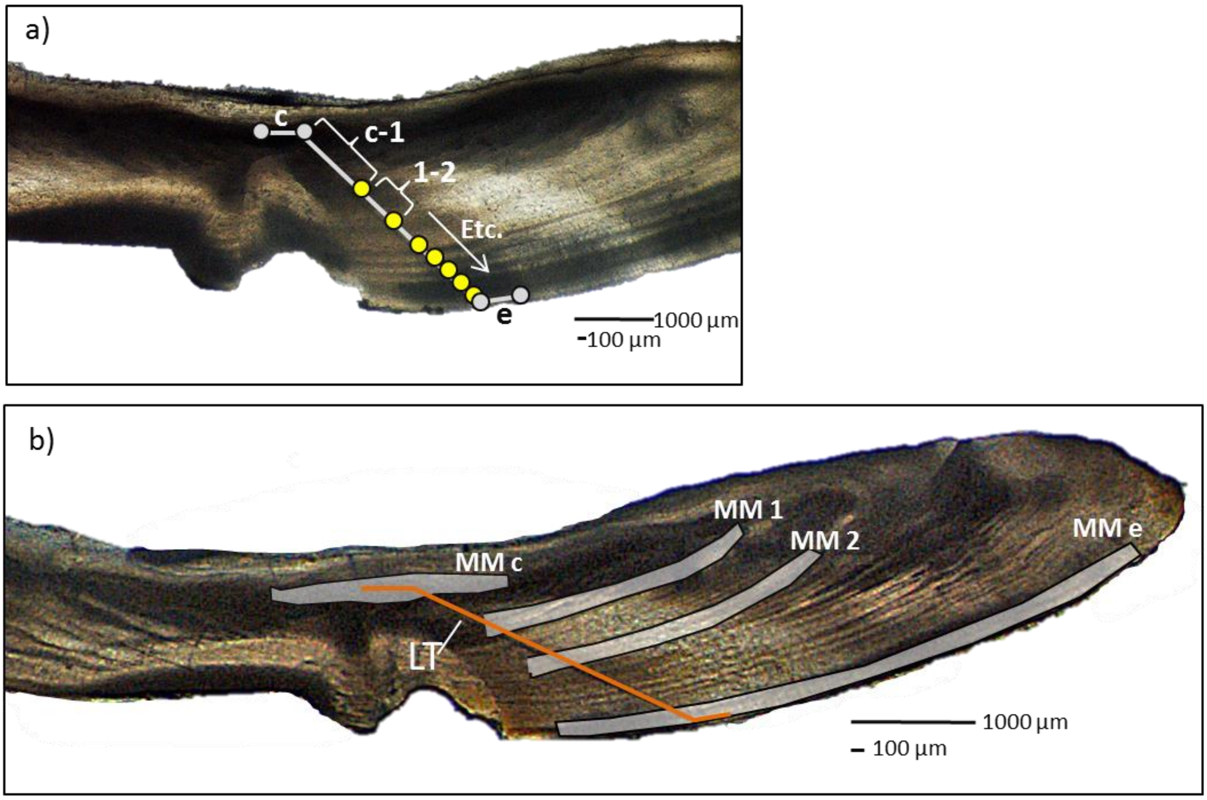

Figure 42 Images of transverse sections of Blue-eye Trevalla otoliths showing sampling protocols for a) laser ablation life history profiles (c = core, e = edge, increments indicated by yellow circles) and b) stable isotope analyses, MM c = micro-mill zone core, MM 1 = micro-mill increment zone 1, MM 2 = micro-mill increment zone 2, MM e = micro-mill increment zone edge, LT = laser transect path

Stable Isotope analysis

After otolith sections had been analysed by LA-ICP-MS they were then sampled using a micro-mill (New-Wave Research) (Figure 43). The micro-mill was programmed to remove otolith material (80–100 µg) from the core region and the marginal region (edge) of all otoliths (Figure 42b). For a sub-set of otoliths, two other regions were sampled, one region at around the first increment zone (i.e. pelagic juveniles prior to transition to demersal adult habitat), and another around the second increment zone (i.e. hypothesised time of transition to the demersal habitat) (Figure 42b). These additional zones were chosen as an exploration of shifts in temperature exposure during life history and to confirm the timing of the transition to deep water habitat at 2-years of age. For these analysis 24 seamount, and 19 slope samples were used. Seamount samples consisted of Fraser (2), Britannia (3), UQld (2), Barcoo (3), Taupo (2), Derwent Hunter (3), Lord Howe 3 (1), Lord Howe 4 (2), Gascoyne (2) and Cascade Plateau (4). Slope samples consisted of sth-NSW (3), Bass Canyon/East Flinders Is. (4), west Tasmania/west Bass Strait (4), WestKI/Gab (4), WA-Esperance (4).

The micro-mill zone in the core (c) region extended for approximately 800–1000 µm to the dorsal and ventral sides of the core (Figure 42b). Micro-mill trenches were approximately 150 µm wide and up to 300 µm deep. The sample of the core region is estimated to have incorporated approximately the first 3–4 months of life (refer to daily age estimates of the inner otolith zones in Results Chapter 2), whereas the samples along the otolith edge would have captured at least the last year of life.

The otolith powders from each sampling zone were transferred into individual 0.2 ml Eppindorf PCR tubes for storage prior to analysis. Stable carbon and oxygen isotope composition were determined using a ThermoFisher GasBenchIII gas preparation and introduction system coupled to a ThermoFisher DeltaVPLUS isotope ratio mass spectrometer via the ThermoFisher ConFloIV (Advanced Analytic Centre's Environmental Isotope Laboratory, James Cook University, Cairns). Carbon dioxide was evolved from carbonate powder by reaction with 100% orthophosphoric acid in 15 mL exetainer vials after atmosphere was replaced with He. Repeat samples of NBS-18 and NBS-19 (international standards) with similar mass to unknown samples provided monitoring of accuracy and precision. Precisions (s.d.) for international standards were better than 0.1‰ for both $\delta^{13}C$ and $\delta^{18}O$. Both $\delta^{13}C$ and $\delta^{18}O$ values are reported relative to Vienna PeeDee Belemnite (VPDB).

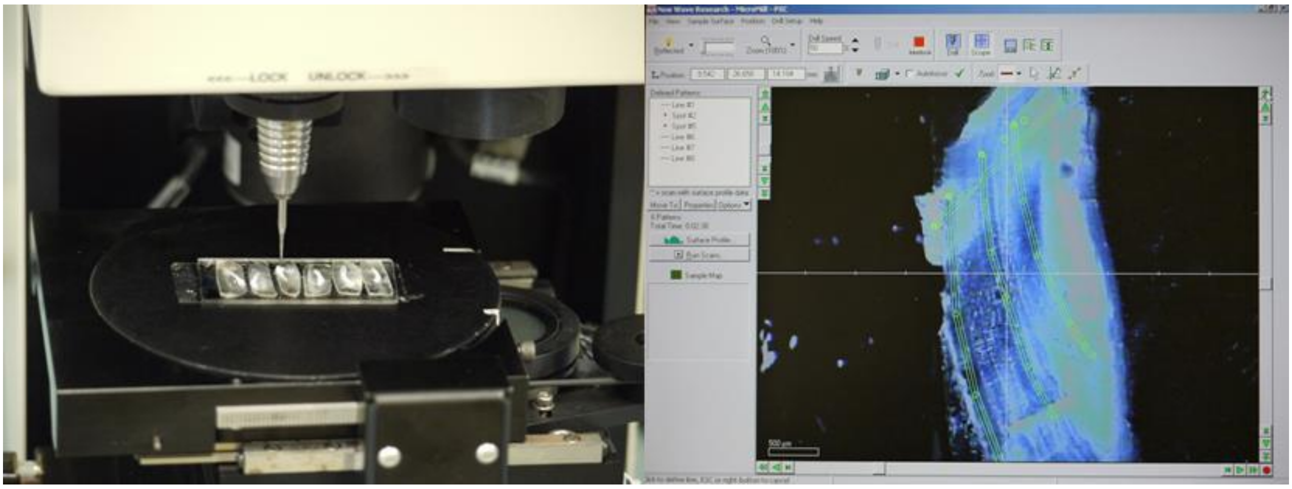

Figure 43 Images of (left) micro-mill drill with blue-otolith sections, (right) screen grab showing programmed micro-mill drill paths (green lines).

Data analysis

The focus of this study was to compare differences among fishery areas for the individual age zones and the cores and edges rather than comparing between the different ages across the profiles. Therefore, the spatial comparisons for each age were conducted as separate analyses, as opposed to a repeated measures approach. The similarities and differences among areas for each age were used to address specific questions about spatial separation with age and to infer stock structure. To achieve these comparisons, it was necessary to simplify the transect data. For each otolith and element, an annual, age-related mean was calculated from the series of elemental concentrations that were assigned to each year of life. For each otolith this provided profiles of age-related mean estimates of the element:Ca ratios for Ba, Sr, Mn and Mg, from all increments from the otolith core to the margin (edge zone). These increments are labelled c, c-1, 1-2, 2-3, 3-4 and so on, C (core) and e (edge), relating to the otolith material deposited between the consecutive opaque zones and for the otolith core and margin. We focussed statistical comparisons on increment zones from the core (c) to increment zone 5-6 (i.e. age 5–6 years) and the edge zone. For the edge zone, however, we only made comparisons for Ba:Ca, Sr:Ca, Mn:Ca, $\delta^{13}C$ and $\delta^{18}O$ as there was clear Mg contamination in many of the edge zone samples indicated by high Mg level relative to the most adjacent increment zone. The period of life up to age 6 years encompassed the pelagic life-stage to about 2 years and 3–4 years of the demersal life phase. Qualitative comparison of otolith profiles for older fish were also used to indicate if any obvious changes with age may occur that may indicate movements at older ages.

For each age and stable isotope sampling zone the among-area comparisons of individual element:Ca ratios and the stable isotopes were achieved using linear mixed models and general linear models (ANOVA). Linear mixed models were initially applied for all comparisons of annual increment zones and the core zone with a random term for cohort nested in sampling area. For the edge zone comparisons of Ba:Ca, Sr:Ca, Mn:Ca, $\delta^{18}O$ and $\delta^{13}C$ random terms were also tested for 'age nested within area' and 'capture year nested within area'. The influence of the random term was assessed by a change in deviance test between models with and without the random term. The change in deviance test statistic has a chi-squared distribution with degrees of freedom (df) equal to the difference in the number of parameters estimated. In this case with df 1 if the difference of the deviance (-2 log-likelihood) between the models with and without the random term was less than 4 then the random term had no significant effect ($p>0.05$), and in these cases the general linear model was applied. The random term 'cohort nested in area' was only significant for the comparisons of Ba:Ca for increment zones 4-5, and 5-6. The random term 'capture year nested within area' was significant for the Mn:Ca edge (e) zone comparison. Tukey's pairwise *post-hoc* comparisons were used to identify which area means were significantly different.

Data for each element:Ca and isotope ratio and otolith zone were checked for assumptions of normality and homogeneity of variances using frequency histograms, Q-Q plots, box and residual plots. The Box-Cox power transform was used to transform data that did not meet these assumptions. All data except for Sr:Ca, Mg:Ca, $\delta^{18}O$ and $\delta^{13}C$ required transformations for analysis. For $\delta^{13}C$ ontogenetic trends in otolith carbonate are well known (Weidman and Millner 2000) and were evident in the data with the inclusion of the older Cascade Plateau and Southern NSW samples (linear regression, $p<0.001$, co-efficient 0.075). Therefore for the samples from these two areas we adjusted the $\delta^{13}C$ values of the otolith edge samples to their age 6 year equivalent using the co-efficient (slope) of the regression of $\delta^{13}C$ on age. The age 6 year equivalent was used as this was average age of the other samples with these areas excluded.

Multivariate otolith chemistry was compared among areas for the individual otolith zones, using MDS (multidimensional scaling) to display patterns of variation among areas and PERMANOVA to indicate areas that were significantly different from each other. For the juvenile zones (c, c-1 and 1-2) we only analysed the element:Ca ratios as these data were available for all three of the early life zones and univariate analyses indicated significant variation among areas for each element:Ca ratio in at least one of the zones. For the multivariate edge analysis we analysed Ba:Ca, $\delta^{18}O$, Sr:Ca, and $\delta^{13}C$ (age adjusted values for Southern NSW and Cascade Plateau). Data for Mg:Ca and Sr:Ca were divided by 100 and 1000 respectively to normalise the scale of variation with the other variables. The data for all variables were log (x+1) transformed, and a Euclidean distance-based matrix was constructed upon which the PERMANOVA was performed. MDS plots were constructed based on the centroids for each sampling area from this Euclidean distance matrix.

To further inform inferences on spatial separation and habitat transition of Blue-eye Trevalla, $\delta^{18}O$ values of otolith zones were converted to water temperature estimates using fractionation equations from the literature (Høie *et al.* 2004) (below) and $\delta^{18}O$ seawater water values extracted from the 'Global Gridded Data Set of Oxygen Isotopic Composition in Seawater' (LeGrande and Schmidt 2006). Equation for converting $\delta^{18}O_{otoliths}$ to water temperature (Høie *et al.* 2004):

$$\delta^{18}O_{Otolith(VPDB)} - \delta^{18}O_{water(VSMOW)} = 3.90 - 0.20T(°C)$$

Temperature estimates derived from $\delta^{18}O$ in otoliths were compared with actual water temperature data obtained for bottom waters at various depths in each of the three fishing regions (sourced from the CSIRO; CARS - Climatology of Australasian Regional Seas program). Water temperatures derived from otoliths are compared to actual water temperature depth profiles at shelf and seamount locations. Because it is uncertain whether individual fish may have originated in their regions of capture, temperature conversion for the core otolith zone are presented using both the average $\delta^{18}O$ water value across all the areas and the local area estimates. For the edge otolith zone the local area $\delta^{18}O$ water value was applied. For the core zone $\delta^{18}O$ water values were applied using estimates from surface waters, and for the edge zones we used values estimated for 400 m depth, the reported residence depth of adult Blue-eye Trevalla (Figure 3, Results Chapter 1).

Results

Univariate otolith chemistry

General patterns

Analysis of Blue-eye Trevalla otolith element:Ca profiles for Mg:Ca, Mn:Ca, Ba:Ca and Sr:Ca showed that variation among sampling areas was greatest for Ba:Ca (Figure 44). There was generally no clear variation among areas for Mg:Ca, except for the Cascade Plateau in the core zone which showed lower mean values than the other areas. For Sr:Ca the only clear variation among areas was for the WA-Esperance samples that diverged to lower values than the other areas from increment zone 4-5 to the edge zone (Figure 44). For Mn:Ca, Derwent Hunter displayed a higher mean value for the core and core-1 (c-1) zones, but similar to Mg:Ca and Sr:Ca, all other areas were similar across the profiles. For Mg:Ca and Mn:Ca there were clear trends of decreasing levels with age out from the core. For Mn:Ca the decreasing trend was greatest between the core and the increment zone 2-3 after which values stabilised, but for Mg:Ca the downward trend was more gradual with age (Figure 44). In contrast, for Sr:Ca there was an increasing trend from the core to increment zone 4-5, after which values plateaued (Figure 44).

For Mn:Ca the only significant difference among areas was for the c-1 increment zone, where the Derwent Hunter (DH) area was significantly higher than the West Tasmania/west Bass Strait (WBS) area (Table 16, Figure 44). For Mg:Ca the only significant differences among areas was for the core zone where Derwent Hunter, Taupo (TPO), and WA-Esperance (WA) were all higher than the Cascade Plateau (Table 16, Figure 44). For Sr:Ca, variation among areas was significant in the older increment zones; 4-5, 5-6 and the edge zone. All the significant differences for Sr:Ca involved WA-Esperance being lower than other areas (Table 16, Figure 44).

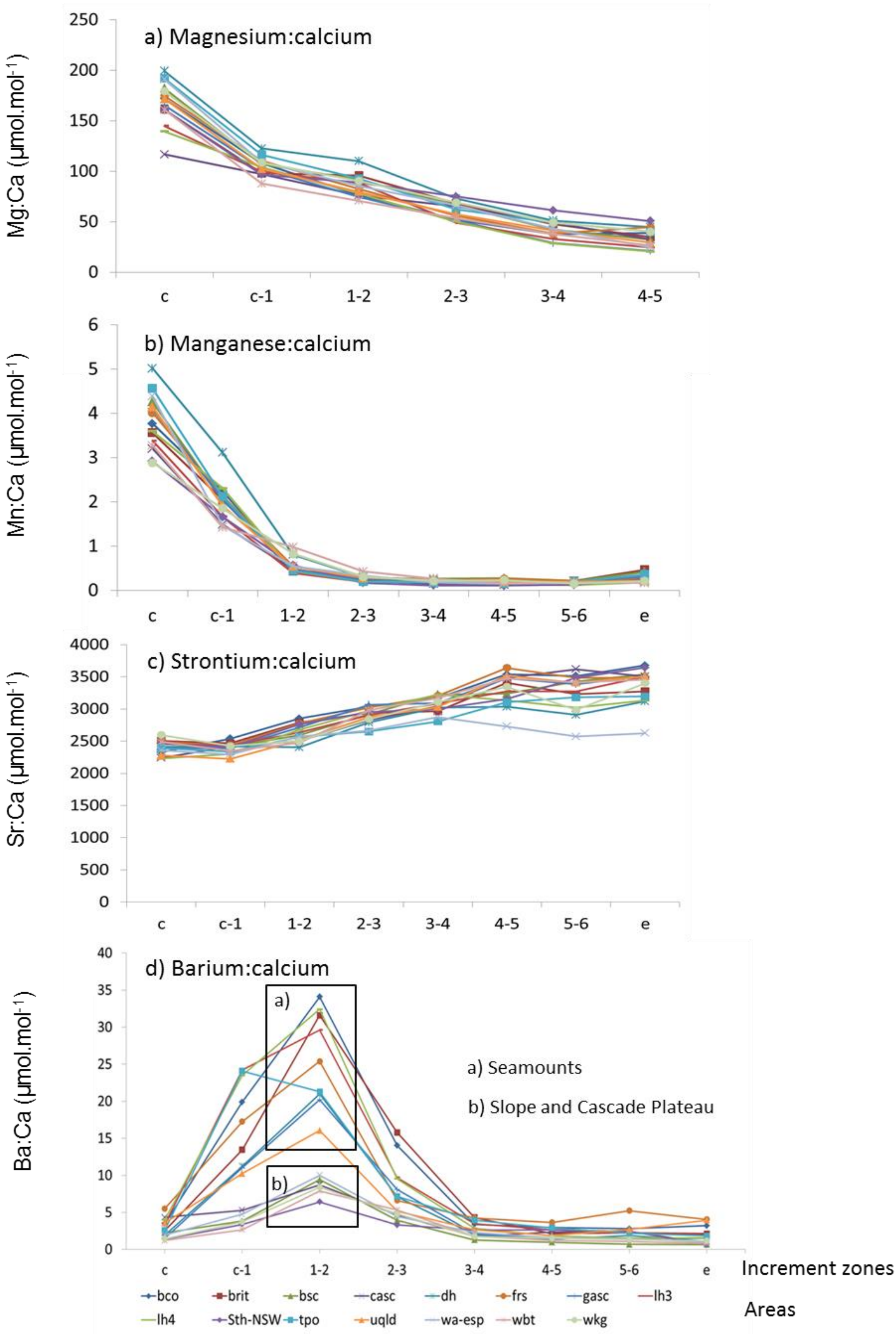

Figure 44 Comparisons of Blue-eye Trevalla otolith element:Ca profiles among sampling areas (data are means for each increment zone); a) Magnesium:Calcium, b) Manganese:Calcium, c) Strontium:Calcium, d) Barium:Calcium. Data for the edge (e) zone not included for Magnesium:Calcium due to indications of Mg contamination at the edge zones. See Appendix 5 for key to site codes.

Table 16 Single factor comparisons (linear mixed models LMM, General linear models GLM) among Blue-eye Trevalla fishery areas of element/Ca ratios in individual otolith increment zones. See Appendix 5 for key to site codes.

Element/Ca	**Otolith zone** *=LMM applied	**Area** (P-value)	**Tukey's pairwise comparisons** P-value * ≤0.05, **≤0.01, ***≤0.001, seamount areas in bold text
Mg:Ca	c	0.019	**DH**>**CASC**** **TPO**>**CASC*** WA>**CASC***
	c-1	ns	ns
	1-2	ns	ns
	2-3	ns	ns
	3-4	ns	ns
	3-4	ns	ns
	4-5	ns	ns
	5-6	ns	ns
Mn:Ca	c	ns	ns
	c-1	0.026	**DH**>WBT**
	1-2	ns	ns
	2-3	ns	ns
	3-4	ns	ns
	4-5	ns	ns
	5-6	ns	ns
	e*	ns	ns
Sr:Ca	c	ns	ns
	c-1	ns	ns
	1-2	ns	ns
	2-3	ns	ns
	3-4	ns	ns
	4-5	0.007	**FRS**>WA** **BCO**>WA* **UQLD**>WA*
	5-6	0.004	**NSW**>WA** **CASC**>WA** **BCO**>WA* **FRS**>WA*
	e	<0.001	NSW>WA*** **BCO**>WA*** BSC>WA** **UQLD**>WA** **LH3**>WA** **CASC**>WA* **FRS**>WA*
Ba:Ca	c	<0.001	**FRS**>WBT, NSW*
	c-1	<0.001	**BCO**>WBT***, WKG**NSW**; BSC*, WA* **LH3**>WBT, WKG, NSW***; BSC, WA**, **LH4**>WBT, NSW, WKG***; BSC,WA** **TPO**>WKG,WBT, NSW***; BSC, WA* **FRS**>WKG*
	1-2	<0.001	**BCO**>NSW, WBT***; WKG**; WA, **CASC*** **BRIT**>NSW,WBT***; WKG**; WA, **CASC*** **FRS>**NSW**; WBT* **LH3**>NSW***; WBT**; WKG, **CASC*** **LH4>**WBT, NSW***; WKG**; WA, **CASC***; **TPO**>NSW**
	2-3	<0.001	**BCO**>NSW* **BRIT**>NSW***; BSC**; **CASC**, WKG, WA, WBT*
	3-4	0.007	**BCO**>BSC* **FRS***>BSC
	4-5*	0.020	**BCO**>BSC*
	5-6*	0.031	**FRS**>BSC* **BCO**>BSC*
	e	<0.001	**BCO**>NSW, WA, WBT, BSC, **CASC, DH*****; WKG** **BRIT**>NSW***; BSC** **FRS**>NSW, BSC***; WBT**; DH, WA, **CASC*** **GASC**>NSW***; BSC** **LH3**>NSW, BSC*** **LH4**>NSW***; BSC** **TPO**>NSW***; BSC** **UQLD**>NSW***; BSC* WKG>NSW*** WA>NSW* WKG>BSC*

Barium:Calcium

There was a clear divergence in Ba:Ca between the seamount and shelf locations, with the exception of the Cascade Plateau, starting from the C-1 zone (core to first annual increment) until the age of 2–3 years (increment zone 2-3) when the profiles merged to similar values by the 4-5 increment zone (Figure 44). Observation of the separate profile charts for each area showed that for all seamount areas, except the Cascade Plateau, the mean Ba:Ca exceeded 10 µmol mol^{-1} for the age 1-2 increment zone (Figure 45), but for all the slope areas and the Cascade Plateau seamount, the mean Ba:Ca was either approximately equal to, or below 10 µmol mol^{-1} for the 1-2 increment zone (Figure 46). The mean integrated Ba:Ca levels for some of the seamount areas were in the order of 20-30 µmol mol^{-1} for the 1-2 year increment zone, with some areas having peaks spread across the c-1 and 1-2 increment zones (i.e. Taupo, Lord Howe 3 and 4). Interestingly all areas, irrespective of seamount or slope, showed peaks in the mean levels corresponding to the 1-2 year increment zone (Figure 45, Figure 46).

While it is not practical to present all 184 individual Ba:Ca otolith profiles, an example set of the variation in profiles observed is provide in Figure 47. These examples represent the range of different profiles that were observed across sampling areas. The difference in the mean annual integrated data reflect the proportions of these various profiles in each sample group (indicated by overlap among areas in Figure 48c). The seamount areas were mostly comprised of samples with larger peaks in Ba:Ca, whereas the slope areas had higher proportions of samples with lower Ba:Ca peaks or flatter profiles. Notable in the profiles was that Ba:Ca peaks generally originated prior to the first increment zone, and in some instances the rise in Ba:Ca levels was abrupt (Figure 47). Generally, the Ba:Ca peaks had reduced to background levels by annual increment 2-3, and beyond this generally showed no further large peaks or notable variation with age. The maximum Ba:Ca levels in numerous otoliths reached up to, and for some, exceed 100 µmol mol^{-1}, extraordinarily high levels for marine fish otoliths. Similar anomalies were not observed for the other element:Ca ratios.

Significant differences in otolith Ba:Ca among areas where detected for all otolith increment zones (Table 16). For the increment zones from the core to increment 5-6, all the significant differences detected involved seamount (excluding Cascade Plateau) areas being significantly higher than slope areas or the Cascade Plateau (Table 16). For these otolith zones most of the significant differences among areas were observed for the c-1 (core to increment 1) and increment 1-2 zones (Table 16, Figure 48b, c). For these two otolith zones Barcoo, Lord Howe 3 and Lord Howe 4 all showed at least one significant difference with each of the slope areas and the Cascade Plateau, Taupo showed differences to all slope areas, but not the Cascade Plateau, Britannia showed differences to Cascade Plateau and all slope areas except, Bass Canyon/East Flinders Is., which was however different for increment zone 2-3. Fraser showed differences to Southern NSW, West KI/GAB and Western Tasmania/Western Bass Strait (Table 16, Figure 48b). For two seamount areas; Derwent Hunter and ‘unknown’ Queensland, no significant differences were observed with any other seamount or slope areas (Table 16, Figure 48b).

For the otolith edge zone (Figure 48a), the patterns of significant variation among areas were more complex, with significant variation detected both within and between seamount and slope areas (Table 16). For slope areas significant differences were detected between WA-Esperance and West KI/GAB (both higher) with Southern NSW, and West KI/GAB (higher) with Bass Canyon/East Flinders Is. (Table 16). Seamount areas, Fraser, Britannia, Barcoo, Gascoyne, Lord Howe 3, Lord Howe 4, Taupo and ‘unknown’ Queensland, were all significantly higher than Southern NSW and Bass Canyon/East Flinders Is. Fraser and Barcoo, were also significantly higher than WA-Esperance, Derwent Hunter, Cascade Plateau, and Western Tasmania/Western Bass Strait. Barcoo was also significantly higher than West KI/GAB (Table 16, Figure 48a).

For the otolith core and edges, spatial patterns of variation in Ba:Ca were similar for both zones except for the Lord Howe 3, Lord Howe 4, Cascade Plateau, and Bass Canyon/East Flinders Is. where levels in the core were relatively higher than for the edge zones (Figure 48a). For the increment c-1 and 1-2, the 1-2 zone was generally a higher than the c-1 zone for all areas except for Taupo. As noted earlier form the observations of the individual un-integrated profiles, the peaks in Ba:Ca often extended across these two zones, therefore differences between the c-1 and 1-2 zones depend on whether the maximum values occurred prior to or after the first increment.

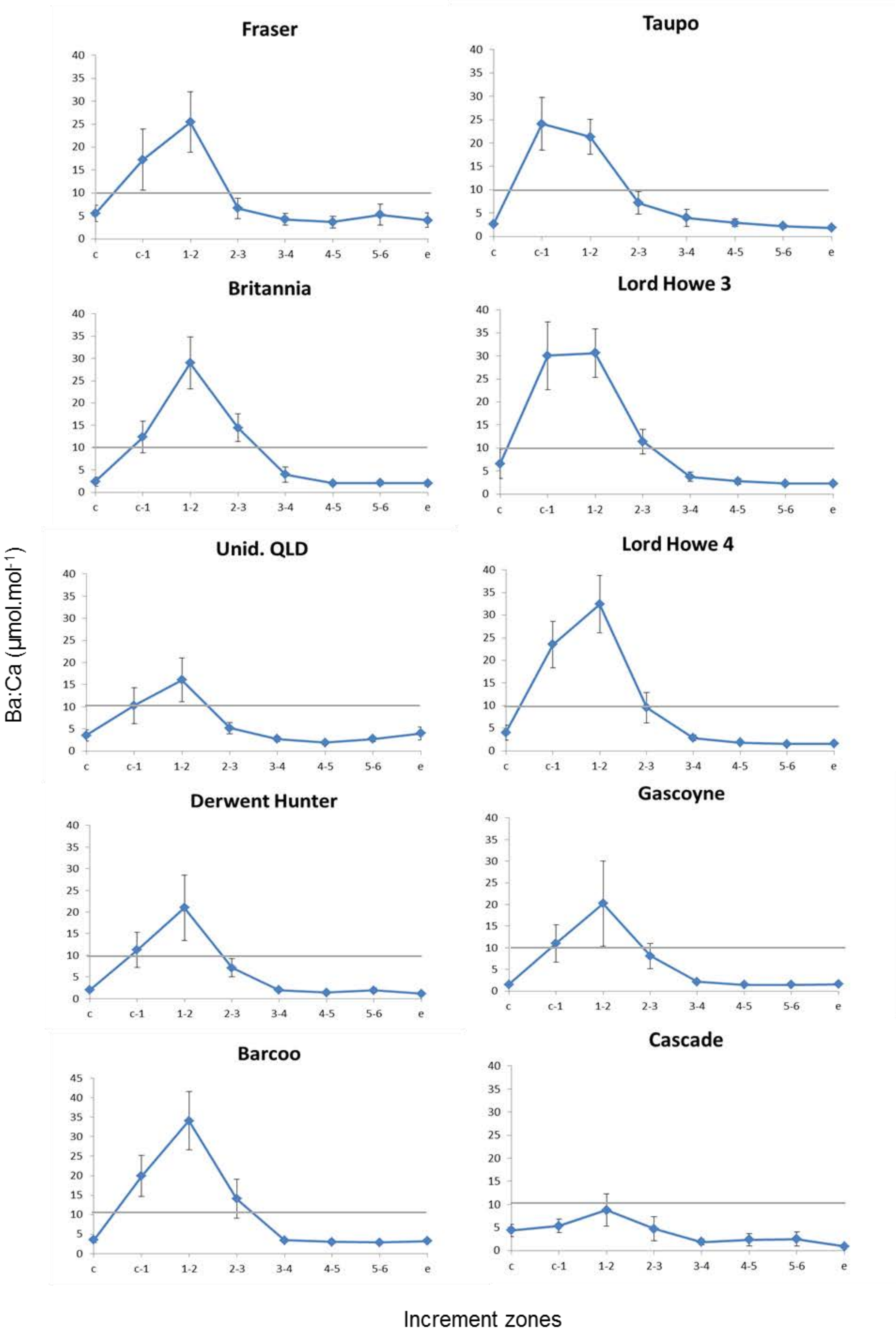

Figure 45 Seamounts: comparisons of Barium:Calcium profiles (mean ±SE for each growth zone) across otoliths sampled from 10 seamount locations.

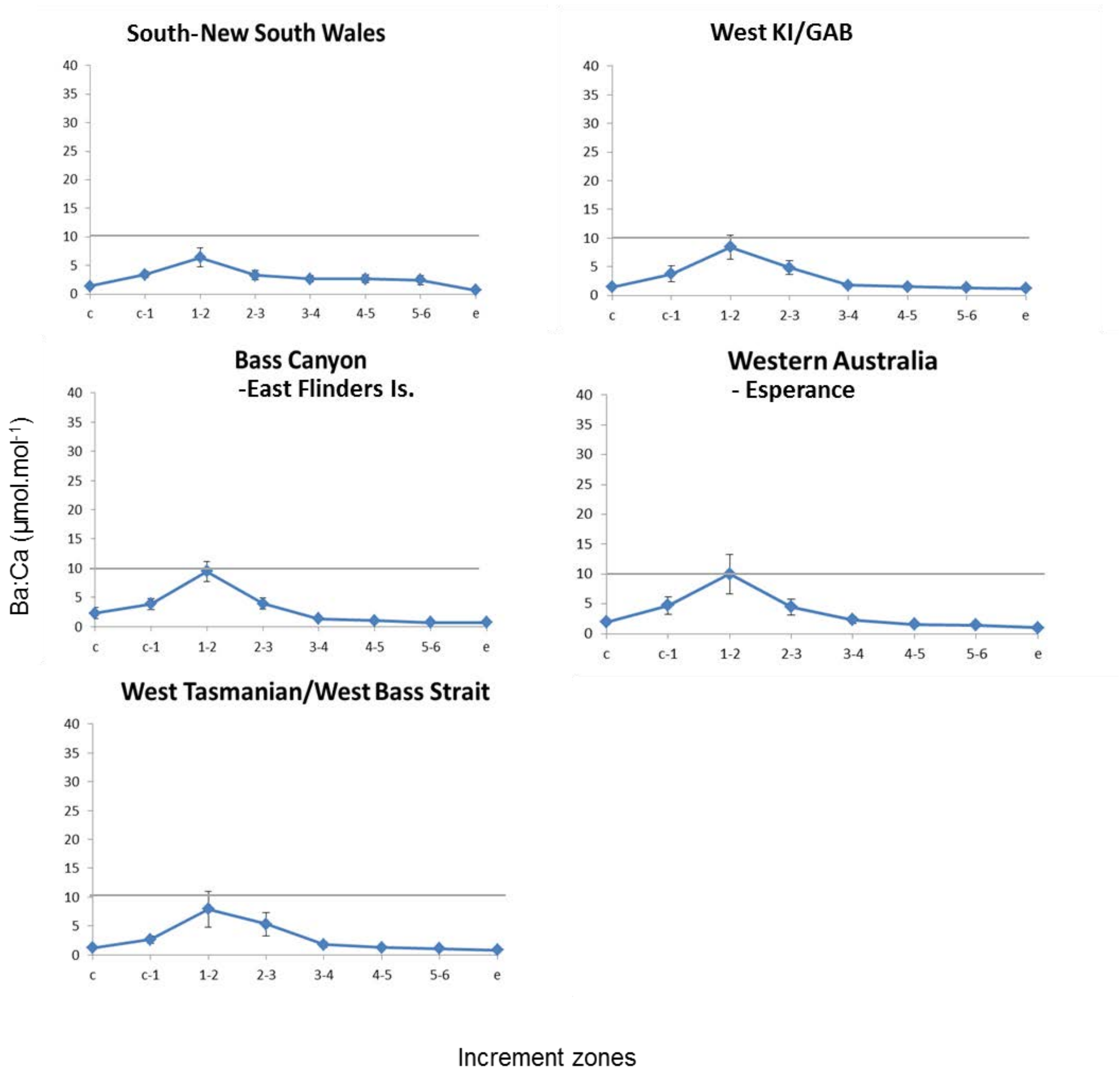

Figure 46 Slope: comparisons of Barium:Calcium profiles (mean ±SE for each growth zone) across otoliths sampled from 5 slope locations.

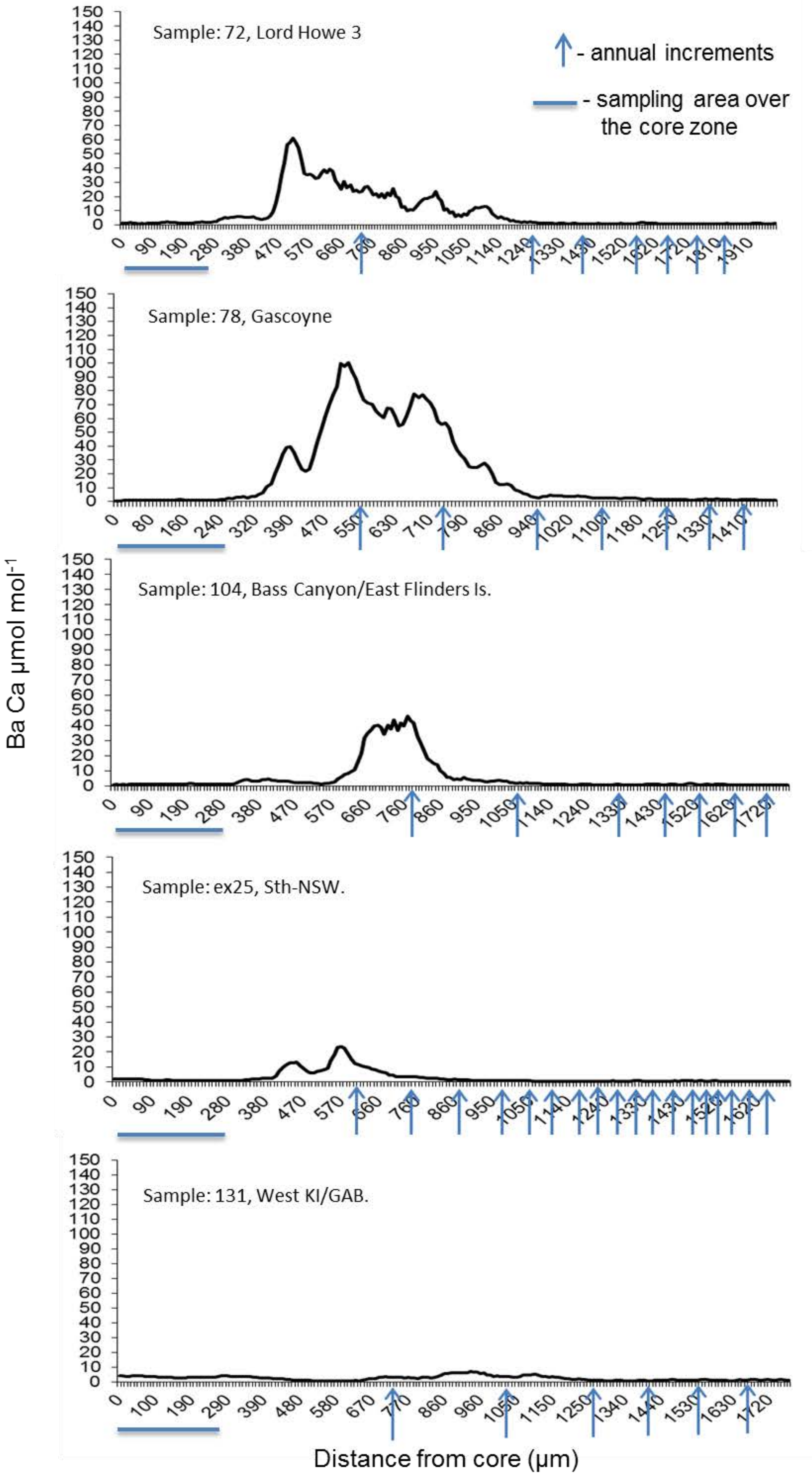

Figure 47 Examples of variation in the un-integrated Ba:Ca profiles observed across Blue-eye Trevalla otoliths. The arrows indicate approximate positions of the annual opaque increment zones, and the horizontal bars indicate the zone sample over the otolith core (i.e. the 'c' zone in Fig. 35a).

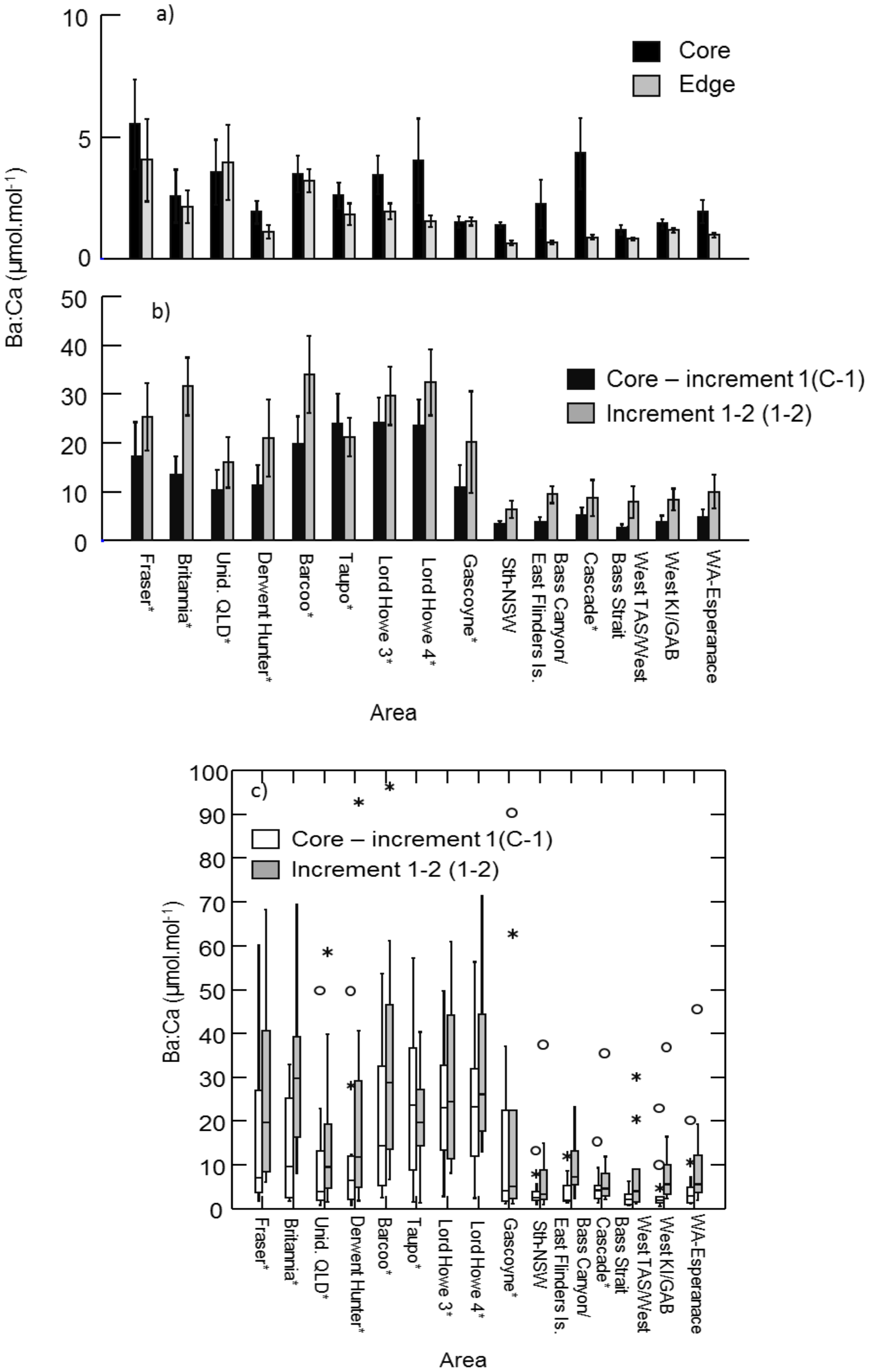

Figure 48 Comparison of Ba:Ca ratios (mean ±SE) of Blue-eye Trevalla otoliths among slope and seamount sites (indicated by*) for different otolith zones, a) core v edge zone, b) core-1 v increment 1-2 and, c) box-plots for the c-1 and 1-2 increment zones to display variation and dispersion of values within and among samping areas.

Stable Isotopes

$\delta^{18}O$

Cores

Variation among sampling areas in $\delta^{18}O$ of Blue-eye Trevalla otolith cores was not significant, reflecting a large amount of individual variability (Table 17Table 17 Single factor comparisons among Blue-eye Trevalla fishery areas of $\delta^{18}O$ and $\delta^{13}C$ ratios in otolith core and edge sampling zones. See Appendix 5 for key to site codes., Figure 49a). The highest (i.e. coolest) mean value was, however, for the West Tasmania/West Bass Strait area, as would be expected based on local water temperature, and the lowest (warmest) were for Taupo seamount and WA-Esperance, but there were no clear overall north-south trends and most seamount areas overlapped with the slope areas (Figure 49a).

Water temperature estimates derived from the $\delta^{18}O$ of Blue-eye Trevalla otolith cores indicated mean temperatures experience by Blue-eye Trevalla during the early-life pelagic phase were between 16–19°C (Figure 50a). For all areas except West Tasmania/West Bass Strait this range was consistent whether or not the average or local area value for $\delta^{18}O_{water}$ was applied. For the West Tasmania/West Bass Strait area, applying the local area $\delta^{18}O_{water}$ value suggested a mean temperature exposure of approximately 14°C. The temperature estimates obtained from conversion of otolith core $\delta^{18}O$ were consistent with the annual average values for surface waters across the sampling areas, albeit being lower than the most northern areas (Figure 50a, b), which may reflect spawning timing (spawning thought to occur in winter in northern areas).

Table 17 Single factor comparisons among Blue-eye Trevalla fishery areas of $\delta^{18}O$ and $\delta^{13}C$ ratios in otolith core and edge sampling zones. See Appendix 5 for key to site codes.

Isotope ratio	**Core** (P-Value, area)	**Tukey's pairwise comparisons**	**Edge** (P-value, area)	**Tukey's pairwise comparisons** P-value * ≤0.05, **≤0.01, ***≤0.00, seamount areas in bold text
$\delta^{18}O$	ns	ns	<0.001	NSW>**BCO, DH, TPO*****; **BRIT*** WBT>**BCO*****; **DH**, **TPO, BRIT, FRS** * BSC>**DH***, **TPO*** **LH4>DH, TPO***
$\delta^{13}C$	ns	ns	<0.001	**FRS**>WKG, **BCO****; **CASC**, **TPO*** **LH4**> WKG, **BCO*****; **CASC**, **TPO**** **LH3**>WKG** **BRIT**>WKG* **GASC**>WKG** NSW>WKG*** WBS>WKG**

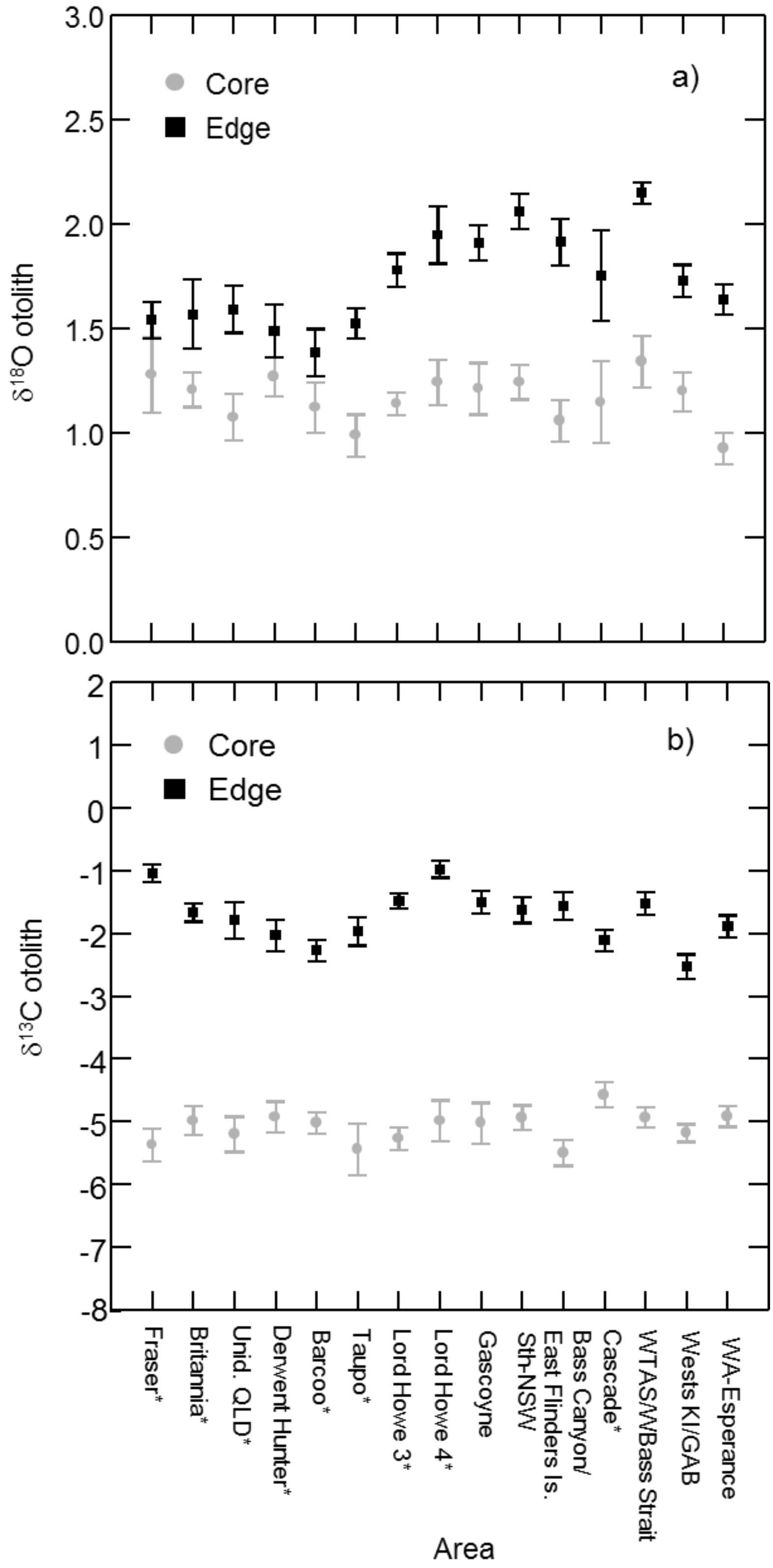

Figure 49 Comparisons of a) $\delta^{18}O$ and b) $\delta^{13}C$ (mean ±SE) for otolith core and edge zones. Sample areas from left to right are ordered from north to south to west. * indicates seamount areas

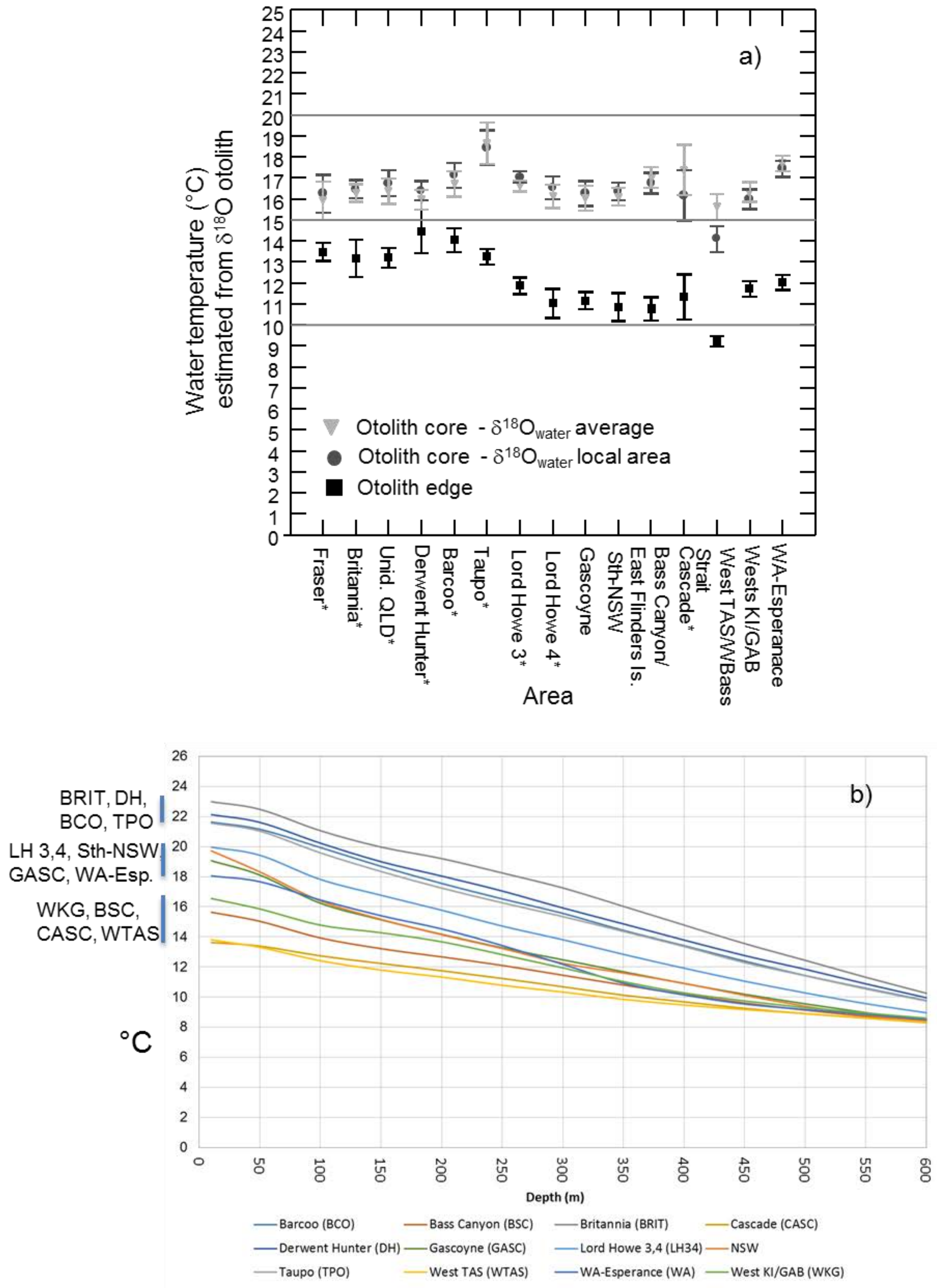

Figure 50 a) Comparisons of water temperatures (mean ±SE) estimated from $\delta^{18}O$ otoliths among sampling areas , and b) actual CARS water temperature depth profiles to 600 m across sampling areas (with exclusion of the Fraser seamount not available). *indicates seamount areas

Edges

In contrast to the otolith cores, $\delta^{18}O$ of Blue-eye Trevalla otolith edges showed clear trends with latitude, with mean $\delta^{18}O_{otolith}$ values increasing from the northern seamounts south to West Tasmania/West Bass Strait, which had the highest (coolest) value, and then decreasing to the western more northerly latitude slope areas of West KI/GAB and WA-Esperance (Figure 49a). Interestingly the Bass Canyon/East Flinders Island and Cascade Plateau areas had lower mean values than the Southern NSW area, although sample sizes were lower and variation was greater for the later areas (Table 15, Figure 49a). Variation among areas was significant, with the West Tasmania/West Bass Strait area being significantly higher (cooler) than the northern Fraser, Britannia, Taupo, Derwent Hunter and Barcoo seamounts (Table 17). Southern NSW was significantly higher than Barcoo, Derwent Hunter, Taupo and Britannia. Bass Canyon/East Flinders Is. and Lord Howe 4 were significantly higher Taupo and Derwent Hunter (Table 17, Figure 49a)

Water temperature estimates derived from the $\delta^{18}O$ of otolith edges indicated mean temperatures experienced by Blue-eye Trevalla during the demersal adult phase were between 9 and 14°C, with clear differences between the seamount and slope areas, and clear separation of the West Tasmania/West Bass Strait area, which had the lowest estimated temperature exposure for the adult demersal phase (Figure 50a).

Comparisons of water temperature estimates from $\delta^{18}O_{otolith}$ edges with actual water temperature data at 400 m depth were remarkably consistent for each area (Figure 51). This consistency reflects not only the reliability of the $\delta^{18}O_{otolith}$ as a temperature indicator, but also the longer period of environmental integration for the edge zone (i.e. at least 1 year) which matched the annual time scale of the water temperature data. The notable differences were for the WA-Esperance and WestKI/GAB areas, where the otolith based predictions indicated warmer water exposure than actually expected at 400 m. For these areas the actual depth where the otolith predicted temperatures occurred was at around 300 m (Figure 50b).

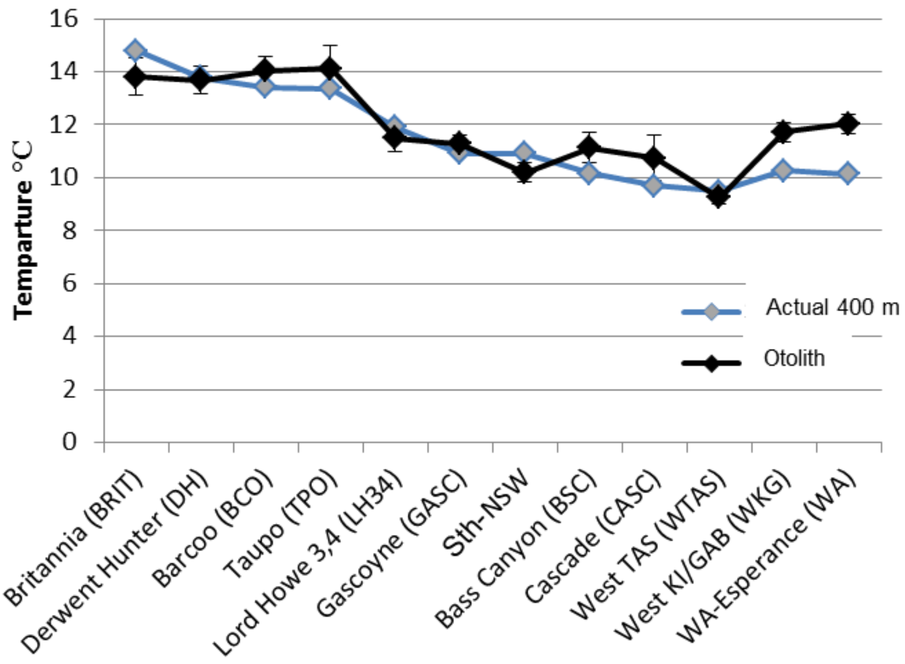

Figure 51 Comparisons of predicted water temperatures from otolith edge $\delta^{18}O$ (last year of life)(mean ±SE) and actual water temperatures at 400 m depth (annual averages) for areas where both data were available.

Temperature variation with age from $\delta^{18}O$ profiles

The estimates of temperature derived from $\delta^{18}O$ of the otolith cores, increments 1, 2, and edge zones showed that for the both the seamount and slope sub-samples the early part (first 3–4 months) of the pelagic life-phase was spent in cooler temperatures, than the period around the formation of the first increment zone (Figure 52), considered to be at approximately 350 days age (Results Chapter 2). While the temperature estimates overlapped between the seamount and slope areas for the core zone, at the first increment zone they had diverged, with the slope samples being exposed to on average colder water. However, for both groups the temperature estimates were considerably higher (i.e. by 2–3°C) than for the core zone (Figure 52). At increment zone 2 the estimated temperatures dropped for both the seamount and slope groups to be lower than the core and increment zone 1, but higher than the edge zone, when the fish were known to be at the adult depth. This indicated that at around age 2 years, the Blue-eye Trevalla sampled from both seamount and slope groups had transitioned to deeper cooler waters, but not as deep as the adult stages.

$\delta^{13}C$

Cores

Similar to $\delta^{18}O$, there was no significant variation among areas in $\delta^{13}C$ for the otolith cores (Table 17). There were also no apparent trends with latitude or broader scale patterns of variation among seamount and slope areas (Figure 49b).

Edges

$\delta^{13}C$ for the otolith edges did show significant variation among areas (Table 17). While there was considerably more spatial variation in $\delta^{13}C$ of the otolith edges than the cores, the main differences involved the West KI/GAB area being significantly lower than the Fraser, Lord Howe 4, Lord Howe 3, Britannia, Gascoyne, Southern NSW, and West Tasmania/West Bass Strait areas (Table 17, Figure 49b). The Fraser and Lord Howe 4 areas were also significantly higher than Barco, Taupo and the 'age adjusted' Cascade Plateau data.

$\delta^{18}O$ and $\delta^{13}C$ bivariate comparisons

The bivariate plots of $\delta^{18}O$ and $\delta^{13}C$ for the otolith cores showed major overlap among seamount and slope area, with exceptions being Taupo and WA-Esperance being separated from the main grouping by their lower average $\delta^{18}O$, and Cascade Plateau separated by higher $\delta^{13}C$ (Figure 53a)

For the edge zone there was more group structure, with Lord Howe 3, Lord Howe 4, Gascoyne, Southern NSW, West Tasmania/West Bass Strait and Bass Canyon/east Flinders Is. showing higher $\delta^{18}O$ and lower $\delta^{13}C$ than the other areas (Figure 53b). The Fraser seamount area was somewhat of an outlier with lower $\delta^{13}C$ and lower $\delta^{18}O$.

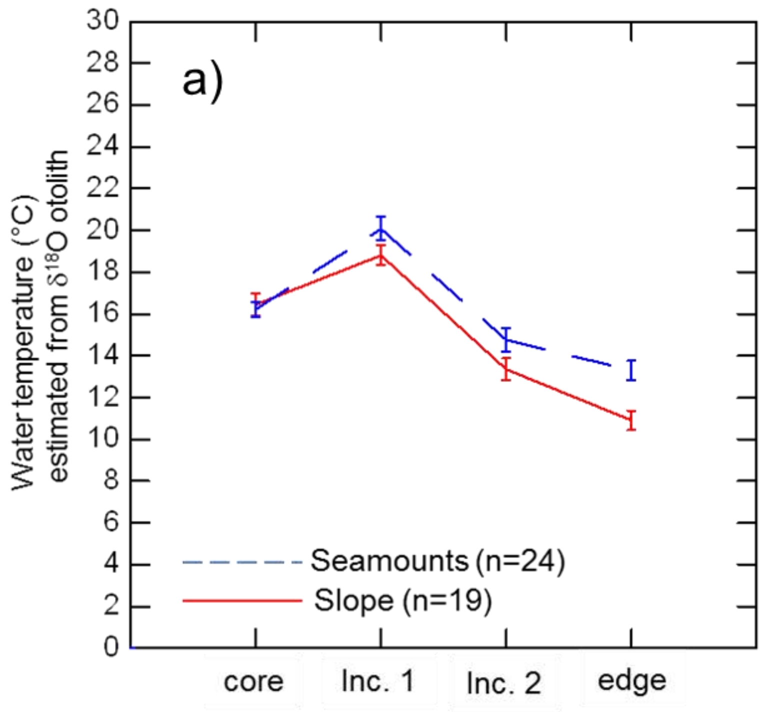

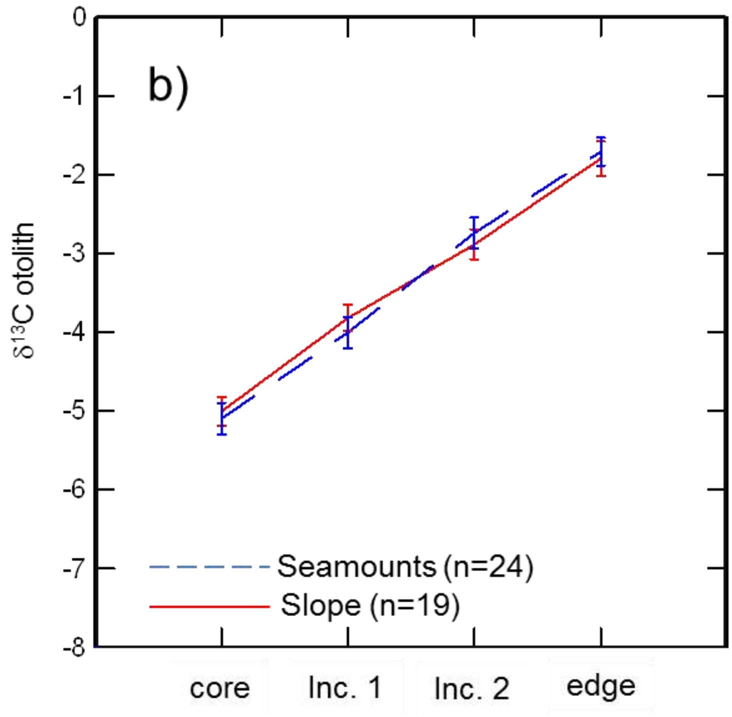

Figure 52 Comparison of a) environmental water temperatures (mean ±SE) estimated from $\delta^{18}O$ otolith and b) $\delta^{13}O$ across otolith growth zones experienced by Blue-eye Trevalla sampled from slope and seamount location. Sub-samples were included from all slope and seamount locations (see methods).

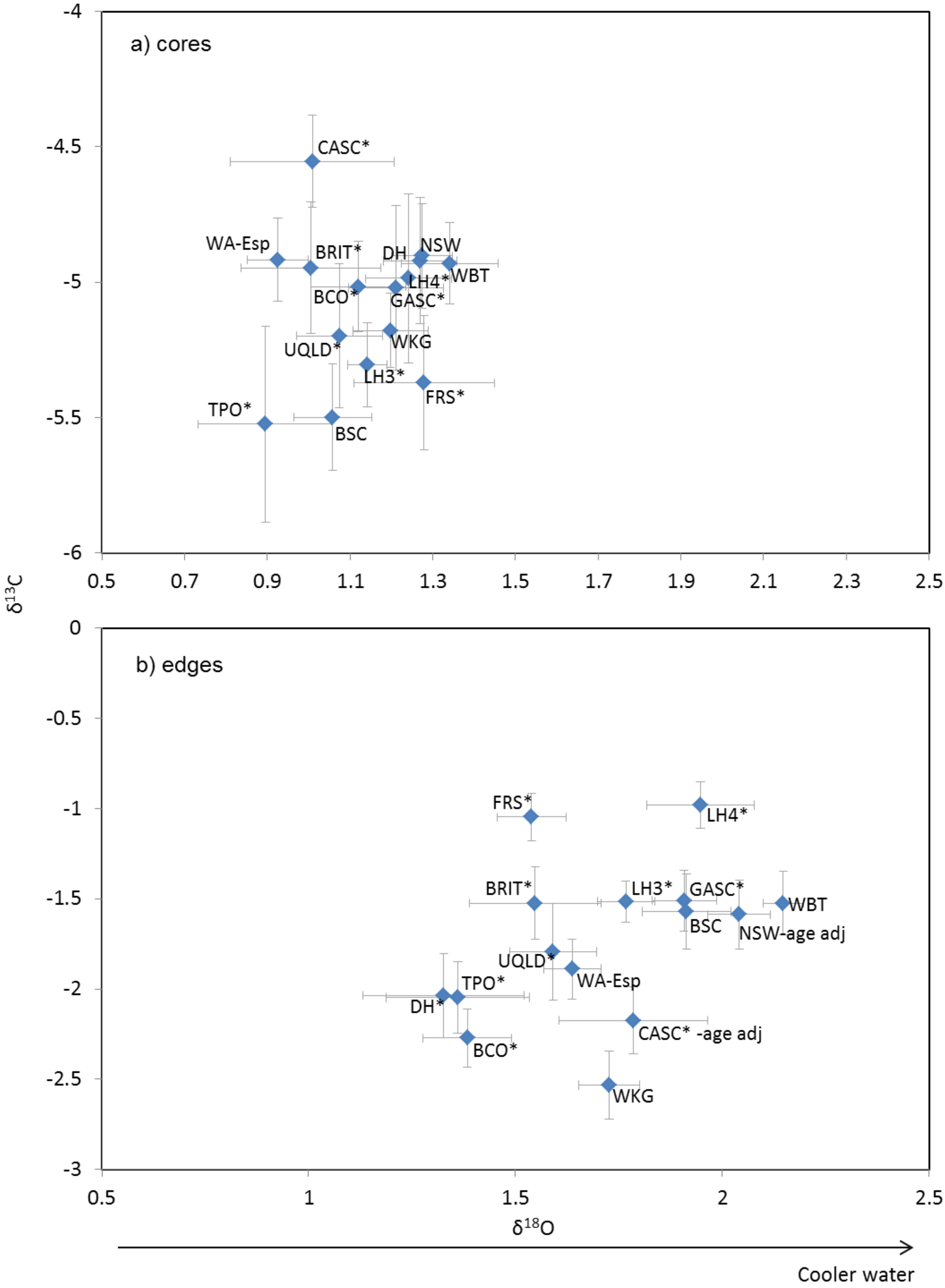

Figure 53 Bi-plots of $\delta^{18}O$ and $\delta^{13}C$ (mean ±SE) of otolith a) cores and b) edges showing variation among shelf and seamount areas. * indicate seamount areas. See Appendix 5 for key to site codes.

Multi-variate otolith chemistry

Early life history stages

Multidimensional scaling plots (Ba:Ca, Mn:Ca, Mg:Ca, Sr:Ca) of the three early life history otolith zones (core, core-increment 1 and increment 1-2) showed clearer separation among the slope and seamount areas for zones c-1 and 1-2 than for the core zone (Fig. 54 a-c). Although for the core zone the seamount areas were still generally more similar to each other than to the slope areas, with the exception of Gascoyne. For increment zones core-1 and 1-2, the tighter grouping of areas, along an almost straight line in the ordination, was related to an over-riding influence of the Ba:Ca ratio on the differences (Figure 54b, c). For the core-1 zone the slope areas and Cascade Plateau were similar to each other, with the seamount areas; 'unknown' QLD and Gascoyne being very similar to each, but intermediate between the slope/Cascade group and the other seamounts, with the exception of Derwent Hunter, which was an outlier for all three otolith zones (Figure 54a-c). For all three otolith zones the Gascoyne seamount tended to be more similar to the slope areas than the majority of the seamount areas (with exception of Cascade Plateau and 'unknown' QLD in zones c-1 and 1-2).

PERMANOVA pairwise comparisons showed the most highly significant differences were between the seamount and slope areas, with the exception of Gascoyne and 'unknown' QLD, where the only differences to slope areas were between 'unknown' QLD and Southern NSW in the otolith core and increment 1-2 zone (Table 18). In the core zone the Cascade Plateau area was highly significantly different to the Southern NSW and WestKI/GAB areas, and Derwent Hunter, but not the other seamount areas. While significant difference were detected among some seamount areas in all three early life zones, these difference were not as highly significant as those between seamount and slope areas (Table 18).

Demersal adult life stage (otolith edges)

Similar to the early life stages, multidimensional scaling plots (Ba:Ca, Sr:Ca, $\delta^{18}O$ and $\delta^{13}C$) of the otolith edge zones showed that seamount areas were generally more similar to each other than to slope areas, with exception of Cascade Plateau and Derwent Hunter (Figure 55). There was more dispersion among the areas in the edge ordination than for the early life zones, (i.e. core-1 and 1-2), suggesting prolonged periods of local area residency prior to capture allowing greater opportunity for otolith chemistry to diverge. The influence of the two stable isotopes was also important, as these integrated over at least an entire year of life prior to capture. Interestingly, the three slope areas most alike were also the closest to each other geographically; Southern NSW, Bass Canyon/east Flinders Is, and West Tasmania/West Bass Strait. However, Cascade Plateau, which is relatively close to these three slope areas, was more similar to WA-Esperance, Derwent Hunter, and West KI/GAB. The seamount areas Lord Howe 4, Fraser and Barcoo, were most different to the slope areas (Figure 55).

PERMANOVA pairwise comparisons showed the most highly significant differences were again between the seamount and slope areas, but that more of the seamount areas were significantly different from each other than for the early life zones (Table 19). Further, highly significant difference occurred between slope areas in south-eastern Australia (Southern NSW, Bass Canyon/east Flinders Is, West Tasmania/West Bass Strait) and those to the west (WA-Esperance, West KI/GAB).

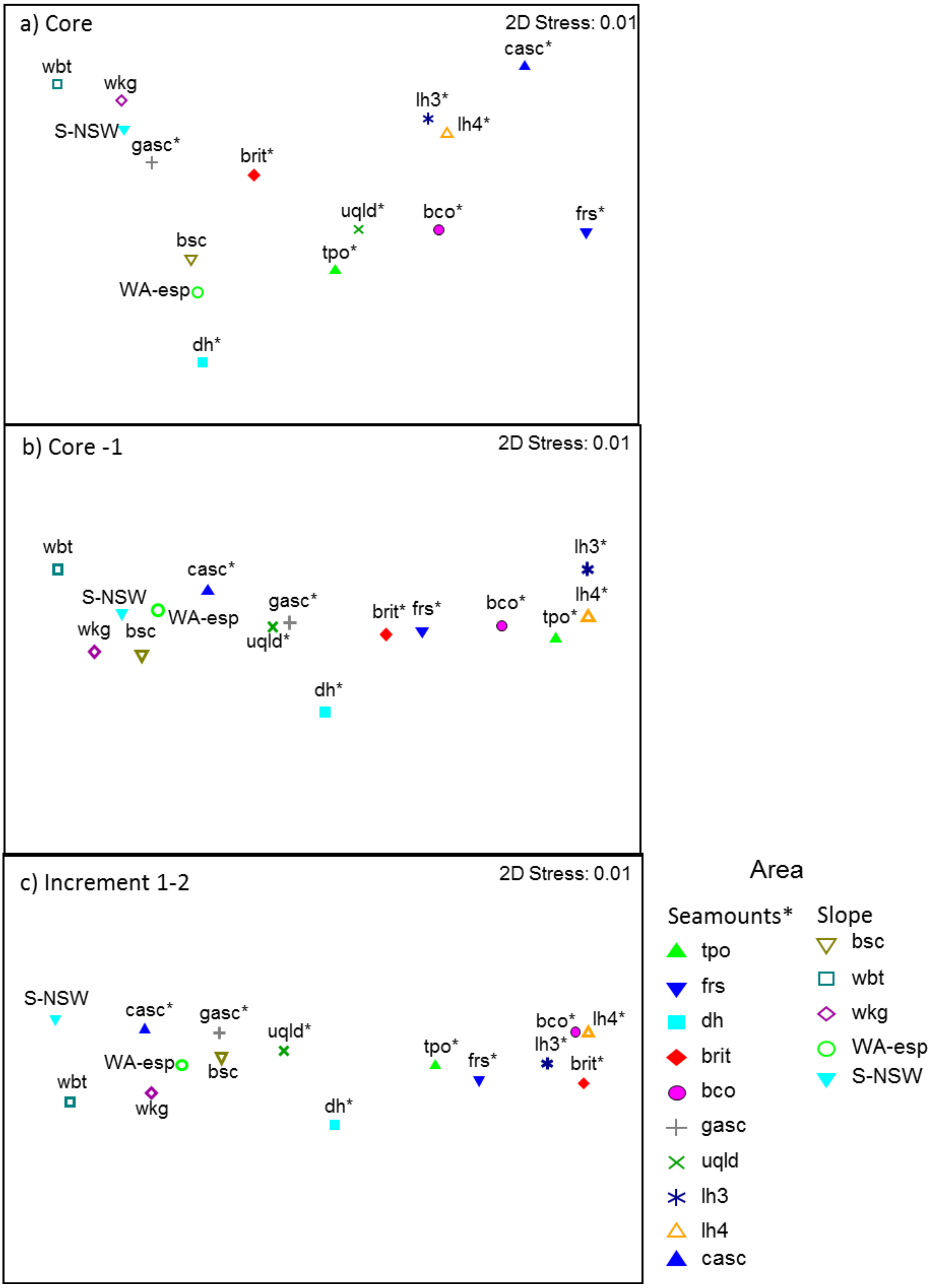

Figure 54 MDS (multidimensional scaling) plot of variation in multi-elemental chemistry (Ba:Ca, Mn:Ca, Mg:Ca, Sr:Ca) of Blue-eye Trevalla otoliths among sampling areas for; a) otolith core zone, b) core –increment zone 1, c) increment zone 1-2. Seamount areas denoted with *. See Appendix 5 for key to site codes.

Table 18 Results of PERMANOVA pairwise comparisons of Blue-eye Trevalla multivariate otolith chemistry (Ba:Ca, Mn:Ca, Mg:Ca, Sr:Ca) among sampling areas for a) otolith core zone, b) core –increment zone 1, c) increment zone 1-2. Seamount locations in blue shaded cells, slope locations in orange shaded cells. See Appendix 5 for key to site codes.

a) core	frs	brit	uqld	dh	bco	tpo	lh3	lh4	gasc	sth-nsw	bsc	casc	wbt	wkg	WA-Esp
frs															
brit															
uqld															
dh															
bco															
tpo															
Lh3															
Lh4															
gasc															
sth-nsw															
bsc															
casc															
wbt															
wkg															
WA-Esp															

p≤0.05

p≤0.01

p≤0.001

b) Core-1	frs	brit	uqld	dh	bco	tpo	lh3	lh4	gasc	sth-nsw	bsc	casc	wbt	wkg	WA-Esp
frs															
brit															
uqld															
dh															
bco															
tpo															
Lh3															
Lh4															
gasc															
sth-nsw															
bsc															
casc															
wbt															
wkg															
WA-Esp															

p≤0.05

p≤0.01

p≤0.001

c) Inc 1-2	frs	brit	uqld	dh	bco	tpo	lh3	lh4	gasc	sth-nsw	bsc	casc	wbt	wkg	WA-Esp
frs															
brit															
uqld															
dh															
bco															
tpo															
lh3															
lh4															
gasc															
sth-nsw															
bsc															
casc															
wbt															
wkg															
WA-Esp															

p≤0.05

p≤0.01

p≤0.001

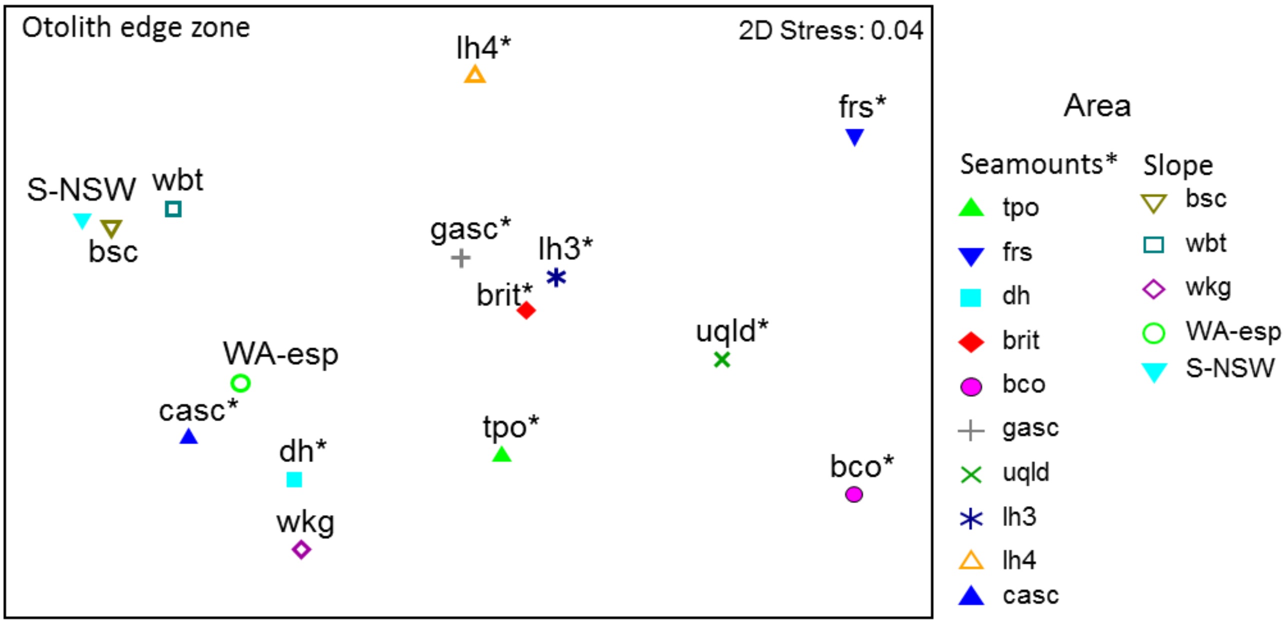

Figure 55 MDS (multidimensional scaling) plot of variation among sampling areas in multivariate (Ba:Ca, $\delta^{18}O$, Sr:Ca and $\delta^{13}C$- age adjusted for casc and S-NSW) chemistry of Blue-eye Trevalla otolith edge zones. Seamount areas denoted with *. See Appendix 5 for key to site codes.

Table 19 Results of PERMANOVA pairwise comparisons of Blue-eye Trevalla otolith edge zone multivariate chemistry (Ba:Ca, $\delta^{18}O$, Sr:Ca and $\delta^{13}C$- age adjusted for casc and S-NSW) among sampling areas. Seamount locations in blue shaded cells, slope locations in orange shaded cells. See Appendix 5 for key to site codes.

Edge	frs	brit	uqld	dh	bco	tpo	lh3	lh4	gasc	sth-nsw	bsc	casc	wbt	wkg	WA-Esp
frs															
brit															
uqld															
dh															
bco															
tpo															
lh3															
lh4															
gasc															
sth-nsw															
bsc															
casc															
wbt															
wkg															
WA-Esp															

p≤0.05

p≤0.01

p≤0.001

Discussion

Comparisons of otolith element:Ca and stable isotope ratios of Blue-eye Trevalla collected across nine seamount and six slope areas around south-eastern Australia, including Tasmania, did not support the current approach of treating Australian Blue-eye Trevalla populations as a single 'global' Australian stock. While the otolith chemistry approaches and sampling regime applied cannot be expected to entirely resolve stock structure of Blue-eye Trevalla across its Australian range, in combination with the other approaches in this report, there is sufficient evidence to support a revised model of Blue-eye Trevalla stock structure in Australian waters.

The clearest results from this study related to the comparison of slope and seamount areas. Most notable, were the differences in otolith Ba:Ca that occurred during the juvenile pelagic phase; until the end of the second year of life. The strong difference in the annually integrated Ba:Ca levels between seamount (higher values) and slope areas during the early life history indicated that separation, and population structuring, was somehow occurring before Blue-eye Trevalla transitioned to the demersal adult habitat. The un-integrated life history profiles demonstrated that the ontogenetic timing of the increases in otolith Ba:Ca during the pelagic phase was generally prior to or around formation of the first annual increment zone. While a variety of individual Ba:Ca profiles were observed, and similar peaks often occurred in slope samples, the slope samples were generally lower in magnitude than those observed in the seamount otoliths. The consistent ontogenetic timing of the Ba:Ca peaks, coupled with low variation along the life history profiles after the third annual increment, suggest that the peaks are related to an ontogenetic/developmental transition. The analysis of $\delta^{18}O$ and associated water temperature predictions showed that the otolith zone characterised by the elevated Ba:Ca corresponded to a period of increased water temperature exposure for both the seamount and slope samples. This confirms that fish would have been in the near surface waters during this phase of otolith Ba:Ca enrichment. While the age integrated mean Ba:Ca ratios showed highly significant differences among most seamount and slope areas, with the exception of Derwent Hunter and 'unknown' QLD, there was overlap in distributions which may reflect individual variability or low level of connectivity between some seamount and slope areas later in the pelagic juvenile phase or after settlement to the demersal habitat. Movement of demersal Blue-eye Trevalla over relatively large distances has been indicated by tag-recapture studies in New Zealand (Horn 2003) and along the NSW slope, but there is currently no evidence for significant migrations between slope and seamount areas in the Tasman Sea.

The fact that the seamount samples could be separated from slope samples based on their early life otolith chemistry (during the pelagic stage), suggests that there is little mixing of fish among seamount and slope areas after they settle to the demersal habitat. Similarly the strong differences between the Western Tasmania/western Bass Strait area with the WA-Esperance and West KI/GAB areas in $\delta^{18}O$ of otolith edges indicates that extensive demersal migration between these areas is unlikely. The high Ba:Ca zones in the otoliths of the seamount samples are consistent with the earlier study of whole otoliths, where the offshore seamounts also showed higher Ba than the slope areas (Hindell *et al.* 2005). It would appear that although the large Ba:Ca peaks are short-lived they were significant enough to effect the whole 'dissolved' otolith composition in the earlier study. Furthermore, the consistent detection of elevated Ba:Ca in the seamount otoliths from the two studies suggests the Ba:Ca enrichment in seamount otoliths is consistent over time.

While slope and seamount areas had clearly different Ba:Ca levels through the first and second years of pelagic life, the analyses focussed on the core region of the otoliths (first 1-2 months of life) showed less variation, and overall lower Ba:Ca levels. While there was a general trend for the seamount areas to have higher mean Ba:Ca than most of the slope areas, the comparison were only significant between the Fraser and Southern NSW, Western Tasmania/western Bass Strait areas. There were interesting similarities in the spatial patterns of variation in the Ba:Ca of the otolith cores and edges, although differences among areas were more significant for the edges zone. This may relate to statistical power issues rather than broad scale homogeneity of larval otolith Ba:Ca. For the multivariate comparisons, the only seamount area that differed from all the slope areas for the otolith cores was also Fraser seamount (the most northerly). This is consistent with this seamount being the most upstream in relation to the predominant direction of likely dispersal along the Tasmantid seamount chain. Interestingly, the Cascade Plateau and Bass Canyon/East Flinders Is areas had higher Ba:Ca in the otolith cores, and were more consistent with the seamount areas, and Gascoyne had low Ba:Ca, which was more consistent with the slope areas. This may indicate that at least Cascade Plateau and Bass Canyon/East Flinders Is. receive some replenishment derived for seamounts further north, and Gascoyne receives some replenishment from the adjacent slope areas.

The analysis of $\delta^{18}O$ in the otolith core region (integrating over the first 3–4 months of life) showed no clear differentiation among seamount and slope areas, and the predicted temperatures experienced during this early life stage overlapped considerably within a range of approximately 15–20°C. This result was intriguing given the differences in Ba:Ca observed among seamount and slope samples later in their juvenile pelagic stages, and the clear latitudinal trends in predicted water temperatures experienced by the demersal adult stages. This could indicate either a high degree of geographic (latitudinal) mixing/dispersal of larval stages (both north and south) sourced from different spawning areas, or that Blue-eye Trevalla larvae are exposed to similar temperature regimes irrespective of latitude due to varying timing of spawning with latitude (i.e. spawning periods are cued to occur in certain optimal temperature windows irrespective of latitude), and or some ability to regulate their depth during the larval stage to remain in an optimal thermal window. Alternatively, survival rates might be maximised when larvae are retained ‘passively’ in water masses/depths with an optimal thermal range. Given that the dispersal modelling did not suggest major south to north dispersal (chapter 5), and surface waters over the northern latitude seamounts would typically be greater than 20 °C all year (CSIRO, unpublished data), it is more likely that a combination spawning timing and/or depth regulation (larvae staying deeper) explains the low larval otolith temperature estimates for the northern seamount samples.

There is limited information on how or if seasonal spawning dynamics of Blue-eye Trevalla vary with latitude, or among slope and seamount areas. Baelde (1996) showed that Blue-eye Trevalla off north eastern Tasmania spawned in late summer-early autumn, with the peak spawning period being March/April. This spawning period was consistent with the study by Jones (1985) off South Australia. Jones (1998) suggested that spawning further north along the eastern Australian (NSW) slope may occur in the winter months, although further studies are required to confirm such a latitudinal trend. There is no information on spawning timing along the Tasmantid seamounts. It is clearly evident from this earlier work that Blue-eye Trevalla spawning likely occurs in many areas across a broad latitudinal range, rather than at a few highly localised spawning aggregation sites, and also that spawning can be spread across several months. If there was a trend for winter spawning in northern areas and late summer spawning in more southerly areas this could explain why the predicted ambient temperatures from the otolith cores showed overlap among adult sampling areas separated across such a broad latitudinal range. More detailed analysis of seasonal variation in water temperature with latitude in relation to the predictions from the otolith core $\delta^{18}O$ may shed further light on this hypothesis.

The dispersal modelling component (Chapter 5) indicated potential for broad dispersal of larval stages along the eastern Australian coast under the influence of the east Australian Current, and importantly, from seamount to slope areas along NSW, in a largely unidirectional fashion. Furthermore, dispersal from southern Western Australia and the GAB region to the east under the influence of the Leeuwin/Flinders/Zeehan currents could clearly connect spawning areas in these regions with demersal population as far east as western Tasmania and western Bass Strait. While dispersal potential may be influenced by variable time of spawning (i.e. seasonal timing of model particle release) in different areas, this was not tested in the current study. Blue-eye Trevalla have a long pelagic phase, and are thought to aggregate around flotsam (Duffey *et al.* 2000, Last *et al.* 1993) which suggests they may tend to behave more like passive particles, even when they are well developed and capable swimmers. However, the fact that both the Ba:Ca and $\delta^{18}O$ of the seamount and slope samples diverged while Blue-eye Trevalla were still in surface waters, does suggest that even if there was broad dispersal during the first few months of life, dispersal becomes more restricted after the first 6 months of life, perhaps due to Blue-eye Trevalla actively controlling there geographic position. Overall, the otolith chemistry data are not inconsistent with the dispersal modelling (Chapter 5).

The variation in composition of the otolith margins, which integrated at least the last year of life in all fish, clearly indicated patterns of extended local residency of the demersal adult life-stages. Variation was evident for Sr:Ca, Ba:Ca, $\delta^{18}O$ and $\delta^{13}C$. The predicted temperatures from otolith $\delta^{18}O$ closely matched the annual average temperatures at 400 m depth in all areas, except for WA-Esperance and WestKI/GAB, where the predicted temperatures suggested residency at around 300 m depth according to the CARS temperature-depth data. The predicted temperatures from otolith $\delta^{18}O$ values at around the first annual increment zones indicated warmer water exposure at the first increment zone, which is consistent with the increment being laid in the spring/summer, but the core region being laid down in the autumn/winter (as expected from the known spawning times). The much lower temperatures predicted from the second increment zone confirm that the transition to deeper water had occurred at this point, as previously hypothesised based on the age at first recruitment to the demersal fisheries. The variation among areas in the $\delta^{13}C$ of the otolith edges could have been influenced by metabolic rate, diet and the dissolved inorganic carbon (DIC) of the ambient water (Schwarcz *et al.* 1998; Weidman and Millner 2000). A consistent trend in $\delta^{13}C$ of otoliths is for increases ($\delta^{13}C$ becomes less depleted) as fish age, related to an increasing trophic level of prey and decreasing metabolic rate (Weidman and Millner 2000, Begg and Weidman 2001). This trend with age was evident for the samples we compared across the core, first and second increment, and edge zones. The $\delta^{13}C/\delta^{18}O$ bi-plot for the otolith edge zone also showed a pattern for increasing $\delta^{13}C$ with increasing $\delta^{18}O$, which is consistent with a temperature related metabolic influence on the levels of $\delta^{13}C$ depletion, i.e. fish in cooler waters have lower metabolic rates, leading more enriched otolith $\delta^{13}C$.

Overall the results of the otolith chemistry study support *hypothesis 2:* recruitment of Blue-eye Trevalla to seamount and continental shelf areas is derived from a broadly dispersed/mixed larval pool, but adult populations constitute separate resident sub-populations (meta-population with local adult residency). Although there is likely an isolation by a distance gradient between more northern and southern areas. Importantly the more northern 'upstream' areas would depend more on locally source replenishment than the 'downstream' (more southerly areas), and would therefore be more vulnerable to overfishing.

While the chemistry of the otolith core was limited in its ability to clearly detect separate larval sources for the demersal adult populations sampled, the dispersal modelling indicated it would be highly unlikely for spawning areas along the eastern Australian slope to be significant sources of replenishment to areas west of Tasmania and west of Bass Strait. The similarity of early life history otolith chemistry among slope areas from eastern and western Australia most likely relates to the similarity in environmental influences on the otoliths rather than significant mixing.

Further comments on the extraordinary peaks in Ba:Ca in Blue-eye Trevalla otoliths

Most studies of Ba incorporation into fish otoliths point to the proximal influence on variation being the ambient levels in the surrounding water relative to calcium (Bath *et al.* 2000; Elsdon and Gillanders 2003; Hamer and Jenkins 2007). While surface waters can become enriched with Ba due to upwellings (Lea *et al*. 1989; Hatch *et al*. 2013) that can occur at seamounts, shelf-breaks and canyons, the influences of upwelling enrichment on surface waters near seamounts is expected to be transient and/or short-lived due to low residence times of the surface waters (Genin and Boehlert 1985; Genin 2004). The extremely high Ba:Ca values, exceeding 100 µmol mol^{-1} in many samples, the abrupt shifts, and consistency of ontogenetic timing of Ba:Ca peaks across samples from widely separated areas is inconsistent with the peaks being driven by exposure to irregular patches of highly Ba enriched ocean surface waters. Indeed, offshore oceanic surface waters are expected to be fairly homogeneous and low in ambient Ba, which typically has a nutrient type profile in ocean waters (Dehairs *et al.* 1997). While ambient Ba can be enriched with depth in the open ocean (Bruland and Lohan 2003, Ashford *et al.* 2005), the $\delta^{18}O$ values of the Ba enriched otoliths zone clearly suggest the enrichment is occurring in warmer surface waters. While we cannot totally rule out the influence of ambient Ba levels, we hypothesise that the Ba enriched zones in the early life of pelagic Blue-eye Trevalla is related to rapid changes in growth, or some other major ontogenic transition, perhaps combined with shifts in water temperature exposure (Izzo *et al.* 2015). The differences observed among sampling areas would therefore relate to environmentally mediated differences in the influences of these environmental/physiological effects on otolith Ba:Ca, rather than direct effects of ambient levels. This could provide an extraordinary example of otolith chemistry showing major variation with a geographic context that is not clearly linked to major changes in ambient water chemistry.

5. Ecological dispersal modelling

Quantifying the potential connectivity of Blue-eye Trevalla between spawning areas and fishing grounds to infer species sub-structure (stock structure) across its Australian range

Introduction

The deepwater fish Blue-eye Trevalla (*Hyperoglyphe antarctica*) is distributed widely on the upper continental slope (~200–1000 m depths) of South Africa, Australia, New Zealand and offshore ridges and seamounts (Haedrich 1967). It is an important commercial species in Australia where it commands a premium price as an iconic seafood species in domestic fish markets. Despite this prominence, important gaps in knowledge of its ecology hamper its fishery management in Australian waters. Thus, although Blue-eye Trevalla ranges across southern temperate Australia and extends to sub-tropical latitudes on both east and west coasts – an along-slope distance of some 6,500 km exclusive of offshore seamounts – it is currently managed as a single stock. The primary developmental need for the Blue-eye Trevalla stock assessment is a spatial framework in which meaningful sub-units of the fishery can be identified, i.e. based on natural sub-populations or processes such as recruitment. Reducing uncertainties about stock structure has the potential to underpin a less risk-averse management strategy and reverse the decline in total allowable catch of the species which in recent years has dropped over 50% from 785 tonne in 2007 to 335 tonne in 2016. A key element in defining the species' stock structure in Australian waters is a knowledge of its ecological connectivity.

Ocean circulation models are potentially powerful tools for estimating ecological connectivity, but remain predictors of hydrological connectivity unless biological parameters are included. Coupled physical-biological (biophysical) models strive for a realistic blending of the physical and biological factors that contribute significantly to dispersal and connectivity, and depend both on a reliable hydrodynamic model, and on obtaining biological inputs such as the behaviour of early life history stages and adult spawning locations (Leis *et al.* 2011). Sophisticated biophysical models may include complex information on mortality, larval swimming and orientation, and ontogenetic vertical migration (e.g. North *et al.* 2009), and where this information is available it has been used to measure potential connectivity at a range of spatial scales, e.g. fine scale/10 km for coral reef fishes versus 100 km for pelagic spp. (Cowen and Sponaugle 2009).

Developing a biophysical model to estimate the ecological connectivity of a deep-sea fish is challenging because there is typically less known about relevant aspects of biology and behaviour during early life compared to well-studied systems such as coral reefs. This remains the case for Blue-eye Trevalla despite its importance as a commercial species. It has long been known (e.g. Jones 1985) that Blue-eye Trevalla appear on Australian and New Zealand commercial fishing grounds at a length of about 35 to 45 cm, when they are estimated to be about 2 years old (Horn 1988), and therefore appear to be fast growing (Horn and Massey, 1989). During this period of fishery recruitment they may school in mid-water or near-surface (Duffy *et al.* 2000) but appear to have a mostly near-seabed (benthopelagic) existence on the upper continental slope, mainly in 200–650 m depth and often in association with abrupt seabed topography including hills and seamounts (Williams *et al.* 2016). In contrast, however, the species' distribution prior to the near-seabed adult phase is unknown because extensive net sampling programs over the Australian continental slope collected only a few larvae (Bruce *et al.* 2000, 2001), and juveniles have been observed only rarely. The elusive nature of juveniles is such that only about 22 juveniles (7 to 9 cm FL) have been captured off New Zealand – two with general flotsam and at least 20 with a discarded and heavily encrusted trawl net (Duffy *et al.* 2000), and 4 individuals (3 to 6 cm FL) off Australia – dip netted beneath a floating raft of the brown kelp, *Phyllospora comosa* (Last *et al.* 1993). This indicates a near-surface, and probably lengthy, juvenile existence in association with floating objects (Result Chapter 1, Figure 10), and is consistent with the behaviour of congeneric species such as the Atlantic Blue-eye, *H. perciforma*, or 'barrelfish', named for its common association with drifting logs and other floating objects. There was some pre-existing information on spawning locations and times of Blue-eye Trevalla (Jones, 1985; Baelde, 1996) but those were for relatively small areas of its Australian distribution.

In this chapter we provide a mapping of the ecological connectivity of Blue-eye Trevalla across its entire Australian range in a four dimensional (3-D x time) object-orientated, biophysical dispersal model (Kool and Nichol, 2015). New and pre-existing data on relevant aspects of Blue-eye Trevalla's biology and ecology, including some inference from the closely related upper slope species Silver Warehou (*Seriolella punctata*) (Bruce *et al.* 2002), were synthesized to provide the best basis for parametrising the model. Factors included were an estimate of pelagic larval/ juvenile duration; ontogenetic vertical distribution; spawning time, locations and depths; and an estimate of (exponential) mortality. The strengths of our model include quantifying and visualising the ecological connectivity between sources (spawning grounds) and sinks (commercial fishing grounds) in a connectivity matrix (Kool and Nichol, 2015). A parallel analysis of isotopic and elemental microchemistry of Blue-eye Trevalla otoliths (Results Chapter 4) provided some ability to compare and validate the model results.

The two sub-objectives for this part of our study were to:

1. quantify the potential connectivity of Blue-eye Trevalla between spawning areas and fishing grounds to infer species sub-structure (stock structure) across its Australian range.
2. interpret the results in the context of fishery management.

Materials and Methods

The model

The model used was Conn4D – an open-source, biophysical dispersal model developed at Geoscience Australia in support of the National Environmental Research Program's Marine Biodiversity Hub. The model uses modelled oceanographic data (here, HYCOM GLBa0.08) in conjunction with individual-based behaviour to evaluate the expected trajectory of marine larvae transported via advection and diffusion in 3D space (including 32 depth bins) over time. The model is described in detail in Kool and Nichol (2015), and source code is available on Github (https://github.com/GeoscienceAustralia/conn4D).

Selection of input parameters

Key relevant elements of Blue-eye Trevalla ecology were identified by reviewing the literature (see Table 3, Results Chapter 1), and through discussions with knowledgeable commercial fishers. This information was used to inform and parameterize the model for Blue-eye Trevalla in the follow ways:

1. spawning season was restricted to autumn (March to May), and spawning pattern was in batches, 4 per season; particles were released for the years 2009–2012 every 21 days beginning at March 1st, and ending on May 24th;

2. spawning depth was 400 m, or as close as possible to this depth given the local bathymetry data at the spawning sites;

3. particles (eggs/larvae/early stage juveniles) initially rise in a linear manner to a 'preferred depth', randomly selected between 0 and 50 m, during a 4-day period at the beginning of the simulation; following the four day mark, particles retain their preferred depth as long as the absolute vertical current velocity is not in excess of 2 cm/s;

4. locations of 31 spawning areas (sources) (Table 20; Figure 56) were a combination of information from Baelde (1996), locations identified from gonad index data, and locations identified by fishers; 'seed' locations were added to sink areas where Blue-eye Trevalla occur but where there is no other information (five areas between Esperance and the Abrolhos Islands in Western Australia);

5. the number of source points per source area was variable, and depended on the above information – however, source areas with more source points were where historical Blue-eye Trevalla catches were highest and where egg release could be expected to be higher; there were single seed locations in each of the five Western Australian source areas.

6. the number of particles released from each source point was equal;

7. locations of 34 sink areas (Table 20; Figure 56) were identified as the area of the upper continental slope in 200–700 m corresponding to the core depth range of the species; the slope was divided into sections corresponding to clusters of fishing ground areas within each of the broad fishery regions identified during analysis of catch and effort data (Results Chapter 1); these sink areas covered the entire upper slope between the Abrolhos Islands off WA and the NSW-Queensland border, and continental slope depths of the Tasmantid Seamount Chain, and the Lord Howe Rise from Lord Howe Island to the Capel Bank.

8. early life history of larvae, juveniles and young adults (<2 years of age) was interpreted to be pelagic and near-surface (to 100 m depth);

9. early life history (up to two years) was assumed to be passive, i.e. no swimming or behavioural orientation parameters were included; this was due to absence of information, and the likely absence of stimuli (settlement cues) for fish drifting or residing with flotsam drifting in surface currents;

10. exceptions to the general assumption of passive movement were vertical ascent during the first 4 days of life (#3 above), and distribution restricted to the top 100 m of the water column and concentrated in 0–50 m;

11. mortality was included in one example using a rate of 0.1 per day (a general value, e.g. Houde, 1989).

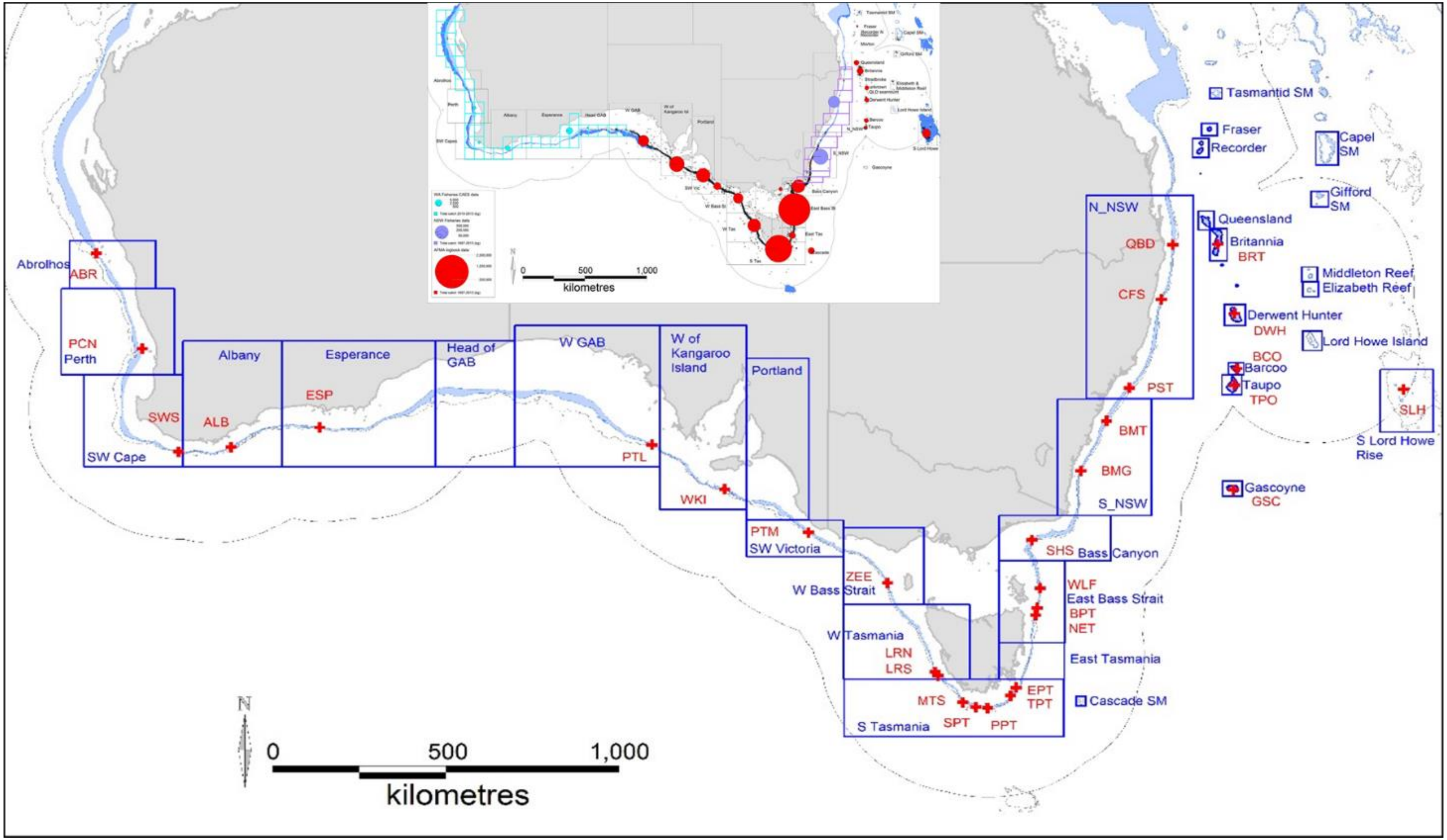

Figure 56 Map showing the locations of 'sources' (Blue-eye Trevalla spawning areas) (red symbols and labels) and 'sinks' (Blue-eye Trevalla commercial fishery areas) (blue boxes and labels) used to model ecological connectivity. Note, 'sink' areas are the upper continental slope (200-700 m depths shown as blue-shaded polygons) within sink rectangles. Grey contours are the 1000 m isobath and 200 n.m. EZ boundary. The full list of source and sink areas (including full names for the red abbreviated labels) is in Table 20. Inset: map showing the distribution of total historical catch (1997 to 2013).

Table 20 Lists of sources (Blue-eye Trevalla spawning areas) and sinks (Blue-eye Trevalla commercial fishery areas) used to model ecological connectivity (and see Figure 2). Yellow-shaded locations are the Lord Howe Rise; green-shaded locations are seamounts forming the Tasmantid Seamount Chain; unshaded locations are on the upper continental slope of NSW, Victoria, Tasmania, South Australia and Western Australia.

Sources		Sinks	
Abrev.	**Name**	**Abrev.**	**Name**
'SLH'	South Lord Howe Rise	'SLH'	South Lord Howe Rise
'GSC'	Gascoyne Seamount	'LHI'	Lord Howe Island
'TPO'	Taupo Seamount	'ELR'	Elizabeth Reef
'BCO'	Barcoo Seamount	'MDR'	Middleton Reef
'DWH'	Derwent Hunter Seamount	'GIF'	Gifford Seamount
'BRT'	Britannia Seamount	'CPL'	Capel Bank
'QBD'	Queensland Border	'GSC'	Gascoyne Seamount
'CFS'	Coffs Harbour	'TPO'	Taupo Seamount
'PST'	Port Stevens	'BCO'	Barcoo Seamount
'BMT'	Browns Mt	'DWH'	Derwent Hunter Seamount
'BMG'	Bermaguie	'BRT'	Britannia Seamount
'SHS'	Seiners HS	'QLD'	Queensland Seamount
'BPT'	Banks Patch	'RCD'	Recorder Seamount
'WLF'	The Wall	'FRS'	Fraser Seamount
'NET'	NE Tas	'TSM'	Tasmantid Seamount
'EMP'	18 Mile Patch	'NNS'	Northern NSW
'TMP'	30 Mile Patch	'SNS'	Southern NSW
'PPT'	Pedra Patch	'BCN'	Bass Canyon
'SPT'	South Patch	'EBS'	Eastern Bass Strait
'MTS'	Maatsuyker Patch	'CSC'	Cascade Seamount
'LRS'	Low Rocky South	'ETS'	Eastern Tasmania
'LRN'	Low Rocky North	'STS'	Southern Tasmania
'ZEE'	Zeehan	'WTS'	Western Tasmania
'PTM'	Pt. MacDonnell	'WBS'	Western Bass Strait
'WKI'	W Kangaroo Is	'SWV'	Southwest Victoria
'PTL'	Port Lincoln	'PRT'	Portland
'ESP'	Esperance	'WKI'	West Kangaroo Island
'ALB'	Albany	'WGA'	Western GAB
'SWS'	SW Site	'HGA'	Head of GAB
'PCN'	Perth Canyon	'ESP'	Esperance
'ABR'	Abrolhos	'ALB'	Albany
		'SWC'	SW Cape
		'PRT'	Perth
		'ABR'	Abrolhos

Data analysis

Analysis focused on the potential movement (ecological connectivity) of early life history stages of Blue-eye Trevalla between spawning grounds ('sources') and commercial fishing grounds ('sinks'). 'Particles' representing the eggs, larvae, juvenile and young adult phases of Blue-eye Trevalla, all believed to be pelagic in the upper water column and constrained to the top 100 m in this model, were released from sources. The movement (forwards in time) of particles to sinks was visualized by animating their positions over time using ArcGIS 10.2 software package. Simulated particle locations were estimated at four points in time. First, their locations on the day at t = 0, 50, 100 and 150 days, and second, as a density surface by calculating the number of points on or within a set radius (12 km) of a given pixel location at t = 0, 50, 100 and 150 days. The surfaces show the relative probability of finding a particle at a location at a particular point in time. The density surface itself can be considered as a 2-dimensional form of a dispersal kernel.

The dispersal patterns are summarised in connectivity matrices that quantify and map the number of particles dispersing from each source to each sink, and provide a visualization of spatial clusters of connected areas. Rows and columns were ordered on the basis of spatial proximity so that blocks in the matrix can be used to identify spatial clusters of connected areas. The numbers of simulated particles on a $\log_{10}$ scale were used to generate matrices showing patterns of relative connection strength, with blue indicating a weak connection and yellow and red values increasingly stronger connection. The results are for the full time period 2009–2012. Without a mortality factor in the model, these patterns reflect 'potential' rather than 'realised' connectivity.

Results

Dominant patterns of dispersal

Particle movement at points in time (Figure 57) and integrated through time (Figure 58) reveal several dominant patterns of potential connectivity. Most broadly, at the whole-of-range spatial scale for Blue-eye Trevalla, there is a contrast between along-slope (mostly unidirectional) dispersal in the west and central range, and more dissipated dispersal (relatively multidirectional) in the eastern range, i.e. within the Tasman Sea. Particle supply to open ocean areas appears limited: the 2-year time-integrated dispersal (without mortality in the model) shows a rapid gradient of decline in particle density with increasing distance offshore (Figure 58 D). The along-slope, mostly west to east, movement of particles is strongly apparent on the Western Australian, South Australian and western Victorian continental margin where particles move towards and around Tasmania (e.g. Figure 58 D). This is driven by the combined influence of the Leeuwin current at the shelf edge and wind-associated drift further offshore (Middleton and Bye 2007).

Supply of particles from the west is part of a complex pattern of particle movements around Tasmania and off Victoria. There is considerable particle mixing, including southwards movement from Eastern Victoria (eastern Bass Strait) driven by the East Australian Current (EAC) (Boland and Church 1981; Ridgway and Dunn 2003), and east and southeast movements from western Victoria driven by the Flinders Current (Bye 1968; Middleton and Bye 2007). These patterns around Tasmania also include strong along-slope movement though the relatively shallow (<80 m depth) Bass Strait, and mixing offshore – particularly off eastern Tasmania and Victoria. Further north, and rather separately, multiple semi-independent plumes facilitate broad mixing between the continental slope of NSW and the Tasmantid Seamount Chain, extending across the western-central Tasman Sea to the southern boundary of the Coral Sea. This pattern is consistent with contained circulation within the Tasman Sea bounded by the Tasman Front (Tilburg *et al.* 2001) - the path of separated components of the EAC (Condie *et al.* 2003).

Finally, further offshore there appears to be broad dispersal of particles from the Lord Howe Rise into the central and eastern Tasman Sea, but with limited movement to other areas, i.e. only relatively minor exchange with the central section of the Tasmantid Seamount Chain. There appears to be some movement of particles from the Lord Howe Rise further westwards towards New Zealand, but the model cannot simulate dispersal beyond its eastern boundary at 180˚E.

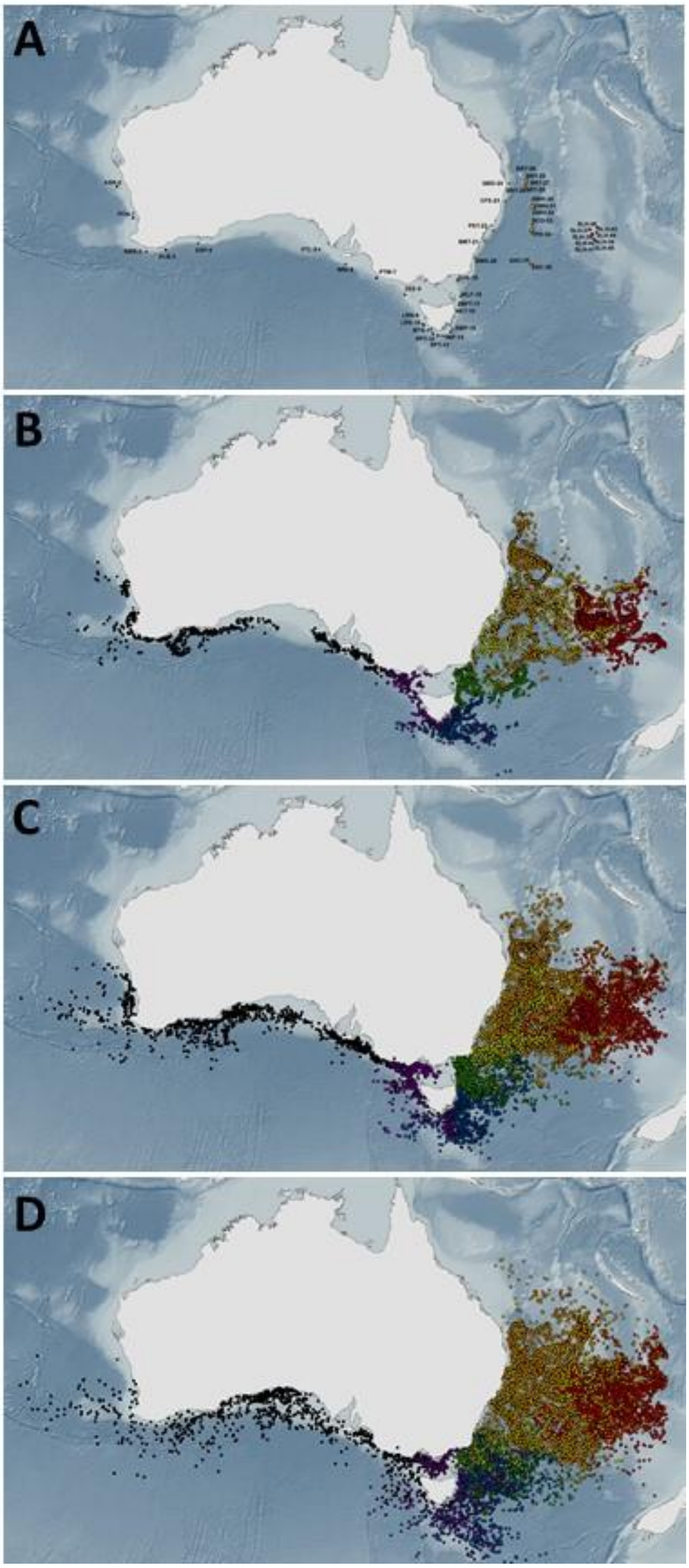

Figure 57 Maps showing simulated particle locations at four points in time: (A) source locations (see Table 20 for names), t=0; (B) t=50 days; (C) t=100 days; (D) t=150 days. Point maps show particle locations on the day, as opposed to integrated up until that day. Colour codes represent regional groupings to simply visualisation.

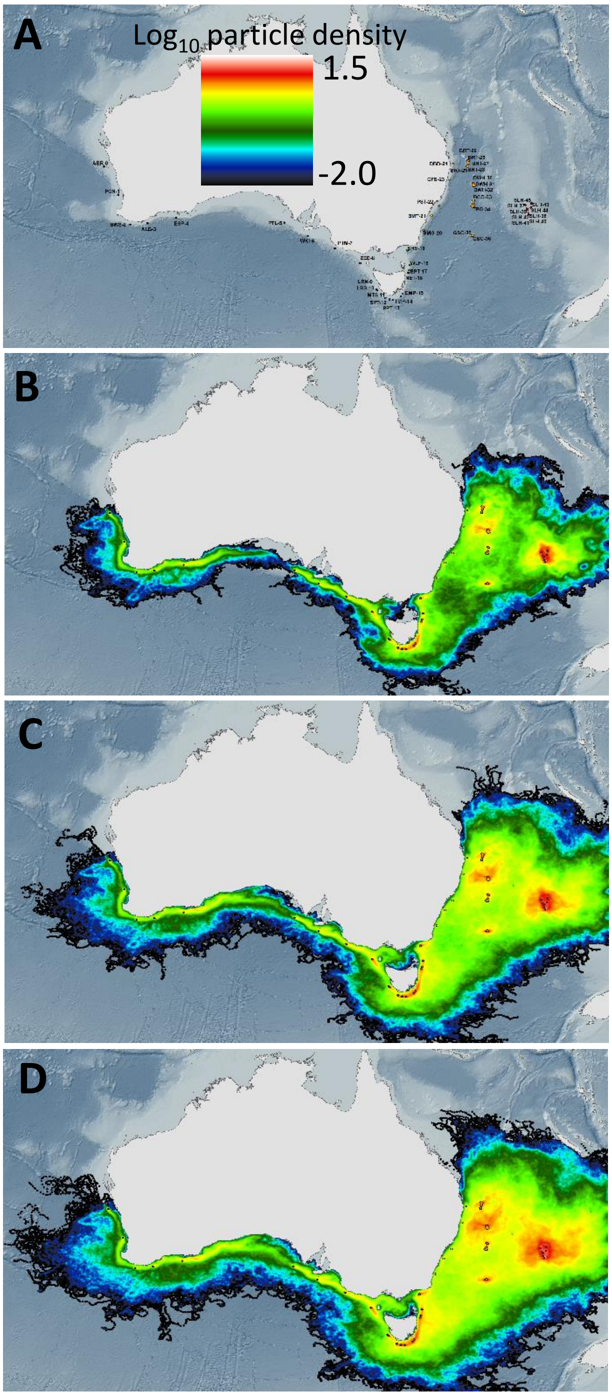

Figure 58 Maps showing simulated dispersal surfaces of particles integrated at four points in time: (A) source locations, t=0; (B) t=50 days; (C) t=100 days; (D) t=150 days. Colour bar shows the relative particle density on log scale.

Source-sink relationships

These dominant dispersal patterns create strong asymmetries in the connectivity matrices (Figure 59) that clearly show the unidirectional and restricted linkages between particular source and sink areas. For example, sources off Western Australia and South Australia contribute strongly to sink areas off western Tasmania, but contributions in the reverse direction are relatively weak.

The continental slope of Eastern Bass Strait (defined here as between Bass Canyon and northeast Tasmania, Figure 56) appears to have the broadest potential range of strong sources of Blue-eye Trevalla recruits, over short and long time periods (Figure 59). Thus, it receives relatively high numbers of particles from sources between southern NSW and western Bass Strait, and to a much lesser extent from the Gascoyne Seamount. This diversity of sources identifies eastern Bass Strait as likely to have relatively high genetic diversity. The potential for genetic mixing linked to along-slope movements of adult (spawning age) Blue-eye Trevalla between source and sink areas is unknown, although some extensive movements have been recorded off New Zealand by Horn (2012). Two other sink areas – the South and North New South Wales continental slope to the north, and the East and South Tasmanian slope to the south – also receive particles from a broad range of sources over short and long time periods (Figure 59). The NSW sinks receive a relatively high supply of particles from all Tasmantid seamounts, and the continental margin between the NSW-Queensland border and eastern Bass Strait; supply is much reduced from sources further south, i.e. south and southwest Tasmania. The East and South Tasmania sinks receive particles from sources from as far west as Kangaroo Island. All three sink areas (NSW, eastern Bass Strait and East/South Tasmania) have patterns of strong self-supply, lower supply to each other, and little supply beyond the eastern seaboard – although there is widespread but relatively very low supply to the Tasmantid Seamounts and Lord Howe Rise.

In contrast, the South Lord Howe Rise source has very limited connection, with potential external supply from only the Tasmantid Seamount chain (Figure 59). The South Lord Howe Rise appears able to supply only the islands, reefs, and seamounts that make up the Rise, and otherwise provides only minor supply to the NSW slope. The Capel Seamount at the northern end of the Rise receives particles from the Derwent Hunter and Britannia Seamounts in the Tasmantid chain, but this is in part because it is the largest sink on the Lord Howe Rise in terms of Blue-eye Trevalla habitat area. The Tasmantid Seamount chain shows a broadly similar pattern of limited connection, appearing to receive strong supply of particles mainly from other seamounts in the chain, over short and long periods of time; there is potential for some minor contribution from the NSW margin to Derwent Hunter and Britannia Seamounts over the long duration (2 years) (Figure 59 D). The northernmost seamounts (unnamed, Fraser and Recorder) receive very low numbers of particles – although there is no self-supply because none were included as source areas, and all have very small Blue-eye Trevalla habitats relative to other seamounts in the chain.

Sink areas to the west of Tasmania (Western Tasmania through to the Abrolhos Islands) show a strong unidirectional (west to east) pattern of supply and receipt. This is consistent with the clearly visible patterns in point-in-time and integrated particle tracks seen in maps (Figure 57 and Figure 58, respectively), and is attributable to influence of the Leeuwin and Flinders Currents.

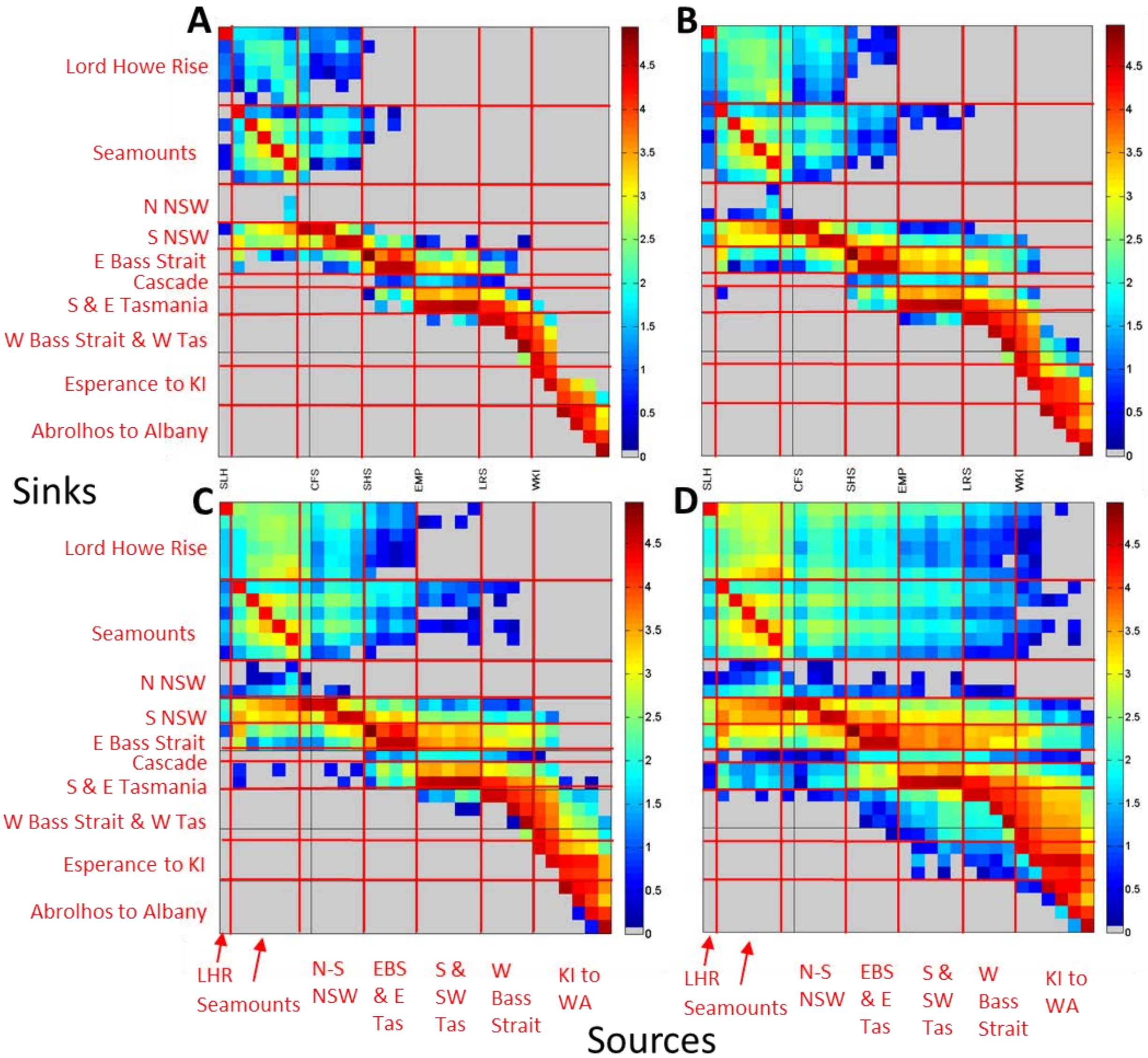

Figure 59 Connectivity matrices showing the number of particles dispersing from each source to each sink (with no mortality) at release durations of (A) 50 days; (B) 100 days; (C) 150 days; and (D) 730 days (equal to the full 2-year early pelagic life history phase). 'Heat-map' (particles on a log10 scale) show patterns of relative connection strength, with blue indicating a weak connection and yellow and red values increasingly stronger connection. The results are for the full time period 2009–2012. Regional boxes between source and sink differ slightly because they are not the same areas. Ignore lines and source codes in black.

Mortality effect on source-sink relationships

Modelling dispersal without allowing for particle mortality provides a simulation of 'potential connectivity', whereas layering in functional aspects such as mortality (and other factors such as differential supply across sources) provides a simulation of 'realized connectivity' (Watson *et al.* 2010). A comparison of 'with' and 'without' mortality (rate of 0.1 per day) for Blue-eye Trevalla dispersal over the 2-year period (Figure 59) shows the connectivity pattern with mortality is restricted to a substantial degree. The primary patterns observed without mortality (previous section) are repeated, but are less clear and more dominated by self-supply (Figure 60 B). Unfortunately, there is not an estimate of larval Blue-eye Trevalla mortality that can be applied, despite it potentially having a significant effect on determining realized connectivity.

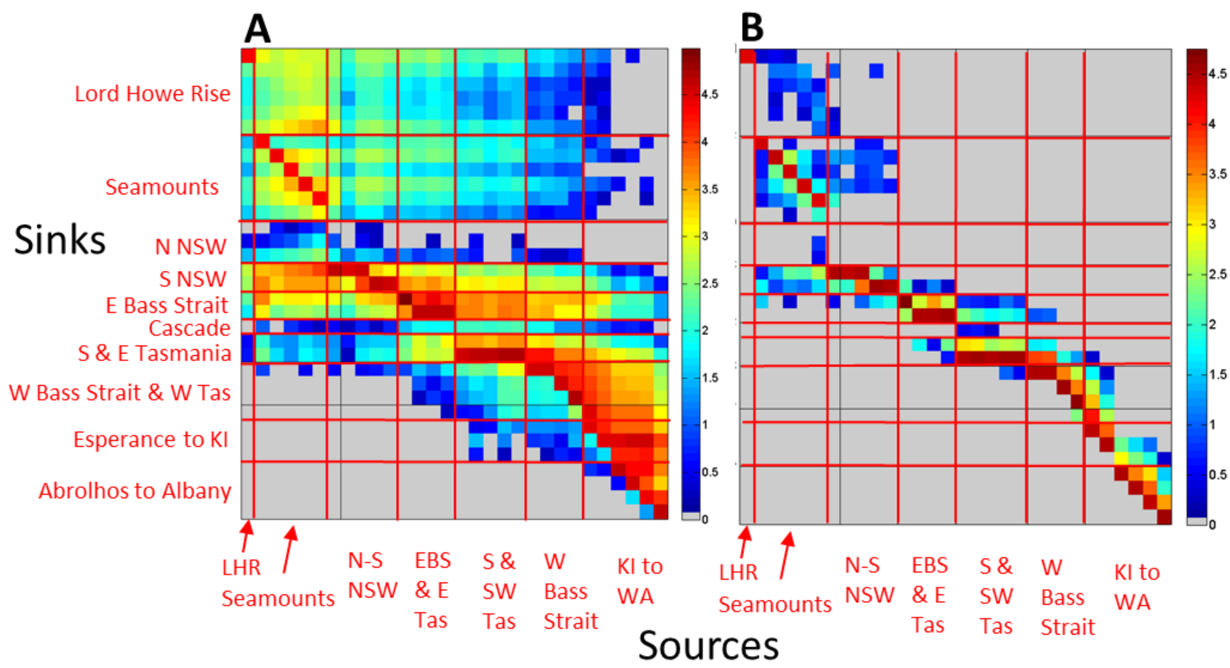

Figure 60 Connectivity matrices showing the number of particles dispersing from each source to each sink at release durations of 730 days (equal to the full 2-year early pelagic life history phase); (A) no mortality; (B) with a mortality rate of 0.1 per day. 'Heat-map' (particles on a log10 scale) show patterns of relative connection strength, with blue indicating a weak connection and yellow and red values increasingly stronger connection. The results are for the full time period 2009–2012. Regional boxes between source and sink differ slightly because they are not the same areas. Ignore the black lines.

Discussion

Application to Blue-eye Trevalla stock assessment

Blue-eye Trevalla ranges across southern temperate Australia and extends to sub-tropical latitudes on both east and west coasts, but is currently managed as a single stock. Attempts to refine the spatial management of catch and effort using harvest control rules (Faye *et al.* 2011) proved difficult because of high spatial and seasonal variability in the availability of different age classes combined with low levels of sampling effort across the fishery (Smith and Wayte, 2002; Fay, 2007). A previous attempt to identify suitable methods for examining Blue-eye Trevalla population structure (Hindell *et al.* 2005) detected sub-regional differences between fish from the Tasmantid seamounts, the Australian southeastern continental slope, and New Zealand using otolith stable isotope and elemental analysis. Whilst these patterns were not consistent, potentially because otolith microchemical differences were partially masked by analysis of whole otoliths and not seen in otolith shape or mitochondrial genetic analysis, the study was able to show that intra-regional differences in population structure (stock structure) would be detected if suitable methods and samples could be applied. Here we have applied another means of identifying natural sub-populations for stock assessment purposes using dispersal inferred from 3-dimensional current modelling over time.

Complex patterns of potential ecological connectivity (movement of Blue-eye Trevalla early life history stages between spawning grounds and adult fishing grounds) corroborate and extend the earlier findings of Hindell *et al.* (2005). The dispersal patterns can be interpreted as four sub-regional stock areas: 'West' – comprising continental slope fishing grounds off Western Australia, South Australia and western Victoria to western Tasmania; 'South' – continental slope grounds around Tasmania and north eastwards to eastern Bass Strait; 'East' – fishing grounds on the NSW continental slope and Tasmantid seamounts; and 'Offshore' – fishing grounds on the Lord Howe Rise (Figure 61).

A better understanding of ecological connection informs options for management intervention in two particular ways. First, for spatial management of catch and effort to prevent serial depletion (sequential over-catch in certain areas), and second because 'upstream' management actions will have the greatest effect on the entire system. Maintaining upstream 'source areas' will help ensure that downstream 'sink' areas will be replenished. The implications of our results for Australian Blue-eye Trevalla are that the South stock appears relatively resilient in having the broadest potential range of strong sources of Blue-eye Trevalla recruits, which is likely to lead to a relatively high genetic diversity. However, it is also the area of greatest economic importance for Blue-eye Trevalla being the area from which the highest historical catches have been taken (Figure 56, inset). Refinement of the species' stock assessment could include a sub-regional allocation of allowable catch to explicitly spread fishing effort into the adjacent West and East stocks. Both these areas receive recruits from a broad range of sources: the East stock includes exchange between all Tasmantid seamounts and the continental slope between the NSW-Queensland border and eastern Bass Strait, and the West stock an extensive along-slope supply from Western and South Australia.

Model validation

While the model provides a powerful means of evaluating potential patterns of connectivity driven by ocean circulation, it only represents the expected distribution pattern based on a perceived understanding of the system. Ultimately, however the information requires testing and validation using independent empirical information. Otolith data provides an empirical record of conditions encountered by individual fish that can be explicitly linked to their age and duration of travel, and a parallel study to this (Results Chapter 4) has provided that opportunity. It is also possible to overlay the simulated particle tracks with chemical oceanographic conditions to generate a suite of chemical signatures over time. From the suite of simulated signatures, it would be possible to identify the particle track most likely to generate the observed empirical chemical signature derived from the otolith information, providing strong testing and validation of the model thereby increasing confidence in its predictive capabilities.

Future development

One of the key strengths of the model is its ability to represent the behaviour of individual organisms in response to localised conditions. The simulated organisms can respond in flexible ways to a range of environmental parameters. The model can equally use generalized life history patterns, or alternatively can incorporate highly detailed behaviour, as long as the underlying parameters are available. As more information becomes available, it is expected that the model will increase in its fidelity to actual conditions. It is also possible to compare results of generalized versus specialized simulations in order to evaluate whether the effort of collecting additional information provides significant value. In some cases, generalized results may be sufficient for making decisions and taking action.

It is possible to perform predictive work with the model by using ocean current forecasts (short or long-term) to drive the simulations. Taking this approach, it would be possible to evaluate the potential consequences of climate change in driving changes in oceanographic patterns, and the resultant potential effect on fisheries.

It is noted that applying mortality to the model does dramatically affect the extent of particle dispersal (relative connection between regions). It is expected that water temperature will affect the larvae mortality, with larvae on some trajectories surviving better than others. Taking this into account would be a further improvement to the model.

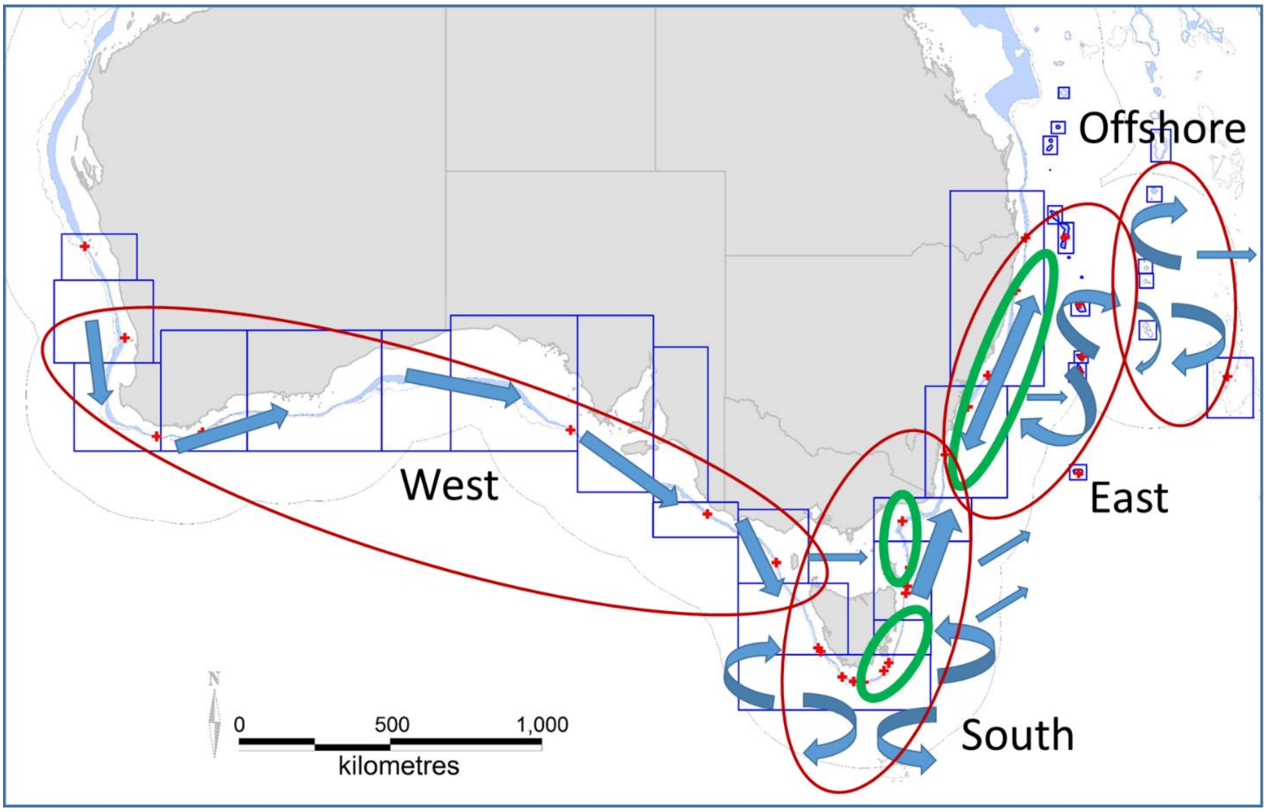

Figure 61 Diagram representing broad patterns of potential dispersal (ecological connectivity) of Blue-eye Trevalla early life history stages based on connectivity matrices (Figure 59 and Figure 60). Blue arrows indicate predominant directions of dispersal; red ellipses show four broad sub-regions based on: (1) unidirectional eastwards along-slope dispersal west of Tasmania; (2) multidirectional, dissipated dispersal around and east of Tasmania; (3) exchange between NSW and Seamounts; (4) local self-supply within all modelled areas. Green ellipses are the primary sink areas: S-E Tasmania, E Bass Strait, New South Wales.

Conclusion

Stock structure

Each of our three analyses provided evidence for stock structure within the broad southern Australian distribution of Blue-eye Trevalla. Spatial differences in age and growth (phenotypic variation) (Chapter 3) and otolith chemistry of the adult life stage implied there was local and regional residency by adult Blue-eye Trevalla (Chapter 4). Dispersal potential indicated by the dispersal modelling (Chapter 5) indicated a broader scale connectivity amongst regional populations was likely during early life. Broad-scale overlap of stable isotope and elemental signatures in otoliths of the pelagic larval stage were consistent with the hypothesis of broad dispersal during the first few months of life, but indicated the environmental histories of seamount fish diverged from those of slope fish during the first year of pelagic life (Chapter 4). By overlaying the spatial patterns identified by each of the independent lines of evidence we identified four broad 'stock areas': (1) West, (2) South, (3) East, and (4) Seamounts-Lord Howe (Figure 62). Each of these stock areas represents an interconnected meta-population (i.e. group of discrete adult sub-populations) with higher levels of larval/ juvenile connectivity and higher self-recruitment within than between areas. However, connectivity within each area is complex, some with a largely unidirectional flow of propagules (i.e. West Australia to western Bass Strait – West stock area) and others with flow of propagules in multiple-directions (i.e. NSW coast – East stock area). The rationales for the stock areas are detailed separately below (Table 21).

Importantly, the Blue-eye Trevalla stock areas do not reflect truly separated biological stocks because there is some exchange between them during pelagic early life history. However, local-scale residency by adults implies there are discrete adult populations on the continental slope and seamounts – perhaps individual seamounts – and that there is not extensive migration between them, e.g. between the Tasmantid seamounts and the NSW continental slope. Furthermore, some of the adult sub-populations act as larger sinks than others, i.e. benefiting more from recruitment derived from 'upstream' spawning areas.

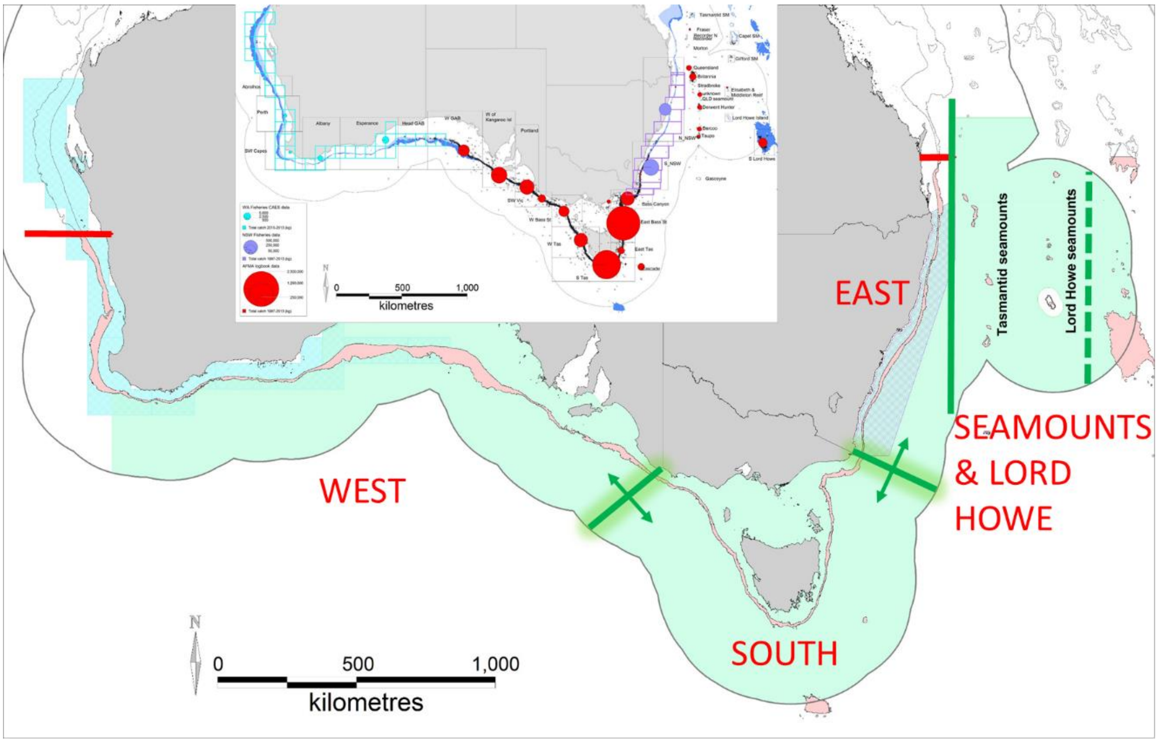

Figure 62 A suggested 'stock area' map for Blue-eye Trevalla based on (1) patterns of age and growth (Figure 40 and Figure 41); (2) evidence from otolith microchemistry for the similarities of sites in the South region (Figure 55) and local-scale adult residency; and (3) potential larval dispersal (Figure 61). The stock areas are defined by boundaries (green lines) within the geographical limits of the Blue-eye Trevalla Australian distribution (red lines); the depth range occupied by adult Blue-eye Trevalla (red hashed area). A rationale for the areas and boundaries is provided separately (Table 20). Map shading shows relevant fishery jurisdictions: cyan – Western Australia, green – Commonwealth (SESSF), and hatched – New South Wales. Inset: map showing the distribution of total historical catch (1997 to 2013).

Table 21 The rationale for suggested areas and boundaries for Blue-eye Trevalla stocks (Figure 62) based on (1) patterns of age and growth (Figure 40 and Figure 41), (2) evidence from otolith microchemistry for the similarities of sites in the South region (Figure 55) and local-scale adult residency, and (3) potential larval dispersal (Figure 61).

Area and Boundary	Rationale
All areas	There are consistent (phenotypic) differences in growth rates (length-at-age) and otolith chemistry among areas (fishing grounds) within all proposed stocks indicating that there is probably limited movement of adult fish following recruitment to the seabed at about 2 years of age. This follows an extended period of oceanic dispersal when there is a strong potential for both broad-scale dispersal and self-supply of recruits within in all areas, although there is strong and uniquely unidirectional (west to east) dispersal off WA and in the GAB.
West	There was no significant difference in growth of Blue-eye Trevalla (length-at-age) in the GAB compared to the slope around Tasmania (Figure 40 and Figure 41), but strong unidirectional (west to east) dispersal across the GAB from WA to Western Bass Strait (Figure 61 and Figure 62). A West-South boundary is diffuse, but would lie in the region of the SA-VIC State border based on differences in adult otolith chemistry.
South	Growth of Blue-eye Trevalla is significantly slower (smaller length-at-age) on the continental slope around Tasmania compared to the slope off NSW (Figure 40 and Figure 41). There is (1) weak connection between Tasmania/ Eastern Bass Strait and NSW, whilst (2) relatively strong evidence for potential dispersal between Western Bass Strait and South/ East Tasmania, and between South/ East Tasmania and Eastern Bass Strait, at all durations of dispersal (50, 100, 150 and 730 days), including with mortality in the model (Figure 59 and Figure 61). Otolith chemistry of adults groups the South sites together (Figure 55). A South-East boundary would be diffuse, but would lie in the region of VIC-NSW State border.
East	Growth of Blue-eye Trevalla is significantly slower (smaller length-at-age) on the NSW continental slope compared to the Seamounts, and significantly faster (greater length-at-age) than on the continental slope around Tasmania (Figure 40 and Figure 41). There is evidence for connection between East and Seamounts at all durations of dispersal (50, 100, 150 and 730 days), including with mortality in the model (Figure 60 and Figure 61). An East-Seamounts boundary would be distinctly defined in that it would need to separate the NSW continental slope from the Tasmantid seamount chain. Otolith chemistry of NSW slope and seamount fish diverged in the first year of life and remained different in the adult demersal stage.
Seamounts and Lord Howe	Growth of Blue-eye Trevalla is significantly faster (greater length-at-age) on the Seamounts compared to the NSW continental slope (Figure 40 and Figure 41), and there is evidence for connection with NSW at all durations of dispersal (50, 100, 150 and 730 days), including with mortality in the model (Figure 60 and Figure 61). The southernmost Gascoyne Seamount appears different to the remainder of the Tasmantid seamounts, but is outside the Australian EZ. In general, otolith chemistry of all slope and most seamount fish diverged in the first year of life and remained different in the adult demersal stage. Growth of Blue-eye Trevalla is significantly different on the Lord Howe Rise compared to all other areas, including Seamounts (Figure 40 and Figure 41), and there is limited connection with the Seamounts at all durations of dispersal (50, 100, 150 and 730 days), but none with mortality in the model (Figure 60 and Figure 61). A boundary between the Seamounts and Lord Howe is not suggested because ‘stock’ differences are not strong, and catches are small.

Management implications

Collectively, these broad stock areas and the existence of relatively discrete adult sub-populations suggests that a risk of serial depletion will arise if fishing effort and catch is not spread appropriately across the complete distribution of the fishery. When assessing the risks of serial or local depletion in particular fishery areas managers should not only consider the local fishery indicators but also the level of likely propagule supply from other areas, i.e. the source – sink relationships indicated by the dispersal modelling. It may be important to consider reducing impacts on source areas which supply recruits to important fishery areas, e.g. those around Tasmania, or where dispersal appears to be predominantly in one direction, e.g. from west to east across southern Australia.

The current fishery developed initially on the east coast of Tasmania (primarily using drop-line as a method) and that area remained the most heavily fished (Figure 62, inset), leading to noticeable depletion and depression of the CPUE (Haddon 2015). The 'north-eastern' Tasmantid Seamounts were far less depleted than other areas because they were only occasionally fished due to being more isolated and difficult to fish successfully. The uneven distribution of depletion and consequent CPUE depression constitutes strong evidence that uneven fishing mortality has been occurring and, to avoid the risks inherent in such spatially uneven harvest rates, the spread of effort and subsequent catch of Blue-eye Trevalla is in need of more explicit spatial management. The potential benefit is an appropriately set TAC, including the possibility of an increase, and a greater certainty for quota availability.

Any consideration of spatial management would need to account for the area of Blue-eye Trevalla habitat already protected in each of the stock areas. An initial assessment (Appendix 4) shows that Blue-eye Trevalla habitat, the upper slope in 200-1100 m depths from southern Queensland to the Abrolhos Islands, and including the Tasmantid seamounts and Lord Howe Rise, encompasses an approximate area of 142,200 km^2. A total of 4% of this depth range (5,754 km^2) is closed to all hook and line methods, with an additional 1% (1,625 km2) restricted to fishing only with hydraulic reel. Trawl gears are more restricted, with a total of 19% (26,980 km^2) of Blue-eye Trevalla habitat closed to this fishing method. Note that these closure areas are not additive, as some areas of the upper slope are closed to all fishing gears. It is also the case that Blue-eye Trevalla are not evenly distributed and whilst some closed areas were relatively unimportant for Blue-eye Trevalla fishing, others closures cover fishing areas that have produced large historical yields and could be termed Blue-eye Trevalla 'hot-spots'. The effects of these closures on availability of Blue-eye Trevalla to the fishery is not yet known, but closed hot-spot areas off eastern Tasmania and eastern Bass Strait - Flinders Commonwealth Marine reserve, Flinders gulper shark closure, and on Pink Ling (*Genypterus blacodes*) spawning areas off Maria Island and in Bass Canyon - may have a beneficial effect by protecting source areas of Blue-eye Trevalla recruits.

The South-east region CMRs have been implemented and enforced since 2007. These CMRs exclude all bottom trawling from their areas; however only two areas affect hook and line fisheries in the Blue-eye Trevalla depth range: the Freycinet Recreational Use Zone and a small portion of the Tasman Fracture Sanctuary Zone. A full analysis of spatial overlaps is complex due to the number of closures involved (Appendix 4, Figure 63), and by their differential effect on gears (e.g. trawl vs non-trawl), and permanency (Appendix 4, Table 22), and is therefore outside the scope of this study. We have provided the data to enable a full analysis to be completed if spatial management is further considered as a management option for this species.

Our study of Blue-eye Trevalla provides indications on how to develop and evaluate options for other species with the shared characteristics of broad distribution, unknown spatial sub-structure, and management plans that lack spatial and temporal dimensions. In particular, applying an analysis of age and growth characteristics, which was an important element of the approach applied to Blue-eye Trevalla, should be tractable for other species resident on the continental slope. There should be ample existing data for some species, e.g. Pink Ling (*Genypterus blacodes*), while others such as Mirror Dory (*Zenopsis nebulosa*) may require a targeted regional supplement of otolith analysis to fill gaps across the species' range.

Implications

The main implication of these findings is that some form of spatial management (other than additional spatial closures) is required to ensure that catches are spread across the complete fishery to better optimise the productivity and economic performance of the fishery and lower the risk of serial depletion, whether or not Blue-eye Trevalla are treated as multiple biological stocks.

There is sufficient spatial structuring of Blue-eye Trevalla populations (stock areas) to mean that the current approach of setting a single TAC for the whole species' range without further regulation has a high risk of severely depleting the most convenient regions for fishing. The current approach needs to change if the risk of such depletion is to be reduced. This risk is real and has been demonstrated by the relatively depleted state of the east coast of Tasmania where the fishery has been concentrated for decades. The intent of explicit spatial management would be to avoid depleting any single area at the expense of allowing relatively untouched populations to develop in other areas. The potential benefit is an appropriately-set TAC, including the possibility of an increase, and a greater certainty for quota availability that may accompany a greater certainty in management arrangements.

Catch levels that should be sustainable can be estimated for such spatially structured stocks. The problem of distributing those catches across such a wide-ranging and spatially structured species is common to many other spatially heterogeneous species. Focussing effort and catch in the most convenient areas rather than spreading effort and resulting catch across a wide geographical area is understandable as it is more profitable and efficient to do so, at least until catch rates decline. Localization of fishing effort is not necessarily a problem for well-mixed species, but for species such as Blue-eye Trevalla that exhibit different degrees of sub-population structuring across their geographical range, spatially explicit input controls, are required on top of the standard output controls. This is especially important where the stock assessment for the species is focussed in the area most convenient for fishing as this can generate a biased view of the stock status. An input control might be a risk-based approach informed by the data provided by this project.

Recommendations

Some form of spatial management of Blue-eye Trevalla – other than additional spatial closures – is needed to reduce the risk of locally depleting the most convenient areas for fishing. These options include separate TACs for different stocks, a voluntary agreement about the spread of catch across stock areas, or some other management initiative that helps prevent serial depletion (sequential over-catch in certain areas), and considers 'upstream' management of 'source areas' to help ensure that downstream 'sink' areas are replenished. Any one of these options should help ensure that proposed catches remain sustainable as long as the objective of spreading effort and catch is approximately in line with the species' relative availability in the different fishery areas. The potential benefit is an appropriately set TAC, including the possibility of an increase, and a greater certainty for quota availability.

This project will help develop management options through further dissemination of the research findings to the relevant fishery fora (i.e. RAGs or alternatives). Project data were contributed and discussed at RAG meetings in October and November 2016, and discussion of TAC regionalisation is ongoing.

Extension and Adoption

The project was extended in line with the Extension and Adoption Plan. All outputs planned during the project were completed. The media release and blog (Appendix 3) and accompanying video were released on time, regular updates were presented at SlopeRAG and SESSFRAG (with PowerPoint presentations circulated to AFMA and selected stakeholders), and all milestones were completed.

Method	Responsibility	Completion date
Media release and visual (video) clip in early stage of project for general release (inc. social media)	Principal Investigator, Co-PIs, CSIRO Communications	February 2014
Presentations to SlopeRAG and SEMAC	PIs, especially Malcolm Haddon	Regular (6-monthly) Throughout the project, whenever opportunities arise or when requested by stakeholders.
Milestone Reporting to FRDCs	Principal Investigator and Co-PIs	As per milestone schedule

Future presentations will be provided via the RAGs or alternative fora, and a list of scientific publications is planned and partially completed in the 'chapter' style of this report.

Method	Responsibility	Completion date
Final Report to FRDC	Project Team and publisher	Within 3 months of project completion
Presentations to SlopeRAG and SEMAC	Malcolm Haddon	Following project if results have ongoing uptake
Peer-reviewed scientific paper(s)	Lead author(s) with support of Project Team	During and following project

We expect adoption (use of project findings to enhance the stock assessment for Blue-eye Trevalla) to be considered following the publication of the Final Report and presentations to AFMA and stakeholders.

Project coverage

- Blue-eye Trevalla YouTube release: 'Sustainable catch: Blue-eye Trevalla' (mp4) (https://www.youtube.com/watch?v=fLjKeicR9C4&feature=youtube)
- Media release: 'Keeping an eye on Blue-eye' (see Appendix 3)
- Blog: 'Baby's got blue eyes' (see Appendix 3)

References

AFMA. 2015. Australian Fisheries Management Authority Catchwatch reports. Available online at http://www.afma.gov.au/fisheries-services/catchwatch-reports/ . Accessed on 30 November 2016.

Anderson, J.R., Morison, A.K. and Ray, D.J. 1992. Age and growth of Murray cod, *Maccullochella peeli* (Perciformes: Percichthyidae), in the lower Murray-Darling Basin, Australia, from thin-sectioned otoliths. In Smith, D.C. (ed) (1992) Age Determination and Growth of Fish and Other Aquatic Animals. Australian Journal of Marine and Freshwater Research 43, 983-1013.

Ashford, J., Jones, C., Hofmann, E., Everson, I., Moreno, C., Duhamel, G. and Williams, R. 2005. Can otolith elemental signatures record the capture site of Patagonian toothfish (*Dissostichus eleginoides*), a fully marine fish in the Southern Ocean? Canadian Journal of Fisheries and Aquatic Sciences 62, 2832–2840.

Baelde, P. 1996. Biology and dynamics of the reproduction of Blue-eye Trevalla *Hyperoglyphe antarctica* (Centrolophidae), off Tasmania, southern Australia. Fishery Bulletin 94, 199-211.

Bath, G.E., Thorrold, S.R., Jones, C.M., Campana, S.E., McLaren, J.W. and Lam, J.W.H. 2000. Strontium and barium uptake in aragonitic otoliths of marine fish. Geochimica et Cosmochimica Acta 64, 1705-1714.

Beamish, R. and Fournier, D.A. 1981. A method for comparing the precision of a set of age determinations. Journal of the Fisheries Research Board of Canada 36, 1395-400.

Begg, G.A. and Waldman, J.R. 1999. An holistic approach to fish stock identification. Fisheries Research 43, 35-44.

Begg, G.A., and Weidman, C.R. 2001. Stable $\delta^{13}C$ and $\delta^{18}O$ isotopes in otoliths of haddock *Melanogrammus aeglefinus* from the northwest Atlantic Ocean. Marine Ecology-Progress Series 216, 223-233.

Boland, F.M. and Church, J.A. 1981. The East Australian Current 1978. Deep Sea Research 28, 937-957.

Bolch, C.J.S., Elliott, N.G., Ward, R.D. (1993). Enzyme variation in south-eastern Australian samples of the blue-eye or deepsea trevalla, *Hyperoglyphe antarctica* Carmichael 1818 (Teleostei : Stromateoidei). Australian Journal of Marine and Freshwater Research 44, 687-697

Bradford, M.J. 1981. The use of otolith daily increment widths to estimate the size and growth of juvenile chinook salmon (*Oncorhynchus tshawytscha*). M.Sc thesis, Simon Fraser University 84pp.

Bruce, B.D., Neira, F.J. and Bradford, R. 2001. Larval distribution and abundance of blue and spotted warehous (*Seriolella brama* and *S. punctata*: Centrolophidae) in south-eastern Australia. Marine and Freshwater Research 52, 631-636.

Bruce, B.D., Bradford, R., Daley, R., Green, M. and Phillips, K. 2002. Targeted review of biological and ecological information from fisheries research in the south east marine region - Final Report to the National Oceans Office. CSIRO, Hobart, Australia.

Bruland, K.W. and Lohan, M.C. 2003. Controls of trace metals in seawater. Pp. 23–47. In Holland, H.D. and Turekian, K.K. (eds.) (2003) Treatise on Geochemistry. 6: The Oceans and Marine Geochemistry. Amsterdam: Elsevier.

Bye, J.A.T. 1968. The hydrology of the Southern Ocean: 1. The Australian sector – north. Horace Lamb Centre for Oceanographical Research, Research Paper 26, Flinders University, South Australia.

Campana, S.E. 1999. Chemistry and composition of fish otoliths: pathways, mechanisms and applications. Marine Ecology-Progress Series 188, 263-297.

Campana S.E. 2001. Accuracy, precision and quality control in age determination, including a review of the use and abuse of age validation methods. Journal of Fish Biology 2001 59, 197-242.

Campana, S.E. and Thorrold, S.R. 2001. Otoliths, increments, and elements: keys to a comprehensive understanding of fish populations? Canadian Journal of Fisheries and Aquatic Sciences 58, 30-38.

Condie, S., Ridgway, K., Rintoul, B., Griffiths, B.R.S. and Dunn, J. 2003. National oceanographic description and information review for national bioregionalisation. CSIRO Marine Research, Hobart Australia.

Connell, A. 2012. Marine fish eggs and larvae from the east coast of South Africa, originally posted May 2007 and updated October 2012, South African Institute for Aquatic Biology, viewed 27 May 2016, http://fisheggs-and-larvae.saiab.ac.za/Default.htm

Cowen, R.K. and Sponaugle, S. 2009. Larval dispersal and marine population connectivity. Annual Review of Marine Science 1, 443–466.

Dehairs, F., Shopova, D., Ober, S., Veth, C. & Goeyens, L. 1997. Particulate barium stocks and oxygen consumption in the Southern Ocean mesopelagic water column during spring and early summer: relationship with export production. Deep Sea Research II 44, 497–516.

de Vries, M.C., Gillanders, B.M. and Elsdon, T.S. (2005). Facilitation of barium uptake into fish otoliths: Influence of strontium concentration and salinity. Geochimica et Cosmochimica Acta 69, 4061–4072.

Dougherty, A.B. 2008. Daily and sub-daily otolith increments of larval and juvenile walleye pollock, *Theragra chalcogramma* (Pallas), as validated by alizarin complexone experiments Fisheries Research 90, 271–278.

Duffy, C.A.J., Stewart, A.L. and Yarrall, R. 2000. First record of pre-settlement juvenile bluenose, *Hyperoglyphe antarctica*, from New Zealand. New Zealand Journal of Marine and Freshwater Research 34(2), 353-358.

Dufour, V., Pierre, C. and Rancher, J. 1998. Stable isotopes in fish otoliths discriminate between lagoonal and oceanic residents of Taiaro Atoll (Tuamotu Archipelago, French Polynesia). Coral Reefs 17, 23-28.

Efron, B. and Tibshirani, R.J. 1993. An Introduction to the Bootstrap. Chapman and Hall, New York.

Elsdon, T.S. and Gillanders, B.M. 2003. Relationship between water and otolith elemental concentrations in juvenile black bream, *Acanthopagrus butcheri*. Marine Ecology Progress Series 260, 263-272.

Elsdon, T.S., Wells, B.K., Campana, S.E., Gillanders, B.M., Jones, C.M., Limburg, K.E., Secor, D.H., Thorrold, S.R. and Walther, B.D. 2008. Otolith chemistry to describe movements and life-history parameters of fishes: hypotheses, assumptions, limitations and inferences. Oceanography and Marine Biology: An Annual Review 46, 297-330

Fay, G., Punt, A.E. and Smith, A.D.M. 2011. Impacts of spatial uncertainty on performance of age structure-based harvest strategies for blue eye trevalla (*Hyperoglyphe antarctica*). Fisheries Research 110, 391-407.

Fisher, R.A. 1936. “The coefficient of racial likeness” and the future of craniometry. Journal of the Royal Anthropological Institute of Great Britain and Ireland 66, 57-63.

Gao, Y.W. and Beamish, R.J. 1999. Isotopic composition of otoliths as a chemical tracer in population identification of sockeye salmon (*Oncorhynchus nerka*). Canadian Journal of Fisheries & Aquatic Sciences 56, 2062-2068.

Genin, A., and Boehlert, W. 1985. Dynamics of temperature and chlorophyll structures above a seamount: An oceanic experiment. Journal of Marine Research 43, 907-924.

Genin, A. 2004. Bio-physical coupling in the formation of zooplankton and fish aggregations over abrupt topographies. Journal of Marine Systems 50, 3-20.

Gillanders, B.M. 2002. Temporal and spatial variability in elemental composition of otoliths: implications for determining stock identity and connectivity of populations. Canadian Journal of Fisheries & Aquatic Sciences 59, 1-11.

Good, P. 1994. Permutation Tests. A Practical Guide to Resampling Methods for Testing Hypotheses. Springer-Verlag, Berlin.

Haddon, M. 2011. Modelling and Quantitative Methods in Fisheries. Chapman and Hall, CRS Press. 449 p.

Haddon, M. 2015a. Blue Eye Fishery Characterization 1986 – 2013. Pp 277-327. In Tuck, G.N. (ed.) (2015) Stock Assessment for the Southern and Eastern Scalefish and Shark Fishery 2014. Part 2. Australian Fisheries Management Authority and CSIRO Oceans and Atmosphere Flagship, Hobart. 432 p.

Haddon, M. 2015b. Blue-eye Auto-Line and Drop-Line CPUE Characterization 1986 – 2014. CSIRO report to the SESSF SLOPE RAG, November 2015. CSIRO Oceans and Atmosphere, Hobart. 41p.

Haddon, M. 2015c. Tier 4 Analyses of Selected Species in the SESSF. Data from 1986 – 2014 CSIRO report to the SESSF RAGs, November 2015. CSIRO Oceans and Atmosphere, Hobart. 23p.

Haddon, M. and Willis, T.J. 1995. Morphometric and meristic comparison of orange roughy (*Hoplostethus atlanticus*: Trachichthyidae) from the Puysegur Bank and Lord Howe Rise, New Zealand, and its implications for stock structure. Marine Biology 123, 19 – 27.

Haedrich, R. L. 1967. The stromateoid fishes: systematics and a classification. Bulletin of the Museum of Comparative Zoology, Harvard University 135, 31-139.

Hamer, P.A., Acevedo, S., Jenkins, G.P. and Newman, A. 2011. Connectivity of a large embayment and coastal fishery: spawning aggregations in one bay source local and broad-scale fishery replenishment. Journal of Fish Biology 78, 1090-1109.

Hamer, P.A. and Jenkins, G.P. 2007. Comparison of spatial variation in otolith chemistry of two fish species and relationships with water chemistry and otolith growth. Journal of Fish Biology 71, 1035-1055.

Hatch, M. B. A., Schellenberg, S.A., and Cartera, M.L. 2013. Ba/Ca variations in the modern intertidal bean clam *Donax gouldii*: An upwelling proxy? Palaeogeography, Palaeoclimatology, Paleoecology 373, 98-107.

Hindell, J., Hamer, P., McPartlan, H. and Robertson, S. 2005. Preliminary assessment of the utility of otolith microchemistry, otolith shape analysis and mitochondrial DNA analyses in stock discrimination of Blue-eye Trevalla (*Hyperoglyphe antarctica*) from Australian shelf waters and offshore seamounts and New Zealand - Final report to Fisheries Research and Development Corporation Project No. 2003/045. Primary Industries Research Victoria, Queenscliff, Victoria.

Høie, H., Otterlei, E., and Folkvord, A. 2004. Temperature-dependent fractionation of stable oxygen isotopes in otoliths of juvenile cod (*Gadus morhua* L.). ICES Journal of Marine Science 61, 243-251.

Horn, P.L. 2003. Stock structure of bluenose (*Hyperoglyphe antarctica*) off the north-east coast of New Zealand based on the results of a detachable hook tagging programme. New Zealand Journal of Marine and Freshwater Research 37(3), 623-631.

Horn, P.L. 1988. Age and growth of bluenose, *Hyperoglyphe antarctica* (Pisces: Stromateoidei) from the lower east coast, North Island, New Zealand. New Zealand Journal of Marine and Freshwater Research 22(3), 369-378.

Horn, P.L. and Massey, B.R. 1989. Biology and abundance of alfonsino and bluenose off the lower east coast North Island, New Zealand - New Zealand Technical Report No. 15. MAF Fisheries, Wellington, NZ.

Horn, P.L., Neil, H.L., Paul, L.J. and Marriot, P. 2010. Age validation and growth of bluenose *Hyperoglyphe antarctica* using the bomb chronometer method of radiocarbon ageing. Journal of Fish Biology 77(7), 1552–63.

Houde, E.D. 1989. Comparative growth, mortality and energetics of marine fish larvae: temperature and implied latitudinal effects. Fishery Bulletin: 87, 471-495.

Iacumin, P., Bianucci, G. and Longinelli, A. 1992. Oxygen and carbon isotopic composition of fish otoliths. Marine Biology 113, 537-542.

Izzo C, Doubleday Z.A., Schultz A.G., Woodcock, S.H. and Gillanders, B.M. 2015.Contribution of water chemistry and fish condition to otolith chemistry: comparisons across salinity environments. Journal of Fish Biology 86(6), 1680-98.

Jones, G.K. 1985. An exploratory survey for deepsea trevalla (*Hyperoglyphe antarctica*) in continental slope waters off South Australia - Fisheries Research Paper No 15. Department of Fisheries SA, Adelaide, SA.

Kailola, P.J. and Fisheries Research and Development Corporation (Australia). Bureau of Resource Sciences. 1993. Australian fisheries resources. Canberra, A.C.T: Bureau of Resource Sciences and the Fisheries Research and Development Corporation

Kalish, J. M. 1989. Otolith chemistry: validation of the effects of physiology, age and environment on otolith composition. Journal of Experimental Marine Biology & Ecology 132, 151-178.

Kalish, J.M. 1991a. 13C and 18O isotopic disequilibria in fish otoliths: metabolic and kinetic effects. Marine Ecology Progress Series 75, 191-203.

Kalish, J.M. 1991b. Oxygen and carbon stable isotopes in the otoliths of wild and laboratory-reared Australian salmon (*Arripis trutta*). Marine Biology 110, 37-47.

Kalish, J. and Johnston, J. 2002. Application of the bomb radiocarbon chronometer to the validation of blue eye trevalla (*Hyperoglyphe antarctica*) age. Pp. 148–163. *In* Kalish, J. (ed) (2002) Use of the Bomb Radiocarbon Chronometer to Validate Fish Age. Final Report FRDC Project 93/109, Canberra: Fisheries Research and Development Corporation and Australian National University.

Kool, J.T. and Nichol, S.L. 2015. Four-dimensional connectivity modelling with application to Australia's north and northwest marine environments. Environmental Modelling & Software 65, 67-78.

Last, P.R., Bolch, C. and Baelde, P. 1993. Discovery of juvenile Blue-eye. Australian Fisheries August, 16-17.

Lea, D.W., Shen, G.T. and Boyle, E.A. 1989. Corraline barium records temporal variability in equatorial Pacific upwelling. Nature 340, 373-375.

Lahaye, Y., Lambert, D. and Walters, S. 1997. Ultraviolet laser sampling and high resolution inductively coupled plasma-mass spectrometry of NIST and BCR-2G glass reference materials. Geostandards Newsletters 21, 205-214.

La Mesa, M., Sinopoli, M. and Andalordo, F. 2005. Age and growth rate of Juvenile bluefin tuna *Thunnus thynnus* from the Mediterranean Sea (Sicily, Italy). Scientia Marina, 69 (2), 241-249.

LeGrande, A.N. and Schmidt, G.A. 2006. Global gridded data set of oxygen isotopic composition in seawater. Geophysical Research Letters 33(12), DOI: 10.1029/2006GL026011.

Leis, J.M., Van Herwerden, L. and Patterson, H.M. 2011. Estimating connectivity in marine fish populations: What works best? Oceanography and Marine Biology: An Annual Review, 2011, 49, 193–234.

Manly, B.F.J. 1991. Randomization and Monte Carlo Methods in Biology. Chapman & Hall, London.

Manly, B.F.J. 1997. Randomization, Bootstrap and Monte Carlo Methods in Biology. 2nd edn. Chapman & Hall, London.

Maria, R.A., Miller, J.A. and Hurst, T.P. 2010. Temperature and growth effects on otolith elemental chemistry of larval Pacific cod, *Gadus macrocephalus*. Environmental Biology Fishes 89, 453-462.

Martin, G.B. and Thorrold, S.R. 2005. Temperature and salinity effects on magnesium, manganese, and barium incorporation in otoliths of larval and early juvenile spot *Leiostomus xanthurus*. Marine Ecology Progress Series 293, 223-232.

Middleton, J.F. and Bye, J.A.T. 2007. A review of the shelf slope circulation along Australia's southern shelves: Cape Leeuwin to Portland. Progress in Oceanography 75, 1-41.

Morison, A.K. and Robertson, S.G. 1998 Age of Blue-eye Trevalla (*Hyperoglyphe antartica*): As Part of Fisheries Research and Development Corporation. FRDC 91/20.

Morison, A.K., Robertson, S.G. and Smith, D.C. 1998. An integrated production fish ageing system: quality assurance and image analysis. North American Journal of Fisheries Management 18, 587–598.

Namiki, S., Tanaka, H., Katayama, S., Funaki, O. and Oozeki, Y. 2010 Validation of daily increment formation in otoliths of immature and adult Japanese anchovy *Engraulis japonicus*. Fisheries Science (2010) 76: 951.

North, E.W., Gallego, A. and Petitgas, P. 2009. Manual of recommended practices for modelling physical-biological interactions in fish early-life. Copenhagen: International Council for the Exploration of the Sea Cooperative Research Report 295, 1–112.

Ridgway, K.R. and Dunn, J.R. 2003. Mesoscale structure of the mean East Australian Current System and its relationship with topography. Progress in Oceanography 56(2), 189-222.

Robinson, N., Skinner, A., Sethurama L.A, McPartlan, H., Murray, N., Knuckey, I., Smith, D.C., Hindell, J. and Talman, S. 2008. Genetic stock structure of Blue-eye Trevalla (*Hyperoglyphe antarctica*) and warehous (*Seriolella brama* and *Seriolella punctata*) in south-eastern Australian waters. Marine and Freshwater Research, 59: 502-514

Robbins, W.D. and Choat, J.H. 2002. Age-based dynamics of tropical reef fishes; A guide to the processing, analysis and interpretation of tropical fish otoliths. Townsville, Australia, p 1-39.

Schaefer, K.M. and Fuller, D.W. 2006. Estimates of age and growth of bigeye tuna (*Thunnus obesus*) in the eastern Pacific Ocean, based on otolith increments and tagging data. Bulletin of the Inter-American Tropical Tuna Commission 23(2), 35−76.

Schwarcz, H.P., Gao, Y., Campana, S., Browne, D., Knyf, M. and Brand, U. 1998. Stable carbon isotope variations in otoliths of Atlantic cod (*Gadus morhua*). Canadian Journal of Fisheries and Aquatic Sciences 55, 1798-1806.

Smith, A.D.M. and Wayte, S.E. (Eds.), 2002. The South East Fishery 2001. Fishery Assessment Report compiled by the South East Fishery Assessment Group. Australian Fisheries Management Authority, Canberra.

SPRFMO 2007. Information describing bluenose (*Hyperoglyphe antarctica*) fisheries information relating to the South Pacific Regional Fisheries Management Organisation http://www.sprfmo.int/assets/Fisheries/Species-Profiles/H-antarctica-species-profile-230607-Science-III.pdf. Website last visited 30/5/2016.

Sturrock, A.M., Trueman, C.N., Darnaude, A.M. and Hunter, E. 2012. Can otolith elemental chemistry retrospectively track migrations in fully marine fishes? Journal of Fish Biology 81, 766-795.

Sturrock, A.M., Trueman, C.N., Milton, J.A., Waring, C.P., Cooper, M.J. and Hunter, E. 2014. Physiological influences can outweigh environmental signals in otolith microchemistry research. Marine Ecology Progress Series 500, 245-264.

Thomson, R., Sporcic, M., Klaer, N., Fuller, M., Krucic-Golub, K. and Upston, J. 2015. Data summary for the Southern and Eastern Scalefish and Shark Fishery: Logbook, Landings and Observer Data to 2014. Australian Fisheries Management Authority and CSIRO Oceans and Atmosphere, Hobart. 280p.

Thorrold, S.R., Campana, S.E., Jones, C.M. and Swart, P.K. 1997. Factors determining δ13C and δ18C fractionation in aragonite. Geochimica et Cosmochimica Acta 61, 2909-2919.

Thresher, R.E. 1999. Elemental composition of otoliths as a stock delineator in fishes. Fisheries Research 43, 165-204.

Tilburg, C.E., Hurlburt, H.E., O'Brien, J.J. and Shriver, J.F. 2001. The dynamics of the East Australian Current system: the Tasman Front, the East Auckland Current, and the East Cape Current. Journal of Physical Oceanography 31, 2917-43.

von Bertalanffy, L. 1938. A quantitative theory of organic growth. Human Biology 10, 181-213

Wakefield, C.B., and Newman, J. 2008. Age estimation and reproductive status of an exceptionally large Blue-eye Trevalla (*Hyperoglyphe antarctica*, Centrolophidae) captured off the south coast of Western Australia. Cybium 32(4), 321-324.

Walther, B.D. and Thorrold, S.R. 2006. Water, not food, contributes the majority of strontium and barium deposited in the otoliths of marine fish. Marine Ecology Progress Series 311, 125-130.

Waples, R.S. 1998. Separating the wheat from the chaff: patterns of genetic differentiation in high gene flow species. Journal of Heredity 89, 438-450.

Watson, J.R., Mitarai, S., Siegel, D.A., Caselle, J.E., Dong, C and McWilliams, J.C. 2010. Realized and potential larval connectivity in the Southern California Bight. Marine Ecology Progress Series 401, 31-48.

Weidman, C.R. and Millner, R. 2000. High-resolution stable isotope records from North Atlantic cod. Fisheries Research 46, 327-342.

Williams, A., Althaus, F. and Furlani, D. 2005. Assessment of the conservation values of the Norfolk Seamounts area: A component of the Commonwealth Marine Conservation Assessment Program 2002-2004: report to the Department of the Environment and Heritage. CSIRO Marine and Atmospheric Research, Hobart, Tas. 173p.

Williams, A., Green, M., Graham, K., Upston, J., Barker, B. and Althaus, F. 2013. Determining the distribution of gulper sharks on Australia's eastern seamount chain and the selectivity of power handline fishing in regard to seamount populations of Blue-eye Trevalla and Harrisson's Dogfish. Final report to AFMA. CSIRO Marine and Atmospheric Research, Hobart, Tasmania. 42p.

Williams, A., Upston, J., Green, M. and Graham, K. 2016. Selective commercial line fishing and biodiversity conservation co-exist on seamounts in a deepwater marine reserve. Fisheries Research 183, 617-624

Woodcock, S.H., Munro, A.R., Crook, D.A. and Gillanders, B.M. 2012. Incorporation of magnesium into fish otoliths: Determining contribution from water and diet. Geochimica et Cosmochimica Acta 94, 12–21

Yoshinaga, J., Masatoshi, M. and Edmonds, J.S. 1999. Determination of copper, zinc, cadmium and lead in a fish otolith certified reference material by isotope dilution inductively coupled plasma mass spectrometry using off-line solvent extraction. Journal of Analytical Atomic Spectrometry 14, 1589-1592.

Project materials developed

Planned papers from this project (linked to the main results sections)

Results Chapter 2

Daily and annual ageing methods for otoliths of the Blue-eye Trevalla (*Hyperoglyphe antarctica*)

Results Chapter 3

Spatial variation in age and growth in Blue-eye Trevalla (*Hyperoglyphe antarctica*) supports the concept of separate populations on seamounts and the continental slope

Results Chapter 4

Application of otolith chemistry life history profiles and stable isotope analysis to resolve population structure of Blue-eye Trevalla (*Hyperoglyphe antarctica*)

Results Chapter 5

Ocean circulation models and otolith chemistry infer patterns of ecological dispersal and recruitment in Australian populations of the Blue-eye Trevalla (*Hyperoglyphe antarctica)*

Appendices

Appendix 1: List of researchers and project staff

Name	Affiliation	Status	Role
Alan Williams	CSIRO Wealth from Oceans (Marine Resources and Industry)	Principal Investigator	Project management; written contributions to Final Report, especially Section 5 (Ecological Dispersal Modelling)
Paul Hamer	Fisheries Victoria	Co-Investigator	Otolith microchemistry; written contributions to Final Report, especially Section 4 (Otolith Chemistry)
Malcolm Haddon	CSIRO Wealth from Oceans (Marine Resources and Industry)	Co-Investigator	Age and growth models; stock assessment; written contributions to Final Report, especially Section 3 (Spatial analysis of age and growth)
Simon Robertson	Fish Ageing Services (FAS)	Project team	Otolith ageing; written contributions to Final Report, especially Section 2 (Otolith Ageing)
Franziska Althaus	CSIRO Wealth from Oceans (Marine Resources and Industry)	Project team	Data collation and analysis; written contributions to Final Report, especially Methods and Section 1 (Data collation and biology)
Mark Green	CSIRO Wealth from Oceans (Marine Resources and Industry)	Project team	Literature review and data acquisition; written contributions to Final Report, especially Methods and Section 1 (Data collation and biology)
Johnathan Kool	Geoscience Australia	Project team	Design of dispersal model and data analysis; written contributions to Final Report, especially Section 5 (Ecological Dispersal Modelling)

Appendix 2: Intellectual property

No special consideration necessary because the methods and data inputs and anticipated outputs will all be in the public domain.

Appendix 3: Media release and blog

Keeping an eye on Blue-eye

Blue-eye Trevalla is one of Australia's premium seafoods, and an iconic fish species in south eastern regions including Tasmania.

To help ensure the fishing industry has healthy stocks to catch, CSIRO's Wealth from Oceans Flagship and the Department of Primary Industry (DPI), Victoria, are researching the life history and movement of the fish in a study off eastern Australia.

CSIRO project leader Dr Alan Williams said that the work on Blue-eye will be critical to understanding stock size and distribution. "Our research will help the fishing industry understand more about the Blue-eye's life history, and hopefully lead to a bigger and sustainable catch," he said.

"Blue-eye catches have reduced by 50 per cent in recent years, and shortages in fishing quota have led to some fishing boats lying idle."

The research team will identify where Blue-eye spawn, and track when they move to eastern Australia's fishing grounds as adults. The information will be used in advanced computer models to predict how many fish can be caught sustainably in different fishery areas.

Dr Paul Hamer, a marine scientist with DPI, said computer models rely on information extracted from the ear bones of Blue-eye using new laser techniques. "Chemical signatures in Blue-eye's ear bones tell us where fish are spawned and spend their early years of life."

"We will combine this information with models of ocean currents to predict how fish stocks are distributed, and to understand the fluctuations in stock sizes," Dr Hamer said.

The information gathered in this project will help to manage the species sustainably and ensure the Blue-eye's future on consumers' plates in years to come.

The project is funded by the Australian Government through the CSIRO Wealth from Oceans Flagship, DPI Victoria, and the Fisheries Research and Development Corporation.

For more information contact:

Dr Alan Williams, CSIRO Marine Laboratories, Hobart, Tasmania: 03 6232 5222

Kirsten Lea, Communication Manager, CSIRO Wealth from Oceans Flagship: 0457 563 684

Baby's got Blue Eyes ...

Grilled with garlic, oven baked, or lightly pan fried with a hint of lemon, Blue-eye Trevalla is one of Australia's premium seafoods, and an iconic fish species for commercial fishers and seafood lovers alike.

Caption: Mmmmmm Blue-eye. Easy to cook, easy to prepare ... it's hard to get it wrong according to the owner of the Mures seafood restaurant in Hobart.

Despite having been fished commercially for over 40 years in deep waters off southern Australia, the Blue-eye's early life history and movement is still shrouded in mystery.

Our research into these aspects of the Blue-eye's biology aims to inform the Australian Fisheries Management Authority's process to set commercial catch quotas, and hopefully lead to increases in the quota, which, in recent years, has dropped by 50 per cent due to apparent decreases in the fish's abundance.

Ear bone's connected to the catch quota

Using chemical signatures in the make-up of the Blue-eye's ear bones, we aim to determine the fish's population structure, early life history and movement in the fishery area - which extends roughly from Brisbane to Adelaide, and includes several offshore seamounts.

Once the ear bone is daintily plucked from inside a fish's head, we use laser-based sampling techniques to identify its chemical signature and from this we can infer each individual fish's geographical origin.

With sufficiently large numbers of sampled fish in specific age groups, and when combined with models of ocean currents, the origins of Blue-eye populations in different fishery areas can be estimated.

These insights enable our analysis of the commercial catch to become location-specific or 'regionalised' and reduce many of the uncertainties in the assessment of total stock size.

Caption: CSIRO's Dr Alan Williams holds a tiny ear bone from this fresh Blue-eye (Hyperoglyphe antarctica). Under our no-waste policy we can confirm the rest of the fish was enjoyed by Alan and his family!

A greater confidence in the stock assessment will ensure a sustainable catch for Australia's fishing industry and the continued availability of Blue-eye for consumers' plates.

Find out more about the project in the video <imbed video>

The project is funded by the Australian Government through the CSIRO Wealth from Oceans Flagship, DPI Victoria, and the Fisheries Research and Development Corporation. Footage and images were taken in Hobart, thanks to the Captain, Russell Potter, and crew of the fishing vessel *Diana*, and Will Mure and head chef from the Mures Restaurant.

Media contact: Kirsten.lea@csiro.au or 02 4960 6245

Appendix 4: Closures

Table 22 List of closures that potentially overlap the upper slope Blue-eye habitat, classified by excluded fishing methods.

AFMA Fishey closures	1st implemented (by area)	Date ceasing	Current applicable Commlaw Doc Code*
Closed to all fishing methods			
South Australian Shark Closure – Victor Harbor to the Victorian Border	13/07/2007	1/12/2018	F2013L00168_12
Seal Bay	13/07/2007	1/12/2018	F2013L00168_6
Pages Island	13/07/2007	1/12/2018	F2013L00168_7
Kent Group National Park	13/07/2007	1/12/2018	F2013L00168_3
			F2011L02144_1-a; F2011L02154_1-a;
South Australian Shark Closure – Kangaroo Island / Kangaroo Island gillnet strip	13/07/2007	1/12/2018	F2013L00168_11
Head of the Great Australian Bight / Head of the Great Australian Bight gillnet strip	13/07/2007	1/04/2022	F2013L00168_8; F2011L02144_1-b
Flinders Research Zone Closure	15/02/2013	1/12/2018	F2013L00170_1; F2013L01827_1
Port Macdonnell Closure 2013	15/02/2013	1/12/2018	F2013L00168_40
Derwent Hunter Seamount Closure	15/02/2013	1/12/2018	F2013L00168_39
Gulper Shark Closure – Endeavour Dogfish 2013	15/02/2013	1/12/2018	F2013L00168_18
Gulper Shark Closure – Harrisson's Dogfish	15/02/2013	1/12/2018	F2013L00168_19
Closed to all fishing methods except Hydraulic Reel			
Queensland and Britannia Seamounts Closure	15/02/2013	1/12/2018	F2013L00168_38
Closed to hook fisheries			
Commonwealth Scalefish Hook Sector Gulper Shark Closure – Southern Dogfish	13/07/2007	1/12/2018	F2013L00168_16
Cascade Plateau	13/07/2007	1/12/2018	F2013L00168_2
Closed to auto-longline fisheries			
Automatic Longline Shallow Water Closure	15/02/2013	1/12/2018	F2013L00222_2
Closed to all trawl methods and a trigger applied to all other methods			
St Helens Hill Closure	13/07/2007	1/12/2018	F2013L00168_5
Barcoo and Taupo Seamounts Closure	30/06/2010	1/12/2018	F2013L00168_37
Murray Dogfish Closure	15/02/2013	1/12/2018	F2013L00168_41
Closed to all trawl methods			
GAB Orange Roughy Zone – United Nations	5/07/2008	1/12/2018	F2013L00168_32
GAB Orange Roughy Zone – The Knob	5/07/2008	1/12/2018	F2013L00168_33
GAB Orange Roughy Zone – Racetrack/Hamburger	5/07/2008	1/12/2018	F2013L00168_34
GAB Orange Roughy Zone – Lomvar Gully	5/07/2008	1/12/2018	F2013L00168_31
GAB Orange Roughy Zone – Kangaroo Island Hill	5/07/2008	1/12/2018	F2013L00168_35
GAB Orange Roughy Zone – Humdinger West	5/07/2008	1/12/2018	F2013L00168_29
GAB Orange Roughy Zone – Humdinger/Magic	5/07/2008	1/12/2018	F2013L00168_30
GAB Orange Roughy Zone – Bremmer	30/06/2010	1/12/2018	F2013L00168_28
GAB Orange Roughy Zone – Albany	5/07/2008	1/12/2018	F2013L00168_27
Tasmanian Seamounts Marine Reserve	13/07/2007	1/12/2018	F2013L00168_21
Great Australian Bight Trawl Sector Gulper Shark Closure – Southern Dogfish	13/07/2007	1/12/2018	F2013L00168_17
East Coast Deepwater Trawl Sector Exclusion Zone	13/07/2007	1/12/2018	F2013L00168_9
Western Deepwater Shark Area – opening and trigger limit	10/04/2013	1/12/2018	F2013L00632_1
GAB Far West Gulper Shark Closure	17/12/2010	1/12/2018	F2013L00168_36
South East Trawl Deep Water Closure	15/02/2013	1/12/2018	F2013L00168_20
Closed to demersal ottertrawl, gillnet and Danish seine and a trigger applied to all other			
Freycinet Commonwealth Marine Reserve Closure	15/02/2013	1/12/2018	F2013L00168_13
Murray Commonwealth Marine Reserve Closures (east)	15/02/2013	1/12/2018	F2013L00168_15-a
Murray Commonwealth Marine Reserve Closures (west)	15/02/2013	1/12/2018	F2013L00168_15-b
Closed to demersal ottertrawl			
GAB Deepwater Closure – Far West	5/07/2008	1/12/2018	F2013L00168_26
GAB Deepwater Closure – Salisbury Canyon	5/07/2008	1/12/2018	F2013L00168_25
Portland Area Trawl Closure	5/07/2008	1/12/2018	F2013L00168_23
Eastern South Australia Trawl Closure	5/07/2008	1/12/2018	F2013L00168_22
Bass Strait – Trawl closure	5/07/2008	1/12/2018	F2013L00168_4
GAB Deepwater Closure – Central East Zone	15/02/2013	1/12/2018	F2013L00168_24
Closed to gillnet and hooks from shark hook boats			
West Coast Tasmania Shark Hook Boat Statutory Fishing Right and Gillnet Depth Closure	13/07/2007	1/12/2018	F2013L00168_14
Shark Hook and Gillnet Deepwater Closure	20/02/2013	1/12/2018	F2013L00222_1
Closed to gillnetting			
Murat Bay	13/07/2007	1/12/2018	F2013L00168_1
South Australian Gillnet Closure – Backstairs Passage	13/07/2007	1/12/2018	F2013L00168_10
Commonwealth Marine Reserves			
Closed to all commercial fishing			
Murray [Sanctuary & Marine Nat. Park Zones (IUCN Ia & II)]	2007		
Nelson [Special Purpose Zone (IUCN IV)]	2007		
Zeehan [Special Purpose Zone (IUCN IV)]	2007		
Tasman Fracture [Sanctuary Zone (IUCN IA)]	2007		
Huon [Habitat Protection and Conservation Park Zones (IUCN IV)]	2007		
Freycinet [Recreational Use Zone (IUCN II)]	2007		
Freycinet [Sanctuary & Marine Nat. Park Zones (IUCN Ia & II)]	2007		
Flinders [Sanctuary & Marine Nat. Park Zones (IUCN Ia & II)]	2007		
Closed to all trawl methods			
Murray [Special Purpose Zone (IUCN IV)]	2007		
Murray [Multiple Use Zone (IUCN VI)]	2007		
Tasman Fracture [Multiple Use Zone (IUCN VI)]	2007		
Huon [Multiple Use Zone (IUCN VI)]	2007		
South Tasman Rise [Special Purpose Zone (IUCN IV)]	2007		
East Gippsland [Multiple Use Zone (IUCN VI)]	2007		

* Schedule number and part are appended to the DocCode where applicable

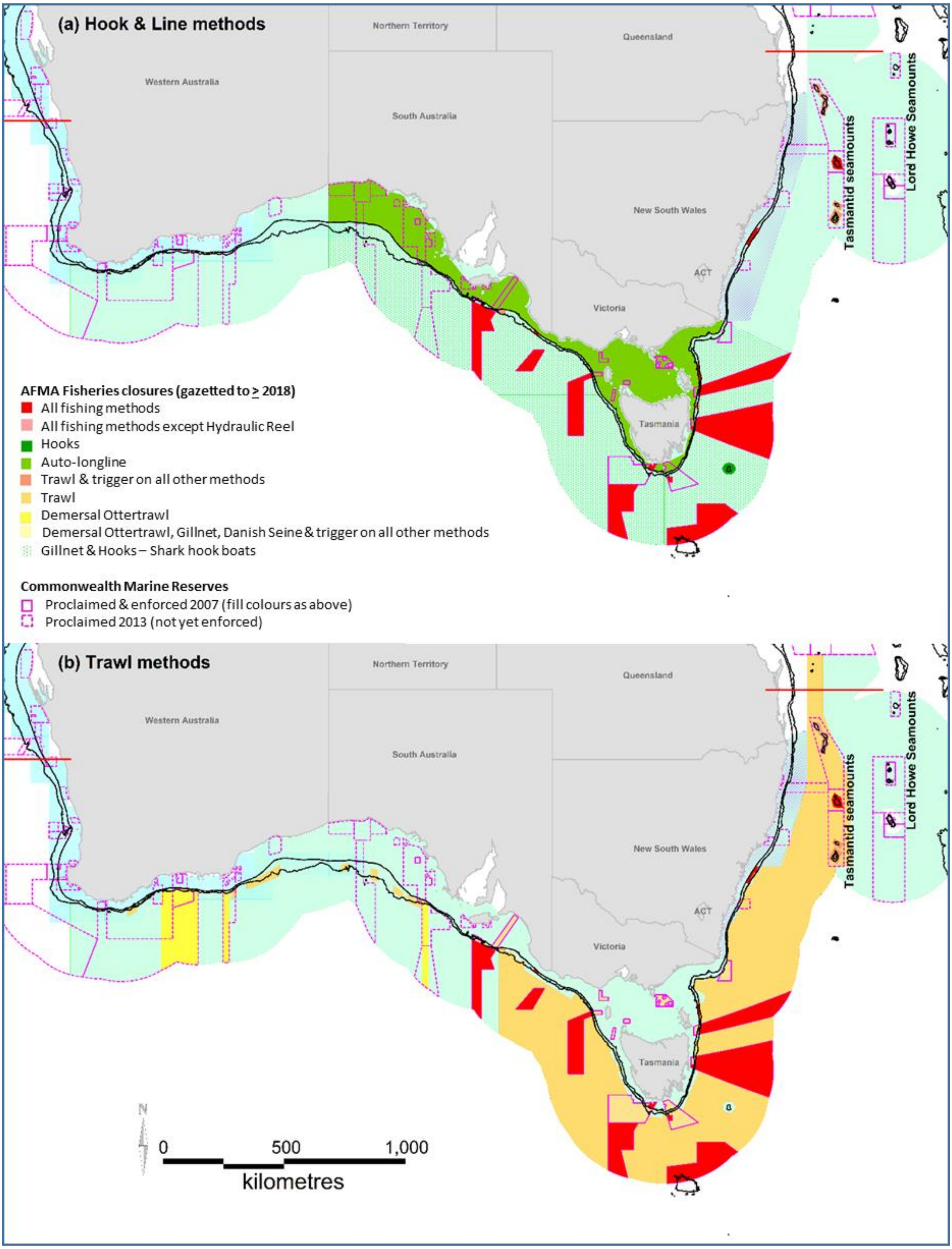

Figure 63 Spatial representation of closures applying to (a) hook and line and (b) trawl fishing methods in relation to the Blue-eye Trevalla habitat o the upper slope (200 – 1100 m depth). Background colours show the fishery areas: SESSF (green), WA fishery (cyan) and NSW fishery (blue).

Appendix 5: Glossary of location abbreviations used in report

UNIFIED TERM	UNIFIED TERM (ABBREV)	Broad area	Ch 1 Catch data Region	CH 2 Aging Region (group)	CH 2 Aging Abbrev	Ch 3 Age & growth	Ch 4 Otolith Chem	Ch 5 disp Model Sink location	Ch 5 disp Model Abbrev	Ch 5 disp Model Source location (within regions)	Ch 5 disp Model Abbrev
Abrolhos	ABR	WA	Abrolhos					Abrolhos	ABR	Abrolhos	ABR
Perth	PRT	cont. slope	Perth					Perth	PRT	Perth Canyon	PCN
SW Capes	SWC		SW Capes					SW Capes	SWC	SW Site	SWS
Albany	ALB		Albany					Albany	ALB	Albany	ALB
Esperance	ESP		Esperance				wa	Esperance	ESP	Esperance	ESP
Head of GAB	HGA		Head GAB					Head of GAB	HGA		
Western GAB	WGAB	West SESSF	W GAB	West King Island/ Western GAB	W KI/ GAB	West KI/GAB	wkg	Western GAB	WGA	Port Lincoln	PTL
West of Kangaroo Island	WKI	cont. slope	W of Kangaroo Isl					W of Kangaroo Isl	WKI	W Kangaroo Is	WKI
Portland	PRT		Portland					Portland	PRT		
Southwest Victoria	SW Vic		SW Vic					SW Vic	SWV	Pt. MacDonnell	PTM
Western Bass Strait	W Bass St		W Bass St					W Bass St	WBS	Zeehan	ZEE
Western Tasmania	W Tas		W Tas	West bass Strait/ West Tas	WBS/ W Tas	WBS/ W Tas	wbt	W Tas	WTS	Low Rocky North	LRN
										Low Rocky south	LRS
Southern Tasmania	S Tas	South cont slope	S Tas					S Tas	STS	Maatsuyker patch	MTS
										South Patch	SPT
										Pedra Patch	PPT
										30 Mile Patch	TPT
										18 Mile Patch	EPT
Cascade seamount	CSC	seamount	Cascade				casc	Cascade	CSC		
Eastern Tasmania	East Tas	East SESSF	East Tas					East Tas	ETS		
East Bass Strait	East Bass St	cont. slope	East Bass St	Bass Canyon/ East Flinders Island		Bass Canyon/ East Flinders	bsc	East Bass St	EBS	NE Tas	NET
										Banks Patch	BPT

UNIFIED TERM	UNIFIED TERM (ABBREV)	Broad area	Ch 1 Catch data	CH 2 Aging		Ch 3 Age & growth	Ch 4 Otolith Chem	Ch 5 disp Model			
			Region	**Region (group)**	**Abbrev**			**Sink location**	**Abbrev**	**Source location (within regions)**	**Abbrev**
Bass Canyon	Bass Canyon		Bass Canyon					Bass Canyon	BCN	The Wall Seiners Horseshoe	WLF SHS
Southern New South Wales	S_NSW		S_NSW	S_NSW		S_NSW	NSW	S_NSW	SNS		BMG
											BMT
Northern New South Wales	N_NSW		N_NSW	N_NSW		N_NSW		N_NSW	NNS	Port Stevens	PST
										Coffs Harbour	CFS
										Queensland Border	QBD
Gascoyne	GSC	Tasmantid	Gascoyne	Gascoyne		Gascoyne	gasc	Gascoyne	GSC	Gascoyne	GSC
Taupo	TPO	seamounts	Taupo	Taupo		Taupo	tpo	Taupo	TPO	Taupo	TPO
Barcoo	BCO		Barcoo	Barcoo		Barcoo	bco	Barcoo	BCO	Barcoo	BCO
Derwent Hunter	DWH		Derwent Hunter	Derwent Hunter		Derwent Hunter	dh	Derwent Hunter	DWH	Derwent Hunter	DWH
'unknown' Queensland Seamount	UQLD		unknown QLD SM	unknown QLD SM		unknown QLD SM	uqld	unknown QLD seamount			
Stradbroke			Stradbroke	Stradbroke		Stradbroke		Stradbroke			
Britannia	BRT		Britannia	Britannia		Britannia	brit	Britannia	BRT	Britannia	BRT
Queensland	QLD		Queensland	Queensland		Queensland		Queensland	QLD		
Recorder	RCD							Recorder	RCD		
Fraser	FRS		Fraser	Fraser		Fraser	frs	Fraser	FRS		
Tasmantid Seamount	TSM		Tasmantid SM	Tasmantid SM		Tasmantid SM		Tasmantid SM	TSM		
Southern Lord Howe Rise	SLH	Lord Howe	S Lord Howe	Lord Howe 3	LH3	LH3	lh3	S Lord Howe	SLH	S Lord Howe	SLH
		seamounts		Lord Howe 4	LH4	LH4	lh4				
Lord Howe Island	LHI							Lord Howe Island	LHI		
Elizabeth Reef	ELR							Elizabeth Reef	ELR		
Middleton Reef	MDR							Middleton Reef	MDR		
Gifford Seamount	GIF		Gifford SM					Gifford SM	GIF		
Capel Bank	CPL		Capel Bank					Capel Bank	CPL		